

Attention Modulates Contextual Processing in Vision

By

Mark Jonathan Roberts

A thesis submitted to
The University of Newcastle Upon Tyne
for the degree of
Doctor of Philosophy

School of Biology and Psychology
The University of Newcastle upon Tyne
January 2006

NEWCASTLE UNIVERSITY LIBRARY

204 26736 3

Thesis L8139

Acknowledgments

I would like to thank Alexander Thiele for excellent supervision, support and encouragement in all parts of this work. I thank Louise Delicato who was involved in gathering data for Chapter 3 and who gathered a large part of the data for Chapter 4, also for her careful reading and helpful comments to Chapter 3. I thank Wolfgang Zinke, Robert Robertson, Kun Guo and Scott McDonald who were involved in gathering data for Chapter 2. I also thank Paul Flecknell, Claire Richardson, Ashley Waddel, Michael Ward and Caroline Fox for their invaluable technical assistance. Finally I would like to thank my wife Katharine, for her complete support throughout and for her practical help proof-reading and preparing the final draft. In this thesis I use the singular personal pronoun, i.e. 'I' instead of 'we'. This was done for simplicity and readability and not to devalue the contributions of others.

The project was supported by Medical Research Council studentship G78/7853, Wellcome grant GR070380, Biotechnology and Biological Sciences Research Council grant BBS/B/09325 and Royal Society small grant scheme 57400.G503/2936.

Contents

ATTENTION MODULATES CONTEXTUAL PROCESSING IN VISION.....	1
ACKNOWLEDGMENTS	2
FIGURES LIST	4
TABLES LIST	6
ABBREVIATIONS	7
ABSTRACT.....	8
PREFACE.....	9
CHAPTER 1: THE INTERACTION OF CONTEXT, CONTRAST, AND ATTENTION ON ORIENTATION DISCRIMINATION IN HUMAN SUBJECTS	13
1.1 ABSTRACT	13
1.2 INTRODUCTION	14
1.3 METHODS	18
1.4 RESULTS	28
1.5 BIOLOGICALLY MOTIVATED MODEL.....	47
1.6 A SIMPLIFIED MODEL FOR FITTING	60
1.7 AN ERROR MODEL TO ACCOUNT FOR THE LOW CONTRAST DATA.....	67
1.8 DISCUSSION	71
CHAPTER 2: ACETYLCHOLINE DYNAMICALLY CONTROLS SPATIAL INTEGRATION IN MARMOSET PRIMARY VISUAL CORTEX	76
2.1 ABSTRACT	76
2.2. INTRODUCTION	77
2.3 MATERIALS AND METHODS	81
2.4 RESULTS	94
2.5 DISCUSSION	113
2.6 CONCLUSION	118
CHAPTER 3: THE INTERACTION OF ATTENTION, CONTRAST AND ECCENTRICITY IN THE DYNAMIC CONTROL OF SPATIAL INTEGRATION IN ALERT MACAQUE PRIMARY VISUAL CORTEX.....	119
3.1 ABSTRACT	119
3.2 INTRODUCTION	120
3.3 METHODS	124
3.4 RESULTS	143
3.5 DISCUSSION	186
3.6 CONCLUSIONS.....	193

CHAPTER 4: THE CHOLINERGIC CONTRIBUTION TO ATTENTIONAL MODULATION IN ALERT MACAQUE PRIMARY VISUAL CORTEX.....	194
4.1 ABSTRACT	194
4.2 INTRODUCTION	195
4.3 METHODS	196
4.4 RESULTS	203
4.5 DISCUSSION	221
GRAND SUMMARY, CONCLUSIONS AND OUTLOOK	224
FUTURE WORK.....	226
REFERENCES.....	227

Figures list

Chapter 1

Figure 1.1a Representation of stimulus in the single task	19
Figure 1.1b Detailed description of target and reference presentation	19
Figure 1.2 Representation of experimental design	24
Figure 1.3 Pictorial explanation of data transformation	26
Figure 1.4 Example of raw data from high contrast experiment	29
Figure 1.5 Example of transformed data and fitted plane from high contrast experiment.....	31
Figure 1.6 Example of raw data from low contrast experiment	33
Figure 1.7 Example of transformed data and fitted plane from low contrast experiment.....	34
Figure 1.8 Within-subject demonstration of contrast reversal effect.....	35
Figure 1.9 Comparison of 3D plane fitting parameters between single and dual task.....	357
Figure 1.10 Target responses in conditions where the target was not presented	40
Figure 1.11a ... Method for testing the effect of false alarms.....	42
Figure 1.11b ... Example of comparison between manipulated high contrast data and low contrast data.....	42
Figure 1.12 Transformed data set from ‘no context bars’ experiments.....	45
Figure 1.13 Vector model for orientation coding	48
Figure 1.14 The effect of population size on orientation tuning accuracy	49
Figure 1.15 The effect of model neuron response variance and orientation tuning bandwidth on orientation coding accuracy.....	49
Figure 1.16 Example of model neuron’s orientation tuning and spatial sensitivity profile	51
Figure 1.17 Surround inhibition and facilitation in the vector model.....	53
Figure 1.18 The interaction between the spatial sensitivity profile and the temporal decay function in determining the nature of contextual influence	55
Figure 1.19 Model prediction across large orientation differences between context and target bars	56
Figure 1.20 Simplified model for fitting to data.....	61
Figure 1.21 Examples of simplified model data fits.....	63
Figure 1.22 Comparison of simplified biological model fitting parameters between the single and dual task conditions	66
Figure 1.23 Comparison of each subject’s false alarm rate and model-predicted false alarm rate	70

Chapter 2

Figure 2.1	Example of a single unit autocorrelation and a multi-unit correlation	83
Figure 2.2	Autocorrelation of a burst cell and a multi-unit	85
Figure 2.3	Demonstration of difference of Gaussians (DOG) model	89
Figure 2.4	Demonstration of ratio of Gaussians (ROG) model	90
Figure 2.5	Relationship between response mean and response variance	92
Figure 2.6	Comparison of fit quality from DOG and ROG models	96
Figure 2.7	Examples of the effect of Acetylcholine (ACh) application on length tuning in facilitated and inhibited cells	98
Figure 2.8	Effect of ACh on DOG fitting parameters	100
Figure 2.9	Effect of ACh on ROG fitting parameters	101
Figure 2.10	Comparison of fit quality between three forms of the DOG and ROG models	104
Figure 2.11	Effect of ACh on fitting parameters in three forms of the ROG model	105
Figure 2.12	Time course of length tuning (DOG model)	107
Figure 2.13	Time course of length tuning (ROG model)	108
Figure 2.14	Population responses from animals 1 and 2	110
Figure 2.15	Population response from animals 3 and 4	111
Figure 2.16	Effect of ACh on the tonic index	112

Chapter 3

Figure 3.1	Example of raw data from receptive field (RF) mapping	127
Figure 3.2	Processed RF mapping data	128
Figure 3.3	Representation of main experimental task	130
Figure 3.4	Example of orientation tuning data	131
Figure 3.5	Example of contrast response function	133
Figure 3.6	Timing of behaviourally relevant events	134
Figure 3.7	Examples of the stereotyped saccade made by monkey D and its effect on neuronal response ...	137
Figure 3.8	Example of length tuning data	140
Figure 3.9	Explanation of receiver operating characteristic (ROC) analysis	143
Figure 3.10	Effect of bar length on reaction time (RT)	146
Figure 3.11	Performance across bar lengths	147
Figure 3.12	Performance across bar lengths, excluding fixation error trials	148
Figure 3.13	Performance as a function of contrast and trial type	150
Figure 3.14	Monkey B, RT in early and late sessions (high contrast stimuli)	152
Figure 3.15	Monkey B, performance in early and late sessions (high contrast stimuli)	153
Figure 3.16	Comparison between performance in block change trials and performance in all trials	154
Figure 3.17	Examples of the effect of attention on length tuning	155
Figure 3.18	Effect of restricting eye position on attentional modulation	157
Figure 3.19	The effect of attention on length tuning at high contrast	159
Figure 3.20	The effect of attention on length tuning at medium contrast	159
Figure 3.21	The effect of attention length tuning at low contrast	160
Figure 3.22	The distribution of RF size and eccentricity	159
Figure 3.23	Examples of the effect of attention on length tuning at $\sim 7^\circ$ eccentricity	163
Figure 3.24	The effect of attention on length tuning across the population at $\sim 7^\circ$ eccentricity	163
Figure 3.25	Percentage change in firing rate across bar length and contrast	166

Figure 3.26 ROC analysis of attentional effect across bar length and contrast	167
Figure 3.27 ROC analysis in the $\sim 7^\circ$ eccentricity sample	168
Figure 3.28 Comparison of ROC values in raw data and data filtered by eye position.....	169
Figure 3.29 The effect of attention on response profiles to high contrast stimuli.....	172
Figure 3.30 The effect of attention on response profiles to mid contrast stimuli ($\sim 2^\circ$ eccentricity).....	173
Figure 3.31 The effect of attention on response profiles to mid contrast stimuli ($\sim 7^\circ$ eccentricity).....	174
Figure 3.32 The effect of attention on response profiles to low contrast stimuli ($\sim 7^\circ$ eccentricity).....	175
Figure 3.33 Tonic index as a function of bar length and attention	176
Figure 3.34 The effect of task demands on response profile	178
Figure 3.35 Cell examples of the effect of contrast and attention on length tuning	180
Figure 3.36 The effect of contrast on length tuning in monkey B.....	181
Figure 3.37 The effect of contrast on length tuning in monkey D.....	182
Figure 3.38 The interaction of attention and contrast on length tuning (monkey B).....	184
Figure 3.39 The interaction of attention and contrast on length tuning (monkey D).....	185

Chapter 4

Figure 4.1 Illustration of electrode manufacture	198
Figure 4.2 Photograph of an example pipette tip.....	199
Figure 4.3 The effect of ACh on contrast response functions	204
Figure 4.4 The effect of ACh on Naka-Rushton fitting parameters	205
Figure 4.5 Example of the effects of attention and of ACh application on neuronal response.....	207
Figure 4.6 Normalised population responses	208
Figure 4.7 The effect of ACh application on attentional modulation	209
Figure 4.8 Attentional modulation as a function of time and bar length	210
Figure 4.9 The effect of attention on response modulation by ACh.....	211
Figure 4.10 The effect of ACh application as a function of time and bar length.....	211
Figure 4.11 Possible explanation for the interaction between ACh application and attention	213
Figure 4.12 The effect of attention and scopolamine application on neuronal responses.....	215
Figure 4.13 Normalised population responses	216
Figure 4.14 The effect of scopolamine on attentional modulation	217
Figure 4.15 Attentional modulation as a function of time and bar length	218
Figure 4.16 The effect of attention on response modulation by scopolamine	219
Figure 4.17 The effect of scopolamine application as a function of time and bar length	219
Figure 4.18 The effect of drug application on reaction time	221

Tables list

Chapter 1

Table 1.1 2D regressing fitting parameters and fit quality from high contrast experiments.....	32
Table 1.2 2D regressing fitting parameters and fit quality from low contrast experiments.....	36
Table 1.3 Subject's ability to correctly discriminate target-absent/target-present trials	38
Table 1.4 Comparison of 2D regression from manipulated high contrast data and low contrast data.....	43
Table 1.5 Effect of colour counting performance in dual task on 2D regression parameters	46
Table 1.6 Simplified model fitting parameters in high contrast experiments	65

Table 1.7 Simplified model fitting parameters in low contrast experiments	66
Table 1.8 Error model fitting parameters for low contrast experiments.....	70

Chapter 2

Table 2.1 Comparison of fit quality from DOG and ROG models using three fitting strategies.....	96
Table 2.2 The effect of ACh on DOG fitting parameters	241
Table 2.3 The effect of ACh on ROG fitting parameters	242
Table 2.4 Comparison of fit quality from three forms of the DOG and ROG models	104

Chapter 3

Table 3.1 The effect of attention on DOG fitting parameters ~2° eccentricity.....	240
Table 3.2 The effect of attention on DOG fitting parameters in monkey B, data cut at 200msec	241
Table 3.3 The effect of attention on DOG fitting parameters at ~7° eccentricity.....	242
Table 3.4 Comparison of peak length and fitting parametrs across eccentricity	243
Table 3.5 Comparison of ROC values across contrasts.....	167
Table 3.6 The effect of contrast on DOG fitting parameters ~2° eccentricity	244
Table 3.7 The effect of contrast on DOG fitting parameters ~7° eccentricity.....	245

Abbreviations

ACh	Acetylcholine
AFC	Alternative Forced Choice
BMI	Bicuculline Methiodide
CNS	Central Nervous System
CRF	Classical Receptive Field
CRT	Cathode Ray Tube (monitor)
DOG	Difference of Gaussians
EPSP	Excitatory Post-Synaptic Potentials
HI	Hazard index
ID	Inner Diameter
IV	Intravenous
LGN	Lateral Geniculate Nucleus
mRF	minimum Response Field
NBM	Nucleus Basalis of Meynert
OD	Outer Diameter
nCRF	non-Classical Receptive Field
RF	Receptive Field
ROC	Receiver Operating Characteristic
ROG	Ratio of Gaussians
RT	Reaction Time
SSE	Summed Squared Error
T-C>R-C	Perceived orientation difference between target and context bars is greater than perceived orientation difference between reference and context bars
T-C<R-C	Perceived orientation difference between target and context bars is less than perceived orientation difference between reference and context bars
TI	Tonic Index
V1	Primary visual cortex
χ^2	Chi squared error
χ^2_N	Chi squared error normalised by the number of fitting parameters

Abstract

Contextual information influences the neuronal processing and perception of visual stimuli. The functional significance of this influence may be to increase the efficiency of visual processing by taking advantage of redundancies in natural scenes. Increased efficiency may come at a cost of introducing errors, especially when stimuli are incongruous with the context. For optimal performance the visual system may therefore balance efficiency with accuracy by dynamically controlling the influence of contextual information. Attention is an appropriate mechanism to set this balance since attention is high when errors are costly and therefore accuracy is preferable over efficiency, but attention is low when accuracy can be sacrificed for efficiency.

States of attention are associated with increased acetylcholine (ACh) efflux into the cortex. The effect of ACh on cortical processing has been investigated in a number of *in vitro* studies. They show that ACh causes a selective inhibition of intracortical synapses while thalamocortical synapses are unaffected or even enhanced. Thus, ACh effectively switches cortical processing in favour of feed-forward inputs. In the visual system this switching would be expected to reduce contextual influences, thought to be mediated by intracortical processing. These findings suggest the hypothesis that attention will reduce contextual influences by the action of ACh.

To investigate this hypothesis I present work from four separate experiments. I found that attention caused a reduction in contextual influences at the level of human perception (Experiment 1) and at the level of neurons in primate V1 (Experiment 3). I also found the application of ACh to cells in V1 of anaesthetised primates caused a reduction in non-classical receptive field modulation (Experiment 2), similar to the effect of attention. Finally I found that attentional modulation of neuronal responses in macaque V1 was partially blocked by the application of a cholinergic antagonist, scopolamine (Experiment 4). Taken together my findings demonstrate that attention causes a suppression of contextual influences at the level of perception and at the level of the primary visual cortex. These effects were at least partly mediated by cholinergic mechanisms.

Preface

There is ample evidence that voluntary attention affects behavioural and neuronal performance (Duncan 1984; Spitzer et al. 1988; Corbetta et al. 1990; Motter 1993; Motter 1994; Motter 1994; Ocraven et al. 1997; Ito et al. 1998; Roelfsema et al. 1998; McAdams and Maunsell 1999; O'Craven et al. 1999; Treue and Martinez-Trujillo 1999; McAdams and Maunsell 2000; Driver and Frackowiak 2001; Roelfsema and Spekreijse 2001; Theeuwes et al. 2001; Treue 2001; Cook and Maunsell 2002) but little is known about the exact neural mechanisms underlying these effects. Several lines of evidence have demonstrated that attention and arousal are associated with activation of the cholinergic system originating in the basal forebrain (Dunnett et al. 1991; Everitt and Robbins 1997). The effect of acetylcholine (ACh) on cortical processing is still debated; however, several *in vitro* studies have suggested that ACh selectively suppresses the efficacy of intracortical synapses whilst the efficacy of thalamocortical synapses is unaffected, or enhanced (Hasselmo and Bower 1992; Gil et al. 1997; Kimura and Baughman 1997; Kimura et al. 1999; Hsieh et al. 2000; Kimura 2000). Thus the action of ACh might be to bias cortical processing in favour of feed-forward inputs (Kimura 2000). In primary visual cortex thalamocortical inputs are thought to provide the major input for the classical receptive field (CRF) whilst intracortical synapses are thought to provide the input for the modulatory non-classical receptive field (nCRF) (Angelucci et al. 2002). These findings suggest the hypothesis investigated in this thesis; that attention will reduce contextual influences by the action of ACh.

The perceptual consequence of nCRF modulation is that local spatial and temporal context can alter the appearance of target stimuli (Albright and Stoner 2002). In Chapter 1 (*The interaction of context, contrast, and attention on orientation discrimination in human subjects*) I present an experiment which uses human psychophysics to investigate attentional modulation of contextual influence at different levels of target contrast. The test stimulus was a dynamic series of 5 bars arranged to produce apparent motion. I assessed how the orientation of bars 1-4 (context) affected the perceived orientation of the fifth bar (target) in relation to an isolated reference bar. Visual attention was manipulated in a single task (full attention) vs. dual task (reduced attention) paradigm. When the target had the same high contrast as bars 1-4 (context) its perceived orientation was shifted away from

the context bar orientation, i.e. context had a repellent influence. When the contrast of the target was low (at a level just above the subject's contrast threshold) with the contrast of the context bars unchanged, the perceived orientation of the target was shifted towards the context bar orientation, i.e. context had an attractor effect. This reversal reveals the dual nature of contextual influences at low and high contrast. Both repulsion at high contrast and attraction at low contrast were strongest in the near-absence of attention (in the dual task condition); directing full attention (in the single task condition) reduced both effects. Thus, in line with the main hypothesis, attention reduced contextual influences independent of the sign of this influence.

In the primary visual cortex, length tuning is a classic demonstration of nCRF modulation (DeAngelis et al. 1994). In Chapter 2 (*Acetylcholine dynamically controls spatial integration in marmoset primary visual cortex*) I present an experiment in which I tested whether length tuning was influenced by external ACh application to cells in the primary visual cortex of anaesthetised primates. In line with my hypothesis, I found that ACh application caused a significant reduction in preferred length, indicating a reduction in spatial summation from the nCRF. I also showed that the response of the majority of cells was enhanced by ACh application, especially in the late (sustained) part of the response. This temporal profile matches the profile of attention-mediated response enhancement as reported by many studies (Motter 1994; Roelfsema et al. 1998; McAdams and Maunsell 1999; Seidemann and Newsome 1999; Reynolds et al. 2000; Roelfsema and Spekreijse 2001; Treue 2001). The finding thus adds support to the idea that ACh may be a part of the neurobiological system responsible for mediating attentional effects in visual cortex.

In Chapter 3 (*The interaction of attention, contrast and eccentricity in the dynamic control of spatial integration in alert macaque primary visual cortex*) I present work in which I tested whether attention affects the length tuning of V1 cells in a similar manner to ACh application. I trained two macaques to perform a task for which they were required to attend either to the location of the RF of the cell under study (attend-RF condition) or to a location in the opposite hemi-field (attend-away condition). A spatial cue indicated to which of these two locations the monkey was required to attend. I then presented two bars (test stimuli) of the preferred orientation and of variable length, one inside the neuron's RF and the other in the opposite hemifield. The monkey had to detect a small change in luminance at the centre of the bar in the cued location, and ignore luminance changes in the bar at the un-cued

location. Neuronal responses and tuning functions were compared between the attend-RF and attend-away conditions. The test stimuli were presented at high, medium or low contrast. I collected data from two monkeys where the stimuli were presented at roughly 2° eccentricity from the fovea, and data from one monkey where the stimuli were presented at roughly 7° from the fovea. In the ~2° eccentricity sample I found that voluntary attention reduced the cell's preferred length, when stimuli were presented at high or medium contrast. These findings show that attention had a similar effect to that of ACh application as demonstrated in Chapter 2. Attention did not affect length tuning at low stimulus contrast. When stimuli were presented at ~7° eccentricity the effect of attention was reversed; that is, high levels of attention increased the preferred length of the cell. The discrepancy between the ~2° and ~7° samples may be explained by differences in centre/surround interactions across eccentricity, as a number of recent studies have reported that facilitation from the nCRF is strongest in (or even exclusive to) regions of visual space near the fovea, whilst nCRF suppression is strongest in the periphery (Xing and Heeger 2000; Petrov et al. 2004). If attention reduces the efficacy of nCRF modulation as I suggest, a reduction in the efficacy of a nCRF dominated by facilitation (as in the near-foveal region) would tend to reduce preferred length. A reduction in the efficacy of a nCRF dominated by inhibition (as in peripheral vision) would tend to increase preferred length. Therefore, results from this chapter demonstrate that nCRF modulation is reduced by attention. Taken together with results from Chapter 1, the hypothesis that contextual processing is suppressed by attention is fully supported.

Results from the experiments detailed in Chapters 2 and 3 demonstrate that attention and ACh have similar effects in V1 cells. In experiments described in Chapter 4 (*The cholinergic contribution to attentional modulation in alert macaque primary visual cortex*) I directly tested the importance of cholinergic transmission for attentional effects by applying a cholinergic agonist (ACh) or antagonist (scopolamine) to cells in the primary visual cortex of an alert macaque engaged in the same attention-demanding task as described in Chapter 3. Cholinergic drugs were applied via a newly developed recording electrode/iontophoresis pipette which allows penetration of the intact dura without the use of guide tubes, thus permitting recording access to V1 with minimal tissue damage. Neuronal responses to stimuli of varying length were measured while the monkey attended to and away from the RF of the neuron under study, with and without drug application. I found that attention

and ACh generally enhanced the response, whilst scopolamine application generally suppressed the response. Moreover I found that the application of either drug reduced the effect of attention; ACh application reduced attentional modulation by causing greater facilitation in the attend-away condition whilst scopolamine reduced attentional modulation by causing greater inhibition in the attend-away condition. Thus ACh had the effect of making responses in the attend-away condition more like responses in the attend-RF condition (potentially mimicking the effect of attention), whilst scopolamine had the effect of making responses in the attend-RF condition more like responses in the attend-away condition (i.e. blocking the effect of attention). These data demonstrate the importance of the cholinergic system in mediating attentional effects in V1 of the macaque. Taken together with other data presented in this thesis, I find good support for the hypothesis that one of the major functions of attention in vision is to rebalance cortical processing in favour of feed-forward inputs and away from contextual processing. The neurobiological mechanism for this dynamic rebalancing of cortical processing is, at least in part, mediated by the action of ACh.

Chapter 1: The Interaction of Context, Contrast, and Attention on Orientation Discrimination in Human Subjects

1.1 Abstract

Contextual information influences neuronal processing and perception. These influences depend on factors such as the stimulus contrast and the allocation of attention. To determine the interaction of these two factors I used human psychophysics to investigate attentional modulation of contextual influence at different levels of target contrast. The test stimulus was a series of five bars arranged to produce apparent motion. I tested how the orientation of bars 1-4 (context) affected the perceived orientation of the fifth bar (target) in relation to an isolated reference bar. Visual attention was manipulated in a single task (full attention) vs. dual task (reduced attention) paradigm.

When the target had the same (high) contrast as bars 1-4 (context), its perceived orientation was shifted away from the context bar orientation, i.e. context caused a repulsion of the perceived target orientation. When the target was presented close to the subject's contrast threshold, with context contrast unchanged, the perceived orientation of the target was shifted towards the context bar orientation; i.e. it was attracted by the context. This reversal reveals the dual nature of contextual influences at low and high contrast. Repulsion at high contrast and attraction at low contrast occurred in the full attention condition but were both enhanced when visual attention was withdrawn in the dual task condition. Thus, attending to the target reduced contextual influences independent of the sign of this influence.

I modelled the data using an ensemble of orientation selective and spatially sensitive V1-like model neurons. The repulsion effect at high contrast could be modelled by centre/surround inhibition, while the attractor effect at near-threshold contrast could be modelled by surround facilitation. This fits well with reports of contrast-dependent switching of surround modulation in V1 neurons.

1.2 Introduction

Visual neurons respond to stimuli presented within a small region of visual space known as the cell's classical receptive field (CRF). Stimuli presented in the so-called non-classical receptive field (nCRF), which surrounds the CRF, cannot elicit a response on their own but may be able to moderate the cell's response to stimuli presented within the CRF. The nature and magnitude of the influence depends on the geometric configuration of stimuli in the centre (CRF) and surround (nCRF). In a similar way the perception of a stimulus can be altered by the spatial and temporal context that surrounds that stimulus. Close parallels have been drawn between electrophysiological findings and psychophysical results (Albright and Stoner 2002; Series et al. 2003; Zenger-Landolt and Heeger 2003). For example, a low contrast line or Gabor patch can be more easily detected by an observer when a collinear stimulus is placed near it (Kapadia et al. 1995; Ito et al. 1998; Kapadia et al. 2000; Freeman et al. 2001; Li and Gilbert 2002; Freeman et al. 2004). The same arrangement boosts the V1 neuronal response relative to the response to the central line on its own (Kapadia et al. 1995; Polat and Norcia 1996; Ito et al. 1998; Kapadia et al. 2000; Khoe et al. 2004). Conversely, pairing a high contrast central grating with an iso-oriented high contrast surround reduces the apparent contrast of the central grating (Zenger-Landolt and Heeger 2003) and depresses neuronal responses (Knierim and Van Essen 1992; Polat and Norcia 1996; Cavanaugh et al. 2002; Williams et al. 2003; Zenger-Landolt and Heeger 2003). Thus, iso-oriented surrounds enhance the perception of and neuronal response to low contrast stimuli, but depress the perception of and response to high contrast stimuli (Levitt and Lund 1997; Polat et al. 1998; Mizobe et al. 2001).

Cross-oriented surrounds interact differently with central stimuli. When the central stimulus is at high contrast a cross-oriented surround enhances its apparent contrast (Yu et al. 2001; Yu et al. 2003), and can enhance the neuronal response (Dragoi and Sur 2000; Cavanaugh et al. 2002). When the centre is at low contrast a cross-oriented surround may have no effect (Mizobe et al. 2001) or may weakly suppress the response to, or perception of, the central stimulus (Polat and Norcia 1996; Cavanaugh et al. 2002). Studies investigating nCRF modulation have thus shown that the nCRF must be regarded as a complex and dynamic part of visual processing. The functional significance of the nCRF is currently debated. One

function may be contrast normalization (Heeger 1992), however the complexity and stimulus specificity of the observed effects points to a role in more complex functions such as contour integration (Fitzpatrick 2000; Li and Gilbert 2002) or filling-in (De Weerd et al. 1995) of low contrast displays, as well as surface segmentation (Born 2000), edge detection, and pop-out (Knierim and Van Essen 1992) in high contrast displays (Stemmler et al. 1995; Mizobe et al. 2001).

Several lines of evidence have suggested that the allocation of voluntary attention is also important in modulating contextual influence, however, relatively few studies have directly tested this proposal. Ito et al. (1998) reported attentional effects on collinear flanker facilitation in a psychophysical study in both humans and monkeys. Their stimulus was a display of four lines presented in the periphery either with or without collinear flankers. One of these four lines (the target) differed in brightness from a centrally presented reference. The subject's task was to report whether the target was brighter or darker than the reference. In the 'distributed attention' condition the target could appear in any one of the four locations. In the 'focused attention' condition a cue indicated at which location the target would appear. This design allowed the authors to investigate how the flanker moderated the perceived brightness of the target under two attention conditions. Their results indicated that the flanker enhanced the perceived brightness of the target, and that this enhancement was roughly four times larger in the distributed attention condition than in the focused attention condition. Ito et al. (1998) therefore propose that contextual interactions are weakened by high levels of attention. Zenger et al. (2000) also studied the effect of attention on contextual effects. In their study four rings of six Gabor patches were presented, one of which contained a central target patch. The subject's task was to indicate which ring contained the target. In a dual task (reduced attention) condition subjects had to perform an additional letter-counting task. The authors report that when the target patch was presented at the same orientation, and at a contrast lower than the surround, detection thresholds were substantially higher in the dual task compared with the single task condition. There are two possible explanations for this result: either the surrounding Gabor patches suppressed the perception of the target, and this suppression was reduced in the single task condition compared with the dual task, or the surrounding Gabor patches caused perceptual filling in of the empty rings during the dual task condition, making real targets harder

to identify. In either case the effect of the surround was reduced in the full attention condition, hence the finding is in line with Ito et al.'s proposition.

Recently Freeman et al. (2001; 2003; 2004) have reported findings apparently at odds with Ito et al.'s and Zenger et al.'s findings. In their studies Freeman et al. showed that collinear flanking stimuli only influenced the perceived contrast of a low contrast target when the flankers were task relevant, and therefore attended, but not when simultaneously-presented orthogonal flankers were task relevant. Thus, in contrast to Ito et al.'s proposition, Freeman et al. suggest that the interaction between targets and flankers *requires* attention rather than being *weakened* by attention. An important difference between Freeman et al.'s experiments and the experiments by Ito et al. and Zenger et al. is that in the latter studies attention was directed either towards or away from the target, whilst in Freeman et al.'s experiments attention was always directed towards the surround but was focused to different parts of the surround. Thus, whilst these experiments show that attention plays a role in the dynamic modulation of contextual influences, it is not yet clear whether attention enhances or suppresses the influence of context.

The anatomical substrate of the CRF and nCRF in primary visual cortex has been a topic of much research. V1 neurons have access to visual information via three types of connection. Thalamocortical synapses carry information into the cortex and are thought to be the main substrate of the CRF (Maffei and Fiorentini 1976; Lund et al. 2003; Series et al. 2003), horizontal synapses recombine information within V1, and feedback synapses carry information from higher areas back to V1. It is thought that the substrate for the nCRF lies within this network of horizontal and feedback (i.e. intracortical) connections (Maffei and Fiorentini 1976; Angelucci et al. 2002; Angelucci and Bullier 2003; Lund et al. 2003; Series et al. 2003).

Feedback and horizontal synapses act through glutamatergic mechanisms whereby the release of glutamate is modulated by presynaptic muscarinic receptors (Parkinson et al. 1988; Sahin et al. 1992). Thalamocortical synapses also act through glutamatergic mechanisms but are modulated by presynaptic nicotinic mechanisms (Prusky et al. 1987; Parkinson et al. 1988; Sahin et al. 1992). When activated by acetylcholine (ACh), muscarinic receptors suppress the efficacy of their associated synapse (Vidal and Changeux 1993; Kimura and Baughman 1997) whilst synapses associated with nicotinic receptors are boosted by cholinergic activation (Vidal and Changeux 1993; Gil et al. 1997). Recent research using brain slices has demonstrated

the significance of this fact. They show that the application of ACh reduces the efficacy of intracortical connections but leaves thalamocortical connections unaffected (Hasselmo and Bower 1992; Hsieh et al. 2000; Oldford and Castro-Alamancos 2003) or even enhances their efficacy (Gil et al. 1997). Thus ACh switches the cortical network in favour of feed-forward processing (Parkinson et al. 1988; Kimura et al. 1999; Kimura 2000; Lucas-Meunier et al. 2003). We have recently demonstrated the functional significance of such network switching *in vivo*, by showing that iontophoretic application of ACh reduces the power of nCRF modulation in primate V1 (Chapter 2; Roberts et al. 2005).

The natural release of ACh is closely bound to attentive states (Everitt and Robbins 1997; Sarter and Bruno 1997; Sarter et al. 2005). In conjunction with the above discussion this suggests the hypothesis that visual processing should become more reliant on feed-forward inputs, with the associated reduction in surround modulation, during states of high attention and ACh release (Sarter et al. 2001; Roberts et al. 2005; Sarter et al. 2005). Here I test this proposal using human psychophysics. The experimental stimulus was a dynamic series of five bars. I found that the orientation of the first four bars (context) influenced the perceived orientation of the final bar (target). The nature of this influence could be either an attraction towards the orientation of the context bars or a repulsion away from it, depending on the contrast of the target. Using a model comprising of an ensemble of orientation-selective and spatially-sensitive model neurons in which responses decayed exponentially with time, I demonstrate that the repulsion effect observed at high target contrast could be due to centre/surround type inhibition (where the target stimulates the 'centre' and the context bars stimulate the 'surround'). The attractor effect that I observed at low target contrast could be due to centre/surround facilitation. Precisely such contrast-dependent switching of surround modulation has been observed electrophysiologically (Polat et al. 1998; Mizobe et al. 2001). Crucially, I found that the effect of the context bars on the perceived orientation of the target was weaker under conditions of full attention than under conditions of reduced attention. This was true under stimulus conditions that promoted attraction and under conditions that promoted repulsion. Thus, I show that the effect of directing voluntary attention was to attenuate the influence of the surround independent of the nature of the surround response. This finding supports my

hypothesis that attention moderates the balance of feed-forward and feedback processing in favour of feed-forward inputs.

1.3 Methods

I performed a series of experiments using the following general stimulus set: five short bars were presented at sequential locations on a uniform grey background (13.6cd/m^2) thereby producing apparent motion (see Figure 1.1a). The size and luminance of each bar was identical (0.8° by 0.07° , 139.6cd/m^2 , 82% Michelson contrast) except in 'low contrast' experiments where the contrast of the fifth bar was reduced to 3.6% (15.0cd/m^2). Bars 1-4 (context bars) were presented for 160msec and shared the same orientation. Bar 5 (target) was presented for 80msec. The target was located 1.1° from the fixation spot either vertically above (Experiment 1) or diagonally to the upper left (Experiments 2-4, see Figure 1.1b). The orientation of the target varied from trial to trial. A sixth bar (reference), of identical size and luminance to the context bars, was presented simultaneously with the target bar. The orientation of the reference also varied from trial to trial. The reference was presented in one of two locations below the fixation spot. The mean location was 1.1° below the fixation spot either vertically below (Experiment 1) or diagonally to the lower right (Experiments 2-4); however, the reference was randomly displaced from this location by half its length (i.e. 0.4°) on a trial-by-trial basis (see Figure 1.1b). This was done to prevent subjects using the separation between the ends of the target and reference to solve the task without explicitly responding to the stimulus orientation. 63 possible combinations (conditions) of target and reference orientation were presented in both the single and dual task conditions of all four experiments described herein (Figure 1.2). In the single task, the subjects were required to report whether the target orientation was clockwise or counter-clockwise from the reference or whether they appeared the same (3AFC). Responses were made on a keyboard using keys 'J', 'K' and 'L' for 'counter-clockwise', 'same', and 'clockwise' responses respectively. In the dual task, the central fixation point was super-imposed by a coloured filled circle. The colour of the circle changed randomly four times during each trial between seven possible colours (red, green, blue, magenta, grey, dark yellow and bright yellow). Colours were presented for 78msec with a 109msec interval between presentations. The first colour was presented 109msec after the presentation of the first bar. The last colour was extinguished 27msec after the

reference and target were extinguished. In addition to performing the orientation task subjects were asked to report the number of times the circle had been either red or green during the trial (which could be between 1 and 4 times) using the numbered keys on the keyboard. The purpose of the colour counting task was to divert attention from the bar stimulus. The single and dual task conditions were divided into separate sessions which were separated by at least one day.

Stimuli were displayed on a 20-inch analogue CRT monitor (75Hz, 1600 x 1200 pixels) positioned 1.4 metres from the subject. Stimuli were presented and responses recorded under the control of Remote Cortex 5.95 (Laboratory of Neuropsychology, National Institute of Mental Health, Bethesda). In all experiments subjects were trained at the start of the first session. During sessions subjects sat in a dark, or dimly lit, quiet room and were able to take breaks when they wished. 7 volunteers (no members of Alexander Thiele's research group) were paid for their participation (£5 per hour). Sessions typically lasted 1 to 2 hours.

Representation of stimulus in the single task

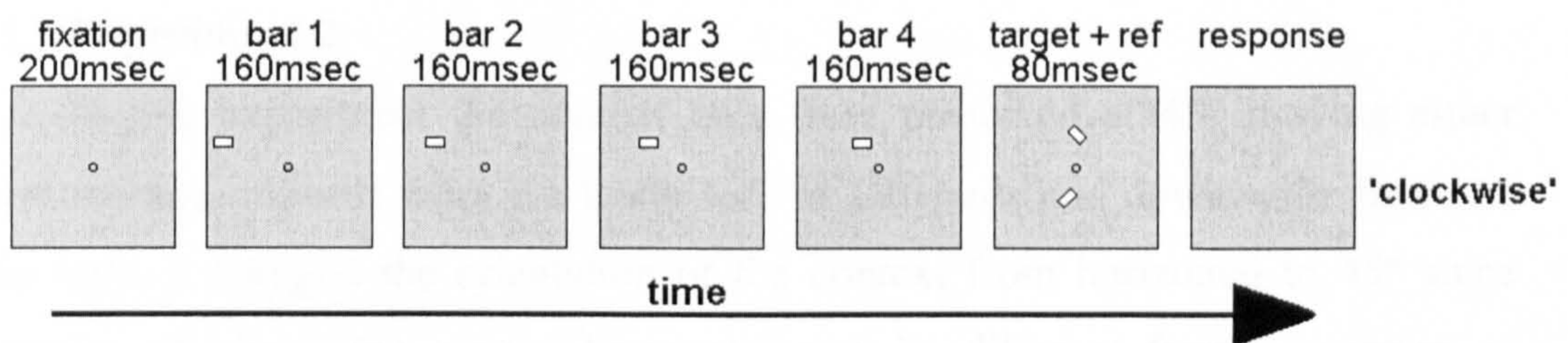


Figure 1.1a Stimulus sequence in the single task condition. Here the context bars are presented horizontally as in Experiment 1. In Experiments 2-4, bars were presented at 45° moving either downwards from the upper right or upwards from the lower left. Stimuli are not presented to scale.

Detailed description of target and reference presentation

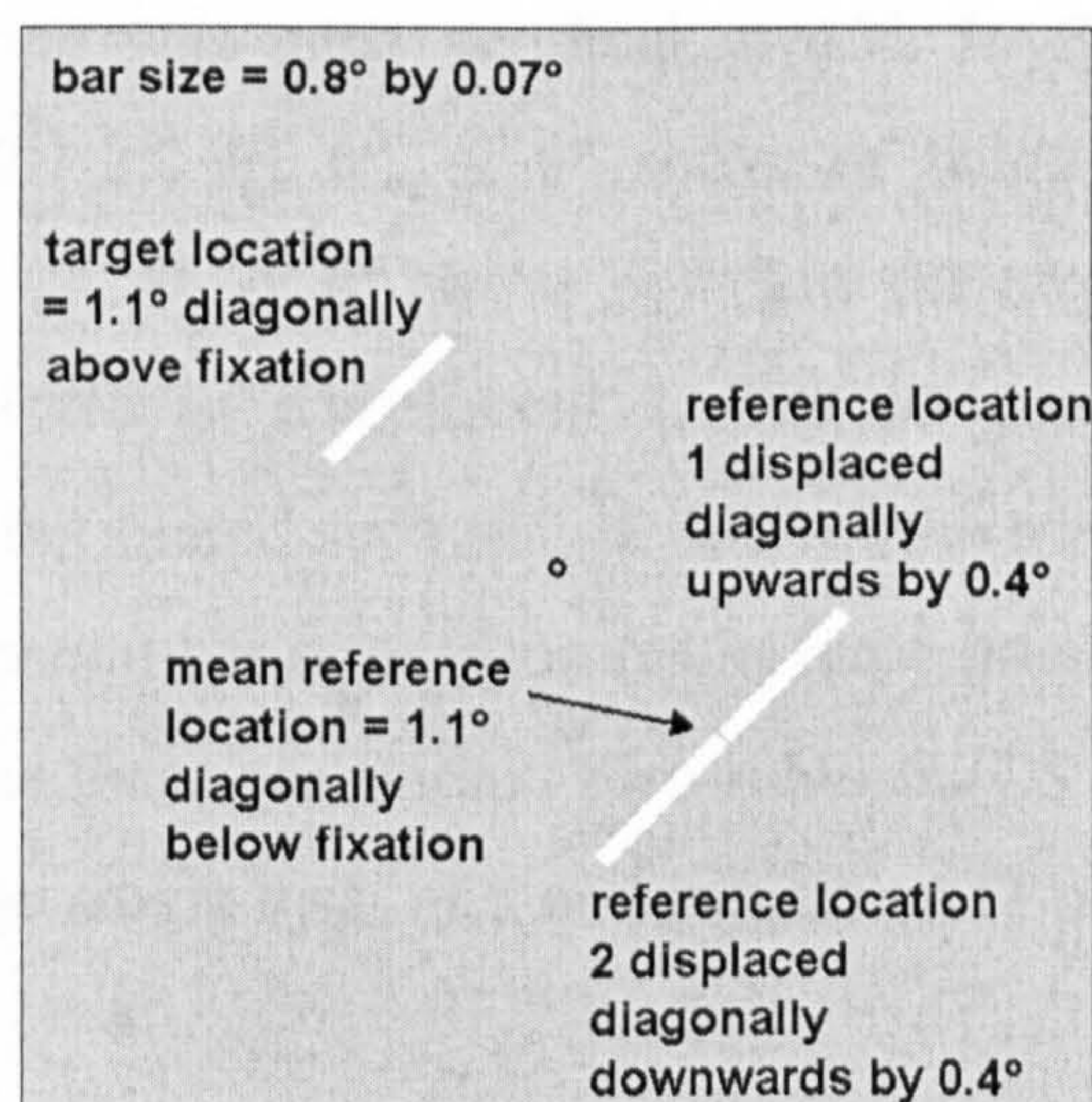


Figure 1.1b Detailed description of the presentation of the target and reference. Here stimuli are presented at 45° as in Experiments 2-4. The reference could appear in either location 1 or location 2, which were displaced diagonally by half of the length of the stimulus from the mean location diagonally below the fixation spot. Stimuli are presented to scale, such that the grey shaded area represents a 5° squared space.

1.3.1 Details of individual experiments

1.3.1.1 Experiment 1

Here the context bars were presented horizontally moving either from the left or the right (randomised from trial to trial). The target orientations were 0°, 1°, 2°, 3°, and 4° above or below the context bar orientation. The reference orientations were 0°, 1°, 2°, and 3° above or below the target orientation. The 63 conditions were presented randomly interleaved, but biased such that conditions where the target had the same orientation as the context were presented in 50% of the trials. These conditions were presented 80 times each; all other conditions were presented 10 times each, giving a total of 1120 trials. Three subjects (2 male, 1 female) participated under these conditions including the author (subject MR). All subjects participated in the single task before the dual task.

1.3.1.2 Experiment 2

In this experiment the context bars were presented at 45° moving either rightwards and upwards from the lower left, or leftwards and downwards from the upper right. I changed the orientation of the context from horizontal to 45° since perception of orientation around horizontal may be different from perception of orientation at other angles (Westheimer 2003; Quinn 2004). Importantly, it has been reported that subjects tend to perceive near-horizontal lines as tilted further from horizontal than they really are (Dick and Hochstein 1989), and that subjects' perception of orientation was most veridical at 45°. In Experiment 2 the target orientation could be 0°, 2°, 4°, 6°, or 8° above or below the context bars. The reference could be 0°, 2°, 4°, or 6° above or below the target. I thus extended the orientation space explored in Experiment 1. The 63 conditions were presented randomly interleaved, but biased such that in 50% of the trials the target orientation was the same as the context bar orientation (as in Experiment 1). Three subjects (all male) participated under these conditions. Two subjects (CS and DB) participated in the dual task before the single task, and one subject (AT) participated in the single task first.

1.3.1.3 Experiment 3a high contrast

In this experiment the context bars were presented at 45°, as in Experiment 2. The target orientation could be 0°, 3°, 6°, 9° or 12° above or below the context bar orientation. The reference orientation could be 0°, 1°, 2° or 3° above or below the target orientation. In this way I increased the space along the target-to-context axis still further than in Experiment 2, but reduced the space along the target-to-reference axis to the same dimensions as in Experiment 1. I did this because data from Experiment 2 suggested that judgments of orientation differences larger than 4° between target and reference were unaffected by the context. The 63 conditions were randomly interleaved and were each presented 20 times (i.e. the 50% bias towards targets that shared the same orientation as the context was removed), giving a total of 1260 trials in both the single and dual task. The coloured circle used for the dual task was presented in both the single and dual task conditions to eliminate any possible confound of presenting the colours or not. Subjects were instructed to ignore the colour changes in the single task. 3 subjects (all male) participated under these conditions. Subjects AG and DH participated in the single task before the dual task, subject JS participated in the dual task first. Two subjects (AG and JS) participated in the low contrast part of this experiment (see next section, *1.3.1.4 Experiment 3b low contrast*) as well as the high contrast part. Both participated in the high contrast part before the low contrast part.

1.3.1.4 Experiment 3b low contrast

In this experiment the luminance contrast of the target bar was reduced from 82% to 3.6%. This contrast was chosen for all subjects without testing their contrast detection thresholds. To check that such a low contrast stimulus was reliably visible, an additional 140 trials (10% of the total trial number) were included in which the target was not presented, giving a total of 1400 trials. Subjects in this experiment faced a four alternative forced choice (4AFC): ‘target counter-clockwise from reference’, ‘target same as reference’, ‘target clockwise from reference’ and ‘target not presented’ using the keys ‘j’, ‘k’, ‘l’ and ‘o’ respectively. In all other respects the design of this experiment was identical to Experiment 3a. Three subjects (all male) including the author MR participated under these conditions. Two subjects (AG and JS) participated in both the high and low contrast parts of this experiment. Although MR had already participated in Experiment 1, more than 2 years separated his

participation in the two experiments. Subjects MR and AG participated in the single task first, subject JS participated in the dual task first.

1.3.1.5 Experiment 4a high contrast

In this experiment the context bars were presented at 45° as in Experiments 2 and 3. The target could be presented at 0°, 3°, 6°, 9°, or 12° above or below the context bar orientation as in Experiment 3. The reference could be 0°, 2°, 4°, or 6° above or below the target. I increased the size of this axis back to the size it had been in Experiment 2, because data from Experiment 3 showed contextual influence up to the limit of the axis. Moreover, data from the dual task low contrast part of Experiment 3 were extremely noisy and difficult to interpret. Increasing the size of the target-to-reference axis reduced the effect of this noise. Each of the 63 combinations of target and reference orientation was presented 20 times, however this was separated into two sessions in which each combination was presented 10 times. Normally one week separated the two sessions. Breaking up the data acquisition forced subjects to take a rest break, since although in Experiments 1-3 subjects had been encouraged to take breaks whenever fatigued, they seemed reluctant to do so. In a number of subjects from Experiments 1-3 there was a clear increase in noise over the course of the session (i.e. responses did not reflect the stimulus), suggesting that the subjects had become fatigued.

1.3.1.6 Experiment 4b low contrast

In this experiment the contrast of the target was set according to the contrast response function of each subject. Each subject's contrast response function was determined using a stimulus which was identical to that used in the main experiment in all respects other than the contrast of the target bar. The contrast of the target was varied between 7 possible contrasts (7.2%, 6.0%, 4.9%, 3.7%, 2.5% 1.2% or 0%); these were the lowest 7 contrasts possible on the 8-bit graphics card of the display computer. The orientation of the target was always the same as that of the context bars. The subjects' task was to report whether or not they saw the target using the letters 'K' and 'O' respectively. Each contrast was presented 15 times. The target contrast used in the main experiment was set to the lowest contrast at which the subject perceived the target in 100% of trials. After the first experimental session (10 presentations per combination of target and reference orientation) the data were examined. If the data showed a high contrast effect (i.e. repulsion of the perceived

target orientation, see section *1.4.1 High contrast experiments*) the contrast of the target was lowered, and the subject re-tested. This was done once for subjects YL and EA and twice for subject ZI (see Figure 1.8). As it happened the contrast I eventually used for all subjects was 3.6%. As in the low contrast part of Experiment 3 an additional 140 trials were included in which the target was not presented, giving a total of 1400 trials in this experiment. Subjects then faced a four alternative forced choice (4AFC): ‘target counter-clockwise from reference’, ‘target same as reference’, ‘target clockwise’ and ‘target not presented’ using the keys ‘j’, ‘k’, ‘l’ and ‘o’ respectively. As in the high contrast part of Experiment 4 the required 20 presentations per combination of target and reference were split into two sessions, separated by a week. Three subjects (NT, YL and EA, all female) participated in both the high and low contrast parts of Experiment 4. Subject ZI participated only in the first half of the low contrast part of the experiment. Data from the dual task of the low contrast part of Experiment 3 showed an overwhelming increase in noise, which I attributed to high task demands. To somewhat reduce the difficulty of the dual task in the low contrast part of this Experiment, subjects were only required to count red coloured patches not red and green.

1.3.1.7 No context bars control experiment

To test whether observed changes in the perceived orientation of the target were due to the presentation of the context bars, and not some other factor, I ran a control experiment in which no context bars were presented. In this experiment the target could be presented at 0°, 3°, 6°, 9°, or 12° above or below 45°. The reference could be 0°, 2°, 4°, or 6° above or below the target. The target was presented at high contrast. Thus this experiment exactly replicated Experiment 4a, apart from the absence of the context bars. Each combination of target and reference orientation (total 63) was presented 10 times, interleaved in a pseudo-random order in one session. Two subjects participated in this control (MR and EA). Both subjects had previously participated in other experiments and shown typical effects.

1.3.2 Data analysis

I first examined proportions of ‘target clockwise to reference’, ‘target same as reference’ and ‘target counter-clockwise to reference’ responses from each combination of target and reference orientation. I represented these proportions as triplets of bars where the height of the bar represented the proportion of responses. I

arranged these triplets into columns representing conditions of equal orientation difference between target and reference and rows representing conditions of equal orientation difference between target and context bar (Figure 1.2). If the only factor influencing responses was the orientation of the target to the reference then 'counter-clockwise' responses should be predominantly present in columns where there was a positive difference between target and reference and 'clockwise' responses should be present in columns where there was a negative difference between target and reference. 'Same' responses should be predominantly in the central column, where there was no orientation difference between the target and reference. An influence of the context bar orientation on the subject's responses would be evident by differences between rows i.e. with changing orientation difference between target and context bars but constant orientation difference between target and reference.

Representation of experimental design

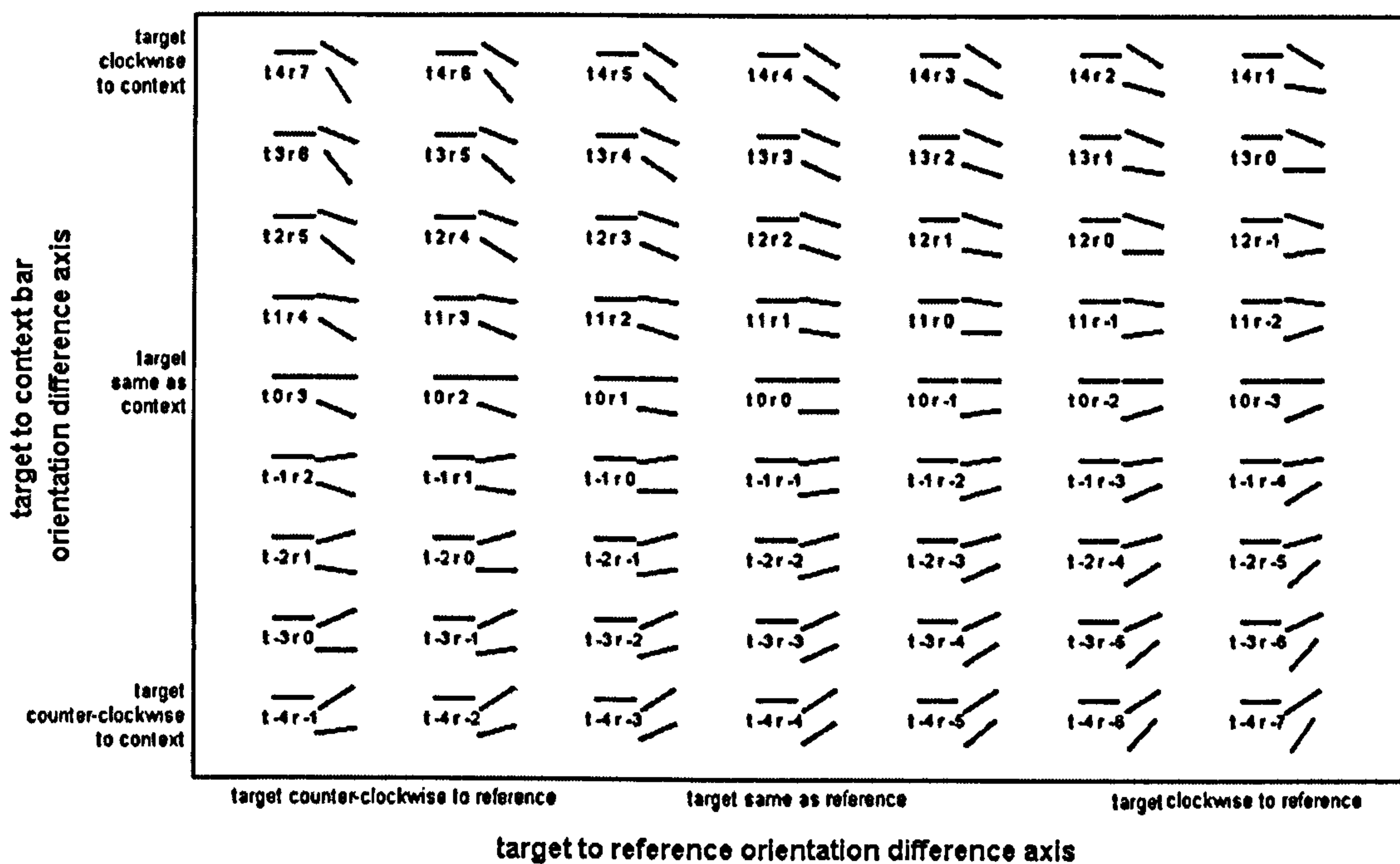


Figure 1.2 Experimental design. Each combination of target and reference orientation is represented as a triplet of lines. The horizontal line on the left represents the final context bar, the line adjacent to it represents the target. The reference is represented below the target. The orientation difference between target and reference changes across columns. Columns to the left show conditions where the target was presented counter-clockwise to the reference. Columns to the right show conditions where the target was presented clockwise to the reference. The central column shows conditions where the target and reference had the same orientation. The orientation difference between the target and the context bars changes across rows. Upper rows show conditions where the target was presented clockwise to the context bar, lower rows show conditions where the target was presented counter-clockwise to the context bars. The central row shows conditions where the target was presented at the same orientation to the context bars. Data in Figures 1.4 and 1.6 are shown in this format. Next to each triplet of lines the relative orientation difference (relative to the step size for each experiment, see

details of individual experiments) between the target and context bars is given by the value 't'. The relative orientation difference between the reference and context bars is given by the value 'r'. I transformed the data set by combining responses from conditions of equal value but opposite sign of t and r, for example the condition at the top left (t = 4, r = 7) is a match for the condition at the bottom right (t = -4, r = -7). I did not combine responses along the central row.

In Figure 1.2 each individual data point is a mirror image of another data point in the set. To find the corresponding mirror image matches it is necessary to first reflect all data points along the central column and then along the central row. Each of these mirror image data pairs can be described in terms of the angular distance of the 'target to context' and of the 'reference to context', thus replacing the nomenclature 'clockwise', 'same', and 'counter-clockwise'. Such a data reduction has three advantages: first, it increases the sampling at fixed orientation differences, second, it removes any bias the subject may have had for 'clockwise' or 'counter-clockwise' responses, and third it allows description of the data in the more meaningful reference frame of the angular distance to context bar orientation. An example of this transformation is given in Figure 1.3. The target and reference bar orientations in the upper left (Figure 1.3A) and lower right panels (Figure 1.3D) in Figure 1.3 are mirror images to one another (reflected along the main axis of context orientation), as are the target and reference bar orientations in the lower left (Figure 1.3C) and upper right panel (Figure 1.3B). In Figure 1.3A the target and reference had an identical angular tilt (pointing upwards), while in Figure 1.3D both had an identical angular tilt (but pointing downwards). For Figure 1.3A, a 'clockwise' response indicated that the *perceived* orientation difference between the target and the context bars was greater than the *perceived* orientation difference between the reference and the context bars (abbreviated as 'T-C>R-C' for the remainder of the text). For Figure 1.3D on the other hand a 'counter-clockwise' decision indicated that the *perceived* orientation difference between the target and the context bars was greater than the *perceived* orientation difference between the reference and the context bars ('T-C>R-C'), i.e. these opposite decisions in a 'clockwise/counter-clockwise' reference frame yield identical decisions in a reference frame where it is the orientation *difference* (rather than direction) from the context bar that is crucial. Figures 1.3B and C also show conditions where the target and reference have an identical angular tilt relative to the context bar orientation (albeit again with opposite sign). Figure 1.3B depicts conditions where 'clockwise' responses indicated that the *perceived* orientation difference between the target and the context bars was less than

the *perceived* orientation difference between the reference and the context bars (abbreviated as 'T-C<R-C' for the remainder of the text). Figure 1.3C depicts a condition where 'counter-clockwise' responses reflected such a 'T-C<R-C' percept. In other words, for Figures 1.3B and C the target was perceived to be tilted less from the context bar orientation than the reference. To obtain this more compact and meaningful reference frame I combined proportions of 'T-C<R-C' responses and proportions of 'T-C>R-C' responses provided they were from stimulus conditions with identical, but opposite, context/target/reference orientations (i.e. the angular difference to the context orientation was identical but had opposite sign).

Pictorial explanation of data transformation

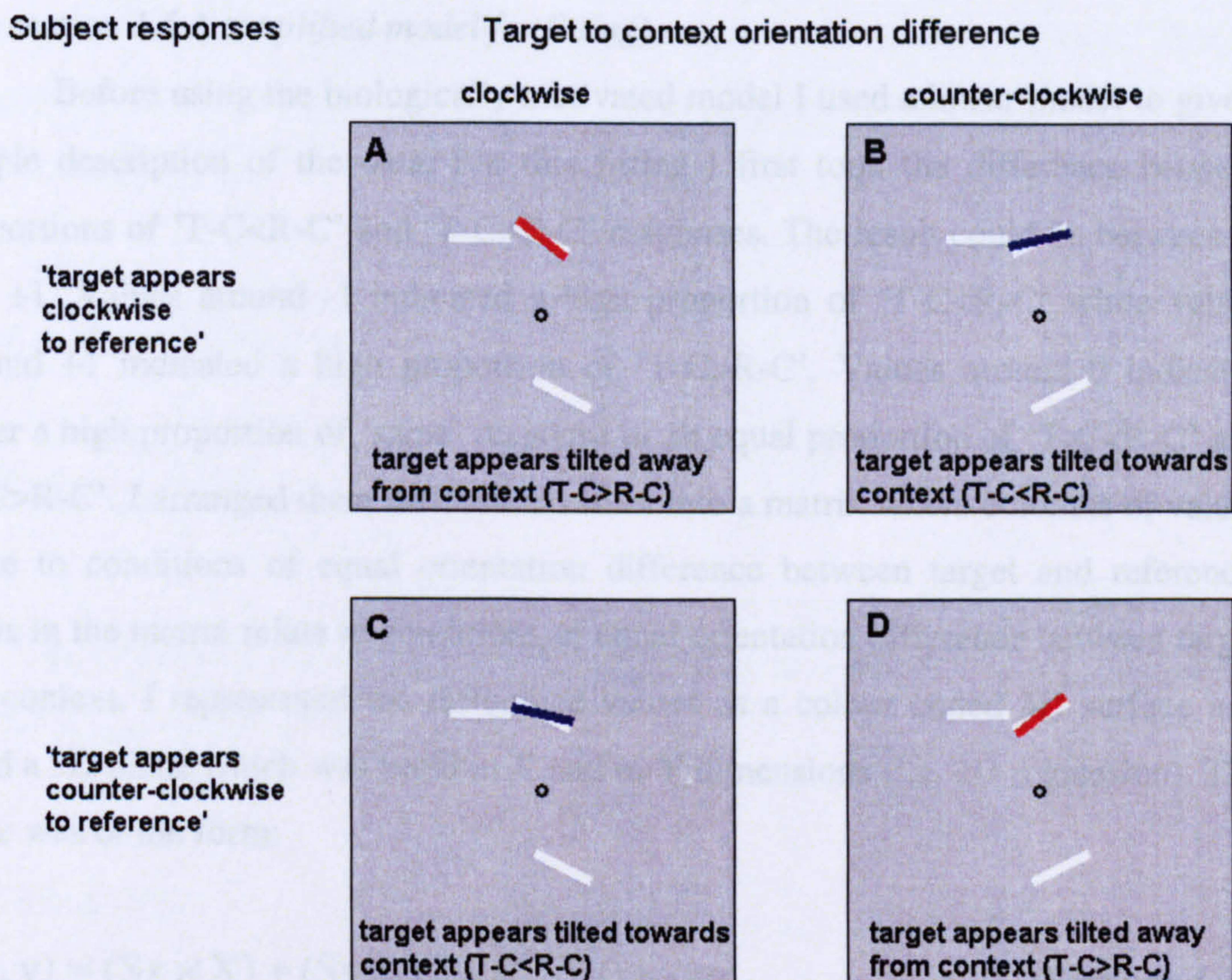


Figure 1.3 Explaining the logic of combining responses to stimuli of equal but opposite orientation difference between target and context bars. White bars represent the final context bar (left), the target (upper right) and the reference (lower right). The target and reference have equal orientations in each representation. The absolute orientation difference between the target and context bars is the same in all four representations, i.e. they represent a 'match'. Parts A and C are the 'lower match', parts C and D are the 'upper match'. Coloured bars overlaying the target represent how the subject perceived the target based on their response. Red bars indicate that the perceived orientation difference between the context bar and the target was greater than the perceived orientation difference between the context bar and the reference ('T-C>R-C', parts A and D). Blue bars indicate that the perceived orientation difference between the context bar and the target was less than the perceived orientation difference between the context bar and the reference ('T-C<R-C', parts B and C). A 'T-C>R-C' response corresponds to 'clockwise' responses when the target is clockwise to the context bar, or a counter-clockwise response when the target is counter-clockwise to the context bar. A 'T-C<R-C' corresponds

to a 'counter-clockwise' response when the target is clockwise to the context bar, or to a 'clockwise' response when the target is counter-clockwise to the context.

I arranged the triplets of proportions of 'T-C>R-C', 'same' and 'T-C<R-C' responses in columns representing conditions of equal orientation difference between target and reference and rows representing conditions of equal orientation difference between target and context bar. If the orientation of the context bars had no effect on the perceived orientation of the target there should be a high proportion of 'T-C<R-C' responses when the orientation of the target was below that of the reference (columns to the left) and high proportion of 'T-C>R-C' responses when the target was at a higher orientation than the reference (columns on the right). I used this matrix of transformed responses to fit a biologically motivated model to the data (see section 1.6 *A simplified model for fitting*).

Before using the biologically motivated model I used a linear model to give a simple description of the data. For this fitting I first took the difference between proportions of 'T-C<R-C' and 'T-C>R-C' responses. The result could be between -1 and +1. Values around -1 indicated a high proportion of 'T-C<R-C' while values around +1 indicated a high proportion of 'T-C>R-C'. Values around 0 indicated either a high proportion of 'same' response or an equal proportion of 'T-C<R-C' and 'T-C>R-C'. I arranged these difference values into a matrix where columns of values relate to conditions of equal orientation difference between target and reference. Rows in the matrix relate to conditions of equal orientation difference between target and context. I represented the difference values as a colour coded 3D surface and fitted a 3D plane which was tilted in X and in Y dimensions (i.e. 2D regression). The plane was of the form:

$$P(x, y) = (S_x \times X) + (S_y \times Y) + C \quad \text{(Equation 1.1)}$$

where the 'X' dimension is the orientation difference between target and reference and the 'Y' dimension is the orientation difference between the target and context bar. 'S_x' is the slope along the target-to-reference dimension and 'S_y' is the slope along the target-to-context bar dimension. 'C' is the plane's offset. I fitted this plane to the matrix of difference values to minimise the summed squared error. I

assessed the goodness of fit by calculating the percentage of variance accounted for by the model (Carandini et al. 1997). Variance accounted for was calculated as:

$$\% \text{Variance} = 100 \times \left(1 - \frac{D(m,r)}{D(R,r)}\right) \quad (\text{Equation 1.2})$$

where ‘D(m,r)’ corresponds to the mean squared difference between the model predicted response (‘P(x,y)’, Equation 1.1), and the subject’s response ‘r’, at each combination of target and reference orientation. ‘D(R,r)’ corresponds to the mean squared difference between the grand mean response (‘R’, calculated across stimulus combinations) and the response to each stimulus separately. Thus ‘D(m,r)’ corresponds to the difference between the model prediction and the data and ‘D(R,r)’ corresponds to the variance of responses across stimulus combinations. I calculated D(m,r) and D(R,r) as:

$$D(m,r) = \frac{1}{N} \sum_s |m_s - r_s|^2, \quad (\text{Equation 1.3})$$

$$D(R,r) = \frac{1}{N} \sum_s |R - r_s|^2, \quad (\text{Equation 1.4})$$

In both cases the sum is over the range of target and reference combinations ‘s’; ‘N’ is the number of combinations.

1.4 Results

1.4.1 High contrast experiments.

From the pattern of responses in these experiments, it seemed that subjects perceived the target to be tilted further from context bar orientation than was the case (Figure 1.4 and 1.5). The orientation of the context bar therefore caused a repulsion of the perceived target orientation. This effect was evidenced by the high proportions of ‘clockwise’ responses when the target was counter-clockwise to the reference but clockwise from the context bars (Figure 1.4A, upper half of columns on the left), and high proportions of ‘counter-clockwise’ responses when the target was clockwise to

the reference but counter-clockwise to the context bars (Figure 1.4A lower half of columns on the right). When I transformed the data set (see Methods), I found high proportions of ‘T-C>R-C’ responses even when in reality orientation difference was T-C<R-C. The proportion of these misjudgments indicated the strength of the repulsion effect by the context bar orientation. The strength of the repulsion effect was dependent on two factors: the orientation difference between the target and context bars, and the allocation of voluntary attention. The repulsion effect was largest in conditions where there was a large orientation difference between the target and context bars (Figure 1.4A compare middle row with upper and lower rows, Figure 1.5A compare bottom row with upper rows). Directing voluntary attention away from the main task towards the colour counting task in the dual task condition generally boosted the magnitude of the effect (Figures 1.4B and 1.5B). Based on visual inspection of the data, the effect of the context was increased in all but two subjects (YL and DB) during the dual task condition. Subject DB showed little effect of the context in either the single or dual task condition. Subject YL showed no change in the size of the effect between the two conditions.

Example of raw data from high contrast experiment

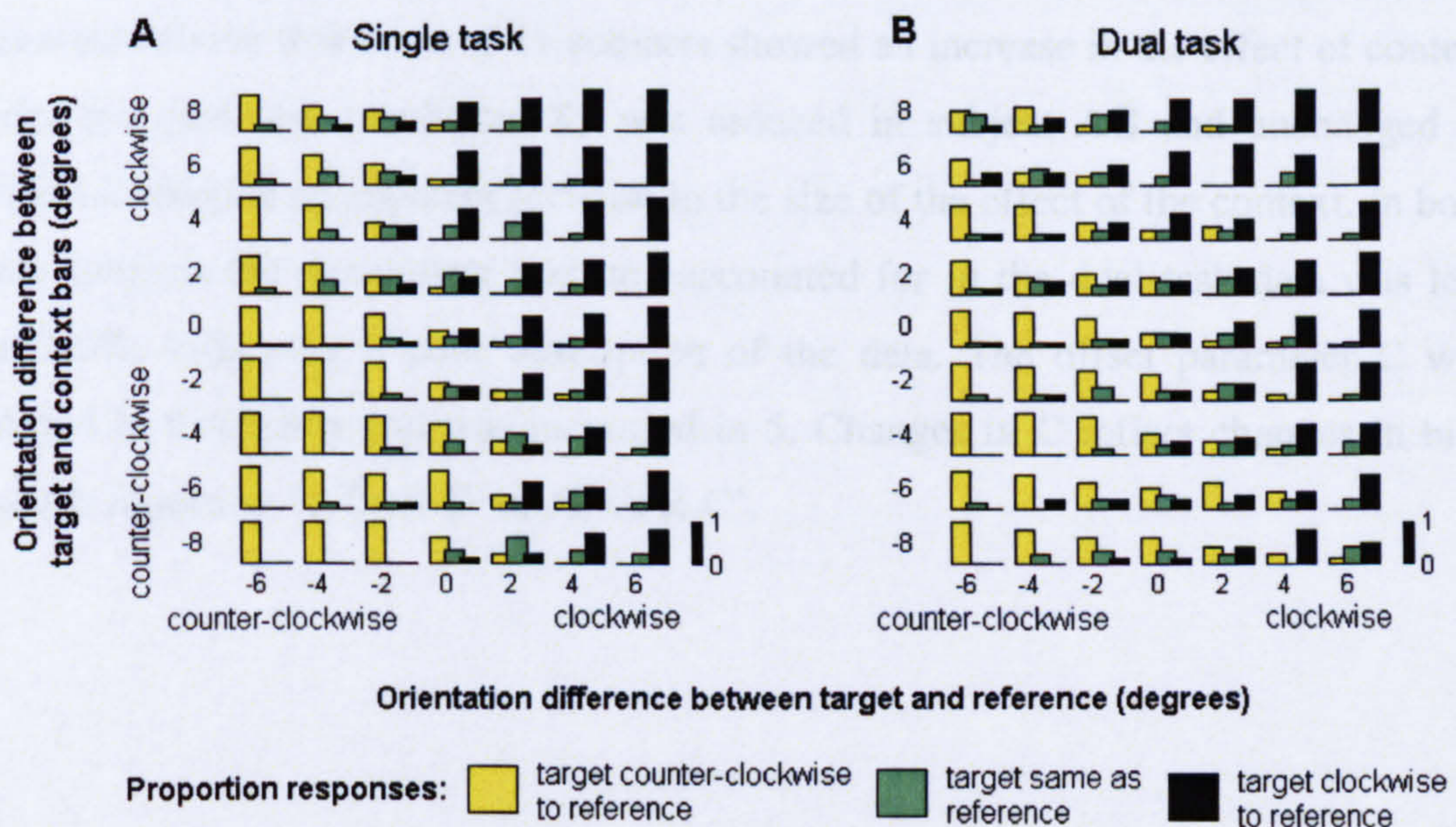


Figure 1.4 Example of a high contrast full data set. Data are arranged as in Figure 1.2 in which the orientation difference between the target and reference varies between columns and the orientation difference between the target and the context bars varies between rows. Negative axis values indicated a counter-clockwise difference and positive values indicate a clockwise difference. For each stimulus condition represented in Figure 1.2, there is a corresponding triplet of bars in this figure for both the single task condition (A) and the dual task condition (B). In each triplet the proportion of ‘counter-

clockwise' responses is shown by the height of the yellow bar, the proportion of 'target same as reference' is shown by the height of the green bar and the proportion of 'clockwise' is shown by the height of the black bar. The data shown are from one typical example subject (AT) in Experiment 2.

I took the difference between proportions of 'T-C>R-C' and 'T-C<R-C' responses and fitted this data with a 3-dimensional surface plane. The surface plane gave generally acceptable fits to the data, evident by a relatively high percentage of variance accounted for (see values in Table 1.1). Table 1.1 also shows the values of S_x (slope along target-to-reference dimension), S_y (slope along target-to-context dimension) and C (offset), fitted to single and dual task data for each subject. The most consistent change in fitting parameters between the single and dual task fits was a reduction in the parameter S_x (reduced in 8 out of 11 subjects, 3 subjects show an increase). This demonstrates a spreading-out of responses and reflects a reduction in the subjects' accuracy of orientation discrimination. Such a reduction could be due either to an increase in noise (subjects choosing responses at random) or an increase in the subjects' threshold for orientation discrimination (subjects more likely to report 'same'). The secondmost consistent change between the single and dual task condition was an increase in the parameter S_y (increased in 6 out of 11 subjects, 3 subjects show no change, 2 show a reduction). This increase reflects an increase in the effect of the context bar orientation on the perceived orientation of the target. It was stated above that 9 out of 11 subjects showed an increase in the effect of context under the dual task condition. S_y was reduced in subject AG and unchanged in subject JS despite an apparent increase in the size of the effect of the context. In both these subjects the percentage variance accounted for in the dual task data was less than 80%, indicating a poor description of the data. The offset parameter C was reduced in 6 subjects and was increased in 5. Changes in C reflect changes in bias towards reporting 'T-C<R-C' or 'T-C>R-C'.

Example of transformed data and fitted plane from high contrast experiment

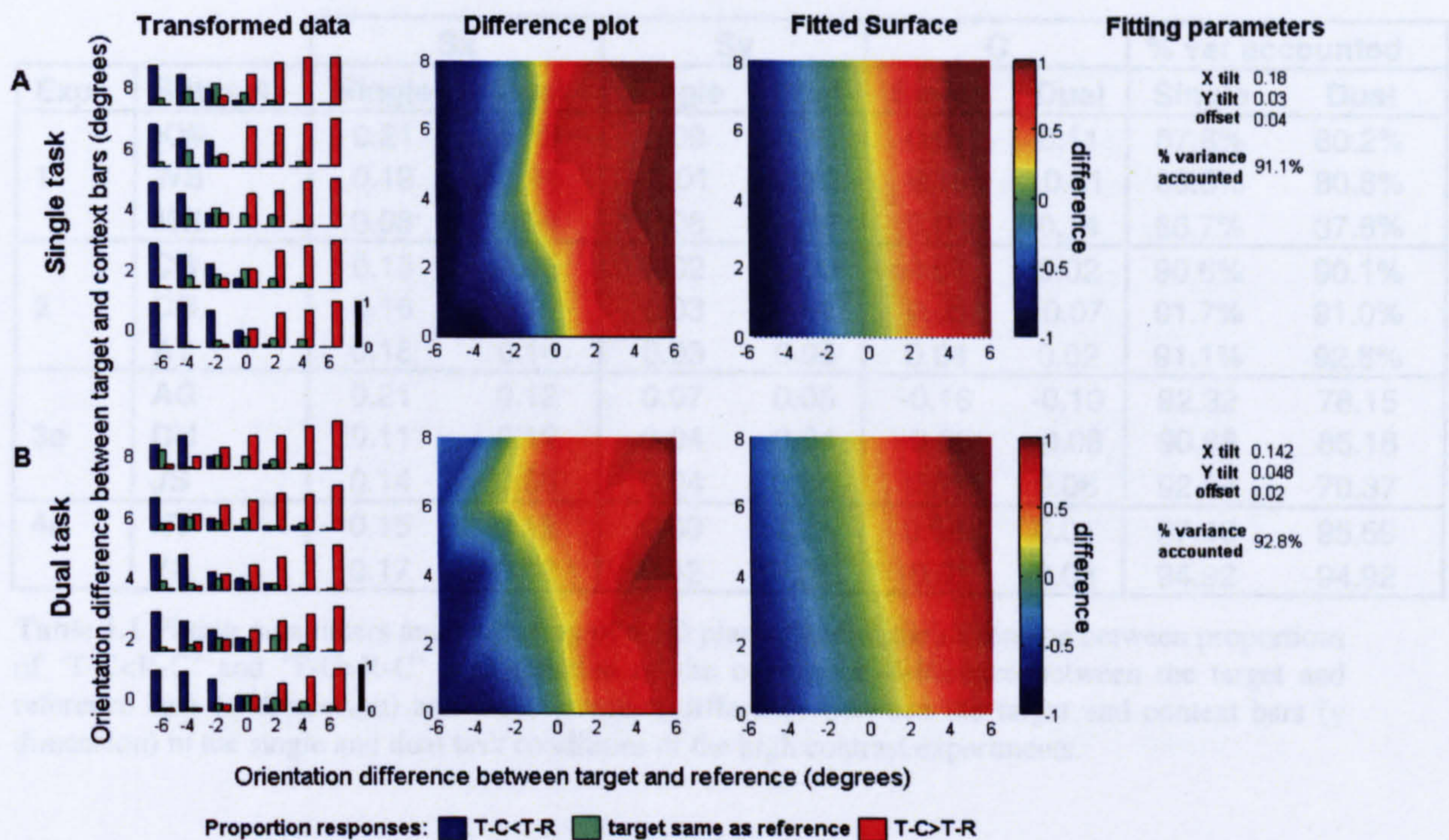


Figure 1.5 Example of transformed high contrast data set in the single task (A) and dual task (B) conditions. Left-hand column of plots ('transformed data') shows proportions of responses indicating either that the perceived orientation difference between the target and context bars was less than the perceived orientation difference between the reference and context bars (blue), or that the target was perceived to be oriented the same as the reference (green), or that the perceived orientation difference between the target and context bars was greater than the perceived orientation difference between the reference and context bars (red). Triplets of bars are arranged such that the orientation difference between target and context bar orientation changes along the y-axis and the orientation difference between target and reference changes along the x-axis. Negative values along the x-axis show that the target was presented tilted closer to the orientation of the context bars than the reference. Positive values on the x-axis show that the target was presented tilted further from the orientation of the context bars than the reference. The central plots (difference plot) show the difference between red and blue bars in the transformed data, plotted as a 3D colour surface. Values close to +1 (shown as red) indicate a high proportion of T-C > R-C responses. Values close to -1 (shown in blue) indicate high proportions of T-C < R-C responses. Values around 0 (shown in green) indicate either an equal proportion of T-C < R-C responses and T-C > R-C responses, or a high proportion of 'same' response. The right-hand column of plots (fitted surface) shows the 3D plane fitted to the difference plots. The tilt in X and in Y and the offset are given to the right of the plot. Data in the top row of plots are from the single task condition, and data on the bottom row are from the dual task condition. The data shown are from one typical example subject (AT) in Experiment 2.

2D regressing fitting parameters and fit quality from high contrast experiments

Exp	Subject	Sx		Sy		C		% var accounted	
		Single	Dual	Single	Dual	Single	Dual	Single	Dual
1	KW	0.21	0.19	0.09	0.13	0.07	0.11	87.8%	80.2%
	WS	0.19	0.21	-0.01	0.10	0.18	-0.01	88.6%	80.6%
	MR	0.08	0.04	0.08	0.09	0.08	0.14	66.7%	37.6%
2	CS	0.13	0.15	0.02	0.06	0.07	0.02	90.6%	90.1%
	DB	0.16	0.12	0.03	0.03	0.05	-0.07	91.7%	91.0%
	AT	0.18	0.14	0.03	0.05	0.04	0.02	91.1%	92.8%
3a	AG	0.21	0.12	0.07	0.05	-0.18	-0.10	92.32	78.15
	DH	0.11	0.12	0.04	0.04	-0.06	-0.08	90.88	85.18
	JS	0.14	0.06	0.04	0.04	0.01	0.08	92.24	70.37
4a	NT	0.15	0.12	0.00	0.01	0.06	0.01	97.46	95.59
	YL	0.17	0.12	0.02	0.01	-0.01	0.08	94.92	94.92

Table 1.1 Fitting parameters and fit quality of a 3D plane fitted to the difference between proportions of 'T-C<R-C' and 'T-C>R-C' as a function of the orientation difference between the target and reference bars (x dimension) and the orientation difference between the target and context bars (y dimension) in the single and dual task conditions of the high contrast experiments.

1.4.2 Low contrast experiments.

In these experiments the pattern of responses was reversed compared with high contrast experiments. That is, I found high proportions of 'counter-clockwise' responses when the target was presented clockwise to the context bars, and high proportions of 'clockwise' responses when the target was presented counter-clockwise to the context bars (Figures 1.6 and 1.7). This pattern indicates that the subjects perceived the target to be oriented closer to the orientation of the context bars than was the case. Thus, lowering the luminance contrast of the target reversed the repulsion effect seen in the high contrast experiments and caused the orientation of the context bars to have an attractor effect on the perceived orientation of the target (Figure 1.8). I tested whether subjects reliably perceived the target by including an additional 10% of trials in which the target was not presented. On these trials the subjects should report that the target was not presented. Two subjects (AG and JS) failed to make any 'no target' responses in the dual task condition (although subject AG performed adequately in the single task condition). Data from these subjects was therefore excluded from further analysis.

Example of raw data from low contrast experiment

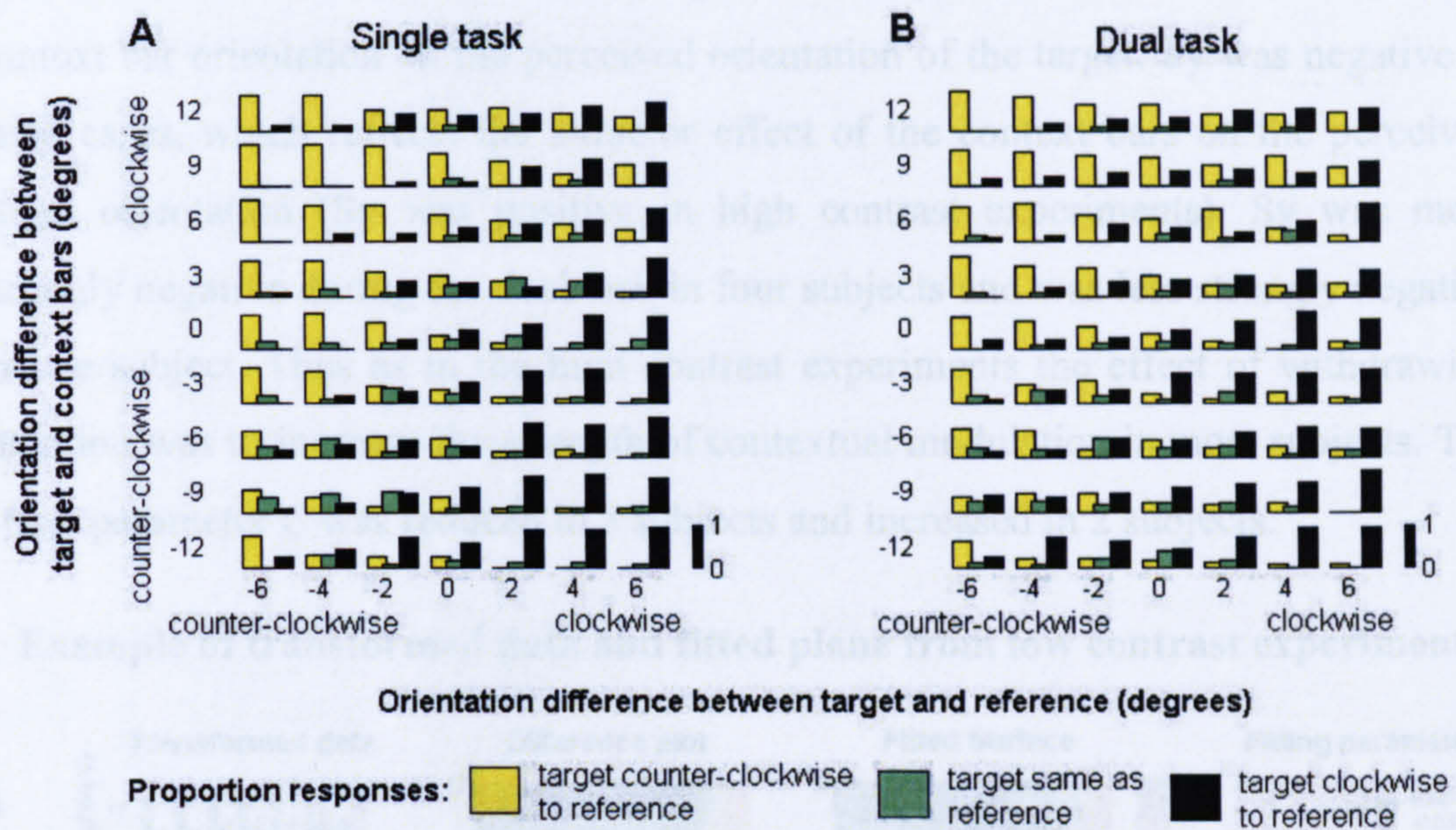


Figure 1.6 Example of a low contrast full data set. Data are shown in the same format as in Figure 1.4. The data shown are from one typical example subject (EA) in Experiment 4.

I transformed the data from the remaining subjects as described in section 1.3 *Methods* and found large proportions of ‘T-C<R-C’ responses, even in conditions when in reality the orientation difference was T-C>R-C (Figure 1.7). This pattern demonstrates that the context bar orientation had an attractor effect on the perceived orientation of the target. The strength of the attractor effect was dependent on the orientation difference between the target and context bars in the same way as it was in the high contrast experiments. That is, the effect was stronger at greater orientation differences between target and context bar. Attention also moderated the strength of the effect. In four subjects the effect of the context was clearly stronger in the dual task condition than in the single task condition. In one subject (YL) the effect was somewhat reduced in the dual task condition compared with the single task condition.

I took the difference between proportions of ‘T-C>R-C’ and ‘T-C<R-C’ responses and fitted the resulting data with a 3-dimensional surface plane (Figure 1.7) as used above. Table 1.2 shows fitting parameters from these fits from each subject in the single and dual task condition. As in the high contrast experiments there was a consistent reduction in S_x (reduced in all five subjects) in the dual task condition. A reduction in S_x reflects a reduction in the reliability of subjects’

responses. This could be due to increased noise, or a reduction in subjects' orientation discrimination acuity. The parameter S_y is related to the effect of the context bar orientation on the perceived orientation of the target. S_y was negative in most cases, which reflects the attractor effect of the context bars on the perceived target orientation (S_y was positive in high contrast experiments). S_y was more strongly negative during the dual task in four subjects and was less strongly negative in one subject. Thus as in the high contrast experiments the effect of withdrawing attention was to increase the strength of contextual modulation in most subjects. The offset parameter C was reduced in 3 subjects and increased in 2 subjects.

Example of transformed data and fitted plane from low contrast experiment

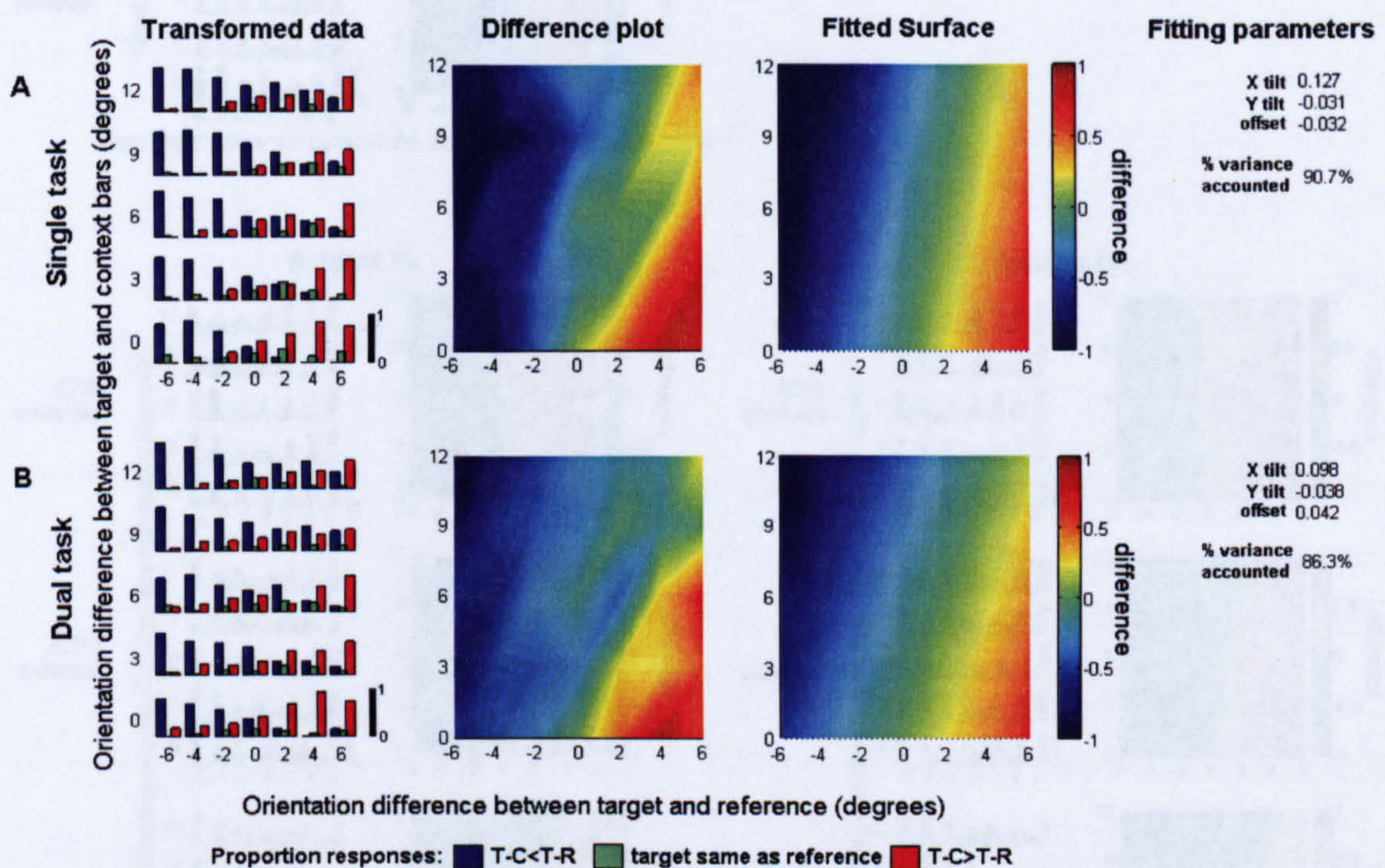


Figure 1.7 Example of a transformed low contrast data set in the single task (A) and dual task (B) conditions. The data are shown in the same format as in Figure 1.5. The data shown are from one typical example subject (EA) in Experiment 4.

Within-subject demonstration of contrast reversal effect

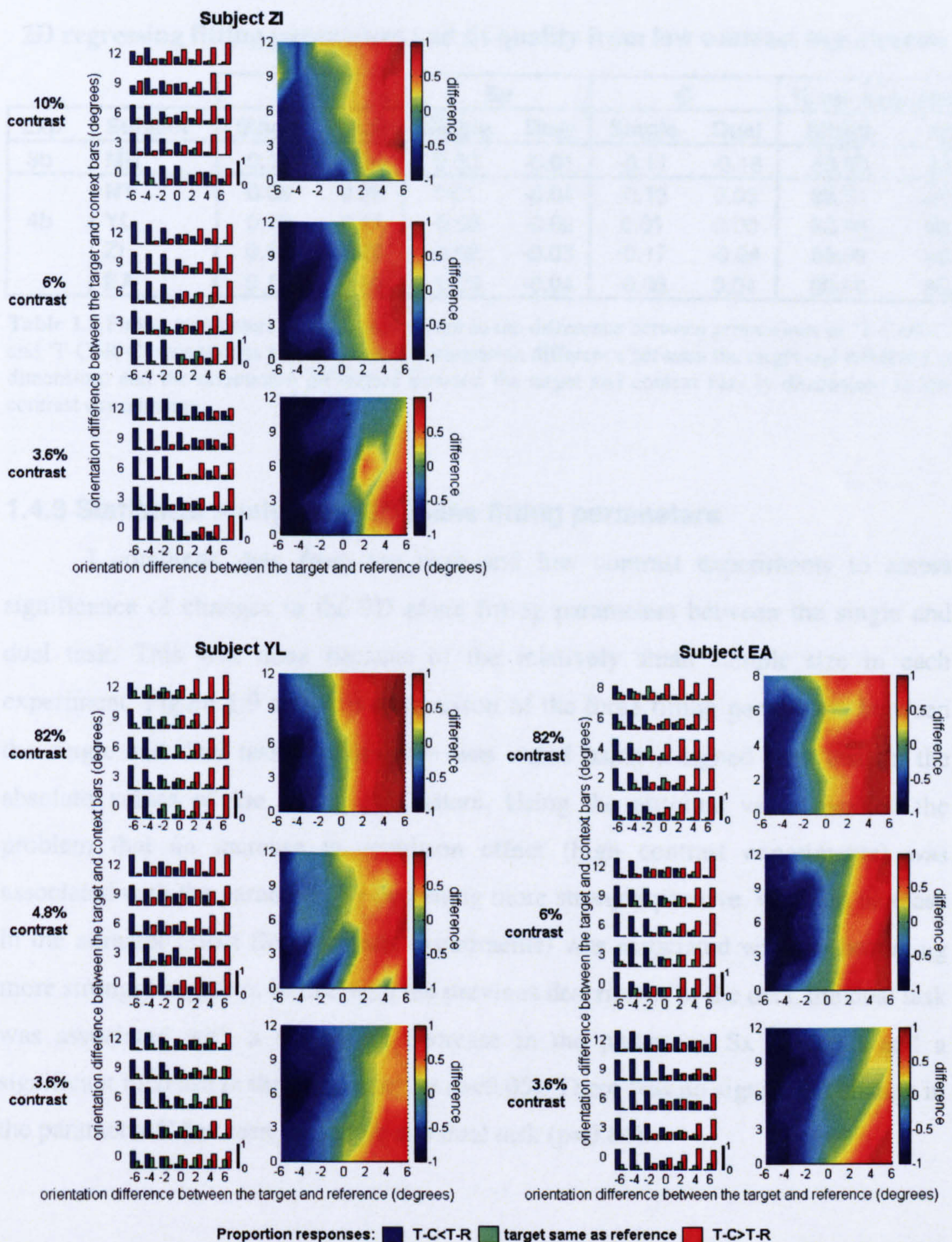


Figure 1.8 Three subjects were tested at three luminance contrasts (see row titles). Plots show transformed data and surface plots, arranged as in Figures 1.5 and 1.7. **Subject ZI)** At 10% contrast the data showed a repulsive effect typical of high contrast data, at 6% contrast no effect of the contrast bars was evident. At 3.6% the effect is of attraction to the context bars, typical of low contrast data. Each data point represents 20 trials per combination of target and reference orientations. **Subject YL)** high contrast data (82%, 40 trials per data point) demonstrates a typical repulsion effect. Using 4.5% contrast there was little effect of the context bars (20 trials per data point). At 3.6% a typical attractor effect was evident (40 trials per data point). **Subject EA)** High contrast data (82%) were obtained under Experiment 2 conditions, a repulsive effect was evident. At 6% contrast a weak attractor effect

was evident (Experiment 4, 20 trials per data point). At 3.6% the attractor effect was stronger (40 trials per data point).

2D regressing fitting parameters and fit quality from low contrast experiments

Exp	Subject	Sx		Sy		C		% var accounted	
		Single	Dual	Single	Dual	Single	Dual	Single	Dual
3b	MR	0.19	0.14	0.00	-0.01	-0.11	-0.18	83.59	80.24
4b	NT	0.08	0.08	0.01	-0.04	-0.13	0.03	89.51	90.87
	YL	0.13	0.11	-0.03	-0.02	0.01	0.00	93.48	93.45
	ZI	0.14	0.10	-0.02	-0.03	-0.17	-0.24	86.09	80.25
	EA	0.13	0.10	-0.03	-0.04	-0.03	0.04	90.66	86.32

Table 1.2 Fitting parameters of a 3D plane fitted to the difference between proportions of 'T-C<R-C' and 'T-C>R-C' response as a function of the orientation difference between the target and reference (x dimension) and the orientation difference between the target and context bars (y dimension) in low contrast experiments

1.4.3 Statistical analysis of 3D plane fitting parameters

I combined data from the high and low contrast experiments to assess significance of changes in the 3D plane fitting parameters between the single and dual task. This was done because of the relatively small sample size in each experiment. Figure 1.9 shows a comparison of the three fitting parameters between the single and dual task. Significance was tested using a signed rank test on the absolute values of the fitting parameters. Using the absolute value avoided the problem that an increase in repulsion effect (high contrast experiments) was associated with the parameter Sy becoming more strongly positive, while an increase in the attractor effect (low contrast experiments) was associated with Sy becoming more strongly negative. In line with the previous description of the data, the dual task was associated with a significant decrease in the parameter Sx ($p < 0.01$) and a significant increase in the parameter Sy ($p < 0.05$). There was no significant change in the parameter C between the single and dual task ($p = 0.84$).

Comparison of 3D plane fitting parameters between the single and dual task

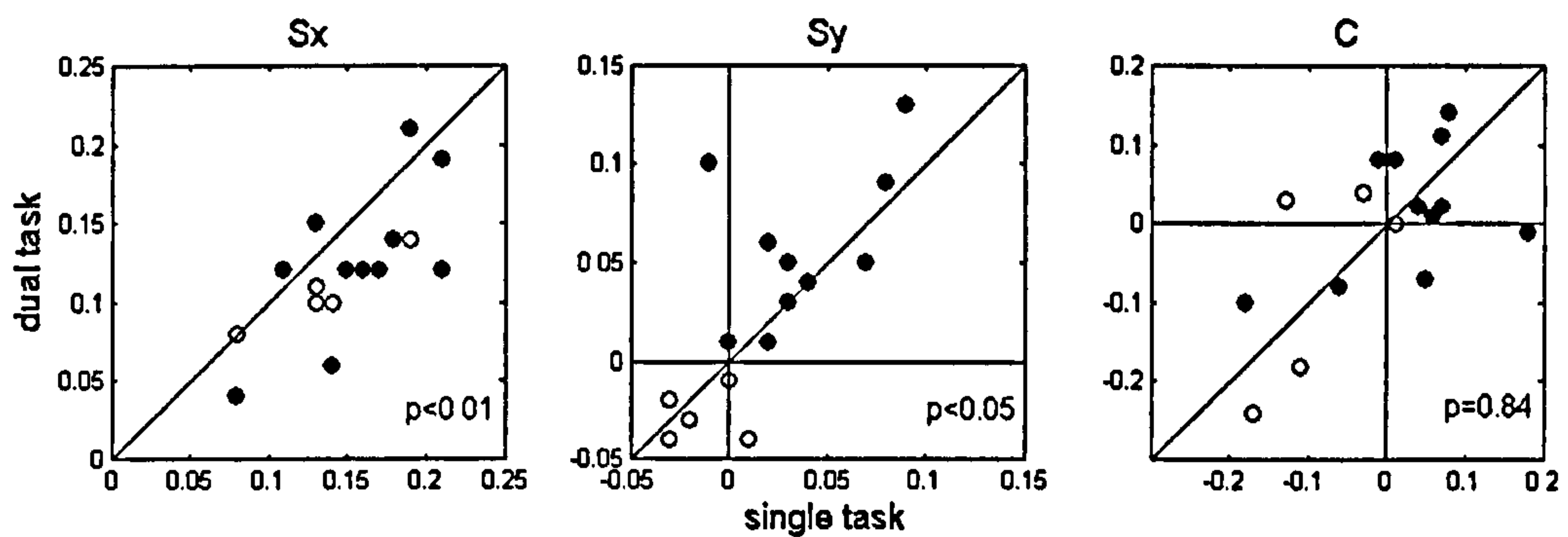


Figure 1.9 A comparison of the three fitting parameters from the 3D plane between the single and dual task. Data from high contrast experiments are marked by filled black circles, data from low contrast experiments are marked by open circles. At the lower right of each plot the significance of differences between the two task conditions is shown (signed rank test). Significance is calculated from the absolute values of data from both contrast conditions combined.

1.4.4 Testing subjects' sensitivity to the low contrast target

I tested whether the subjects reliably perceived the target by including an additional 10% of trials in which the target was not presented. On these trials the subjects should report that the target was not presented. Subject's performance at correctly identifying when the target was and was not presented is shown in Table 1.3. To calculate the subject's sensitivity to the target I calculated D prime (D') as:

$$D' = Z(\text{false alarm rate}) - Z(\text{hit rate}) \quad (\text{Equation 1.5})$$

where ' $Z(\text{hit rate})$ ' is the Z score for the proportion of trials in which the subject correctly identified the presence of the target. ' $Z(\text{false alarm rate})$ ' is the Z score for the proportion of trials in which the subject incorrectly reported that the target was presented. D' scores are presented in Table 1.3, calculated separately for the single and dual task conditions.

On average (median), subjects correctly identified that the target was not presented on 72% of trials in which the target was not presented (correct rejection rate 25th percentile = 39%, 75th percentile = 94%, chance performance = 10%). Subjects correctly identified that the target was presented (by making a 'clockwise', 'counter-clockwise' or 'same' response) on 96.5% of trials in which the target was presented (hit rate 25th percentile 85.5%, 75th percentile 99.0%, chance performance = 90%). Thus it seems that generally subjects could reliably perceive the target. Table 1.3 shows that subjects were poorer at correctly identifying the absence of the

target in the dual task than in the single task conditions (median drop in % of correct rejections = 41%, 25th percentile = 25.8% drop, 75th percentile = 47.5% drop). This is to be expected since it is known that the withdrawal of visual attention reduces contrast sensitivity (Reynolds et al. 2000; Zenger et al. 2000; Reynolds and Desimone 2003; Carrasco et al. 2004; Treue 2004; Huang and Dobkins 2005). However, subjects were also more likely to make an orientation response when the target had been presented (median percentage improvement in hit rate = 2%, 25th percentile = 0.1% improvement, 75th percentile = 4% improvement) suggesting that subjects may have been less willing to respond 'no target' in the dual task condition. I calculated D' as a true measure of the subject's sensitivity to the target unconfounded by their willingness to report 'no target'. D' was reduced in the dual task in all subjects in both conditions. The reduction in D' demonstrates that subjects were indeed less sensitive to the presence of the target in the dual task condition, potentially because of reduced contrast sensitivity in the near absence of attention.

Subject's ability to correctly discriminate target-absent/target-present trials

	Subject	hit rate	Miss rate	correct rejection rate	false alarm rate	Z hit rate	Z false alarm	D'
Single Task	MR	0.99	0.01	0.99	0.01	-2.33	2.33	4.66
	NT	0.87	0.13	0.92	0.08	-1.13	1.41	2.54
	YL	0.95	0.05	1.00	0.00	-1.64	>2.58	>4.93
	ZI	0.98	0.02	0.34	0.66	-2.05	-0.41	1.64
	EA	0.72	0.28	0.94	0.06	-0.58	1.55	2.13
Dual Task	MR	1.00	0.00	0.90	0.10	<-2.58	1.28	3.86
	NT	0.94	0.06	0.41	0.59	-1.64	-0.23	1.41
	YL	0.98	0.02	0.54	0.46	-2.05	0.1	2.15
	ZI	1.00	0.00	0.01	0.99	<-2.58	-2.33	>0.25
	EA	0.70	0.30	0.54	0.46	-0.52	0.1	0.62

Table 1.3 Measures of subjects' sensitivity to the target bar in the single and dual task conditions. *Hit rate* gives the proportion of trials in which the subject gave an orientation response (i.e. 'clockwise', 'counter-clockwise' or 'same') in trials when the target had been presented. *Miss rate* gives the proportion of trials in which the subject responded 'no target' although the target had been presented. *Correct rejection rate* gives the proportion of trials in which the subject correctly responded that the target had not been presented. *False alarm rate* gives the proportion of trials in which the subject gave an orientation response although the target had not been presented. D' prime (D') was calculated from the Z score of the hit rate and false alarm rate and gives a true measure of sensitivity. Z-scores can only be calculated for values greater than 0 and less than 1. For subjects with 100% hit rate I calculated the Z-score for 0.995, for subjects who scored no false alarms I calculated the Z-score for 0.005.

1.4.5 Investigating the consequence of missing the target

A significant concern in the low contrast experiments is that subjects may not have seen the target because of its low contrast, and then mistaken the final context bar for the target. If subjects made that mistake it would be no surprise that their responses appeared to reflect a target bar with an orientation closer to the context bar orientation than was the case. To investigate this possibility I examined the subjects' 'false alarm' responses. A false alarm is defined by the subject responding 'clockwise', 'counter-clockwise' or 'same' in a trial when no target was presented, thus it implies that the subject mistook some other stimulus as the target. The rate of false alarms therefore gives the probability of the subject mistaking some other stimulus (possibly the context bars) for the target. In trials where the target had not been presented the reference bar was presented at 0°, 1°, 2° and 3° above or below the context bar orientation in Experiment 3b and at 0°, 2°, 4° and 6° above or below the context bar orientation in Experiment 4b. Thus the distribution of reference orientations in trials with no target was the same as in trials where the orientation of the target matched the context bar orientation. If the subjects were comparing the reference to the context bar in trials with no target, then the orientation difference between the reference and context bars should be reflected in their responses. Moreover, if subjects were comparing the reference with the context bar even on trials where the target had been presented, the distribution of responses in the 'no target' trials should match the distribution of responses from conditions where the target had been presented with the same orientation as the context bar.

I compared the distribution of the subjects' 'clockwise', 'counter-clockwise' and 'same' responses from false alarm trials with the distribution of responses from trials in which the target had been presented with the same orientation as the context bar orientation. To quantify this comparison I calculated the difference between the proportion of 'clockwise' and 'counter-clockwise' responses and performed a robust linear regression analysis over the difference values across changing reference orientation. I then compared the slopes of the regression between the 'target presented' and 'target not presented' conditions. These comparisons are shown in Figure 1.10 for data where a sufficient number of false alarm responses were made. The figure shows that in some subjects the pattern of responses made when the target was not presented was similar to the pattern of responses subjects made when the target was presented (ZI and EA). This pattern indicates that these subjects may have

mistaken the context bars for the target. For other subjects responses occurred apparently at random (NT and YL), indicating that these probably did not compare the reference with the context bars.

The regression analysis shows that there was a trend for the slope of the difference values to be shallower when the target was not presented than when the target had been presented, even for subjects EA and ZI. This shows that subjects responded more reliably when the target was presented than when it was not. This difference shows that the target bar had a substantial contribution to the subject's response, thus it is likely that when the target was presented subjects responded to the target and not to the context bars. If the subjects usually responded to the context bars and ignored or did not see the target, then no change in slope would be expected (i.e. the presence or absence of the target would not affect the subject's behaviour).

Target responses in conditions where the target was not presented

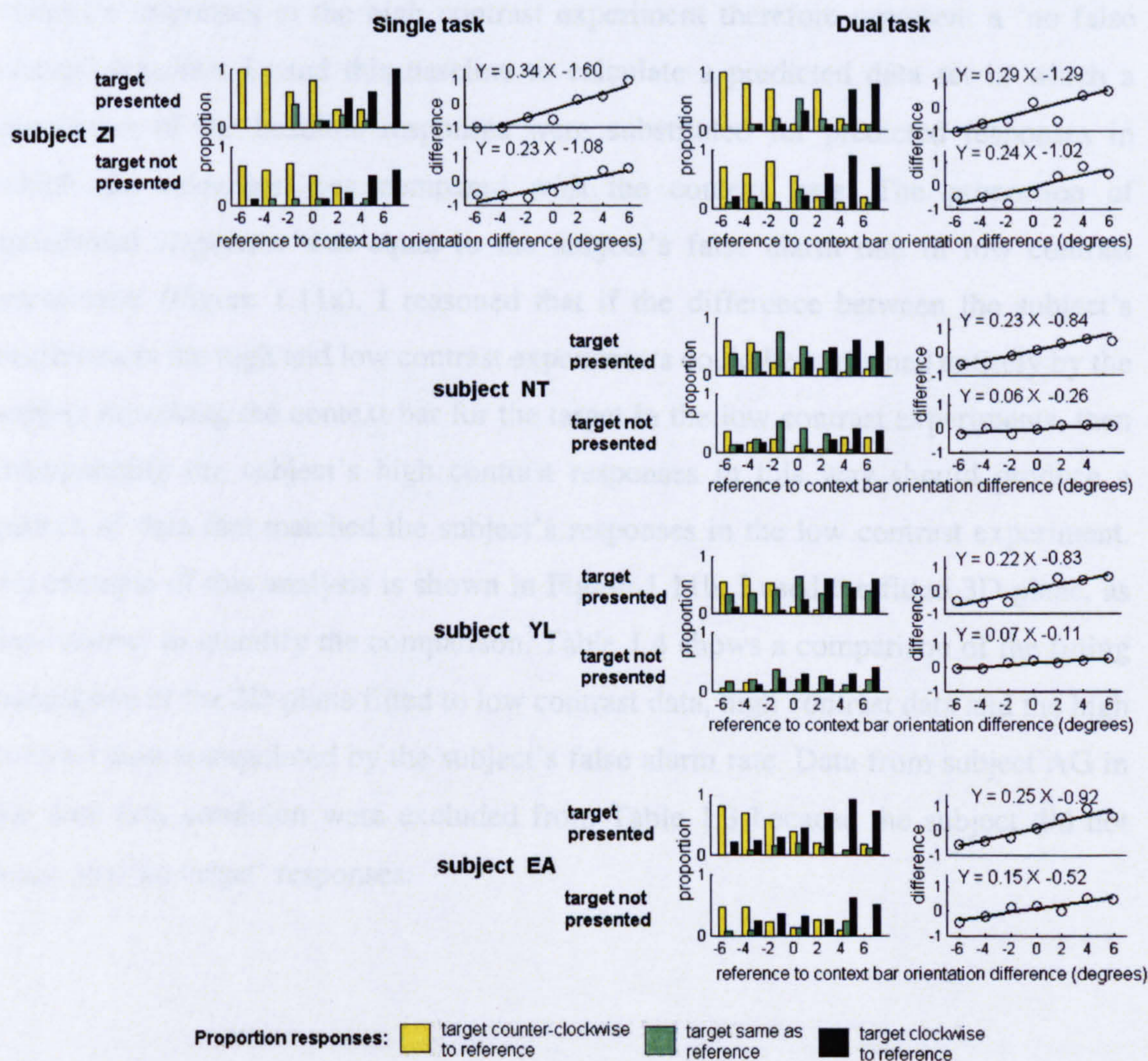


Figure 1.10 A comparison of proportions of 'clockwise', 'counter-clockwise' and 'same' responses from conditions where the target was presented with the same orientation as the context bars, and conditions where the target was not presented. Proportions of responses are shown in bar graphs. Values on the x-axis show the orientation difference between the reference and the target/context bars (degrees). Positive values indicate that the target/context was clockwise to the reference. Only data where subjects made a sufficient number of 'clockwise', 'counter-clockwise' or 'same' responses when the target was not presented are included in the figure. The difference between 'clockwise' and 'counter-clockwise' responses across orientation differences is plotted to the right of the bar graphs. Differences are between -1 and 1; positive values indicate a higher proportion of 'clockwise' responses, negative values indicate a higher proportion of 'counter-clockwise' responses. A regression line is fitted to the difference values. The function of the regression line, in the form $Y = \text{slope} * X - \text{offset}$, is displayed above the respective plot.

To investigate further to what extent the attractor effect in the low contrast experiments could be accounted for by subjects comparing the reference with the context bars rather than with the target bar, I used data from subjects who had participated in both the high and low contrast parts of the experiment. It may be assumed that the subject never (or very seldom) mistook the context bar for the target in the high contrast experiments because of the higher visibility of the target. The subject's responses in the high contrast experiment therefore represent a 'no false alarms' baseline. I used this baseline to calculate a predicted data set in which a proportion of the baseline responses were substituted for predicted responses in which the reference was compared with the context bars. The proportion of substituted responses was equal to the subject's false alarm rate in low contrast experiment (Figure 1.11a). I reasoned that if the difference between the subject's responses in the high and low contrast experiments could be explained entirely by the subject mistaking the context bar for the target in the low contrast experiments, then manipulating the subject's high contrast responses in this way should produce a pattern of data that matched the subject's responses in the low contrast experiment. An example of this analysis is shown in Figure 1.11b. I used the fitted 3D plane, as used above, to quantify the comparison. Table 1.4 shows a comparison of the fitting parameters of the 3D plane fitted to low contrast data, high contrast data and the high contrast data manipulated by the subject's false alarm rate. Data from subject AG in the dual task condition were excluded from Table 1.3 because the subject did not make any 'no target' responses.

Method for testing the proposal that the low contrast data may be explained by subjects missing the target

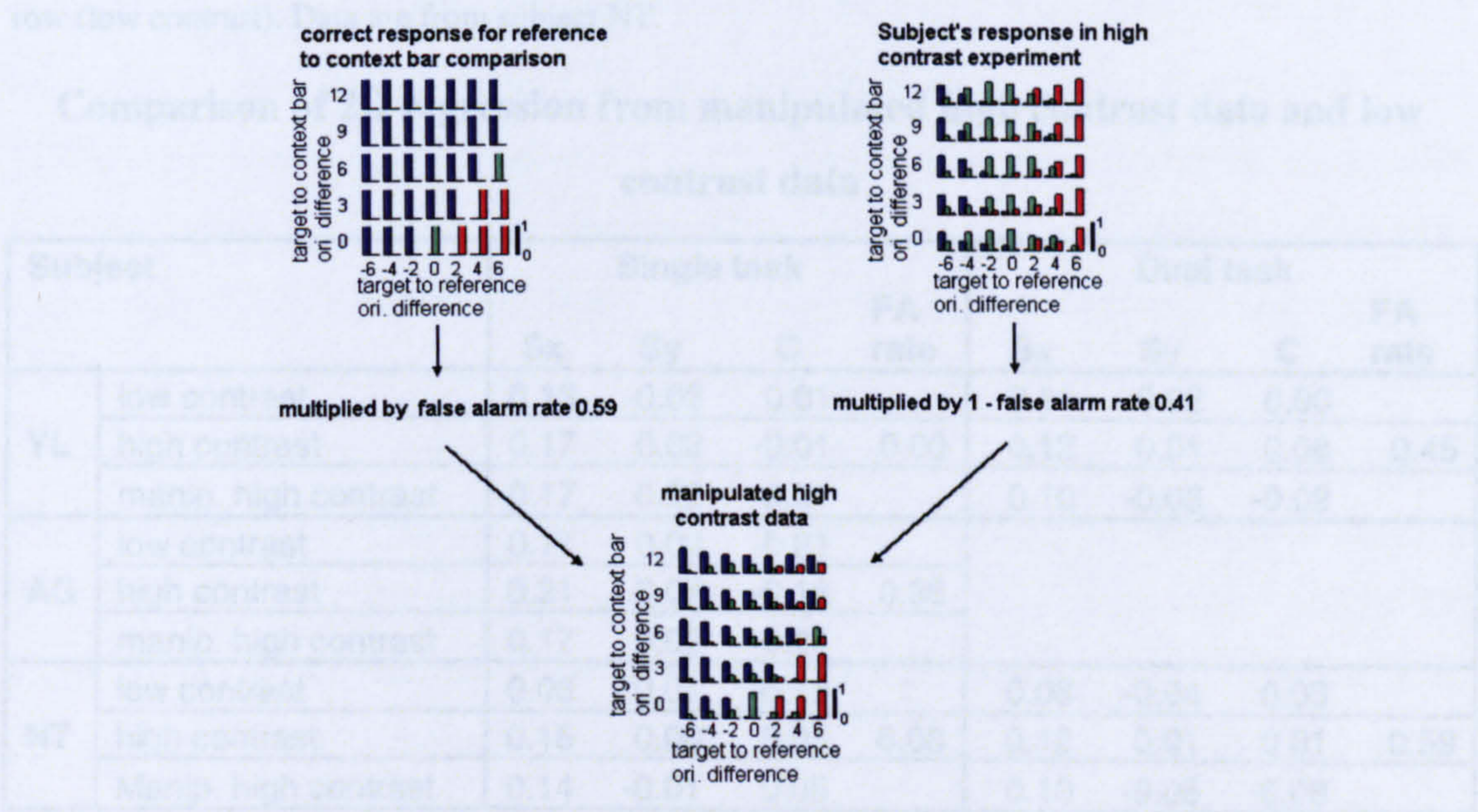


Figure 1.11a Illustration showing method by which high contrast data was combined with predicted responses had the subject compared the reference with the context bars rather than the target on a proportion of trials equal to the false alarm rate. Data shown are from subject NT in the dual task.

Example of comparison between manipulated high contrast data and low contrast data

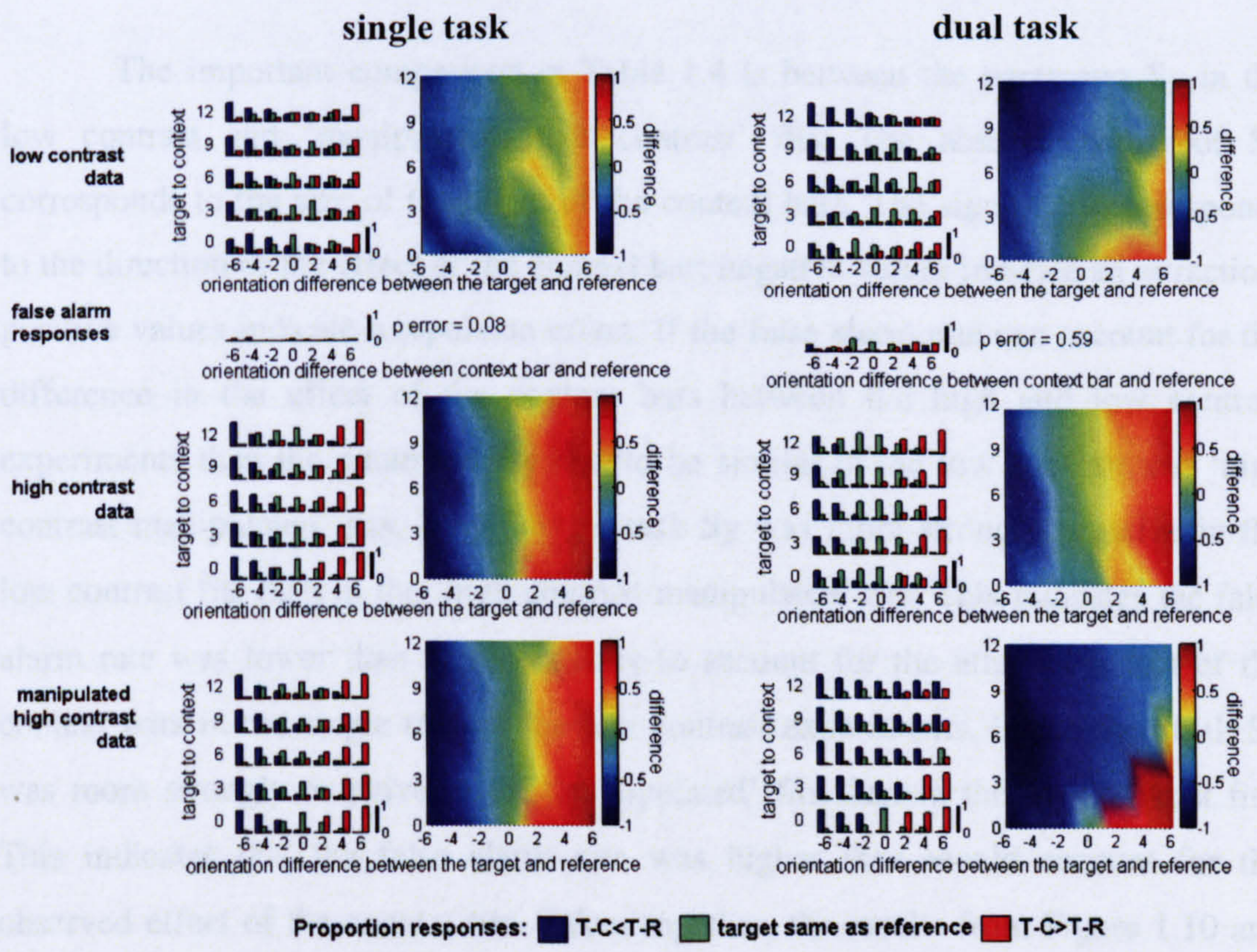


Figure 1.11b Example of combining high contrast data with predicted responses had the subject compared the reference with the context bars rather than the target on a proportion of trials equal to the false alarm rate. If the false alarm rate could explain the low contrast data, then the data shown on the bottom row of the figure (manipulated high contrast) should resemble the data shown on the top row (low contrast). Data are from subject NT.

Comparison of 2D regression from manipulated high contrast data and low contrast data

Subject		Single task				Dual task			
		Sx	Sy	C	FA rate	Sx	Sy	C	FA rate
YL	low contrast	0.13	-0.03	0.01		0.11	-0.02	0.00	
	high contrast	0.17	0.02	-0.01	0.00	0.12	0.01	0.08	0.45
	manip. high contrast	0.17	0.02	-0.01		0.10	-0.03	-0.02	
AG	low contrast	0.17	0.00	-0.21					
	high contrast	0.21	0.07	-0.18	0.36				
	manip. high contrast	0.17	0.02	-0.24					
NT	low contrast	0.08	0.01	-0.13		0.08	-0.04	0.03	
	high contrast	0.15	0.00	0.06	0.08	0.12	0.01	0.01	0.59
	Manip. high contrast	0.14	-0.01	0.05		0.10	-0.05	-0.08	

Table 1.4 Fitting parameters of a 3D plane fitted to the difference between proportions of 'T-C<R-C' and 'T-C>R-C' responses as a function of the orientation difference between the target and reference (x dimension) and the orientation difference between the target and context bars (y dimension). False alarm (FA) rate shows the proportion of trials where no target was presented but the subjects made a target response. This potentially indicates the probability of the subject mistaking the context bars for the target. Data are shown from three subjects who participated in high and low contrast experiments. The rows labelled 'manip. high contrast' refer to data from the high contrast experiment manipulated to simulate the subject mistaking the target for the context bar on the proportion of trials indicated by the false alarm rate.

The important comparison in Table 1.4 is between the parameter S_y in the low contrast and 'manipulated high contrast' fits. The absolute value of S_y corresponds to the size of the effect of the context bars. The sign of S_y corresponds to the direction of the effect of the context bar; negative values indicate an attraction; positive values indicate a repulsion effect. If the false alarm rate can account for the difference in the effect of the context bars between the high and low contrast experiments then the parameter S_y should be similar in the low contrast and 'high contrast manipulated' fits. In the single task S_y was more strongly negative in the low contrast fits than in the 'high contrast manipulated' fits. This indicates the false alarm rate was lower than was necessary to account for the attractor effect of the context bars in the single task of the low contrast experiments. In the dual task S_y was more strongly negative in the 'manipulated' fits than in the low contrast fits. This indicates that the false alarm rate was higher than would account for the observed effect of the context bar. Taken together, the results from Figure 1.10 and

Table 1.4 indicate that, in principal, the attractor effect of the context bars in the low contrast experiments could be partly explained by the subjects mistaking the context bars for the target, because subjects apparently did sometimes compare the reference with the context bars (Figure 1.10) and this error could cause an attractor effect (Table 1.4). However the magnitude of the observed effects of the context bar does not match the magnitude of the attractor effect which could be explained by the false alarm rate. This is especially true for the single task experiments. Here the false alarm rate was generally quite low indicating that subjects very rarely mistook the context bars for the target. Despite this, there is a robust attractor effect in most of the data, thus in the single task the attractor effect cannot be explained by mistaking the context bars for the target. It may be argued that the increase in the size of the effect is due to the increase in the false alarm rate. However there does not seem to be any direct correspondence between the size of the increase in the false alarm rate between the single and dual task and the size of the increase in the attractor effect (see Tables 1.2 and 1.3). For example, the false alarm rate of both subjects NT and YL were increased by ~50% (NT increase by 52%, YL by 46%) however subject NT demonstrates the strongest increase in the attractor effect between single and dual task (single task $S_y = 0.1$, dual task $S_y = -0.4$) while subject YL shows a slight reduction in the size of the attractor effect in the dual task (single task $S_y = -0.3$, dual task $S_y = -0.2$). Thus mistaking the context bar for the target, although potentially contributing to the attractor effect, does not suffice an explanation for the low contrast data.

1.4.6 No context bars control experiment

Two subjects participated in a control experiment in which no context bars were presented. Data from these two subjects is shown in Figure 1.12. Both subjects had participated in previous experiments and had demonstrated attractor effects at low contrast and repulsion effects at high contrast (EA high contrast data shown in Figure 1.8). The patterns of responses in the control experiment did not indicate any shift in the perceived orientation of the target. Thus, the data suggest that the effects on the perceived orientation of the target observed in the previous high and low contrast experiments were due to the presentation of the context bar and not due to some unknown confounding variable.

Transformed data set from 'no context bars' experiments

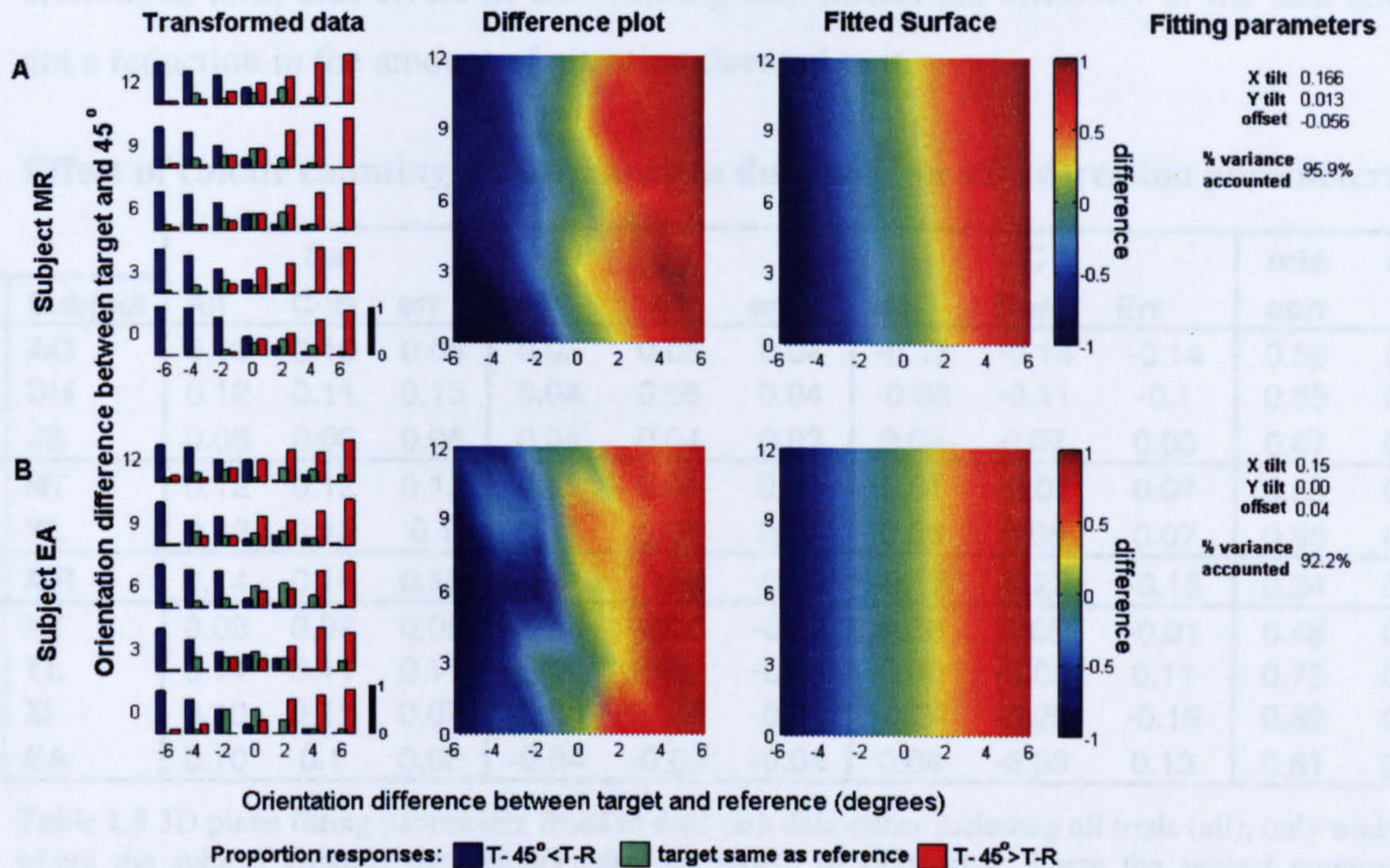


Figure 1.12 Two subjects (MR part A, EA part B) participated in the 'no context bars' control experiment. Stimuli were as in Experiment 4a but the context bars were not presented. Figure shows proportions of responses, the difference surface plots and the fitted 3D plane for each subject. Targets were presented above and below 45°. Each data point represents 20 trials per combination of target and reference orientations. Plots show transformed data, difference plots and 2D regression in the same format as Figure 1.5 and 1.7.

1.4.7 Colour counting performance

Colour counting performance was only recorded in Experiments 3 and 4. In these experiments, subjects were generally quite good at the colour counting task (25th percentile 54% correct, median 63% correct, 75th percentile 74% correct, chance performance = 25% correct). To investigate whether performance on the colour counting part of the task had an impact on the effect of the context bars, I separately analysed data from trials where the subject counted correctly and trials where the subject counted incorrectly. I quantified the size of the effect of the context bars using the 3D fitted plane routine as described previously. Table 1.4 shows the 3D plane fitting parameters fitted to the dual task data sorted to include all trials; only trials where the subject counted correctly and only trials where the subject counted incorrectly.

Sorting the data to only include trials where the subject counted correctly or incorrectly had no consistent effect on any of the fitting parameters. This suggests

that subjects did not switch between attending the counting task and attending the orientation task, thus errors in the counting task reflect the difficulty of the task and not a reduction in the amount of attention devoted to it.

Effect of colour counting performance in dual task on 2D regression parameters

Exp	Subject	Sx			Sy			C			rate	rate
		All	Corr	err	All	corr	err	all	Corr	Err	corr	err
3a	AG	0.12	0.10	0.08	0.05	0.05	0.04	-0.15	-0.14	-0.14	0.65	0.35
	DH	0.12	0.11	0.13	0.04	0.05	0.04	-0.08	-0.11	-0.1	0.53	0.47
	JS	0.06	0.06	0.06	0.04	0.04	0.03	0.08	0.07	0.05	0.87	0.13
4a	NT	0.12	0.12	0.13	0.01	0.01	0.01	0.01	-0.01	0.07	0.56	0.44
	YL	0.12	0.12	0.1	0.01	0.01	0.01	0.08	0.08	0.07	0.95	0.05
3b	MR	0.14	0.14	0.15	-0.01	-0.00	-0.01	-0.18	-0.22	-0.15	0.34	0.66
4b	NT	0.08	0.07	0.08	-0.04	-0.05	-0.03	0.03	0.05	-0.01	0.48	0.52
	YL	0.11	0.11	0.11	-0.02	-0.02	-0.04	0.00	-0.02	0.11	0.75	0.25
	ZI	0.10	0.11	0.07	-0.03	-0.03	-0.04	-0.24	-0.25	-0.15	0.69	0.31
	EA	0.10	0.1	0.08	-0.04	-0.03	-0.04	0.04	-0.03	0.13	0.61	0.39

Table 1.5 3D plane fitting parameters fitted to dual task data either including all trials (all), only trials where the subject counted the colours correctly (corr), or only trials where the subject counted incorrectly (err). The final two columns show the proportion of correct (rate correct) and proportion of incorrect (rate error) trials.

1.4.8 Results summary

The general finding from these experiments was that the orientation of the context bars influenced the perceived orientation of the target. The nature of the influence was dependent on the luminance contrast of the target. At high contrasts the perceived orientation difference between the target and context bar was enhanced, i.e. context bars had a repulsion effect. At low contrast the perceived orientation difference between the target and context bars was reduced, i.e. context bars had an attractor effect. The magnitude of the influence of the context bars was dependent on the orientation difference of the target from the context bars and on the allocation of voluntary attention. In the full attention condition the influence of the context bars was reduced compared with the divided attention condition. This supports the hypothesis that one function of voluntary attention is to attenuate the intracortical processing that gives rise to contextual modulation, and so to shift the balance of cortical processing in favour of feed-forward processing.

1.5 Biologically motivated model

In order to better understand how context affects the visual system's estimate of local features, as seen in the results, it is useful to create a model that relates perception to the properties of a neuronal ensemble. My model was principally based on the model proposed by Vogels (1990; also see Gilbert and Wiesel 1990) and works as follows.

1.5.1 Orientation tuning properties

Each unit in the ensemble had a Gaussian orientation tuning profile (Equation 1.6). The peaks of the unit's tuning profiles were evenly spaced between -90° and 90° (Figure 1.13 left).

$$R(O) = R \times (\exp(-(2 \times (O - O_p)/SD)^2)) \quad (\text{Equation 1.6})$$

where ' $R(O)$ ' is the mean response at orientation ' O ', ' O_p ' is the unit's preferred orientation, ' SD ' is the standard deviation of the tuning width and ' R ' is a normalisation constant determining the maximum response of the unit. I tested the model using a range of values for SD taken from my recent recordings in alert macaque V1 (Chapter 3). The results of these tests are shown in Figure 1.15. For simplicity there was no offset parameter, thus units did not respond to the null orientation. On a trial-to-trial basis, response variance was drawn from a Gaussian distribution with a standard deviation ' $Var(O)$ ' that was proportional to the response mean:

$$Var(O) = CV_{(slope)} \times R(O) + CV_{(offset)} \quad (\text{Equation 1.7})$$

where ' $CV_{(slope)}$ ' and ' $CV_{(offset)}$ ' are constants. I tested the model using a range of values of CV taken from my recent recordings in alert macaque V1 (Chapter 3). The results of these tests are shown in Figure 1.15. The response of each unit was represented as a 'labelled vector' pointing in the preferred orientation of the respective unit, and had a length proportional to the size of the response (Figure 1.13 right). The model's 'perceived orientation' was calculated as the vector sum of the population.

Vector model for orientation coding

Vector model for orientation coding

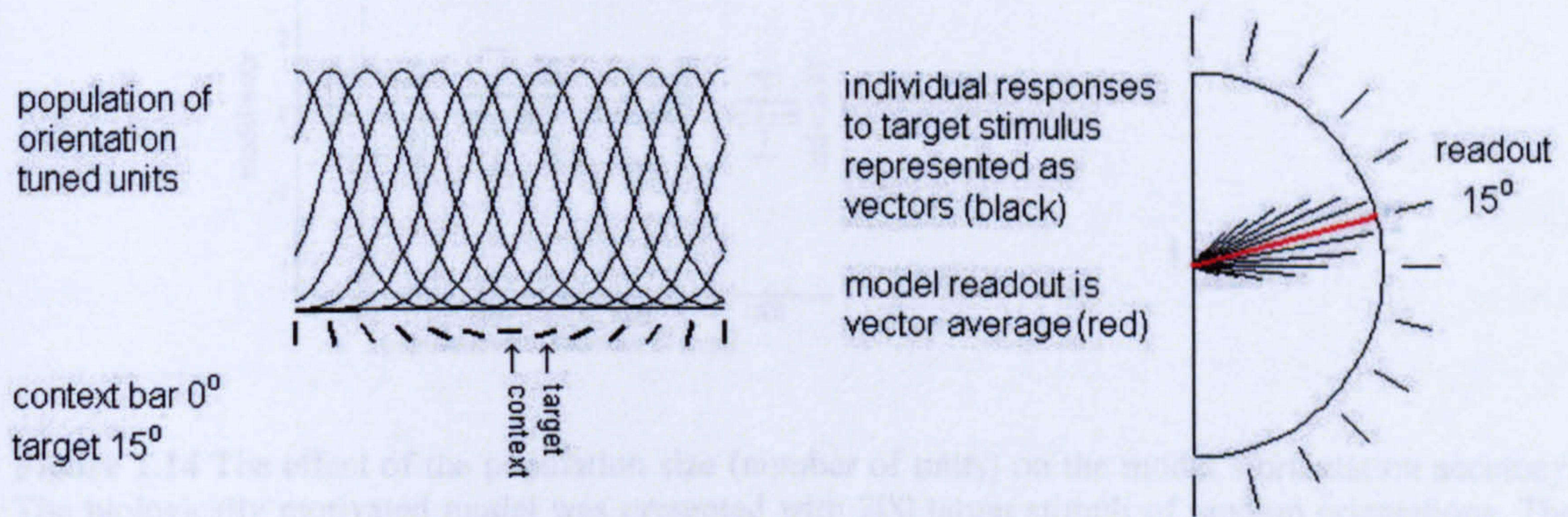


Figure 1.13 Vector model for orientation coding. The plot on the left shows the orientation tuning profiles of a selection of units from the population. These units have orientation preferences (peak of their tuning function) evenly spaced between -90° and 90° (orientation is represented below the x-axis). The plot on the right shows responses from individual units to a stimulus oriented at 15° . The length of each line (vector) inside the semi-circle shows the response from a single unit in the population. Each vector points away from the centre in the direction of the respective unit's preferred orientation. The red vector shows the orientation of the vector average over the population. This gives the model's readout (i.e. 'perceived orientation'). Since in this example response variance was set to 0, the vector average matches the orientation of the stimulus. With response variance above zero the readout would be equal to the true stimulus plus some random noise.

1.5.2 Orientation coding accuracy

Vogels (1990) tested the orientation coding accuracy of his model in relation to human performance. He took the typical human performance as having a mean error of 0° and a standard deviation of $\pm 0.5^\circ$ in reporting the orientation of a stimulus (when measured over 200 trials). Vogels suggested that a population of just 100 units, with orientation tuning properties similar to the units in my model, was sufficient to have an accuracy of orientation coding that was equivalent to human psychophysical performance. When testing my model I found that a population of 100 units was insufficient to produce the same level of orientation coding accuracy as reported by Vogels (1990). For this level of accuracy I found that a population of 1000 neurons was necessary (Figure 1.14). The difference between my model and the model by Vogels is likely to be due to different values for orientation tuning bandwidth (SD, Equation 1.5). Vogels found that 100 units were sufficient when using a bandwidth of 23.6° or 10.6° , values taken from two cells recorded in V1. These values are substantially lower even than the 25th percentile of the distribution I found in V1 (Figure 1.15). In my model I found that 100 units gave adequate performance when I reduced values of SD to similar levels.

The effect of population size on orientation tuning accuracy

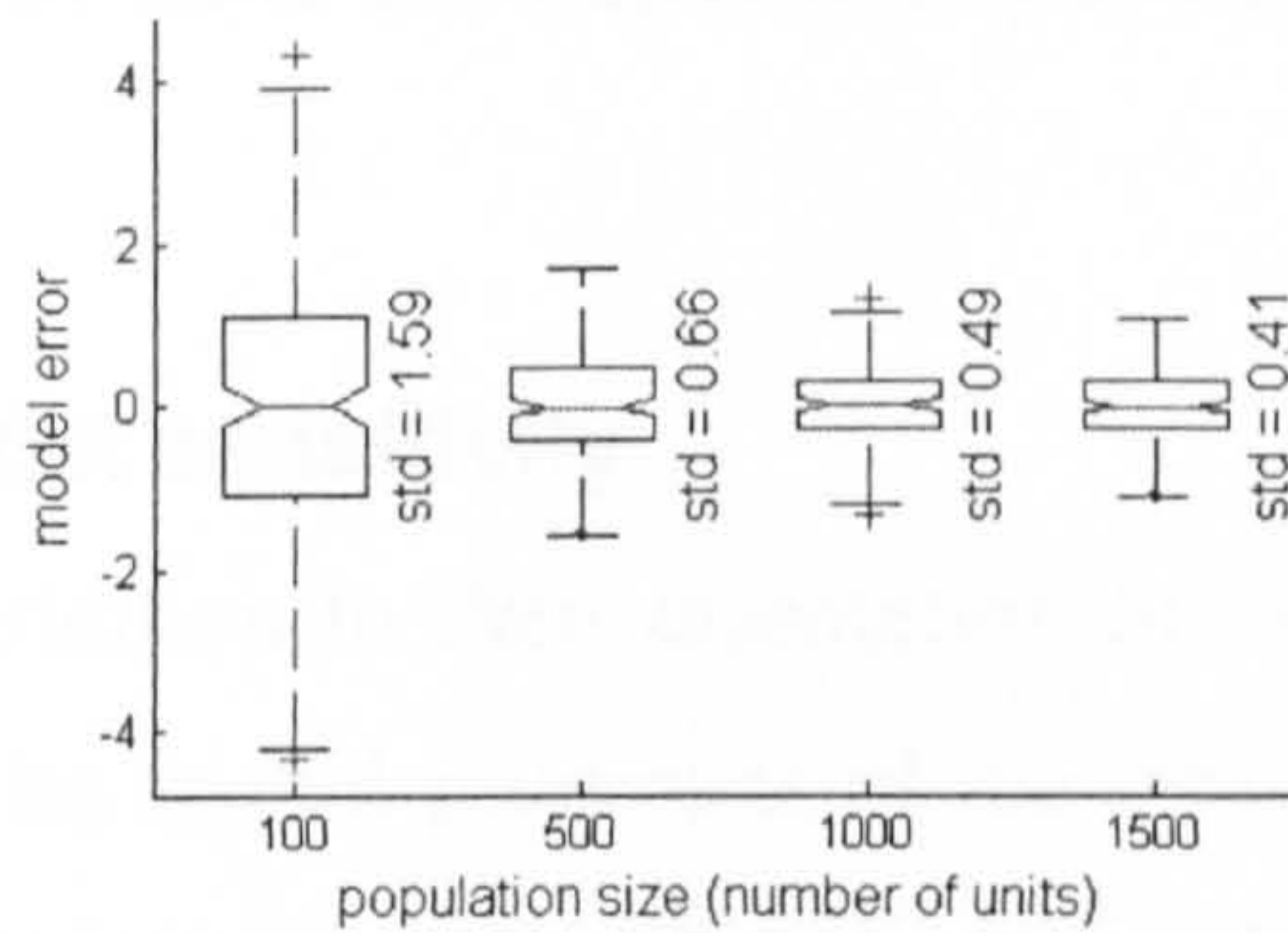


Figure 1.14 The effect of the population size (number of units) on the model's orientation accuracy. The biologically motivated model was presented with 200 target stimuli of random orientations. The model's error was calculated as the difference between the model's output and the presented stimulus. The context bar was not presented. The plot shows box plots (median, upper and lower percentiles, whiskers show the extent of the rest of the data, outliers are marked with a + symbol) of the distribution of errors over 200 trials, the standard deviation (std) is given adjacent to each box plot. I tested the model with a population size of 100 units, 500 units, 1000 units and 1500 units. Values of the variance constants $CV_{(\text{slope})}$ and $CV_{(\text{offset})}$ (Equation 1.7) and the units' orientation tuning bandwidth (SD, Equation 1.6) were set at the median value calculated from V1 recordings.

The effect of model neuron response variance and orientation tuning bandwidth on orientation coding accuracy

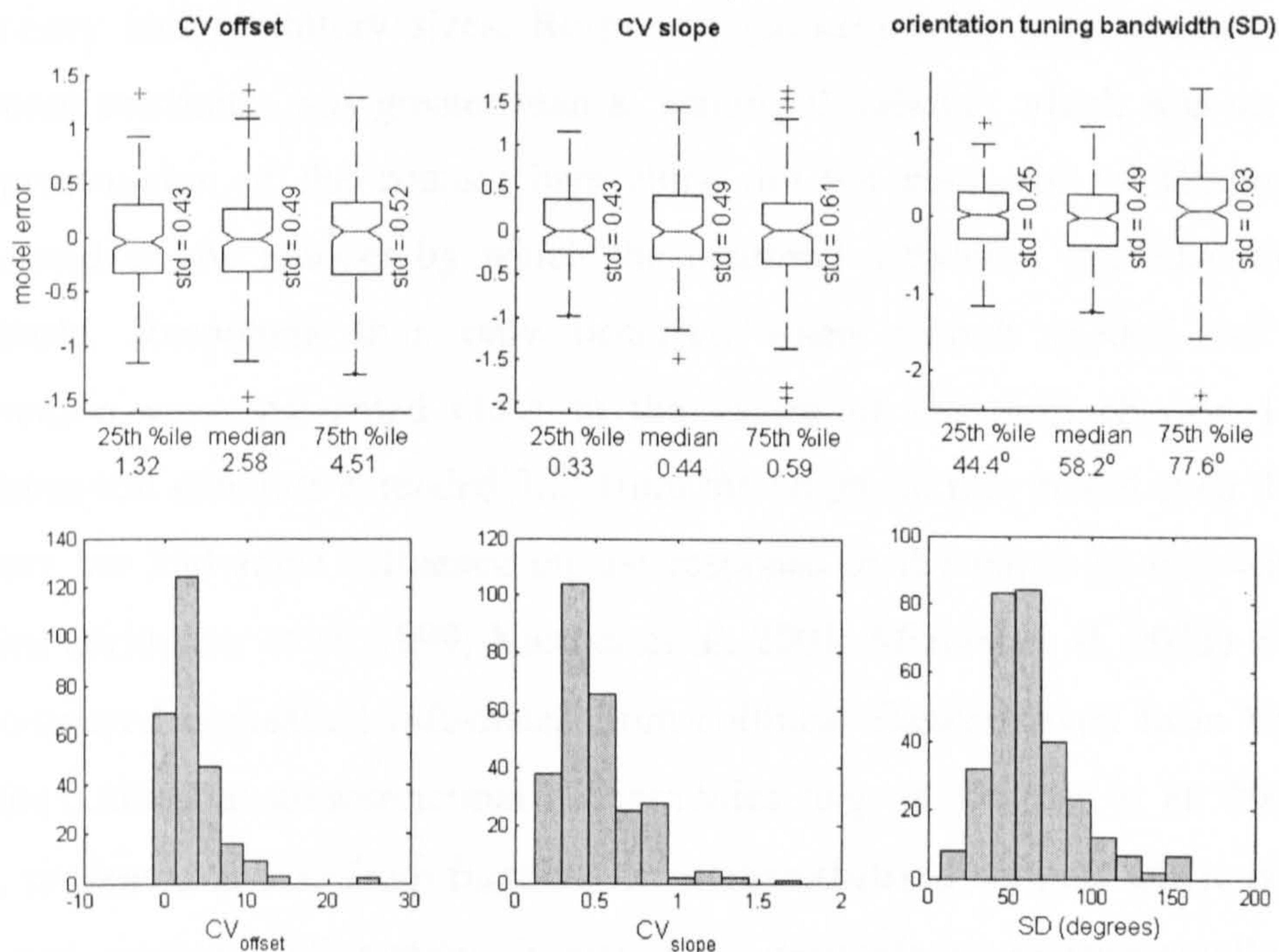


Figure 1.15 The effect of response variance (controlled by parameters $CV_{(\text{slope})}$ and $CV_{(\text{offset})}$) and orientation tuning bandwidth (SD) on the biologically motivated model's orientation accuracy. The model was presented with a set of 200 target stimuli of random orientations. The model's output was compared with the input and the error calculated. Upper row shows boxplots of the model's error over 200 trials; the standard deviation (std) is given adjacent to each boxplot. I calculated realistic values of the three parameters from neuronal recordings taken in V1 of alert primates. Lower plots show the

distribution of each parameter across ~150 cells. I tested the model's orientation accuracy using the median and upper and lower quartiles of each parameter. When varying one parameter the other two parameters were set to their respective median values. The model population size was set to 1000 units.

1.5.3 Spatial sensitivity

In addition to their orientation tuning properties, model units were spatially sensitive. The spatial properties of the units was based on a difference of Gaussians function (DeAngelis et al. 1994; Kapadia et al. 1999; Sceniak et al. 1999; Cavanaugh et al. 2002). This function was derived by the linear combination of a narrow excitatory Gaussian and a wide inhibitory Gaussian and is of the form:

$$R(OX) = R(O) \times \left(\left(K_e \times \left(\exp\left(-\left(\frac{2 \times X}{T_1}\right)^2\right)\right) \right) - \left(K_i \times \left(\exp\left(-\left(\frac{2 \times X}{T_2}\right)^2\right)\right) \right) \right) \quad (\text{Equation 1.8})$$

where 'R(OX)' is the neuronal activation caused by the presentation of a stimulus of orientation 'O' (Equation 1.6) at location 'X'. 'Ke' and 'Ki' respectively are the excitatory and inhibitory gains and 'T1' and 'T2' respectively are the excitatory and inhibitory sizes. Responses (spikes) were only counted when the neuronal activation was greater than a 'spiking threshold', which was set such that the presentation of the context bars alone did not elicit spikes. Responses were calculated as the amount by which the neuronal activation exceeded the spiking threshold. Responses thus only occurred when stimuli around the preferred orientation were presented close to the centre of the field (Figure 1.16). The experimental stimulus extended 3.2° from the target. In this model even the furthest context bar had some influence on the response to the target in line with several studies (Bringuier et al. 1999; Kastner et al. 2001; Mizobe et al. 2001) which have demonstrated contextual influences from collinear flankers even from beyond 10° distance, albeit at greater retinal eccentricities (e.g. in Kastner et al. 2001 stimuli were presented at 5.5° from fixation) or in anaesthetised animals where eccentricity was not assessed. Ultimately, it would be desirable to experimentally assess a realistic estimate of the area over which contextual influences occur, by varying the number of context bars and assessing their influence.

Example of model neuron's orientation tuning and spatial sensitivity profile

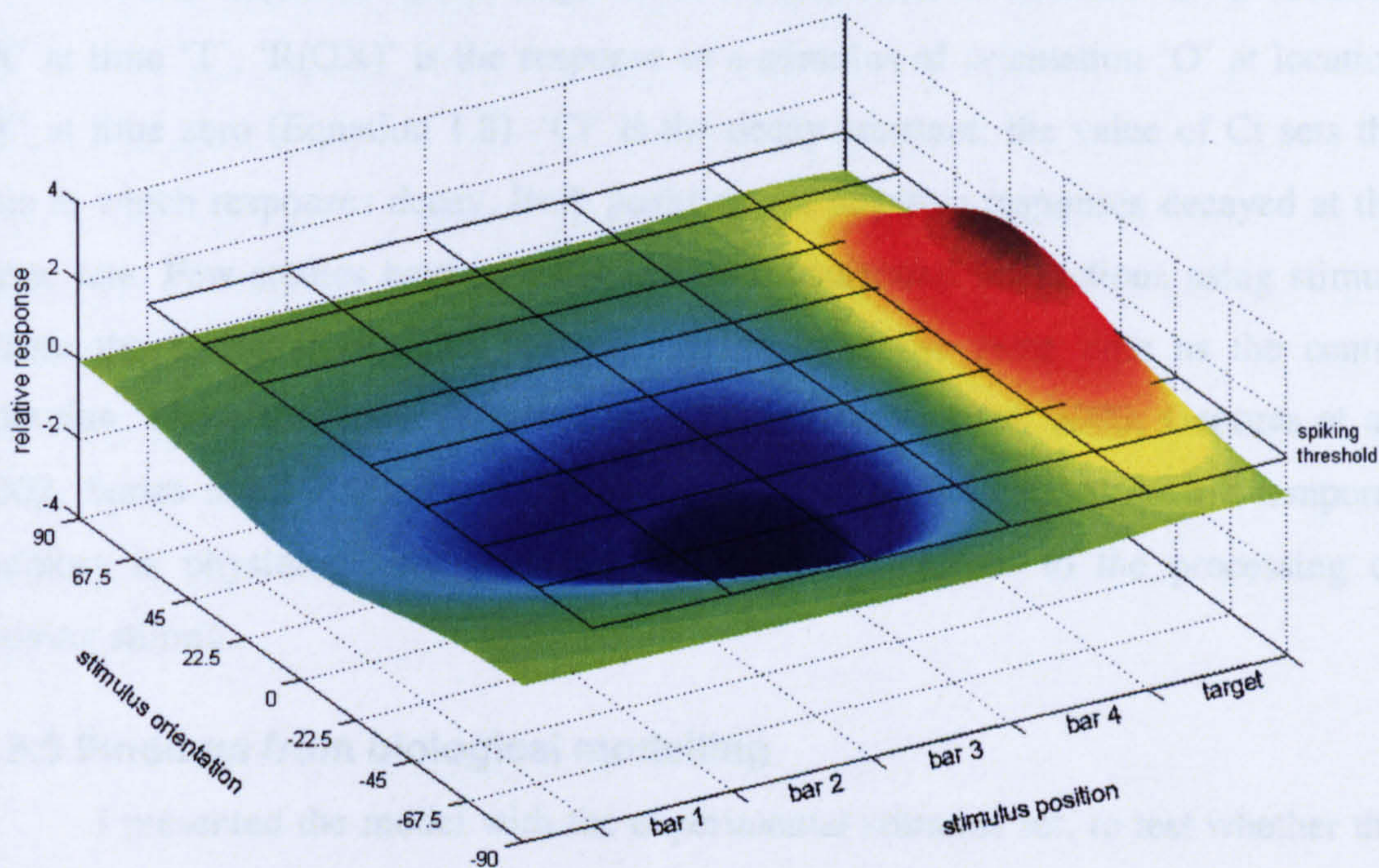


Figure 1.16 Orientation selectivity and spatial sensitivity of model neurons. The neuronal activation caused by the presentation of a stimulus is given by the height of the coloured surface at the relevant stimulus position and orientation. Neuronal activation may be either positive (red) or negative (blue). Whilst neuronal activation can occur in response to the presentation of a stimulus of almost any orientation and at almost any location, spikes are only generated when the level of activation exceeds the spiking threshold (solid black grid), hence this cell only has a spiking response to stimuli oriented away from the null orientation, presented in the target location.

1.5.4 Temporal integration

An important addition to the model was the inclusion of a temporal component, in the form of a decay function for neuronal activation. The effect of this function was to allow the activation caused by the presentation of a stimulus to continue for some time after the stimulus had been extinguished, giving the model a ‘temporal leaky memory’. Hence when the response to the dynamic experimental stimulus was modelled, the activation caused by the presentation of the first context bar could influence the response to the target, even though the presentation of the two stimuli were separated by 640 milliseconds. The decay of the response was modelled by an exponential function. The form of the exponential decay function was:

$$R(\text{OXT}) = R(\text{OX}) \times \exp\left(-\frac{T}{Ct}\right) \quad (\text{Equation 1.9})$$

where 'R(OXT)' is the response to a stimulus of orientation 'O' at location 'X' at time 'T', 'R(OX)' is the response to a stimulus of orientation 'O' at location 'X' at time zero (Equation 1.8). 'Ct' is the decay constant; the value of Ct sets the rate at which responses decay. Both positive and negative responses decayed at the same rate. Few studies have investigated centre/surround interactions using stimuli where the surround stimulus was not presented at the same time as the centre stimulus. Those that have (Westheimer 1990; Chavane et al. 2000; Georges et al. 2002; Series et al. 2002; Jancke et al. 2004) have suggested that such a temporal memory is physiologically plausible, and may be relevant to the processing of moving stimuli.

1.5.5 Findings from biological modelling

I presented the model with the experimental stimulus set, to test whether the model's 'perception' of the target orientation would be influenced by the context bars in the same way as human observers. By independently varying the model's parameters I tested which parameters were critical in determining whether the model reported the target orientation to be closer to the orientation of the context bars (attractor effect) or further from it (repulsion effect). I also tested which parameters could mediate the enhancement of both the repulsion effect and the attractor effect of the context bars that I observed in the dual task paradigm.

The general finding from my modelling was that when the net response to the context bars was negative, and therefore inhibited the response to the target, the model reported that the target orientation was further from the orientation of the context bars than was the case. This finding was consistent with the repulsion effect I observed in high contrast experiments. The reason for this shift in the model's perceived target orientation was that units tuned close to the context bar orientation were inhibited more strongly than units tuned further from the context bar orientation. This was because orientation tuning preference was the same at all points in the spatial sensitivity profile (Figure 1.15). Thus, when the context bars caused inhibition of the response, the vector average shifted away from the context bar orientation (Figure 1.17, centre). By changing the spatial summation parameters or the temporal decay constant, the net surround response to the context bars could become positive and thus facilitate the response to the target. Under these conditions

the model reported that the target orientation was closer to the orientation of the context bars than was the case, due to a larger facilitation of vectors pointing towards the context bar orientation than vectors pointing in other orientations, causing the vector average to move towards the context bar orientation (Figure 1.17, right). This pattern was consistent with the attractor effect that I observed in low contrast experiments. Thus my modelling suggested that the context bars caused inhibition when the target was presented at high contrast but caused facilitation when the target was presented at low contrast. Just such contrast-dependent switching of surround modulation from inhibition at high target contrast to facilitation at low target contrast, has been observed electrophysiologically (Levitt and Lund 1997; Polat et al. 1998; Mizobe et al. 2001).

Surround inhibition and facilitation in the vector model

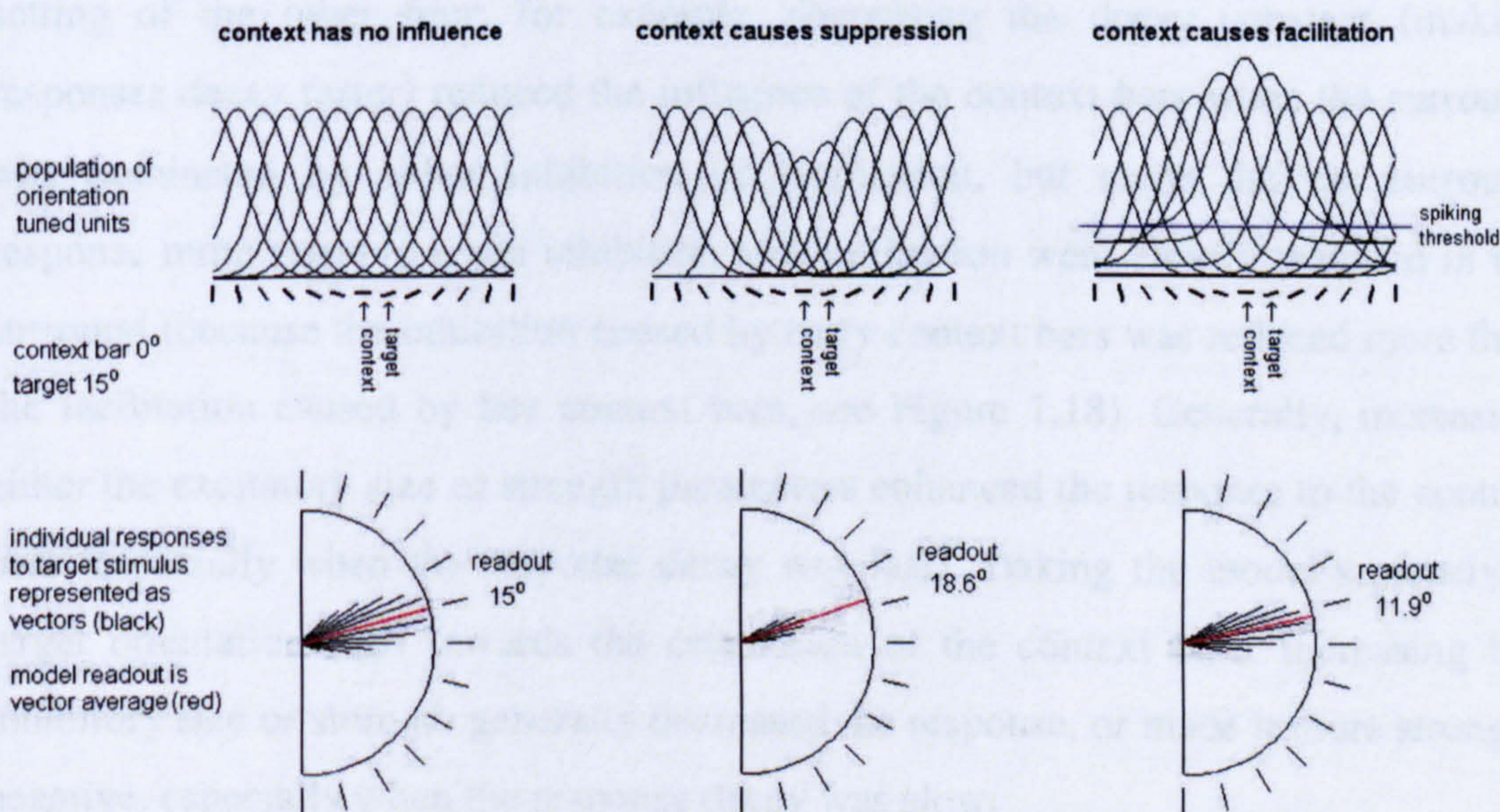


Figure 1.17 Vector model used to investigate the effect of context on the orientation coding of an ensemble of model neurons. Plots along the top row show the orientation tuning profiles of a selection of units from the population. These units have orientation preferences (peak of their tuning function) evenly spaced between -90° and 90° (orientation is represented below the x-axis). In the first column (context has no influence) all units in the population have identical tuning profiles. In the second column (context causes suppression) units whose orientation preference is close to the orientation of the context bar (here 0°) are suppressed more strongly than units whose orientation preference is far from the orientation of the context bar. In the final column (context causes facilitation) units tuned close to the orientation of the context are facilitated more than units tuned far from the orientation of the context. In this column a 'spiking threshold' has been imposed which ensures that units do not respond to the context alone. Only the parts of a unit's orientation tuning profile above the spiking threshold count towards the population vector. Plots along the bottom row show responses from individual units to a stimulus oriented at 15° . The length of each line (vector) inside the semi-circle

shows the response from a single unit in the population. Each vector points away from the centre in the direction of the respective unit's preferred orientation. The red vector shows the direction of the vector average over the population. This gives the model's readout (i.e. 'perceived orientation'). Where context has no influence on units in the population, the model's output matches the stimulus. Where the context causes suppression, the model's output is shifted away from the orientation of the context bar. Where the context causes facilitation, the model's output is shifted towards the orientation of the context bar.

1.5.6 Parameters contributing to the size of surround modulation

The size of the shift in the model's perceived target orientation, both when the shift was towards or away from the context bar orientation, was proportional to the size of the response to the context bars. The size of the response to the context bars was controlled by the spatial summation parameters (size and strength of the inhibitory and excitatory Gaussians) and the temporal decay constant. It is difficult to describe fully how each of these factors independently influenced the size of the response because the influence of any one factor was heavily dependent on the setting of the other four; for example, decreasing the decay constant (making responses decay faster) reduced the influence of the context bars when the surround was dominated by either inhibition or facilitation, but made the net surround response more positive when inhibition and facilitation were closely matched in the surround (because the inhibition caused by early context bars was reduced more than the facilitation caused by late context bars, see Figure 1.18). Generally, increasing either the excitatory size or strength parameters enhanced the response to the context bars (especially when the response decay was fast), making the model's perceived target orientation shift towards the orientation of the context bars. Increasing the inhibitory size or strength generally decreased the response, or made it more strongly negative, especially when the response decay was slow.

The interaction between the spatial sensitivity profile and the temporal decay function in determining the nature of contextual influence

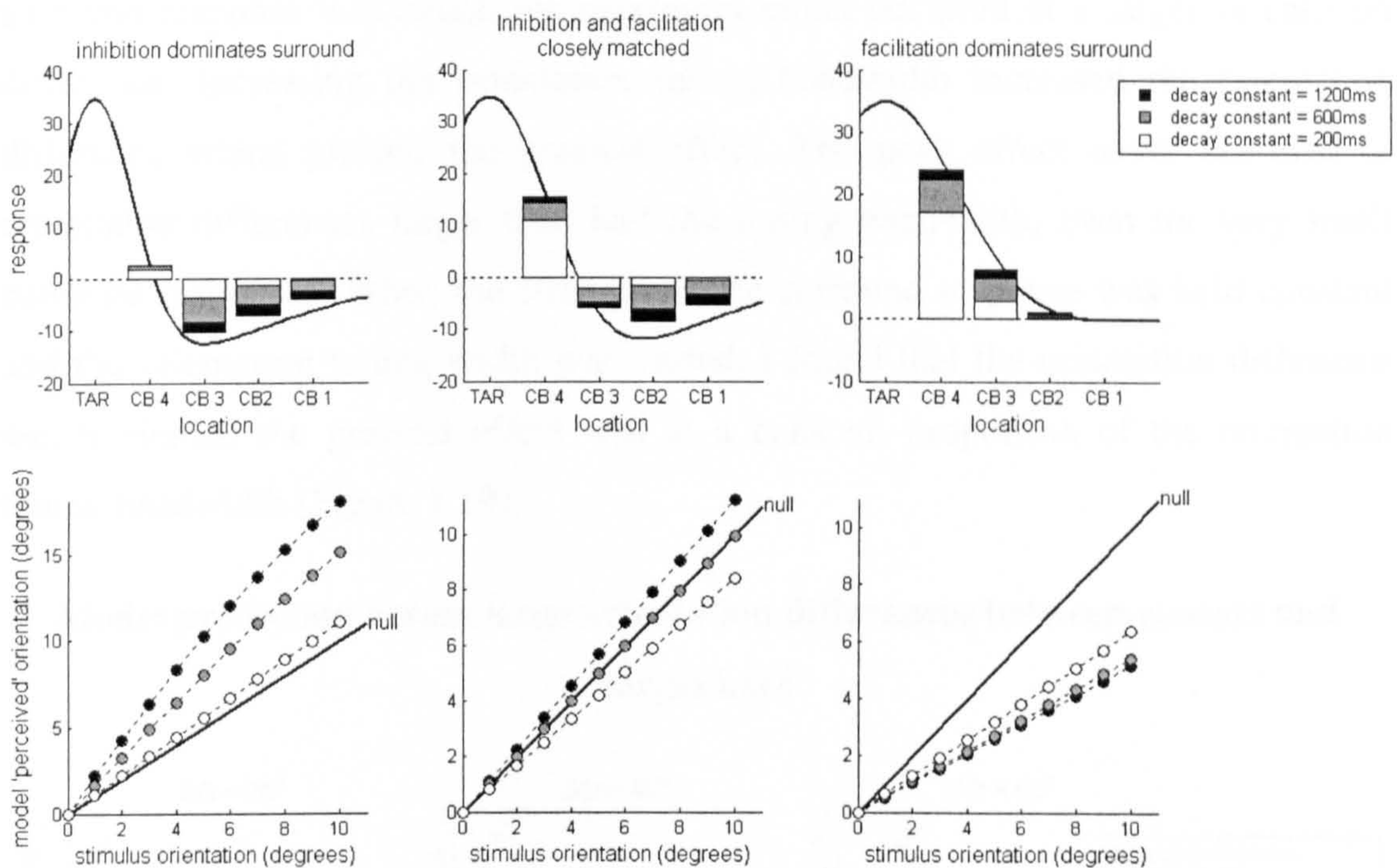


Figure 1.18 The interaction between the model unit's spatial sensitivity profile and the decay constant in determining how the context bars affect the model's 'perception' of the target bar stimulus. Upper plots show spatial sensitivity profile (black solid curve), bars show the response to each of the four context bar stimuli. The height of the bar in black, grey and white indicates the strength of the response at the time the target bar is presented i.e. after the response decay is taken into account. Black bars relate to a slow response decay rate (1200msec), grey bars relate to a medium response decay rate (600msec) and white bars relate to a fast response decay rate (200msec). I presented the model with stimuli oriented between 0° and 10° from the orientation of the context bars. Lower plots show a comparison between the orientation of the presented stimulus (x-axis) and the model's reported 'perceived' orientation (y-axis). Black dots mark the model's output when the response decay rate was slow, grey-filled dots mark the model's output when the response decay was intermediate, and white filled dots mark the model's output when the response decay was fast. The solid black line labelled 'null' shows the line of equality between the presented and 'perceived' stimulus. Dots above the null line indicate a repulsion effect of the context bars, and dots below the line indicate an attractor effect. In order to simplify the figure, the model responses had zero variance for this analysis.

When presenting the model with only the range of stimuli that I had used in the experiment, the orientation tuning bandwidth (full width at half maximum) did not appear to strongly moderate the size of the shift in perceived target orientation. When the model was presented with target stimuli up to 70° away from the context bar, I found that the increase in the size of the effect with increasing target-to-context bar orientation difference (as shown experimentally) was not monotonic. At some point a peak in the size of the effect was reached after which the effect was reduced and eventually abolished. I found that the orientation difference that gave the largest effect was determined by the orientation tuning bandwidth and the size of the net

surround response. When the net surround response was high, the maximum effect occurred at low orientation difference between target and context bar. When the surround response was small, the maximum effect occurred at a larger orientation difference. Increasing the orientation tuning bandwidth increased the orientation difference which yielded the greatest effect. The peak effect never occurred at orientation differences larger than half the tuning bandwidth, even for very small surround responses. When the strength of the surround response was held constant and the orientation tuning width was varied, I found that the orientation difference which yielded the greatest effect was at a constant proportion of the orientation tuning bandwidth (Figure 1.19).

Model prediction across large orientation differences between context and target bars

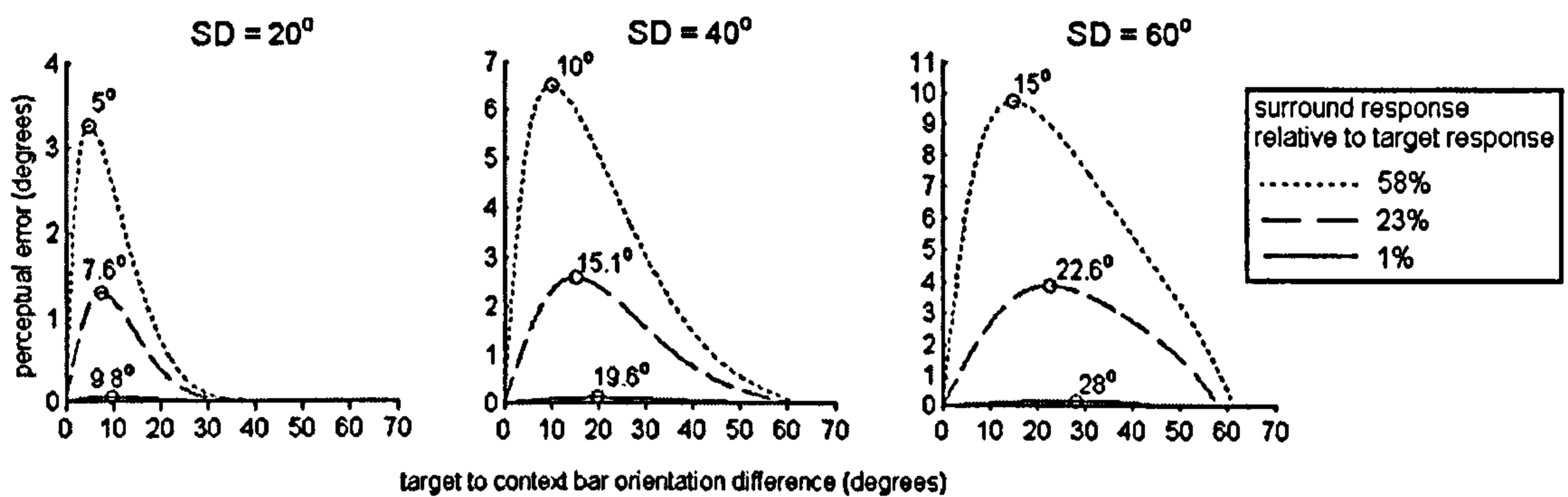


Figure 1.19 The relationship between target-to-context bar orientation difference and the magnitude of the model's 'perceptual' error (i.e. difference between reported orientation and true stimulus orientation) investigated at three levels of orientation tuning bandwidth (SD) and at three levels of net surround response (dotted line, net surround response = 58% of target response, dashed line 23%, solid line, 1%). Net surround response refers to the size of the neuronal activation caused by the presentation of the context bars after temporal decay has been accounted for, thus it is the amount of neuronal activation added to the response to the target stimulus. Along each curve, an open circle marks the target-to-context bar orientation difference which produces the greatest effect; the value is written above. For any level of net surround response the maximum effect of the context bar orientation occurs at a constant fraction of the SD (58% surround response has maximum effect at one quarter of the SD, 23% response has maximum effect at one third of the SD, 1% response has maximum effect at nearly half the SD). Increasing the SD and the surround response increases the size of the perceptual error at any given target-to-context bar orientation difference. Note that y-axes have different scales in each plot.

Changing the variance constant CV added noise to the model's responses. To check whether the variance constant could influence the size of the effect of the context on the model's perceived target orientation, I presented the model with the same combination of target and context bar orientations 100 times, holding all of the model's other parameters constant. I then took the mean of the model's responses

and compared that with the model's response when the variance constant was set to 0. I did this at several levels of CV and with several combinations of target and context bar orientation. I found no evidence that CV affected the influence of the context. The model's responses were normally-distributed with the mean centred at the model's response when CV was set to 0.

1.5.7 Biological model findings summary

From my modelling it seemed that the repulsion effect of the context on the perceived orientation of the target, which I observed in high contrast experiments, could be mediated by an inhibition of cells tuned close to the orientation of the context bars (Figure 1.17 centre). The attractor effect I observed in low contrast experiments, in which the luminance contrast of the target was reduced to 3.6%, could be mediated by a facilitation of cells tuned close to the context bar orientation (Figure 1.17 right). In recent papers, Polat et al. (Polat et al. 1998; Mizobe et al. 2001) investigated how changing the contrast of a stimulus centred on the receptive field of a V1 neuron under study affected the neuronal responses in the presence of high contrast iso-oriented flankers. They showed that when the central stimulus was at high contrast, the addition of high contrast flankers typically suppressed the response to the central stimulus. When the target was at low contrast the same flankers typically facilitated the response, a finding which compliments my modelling. Computer modelling of realistic neural networks has shown the same contrast reversal effect of collinear context (Stemmler et al. 1995). The crucial assumption of this model was that the input-output regime of excitatory neurons (pyramidal cells) differs from that of inhibitory inter-neurons such that at low input levels (low contrast) inhibitory inter-neurons are well below their spiking threshold whilst excitatory neurons are in the steep part of their input-output function. Under these conditions an input from the surround can strongly enhance the response of excitatory neurons but will not elicit a response from inhibitory cells, which are still below their spiking threshold. Thus the activity of the local network is facilitated. At a high input level (high contrast) inhibitory inter-neurons are at their most sensitive whilst excitatory neurons are saturated. Under high contrast conditions an input from the surround does not affect the response of excitatory neurons, which are already saturated, but will enhance the response of the inhibitory population, thereby reducing the activity of the local network. Thus at low target contrast an input from

the surround causes excitation and at high target contrast the same surround input causes inhibition. Stemmler et al. (1995) discuss their findings as a mechanism that can quickly identify high contrast singularities (as in pop-out) but is also able to readily identify low contrast contours.

1.5.8 Mechanisms for reduced contextual influence with attention

My experimental results showed that the strength of the effect of the context bars on the perceived orientation of the target was enhanced in the dual task (reduced attention) compared with the single task (full attention). This was found both in high contrast experiments, where the context repelled the perceived orientation of the target, and in low contrast experiments, where the context had an attractor influence on the perceived orientation of the target. Thus it seems that the effect of withdrawing voluntary attention is to enhance the strength of contextual modulation, independent of whether the stimulus features promote the attractor or repulsion effect. In the biological model the only individual parameter that could be changed to enhance the strength of the surround, both when the net surround response was inhibitory and when it was facilitatory, was the temporal decay constant. Increasing this constant, making responses more persistent, enhanced the effect of both an inhibitory surround and a facilitatory surround as long as the surround was dominated by one or other effect. The hypothesis that the influence of the context on the target became stronger in the dual task condition because neuronal responses became more persistent in the near absence of attention is contrary to the findings of a number of studies which show that the responses of visual neurons become more persistent when voluntary attention is directed towards the cell's receptive field (Roelfsema et al. 1998; McAdams and Maunsell 1999; Reynolds et al. 2000; Scholte et al. 2001). In light of this evidence, a different hypothesis should be formulated.

Current theory suggests that the contextual influence from the so-called non-classical receptive field is mediated by a separate class of synapse from the input to the classical receptive field. A large part of the input to the CRF is thought to arise from thalamocortical/feed-forward connections (Ferster et al. 1996; Gil et al. 1999; Dragoi and Sur 2000; Angelucci et al. 2002; Angelucci and Bullier 2003; Lund et al. 2003). These synapses carry information into a cortical area from the thalamus, or from areas lower in cortical hierarchy to areas higher in the hierarchy (Van Essen et al. 1992). Intracortical (and feedback) synapses recombine information within the

cortex and mediate interactions across visual space; they are thought to mediate contextual nCRF modulation (Das and Gilbert 1999; Angelucci et al. 2002; Angelucci and Bullier 2003; Lund et al. 2003) and can be facilitatory or suppressive in nature. An important feature of these two types of synapses is that they are differently affected by the neuromodulator acetylcholine (ACh); intracortical synapses are suppressed by ACh whilst thalamocortical synapses are unaffected or even enhanced by ACh (Hasselmo and Bower 1992; Gil et al. 1997; Kimura et al. 1999; Hsieh et al. 2000; Kimura 2000). Thus the presence of ACh shifts the cortical network in favour of feed-forward thalamocortical activation. The functional significance of shifting the balance may be to reduce the efficacy of contextual modulation (Roberts et al. 2005). The natural release of ACh is strongly bound to states of attention (Everitt and Robbins 1997; Sarter and Bruno 1997; Sarter et al. 2003), thus the current finding that the influence of context is reduced by attention is in line with the neurophysiological effects of ACh.

The finding that the efficacy of intracortical interactions can be selectively moderated can be incorporated into my model by adding a term which controls the maximum size of the response to the context bars:

$$R(OX) = R(O) \times \left(\left(K_e \times \left(\exp\left(-\left(\frac{2 \times X}{T_1}\right)^2\right)\right) \right) - \left(K_i \times \left(\exp\left(-\left(\frac{2 \times X}{T_2}\right)^2\right)\right) \right) \right) \times S_e$$

(Equation 1.10)

where the additional term 'Se' is the 'surround efficacy' constant and all other terms are as in Equation 1.8. When Se is set to 1, the surround modulation is considered to be 100% effective. Reducing Se below 1 reduces the efficacy of the surround. This reduction occurs irrespective of whether the net surround response is inhibitory or facilitatory. For cholinergic modulation to underlie the observed effect of reduced surround efficacy in the single task condition, ACh would have to be released locally to areas of cortex involved in the processing of attended objects and not to areas involved in processing unattended objects. The specificity of ACh release into the visual cortex is currently unknown. Several recent studies have suggested that ACh release may be more local than was previously thought (Price and Stern 1983; Carey and Rieck 1987; Fournier et al. 2004). Despite these findings it seems doubtful that the basal forebrain, from which cholinergic projections arise (Everitt and Robbins 1997), has the specificity required to influence processing of

the central colour counting stimulus in the dual task, but not to influence the processing of the experimental stimulus located just 1.1° away. Feedback projections from higher cortical areas are also thought to be instrumental in attentional processes (Kastner and Pinsk 2004) and are more likely to have the required level of specificity. It is possible that feedback projections interact with cholinergic projections in order to ‘fine-tune’ cholinergic regulation. This could be achieved by glutamatergic feedback connections directly enhancing ACh release from adjacent cholinergic terminals. In line with this idea, it has been reported that glutamatergic synapses are often found adjacent to cholinergic synapses in cat primary visual cortex (Aoki and Kabak 1992). The consequent rebalancing of the cortical network, by the action of ACh, in favour of processing feed-forward inputs could thus underlie the smaller effect of the context in the full attention condition, as demonstrated in the current experiment.

1.6 A simplified model for fitting

My modelling suggested that surround inhibition could underlie the repulsion effect of the context bar orientation on the perceived orientation of a high contrast target. The model also suggested that surround facilitation could underlie the attractor effect of the context bar on the perceived orientation of a low contrast target. In order to gain some understanding of the magnitude of the supposed inhibition or facilitation, I developed a simplified version of my model that could be fitted to experimental data. In my simplified model (Figure 1.20) I represented the population response to the target and reference as two Gaussians centred at the respective orientations, rather than creating populations of individual vectors. A third Gaussian centred at the context bar orientation was added to the target response distribution, which represented the surround response to the context. On each trial noise was added to each of the three response curves, the effect of which was to shift the curves to the right or the left. The gain of the target and reference responses was fixed at 1. The gain of the response to the context (‘surround gain’) was not restricted. The model reported the reference orientation as the location of the peak of the reference response curve. It reported the target orientation as the location of the peak of the sum of the target and context response curves. This simplified model behaved very similarly to my full model: in the absence of a context bar response, the model made normally-distributed errors with a mean of 0° difference from the

true target orientation. In the presence of a context bar, the model reported that the target was tilted further from the context bar orientation when the surround gain was negative. If the surround gain was positive, the model reported that the target was tilted closer to the context bar orientation than was the case.

Simplified model for fitting to data

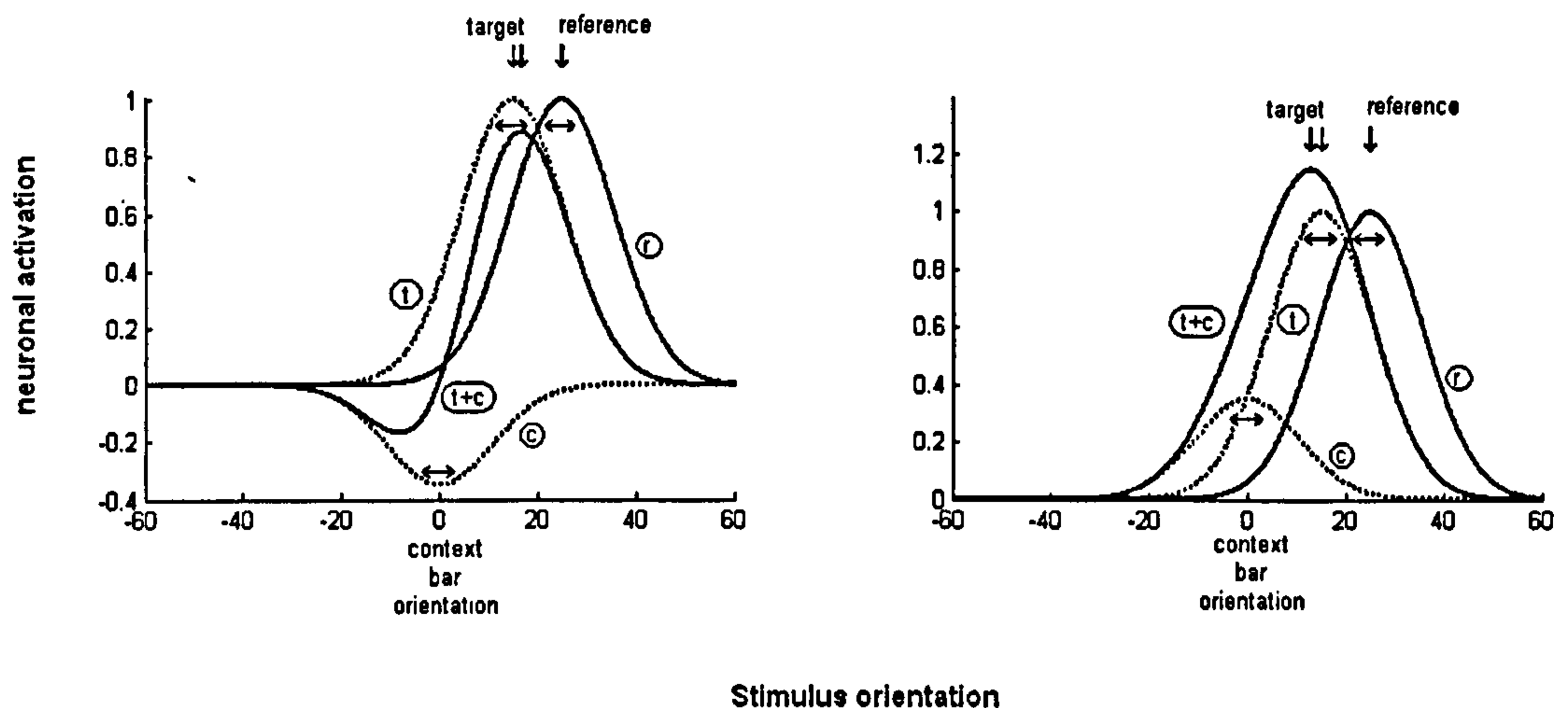


Figure 1.20 Simplified biological model used for data fitting. Information relating to the decision stage of the model is shown in bold (curves and arrows). Information not used at the decision stage is shown as dotted lines and small arrows. The population response to the target, reference and context bars is represented as Gaussians centred at the respective stimulus orientation, labelled *t*, *r* and *c* respectively. The gain of the target and reference curves is set to one. The gain of the context curve is not restricted (here set to -0.35 and +0.35). On each trial noise is added to each Gaussian, which has the effect of shifting the curves to the right or the left. Noise is represented by \leftrightarrow symbols associated with the curves '*t*', '*c*' and '*r*'. The model reports the reference orientation as the location of the peak of the reference curve, marked by a bold downward arrow labelled 'reference'. The target and context curves (dotted curves) are summed to produce the T+C curve (bold). The model reports the target orientation (i.e. 'perceived' target orientation) as the location of the peak of the T+C curve, marked by a bold downward arrow labelled 'target'. A light downward arrow marks the true target orientation. The shift in perceived target orientation is evidenced by the difference between the true orientation and the perceived orientation. When the gain of the 'context' curve is negative (left plot) the perceived target orientation shifts away from the context bar orientation. When the gain is positive (right plot) the perceived target orientation shifts towards the context bar orientation. The model tests the difference between the 'perceived' target and reference orientations. If the difference is less than a 'threshold' value the model reports that the two stimuli are the same, otherwise it reports the orientation difference between the target and context bars as clockwise or counter-clockwise.

I presented this model with combinations of targets and references and gave it the same 3AFC as the experimental participants – 'target clockwise from reference', 'target counter-clockwise from reference' or 'target same as reference'. The model reported that the target and reference 'appeared' to be the same when the difference between the peaks of the target and reference curves was less than a fitted 'threshold' value. I converted the model's 'clockwise' and 'counter-clockwise' responses into 'T-C<R-C' and 'T-C>R-C' responses in the same way that I had converted the

subject's responses (see *1.3 Methods*, Figure 1.3). To fit the model to the experimental data I adjusted the model's three free parameters, which were: the width of the (Gaussian) noise distribution from which noise values were taken on each trial, the surround gain, and the threshold for orientation discrimination.

I presented my simplified model with combinations of target and reference orientations represented in the transformed data set, i.e. the upper 5 rows in Figure 1.2. Each combination was presented 50 times. The model's responses, once converted into 'T-C<R-C' and 'T-C>R-C' responses, were thus comparable to the subject's responses. I used this comparison to optimise the model's three free parameters by minimising the summed squared error between the model's output and the subject's responses. To ensure that the model produced good fits I initially fitted the data with a large number of different starting values. The starting values that produced the best fit were used for the final optimisation. I found that it was necessary to use a standard set of random numbers for the noise distribution (i.e. not using a random number function to generate new noise values on every trial). My standard noise distribution was an array of 3150 random numbers (one for every trial the model would run, i.e. 63 multiplied by 50) with a standard deviation of 1. When fitting the model, numbers from the standard noise distribution were multiplied by the fitted noise parameter, thus the noise distribution took on a standard deviation equal to the noise parameter. I used a standard set of random numbers because I found that generating new random numbers on every trial confused the optimisation program (and lead to worse fits), presumably because using the same parameters twice could produce different errors. Changing the array of random numbers and re-fitting the data caused slight changes to the fitted parameters but did not change the pattern of results. I used the same standard set of random numbers to fit data from all the subjects.

1.6.1 Fitted modelling results

The simplified model provided good fits to the data (Figure 1.21). To compare the fit quality with that of the 2-dimensional regression analysis I converted the model's output into a 3-dimensional surface by taking the difference between the model's 'T-C<R-C' and 'T-C>R-C' responses (see data analysis). I then calculated the percentage variance accounted for by the model in the same way as I had done for the 3D plane (see data analysis). The median percentage variance accounted for

was 84.2% (25th percentile = 76.1%, 75th percentile = 91.1%). These values were slightly lower than the percentage variance accounted for by the regression analysis (median difference = 3.7%, 25th percentile 1.1%, 75th percentile 7.2%).

Examples of simplified model data fits

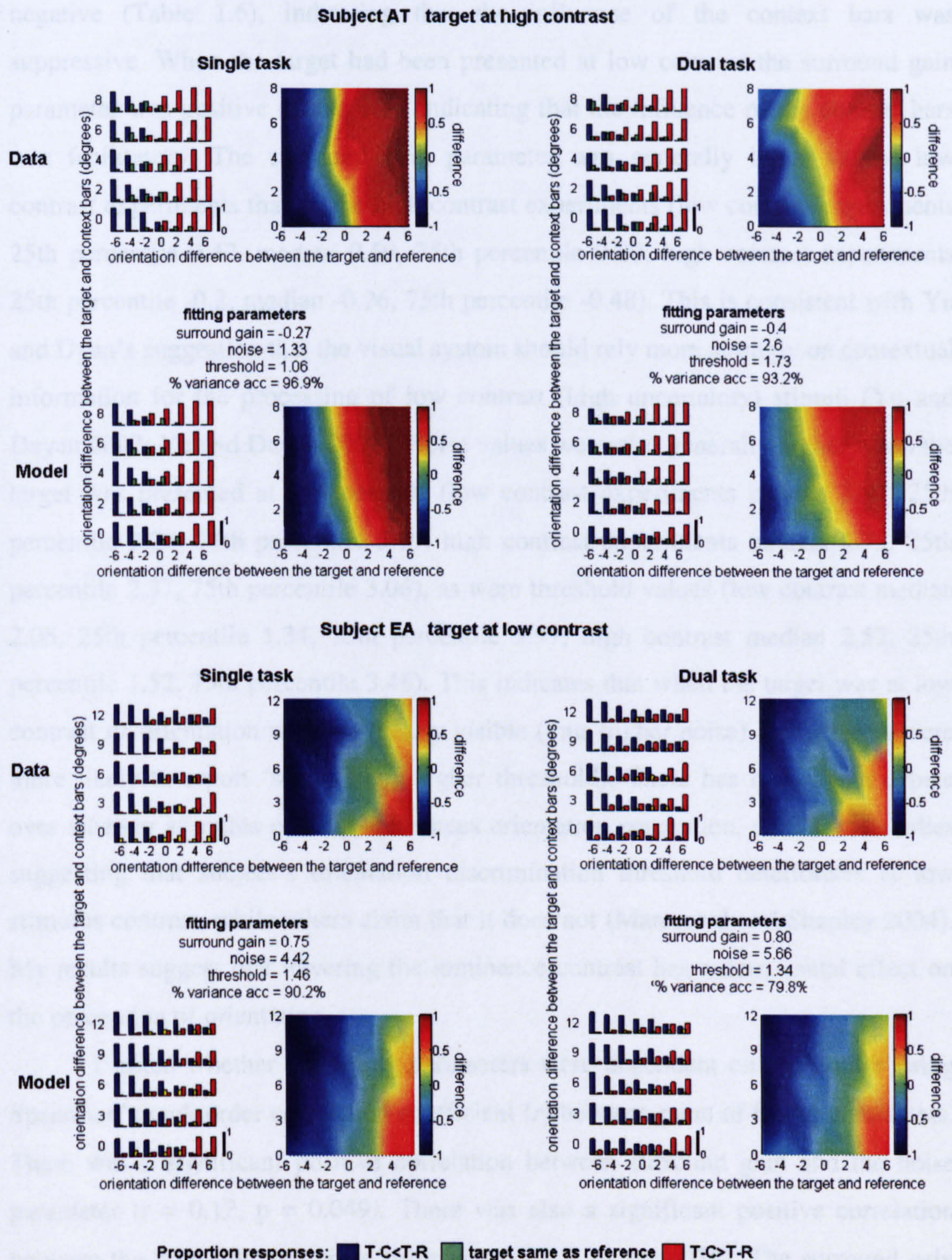


Figure 1.21 First and third rows show data from example subjects (AT and EA). Second and fourth rows show responses from the simplified model fitted to the data. The subject's responses and the model's responses are shown in the same format as in Figures 1.5 and 1.7.

In line with the prediction from the full model (biologically motivated model), and from a number of physiological studies (Polat and Norcia 1996; Polat et al. 1998; Mizobe et al. 2001), I found that when the target had been presented at the same luminance contrast as the context bars the surround gain parameter was negative (Table 1.6), indicating that the influence of the context bars was suppressive. When the target had been presented at low contrast the surround gain parameter was positive (Table 1.7), indicating that the influence of the context bars was facilitatory. The surround gain parameter was generally larger in the low contrast experiments than in the high contrast experiments (low contrast experiments 25th percentile 0.42, median 0.59, 75th percentile 0.80; high contrast experiments 25th percentile -0.2, median -0.26, 75th percentile -0.48). This is consistent with Yu and Dayan's suggestion that the visual system should rely more strongly on contextual information for the processing of low contrast (high uncertainty) stimuli (Yu and Dayan 2002; Yu and Dayan 2003). Noise values were also generally higher when the target was presented at low contrast (low contrast experiments median 3.97, 25th percentile 3.23, 75th percentile 5.19; high contrast experiments median 1.73, 25th percentile 2.37, 75th percentile 3.06), as were threshold values (low contrast median 2.05, 25th percentile 1.34, 75th percentile 3.97; high contrast median 2.52, 25th percentile 1.52, 75th percentile 3.48). This indicates that when the target was at low contrast its orientation was less clearly visible (thus higher noise) and subjects were more likely to report 'same' (thus higher threshold). There has been some debate over whether stimulus contrast influences orientation perception, with some studies suggesting that subject's orientation discrimination threshold deteriorates at low stimulus contrast, while others claim that it does not (Mareschal and Shapley 2004). My results suggest that lowering the luminance contrast has a detrimental effect on the perception of orientation.

I tested whether the fitting parameters were dependent on each other using Spearman's rank order correlation coefficient (r) between pairs of fitting parameters. There was a significant positive correlation between surround gain and the noise parameter ($r = 0.12$, $p = 0.049$). There was also a significant positive correlation between the threshold and noise parameters ($r = 0.14$, $p=0.038$). The surround gain was not related to the threshold parameter ($r = 0.05$, $p = 0.21$). That higher noise should lead to a higher threshold is not surprising; the relationship between surround

gain and noise was less expected. It may be that the higher noise arises from stronger input from the surround (i.e. noise arising from the surround in addition to noise from the feed-forward input), or it may be that the visual system relies more strongly on surround information under conditions of higher noise because of increased uncertainty (Yu and Dayan 2002; Yu and Dayan 2003).

1.6.2 The effect of attention in the fitted model

In the high contrast experiments, the dual task condition was associated with an increase in surround gain (i.e. becoming more strongly negative) in 9 out of 11 subjects; in the remaining two subjects surround gain was unchanged between the single and dual task conditions. The dual task condition was also associated with an increase in threshold in 8 subjects and an increase in noise in 6 subjects.

Simplified model fitting parameters in high contrast experiments

Exp	Subject	Gain		Noise		Threshold		% var accounted	
		Single	Dual	Single	Dual	Single	Dual	Single	Dual
1	KW	-0.46	-0.54	1.55	1.31	1.52	1.10	83.91	76.91
	WS	-0.20	-0.20	2.08	1.46	2.51	1.54	74.55	75.00
	MR	-0.77	-0.80	3.06	2.99	5.25	4.03	49.80	16.07
2	CS	-0.21	-0.47	2.84	1.81	0.95	2.68	86.31	93.60
	DB	-0.20	-0.20	2.00	4.03	1.05	1.52	91.59	87.21
	AT	-0.27	-0.40	1.33	2.60	1.06	1.73	96.87	93.16
3a	AG	-0.24	-0.51	1.39	4.12	1.16	2.53	87.74	65.71
	DH	-0.23	-0.48	1.93	4.65	3.33	3.48	78.56	76.38
	JS	-0.44	-0.81	2.55	5.07	4.15	4.98	83.51	73.18
4a	NT	-0.14	-0.19	2.69	2.18	3.08	4.00	93.29	92.41
	YL	-0.17	-0.22	1.73	3.41	1.95	3.28	95.83	90.60

Table 1.6 Simplified model fitting parameters for each subject in high contrast experiments during the single and dual task conditions.

In the low contrast experiments the dual task condition was associated with an increase in the surround gain parameter in all five subjects. Noise was also increased in all subjects. Threshold was increased in four subjects and reduced in one. Thus the effect of withdrawing visual attention in the low contrast experiments was similar to that seen in the high contrast experiments: a reduction in surround gain, and an increase in noise and threshold.

Simplified model fitting parameters in low contrast experiments

Exp	Subject	Gain		Noise		Threshold		% var accounted	
		Single	Dual	Single	Dual	Single	Dual	Single	Dual
3b	MR	0.10	0.42	3.07	4.32	0.99	2.09	80.73	59.87
4b	NT	0.10	1.03	5.19	5.27	4.81	5.07	84.63	83.39
	YL	0.42	0.43	3.23	3.61	2.55	3.97	92.93	91.00
	ZI	0.74	1.31	2.92	3.60	1.05	2.01	87.09	78.43
	EA	0.75	0.80	4.42	5.66	1.46	1.34	90.24	79.82

Table 1.7 Simplified model fitting parameters for each subject in low contrast experiments during the single and dual task conditions.

To assess significance of changes in the model fitting parameters between the single and dual task I combined data from both contrast experiments. These data are plotted in figure 1.22. Significance was assessed using a signed rank test using the absolute values of the fitting parameters. In line with the previous description of the data, the dual task was associated with a significant increase in all three fitting parameters.

Comparison of the simplified biological model fitting parameters between the single and dual task conditions

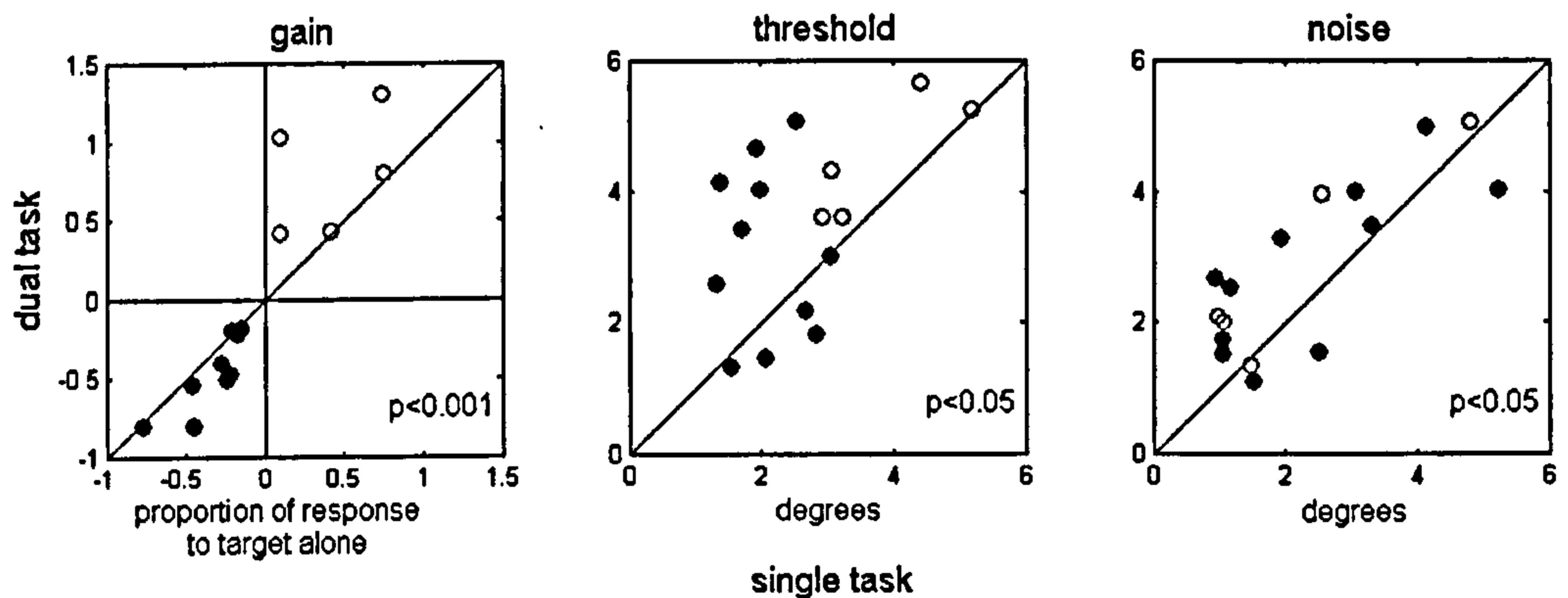


figure 1.22 Comparison of simplified model fitting parameters between the single and dual task conditions. Units of each parameter are given on the x axis. Data from each subject is marked one circle. Data from the high contrast experiments is marked by filled circles; data from the low contrast experiments is marked by open circles. The significance of differences between the single and dual task conditions is shown at the lower right of each plot (signed rank test).

1.6.3 Simplified model results summary

The general finding from my model fitting was that when the target was presented at high contrast the surround gain parameter was negative, indicating that the context bars suppressed the response to the target. When the target was presented at low contrast the surround gain parameter was positive, suggesting that the context

bars facilitated the response to the target. Under both stimulus conditions the absolute value of the surround gain parameter decreased in the single task condition compared with the dual task condition in the majority of subjects. Thus, in line with my previous description of the results, full attention weakened contextual influences independent of the sign of the influence.

Contextual influence tended to be stronger when the target was presented at low contrast compared with when it was presented at high contrast. Lowering the contrast also increased the noise and threshold parameters. These parameters relate to the subject's ability to accurately perceive and report the orientation of the stimuli. Subject's noise and threshold parameters were also increased by the removal of visual attention. Thus, I show that removing visual attention has a similar detrimental effect on subject's perceptual accuracy to that of lowering the stimulus contrast.

1.7 An error model to account for the low contrast data

In an earlier section (*1.4.5 Investigating the consequence of missing the target*) I set out a significant concern that the attractor effect in the low contrast data could, in principle, be explained by subjects having compared the orientation of the reference bar with the orientation of the context bars, rather than with the target bar orientation. To argue against this possibility I showed first that subjects did not respond as consistently when the target had not been presented (Figure 1.10). This demonstrated that the target orientation had a more powerful influence on the subject's responses than the context bar orientation. Thus when the target was presented, the subject's responses were more likely to reflect the orientation difference between the target and reference than the orientation difference between the context bar and the reference. My second argument was that the proportion of trials in which the subjects incorrectly reported that the target had been presented ('false alarm'), by giving a 'clockwise', 'counter-clockwise' or 'same' response, was too low in the single task condition and too high in the dual task condition to explain the magnitude of the observed attractor effect (Figure 1.11, Table 1.4). This was demonstrated by taking the subject's responses in the high contrast experiment and substituting a proportion of those responses (equal to the subject's false alarm rate) with responses that I predicted the subject would make if they compared the reference with the context bars instead of with the target. This analysis has weaknesses. First it assumes that the effect of the context bars in the low contrast

condition will be the same as in the high contrast condition. If this assumption was invalid, and in fact the context bars had no effect on the perceived orientation of the target at low contrast, then the small number of errors the subject made in the single task may be enough to account for the observed attractor effect, because in that case the false alarm rate would not have to cancel out the repulsion effect of the context bars at high contrast before creating an attractor effect. The second problem in the earlier analysis is that it assumes that the subject reported the orientation difference between reference and context bars with perfect accuracy, because I substituted a proportion of accurate comparisons between the reference and context bars into the high contrast data. I showed this assumption to be invalid in the first part of my argument. The effect of this assumption would be to enhance the effect of responding to the context bars in the 'manipulated data set'. It may be that it is because of this assumption that the false alarm rate was apparently too high to explain the observed effects in the dual task condition.

The fitted modelling strategy outlined in the previous section (*1.6 A simplified model for fitting*) offers an alternative way to assess the impact of subjects comparing the reference with the context bars in a proportion of trials. To do this I constructed a new 'error model' which was similar to the earlier 'simplified biological model' but did not assume any interaction between the context bar and the target bar. Instead the error model assumed that the observer mistook the context bar for the target in a proportion of trials. The error model worked as follows: on each trial the model was given the orientation of the target, reference and context bars. Noise was added to these values as in the earlier model. The model could compare the reference orientation either with the target orientation or with the context bar orientation. The probability that the model would compare the reference with the context bar, rather than the target, was controlled by the model's 'false alarm rate'. The model's false alarm rate was a free parameter which was optimised to fit the data. As in the previous model, the error model had a threshold for orientation discrimination which was optimised in the fitting.

I optimised the error model's three free parameters (false alarm rate, noise level and threshold) to minimise the summed squared error between the model's output and the observed response in the low contrast experiments. Thus, I used this model to estimate at what rate the subjects would be required to mistake the context bar for the target in order to explain the data. The fitted parameters from the error

model are shown in Table 1.8. In Figure 1.23 the error model's estimate of the required false alarm rate is compared with the subject's false alarm rate. A robust linear regression demonstrates that the model's prediction was closely related to the observed false alarm rate ($r = 0.64$, $p < 0.01$). The slope of the regression was 0.37 and the offset was 0.27. If the attractor effect observed in the low contrast data could be explained solely by the subject mistaking the context bars for the target then the regression line should have an offset of 0 and a slope of 1. The high offset indicates that in some cases (mostly the single task) the subject's false alarm rate was too low to explain the data. The low slope of the regression indicates that in other examples (mostly the dual task) the subject's false alarm rate was too high to explain the data. These are the same conclusions as given in the earlier analysis, yet they were reached independently of each other and by very different strategies. This therefore corroborates the argument that the attractor effect cannot be fully explained by the subject comparing the reference with the context bars rather than with the target, under the assumption that the false alarm rate indicates the rate at which subjects made this error.

Comparison of each subject's false alarm rate and model-predicted false alarm rate

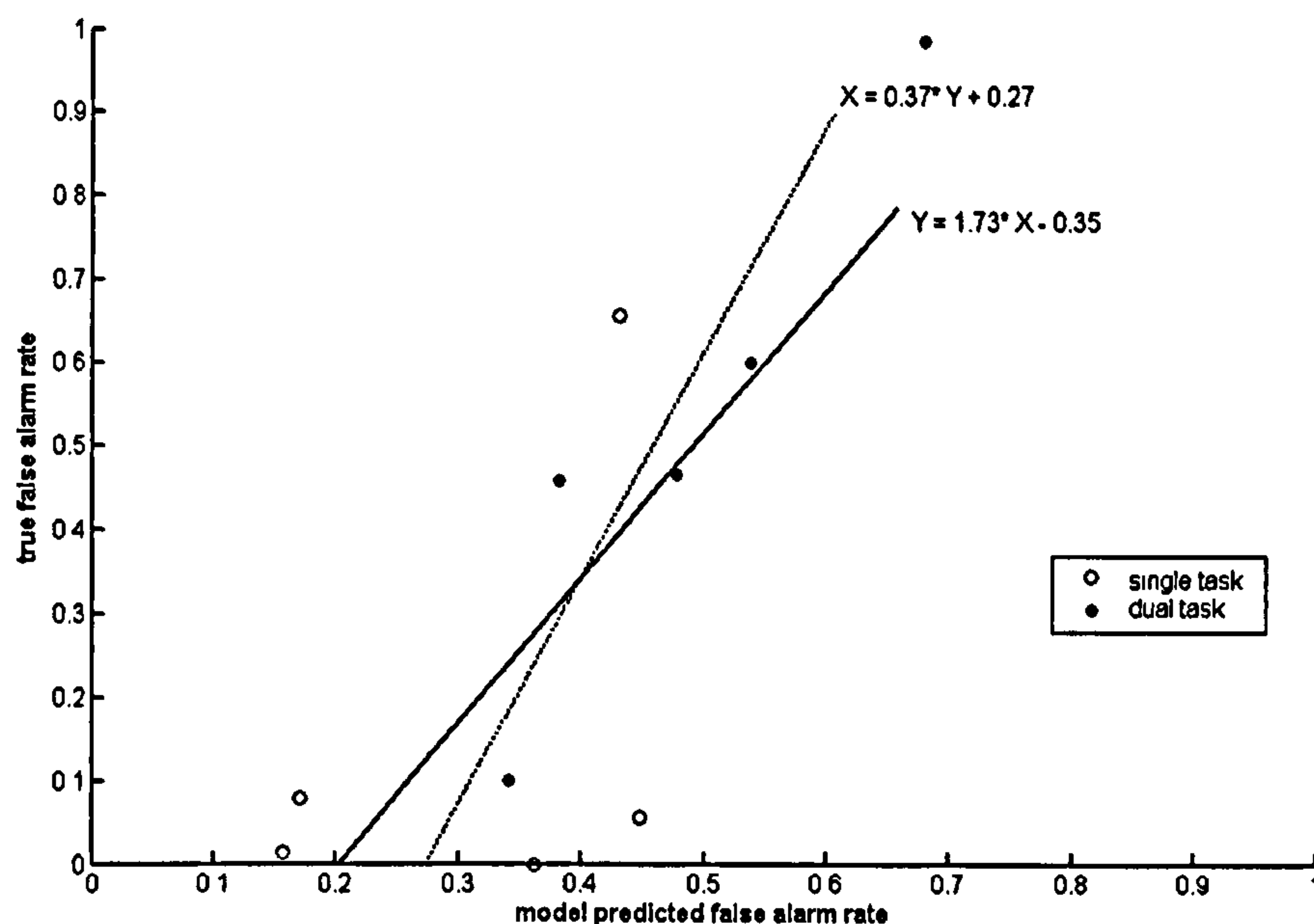


Figure 1.23 Comparison of each subject's false alarm rate in the low contrast experiments with the error model's prediction of what the false alarm rate would have to be in order to explain the observed attractor effect (under the assumption that the false alarm rate reflects the likelihood of subjects comparing the reference with the context bars). Open circles mark data from the single task condition, and filled circles mark data from the dual task condition. Straight lines show the robust linear regression. Solid line shows regression of the subjects' false alarm rate (Y) to the prediction (x-axis). dotted line shows the regression of the prediction (X) onto the subject's false alarm rate (y-axis). The values from the regression are shown at the top end of each line.

Error model fitting parameters for low contrast experiments

Exp	Subject	Subject FA rate		Model FA rate		Model Noise		Model Threshold		% variance accounted	
		Single	Dual	Single	Dual	Single	Dual	Single	Dual	Single	Dual
3b	MR	0.01	0.10	0.16	0.34	2.44	4.28	1.23	2.81	70.16	50.90
4b	NT	0.08	0.60	0.17	0.54	6.55	4.60	5.33	5.37	78.61	83.12
	YL	0.00	0.46	0.36	0.38	2.89	3.81	3.08	4.39	91.62	85.45
	ZI	0.66	0.99	0.43	0.68	1.89	2.85	1.05	1.86	89.78	74.95
	EA	0.06	0.46	0.45	0.48	3.70	5.74	1.67	1.27	86.31	74.74

Table 1.8 Subject's false alarm rate (FA rate) and error model fitting parameters for each subject in the low contrast experiments, single and dual task

1.8 Discussion

In this study I set out to determine how attention and contrast influence contextual modulation in human orientation perception. The test stimulus was a dynamic series of five sequentially presented bars. I measured how the orientation of the first four 'context' bars influenced the perceived orientation of the final 'target' bar relative to a simultaneously presented reference. Results showed that when the target was presented at the same high contrast as the context bars, its perceived orientation was shifted away from the orientation of the context bars. This effect is similar to Westheimer's 'simultaneous orientation contrast' effect (Westheimer 1990). When the target was presented at a low contrast, without changing the contrast of the context bars, the effect was reversed. That is, the perceived orientation of the target was shifted towards the orientation of the context bars. Such contrast-dependent switching has been suggested by a number of studies (Levitt and Lund 1997; Polat et al. 1998; Mizobe et al. 2001), however this is, to the best of my knowledge, the first study to demonstrate it in the domain of orientation perception using a near identical stimulus in the high and low contrast conditions.

I manipulated the allocation of voluntary attention using a single/dual task paradigm. I found that the withdrawal of visual attention in the dual task condition enhanced the effect of the context bars on the perceived orientation of the target. This was true both under stimulus conditions that promoted the attraction of the perceived target orientation, and under stimulus conditions that promoted repulsion. Thus it seems that high levels of attention down-regulate the effect of local context, independent of the sign of the effect. This conclusion is in line with Ito et al.'s finding of reduced surround facilitation under conditions of focused attention versus distributed attention (Ito et al. 1998) and is supported by Zenger et al.'s finding that surround modulation (they make no claim about its nature) is weaker in a single task than a dual task condition (Zenger et al. 2000). However, my conclusion is at odds with Freeman's proposition that attention is required for contextual influences (Freeman et al. 2001; Freeman et al. 2003; Freeman et al. 2004).

In my study and in Zenger et al.'s study, attention was manipulated by a single task/dual task paradigm. Ito et al. used a focused attention/distributed attention paradigm. The task in Ito et al.'s study was to identify a target, which could be presented at one of four locations. In the 'focused attention' condition a cue indicated

at which of the four locations the target would be presented, in the 'distributed attention' conditions there was no cue. The focused attention/distributed attention paradigm has two features in common with the single task/dual task paradigm: in both cases attention was either focused only towards the target location (focused attention, single task condition) or divided between the target location and other locations (distributed attention, dual task condition). Moreover the attentional load was increased in both the distributed attention and in the dual task conditions relative to the focused attention or single task conditions respectively.

In Freeman et al.'s studies (Freeman et al. 2001; Freeman et al. 2003; Freeman et al. 2004), the test stimulus consisted of a low contrast central Gabor patch surrounded by two pairs of flanking Gabors, i.e. five patches arranged in a cross. One pair of flankers was collinear with the central patch; the other pair was presented at an orthogonal orientation. The subjects had two tasks on each trial. First they were to judge the relative alignment of one pair of (cued) flanker Gabor patches, whilst ignoring the other pair, then they were to report whether the central patch was present or not. Thus subjects either attended or ignored the pair of collinear flankers. Freeman et al. report that when the collinear flankers were attended, the perceived contrast of the central patch was enhanced relative to when the flankers were absent, however when the collinear flankers were ignored they had no effect on the perception of the central patch. Thus they conclude that attention is required for contextual influences. Their attentional manipulation is quite different from that used in this study, and from that used in the studies by Ito et al. and Zenger et al. First, the attentional load is constant between Freeman et al.'s conditions. Moreover the collinear flankers change from being task relevant to being task irrelevant. Freeman et al.'s manipulation may thus have prompted subjects to actively ignore the unattended flankers whereas in the current study, Ito et al.'s study and Zenger et al.'s study the flankers would be ignored more passively since they were always irrelevant to the task. Actively-ignored stimuli are known to elicit smaller visual responses than passively-viewed stimuli (Reynolds et al. 1999; Treue and Martinez-Trujillo 1999; Treue 2001; Gazzaley et al. 2005). This attention-mediated suppression may be a mechanism by which the competition for limited processing resources is biased in favour of currently relevant stimuli. The suppression would therefore be expected to be stronger when competition is higher; for example, when competing stimuli are placed in close proximity to one another. Freeman et al.'s experiments may thus have

probed different aspects of attention to our study and that of Ito et al. and Zenger et al. The different findings between the studies are therefore not necessarily contradictory.

The interaction between attention and contrast has been a topic of much debate. It is well known that high levels of attention enhance performance in a number of tasks. Indeed, this effect is demonstrated in the current study, since the effect of the context bars is to promote perceptual errors and this effect is reduced in the full attention condition. Given that increasing the luminance contrast of a test stimulus can also improve performance in a number of tasks, some authors have suggested that the effect of attention is akin to increasing the 'effective contrast' of a stimulus (McAdams and Maunsell 1999; Reynolds et al. 2000). This model of attention is known as the 'contrast gain model' (Huang and Dobkins 2005), and supposes that increasing attention and increasing luminance contrast are essentially interchangeable with one another.

My data are particularly well suited to investigate the interaction between attention and contrast because, unlike in previous studies where lowering the contrast essentially weakened but did not change the perception of the target, I demonstrate a reversal in the perception of the target between high and low contrast. The effect of attention is thus much easier to distinguish from the effect of contrast. In the low contrast experiments I demonstrate that the perceived orientation of the target is shifted towards the orientation of the context bars. This effect was reduced in the full attention condition. In three subjects I demonstrated that the effect of the context bars was also reduced by raising the contrast of the target (Figure 1.8). Hence when the target is presented at low contrast, the effect of attention is similar to increasing the contrast of the target. As target contrast is increased further, the effect of the context bar changes direction from attraction to repulsion (Figure 1.8). At high contrast if attention increased the 'effective contrast' of the target, one would expect to find the strongest repulsion effect in the high contrast, high attention condition, however I find the reverse of this: the strongest repulsion effect is in the high contrast, low attention condition. Increased attention weakens the repulsion effect, rather than increasing it. Reduced repulsion could also be achieved by lowering the contrast of the target. Hence, while data from the low contrast condition demonstrate how the effect of attention can be similar to the effect of increased contrast, data from the

high contrast condition do not support the idea that increasing the level of attention is necessarily interchangeable with increasing the contrast of the target.

In this study I used a biologically inspired model to investigate whether known neurophysiological mechanisms were able to explain my results. I found that a relatively simple model, consisting of an ensemble of V1-type units that were spatially sensitive and had temporal leaky memory, was able to explain my results via a simple centre/surround inhibition or facilitation mechanism. I used a simplified version of my model to fit the experimental data. This method gave almost as good fits to the data as a 2-dimensional regression and had the advantage of providing physiologically relevant parameters.

In a recent study Guo et al. (2004) used a very similar stimulus to that used in my high contrast experiments, yet they found quite different results. In their study subjects were required to compare the orientation of the target bar with the orientation of the final context bar in a 2AFC 'same/different' paradigm. The authors report that subjects became less sensitive to orientation differences between target and context as more context bars were added, suggesting that the context bars attracted the perceived orientation of the target: the reverse of the effect I report from my high contrast experiments. Their experimental design had two major differences from my design. First, in my study the context bars were task irrelevant whereas in Guo et al.'s study the final context bar was task relevant, since it acted as the reference. Furthermore, in Guo et al.'s study the target was presented at the fixation point whereas in my study the target was removed from the fixation point by 1.1° . This difference may be critical since it has been recently reported that surround suppression (which I claim can explain my finding) is absent, or strongly reduced, in the fovea (Xing and Heeger 2000; Williams et al. 2003; Petrov et al. 2004); but see (Westheimer 1990). Guo et al. interpret their finding within a Bayesian framework where the context bars provide the visual system with a prior expectation of what the orientation of the target might be (Young 2000; Mamassian et al. 2002; Kersten et al. 2004). My results from the high contrast experiments are at odds with the Bayesian model, however it might be suggested that the visual system would only rely on a Bayesian approach where there is uncertainty about the visual scene (Yu and Dayan 2002; Yu and Dayan 2003). There may be little uncertainty about high contrast stimuli, whilst there is great uncertainty attached to low contrast stimuli. My low contrast experiments do support the Bayesian prediction that the target should be

perceived to be more like the context bars than it truly is. A Bayesian model differs from a centre/surround model in two major respects. Firstly, the interaction between the prior (i.e. the context bars) and the target is multiplicative rather than a summation (although there may be non-linearities in the brain which make these very similar). Secondly, the power of the prior is expressed by the bandwidth of the prior distribution rather than the gain of the surround response. My simplified model can be quite easily adapted to these differences, simply by adapting the 'surround response' Gaussian to be a 'prior' distribution of varying width but constant gain. The target response and prior distribution are then combined multiplicatively. This model was equally able to explain the low contrast data as my centre/surround model, but of course could not explain the high contrast data. It is important to note that the Bayesian model does not put forward any mechanism by which it may be achieved. Thus to suggest that the perception of low contrast stimuli is influenced by local context in a Bayesian like manner does not cause any conflict with simultaneously suggesting that centre/surround type facilitation could be the mechanism by which the effect is achieved.

In this chapter I have suggested that cholinergic mechanisms may be the neuropharmacological mechanism by which attention causes the observed reduction in surround modulation. In Chapter 2 I test whether the application of ACh can cause the predicted reduction in power of the non-classical RF in V1 neurons of anaesthetised primates.

Chapter 2: Acetylcholine dynamically controls spatial integration in marmoset primary visual cortex

2.1 Abstract

In Chapter 1, I described how local context influenced the perception of target orientation in human subjects. These experiments showed that contextual influences were weaker under conditions of full attention than under conditions of reduced attention. In this chapter I describe an experiment which investigates a possible neuropharmacological mechanism for the reduction in contextual modulation. A number of *in vitro* studies have demonstrated that acetylcholine (ACh) selectively reduces the efficacy of lateral cortical connections via a muscarinic mechanism, whilst boosting the efficacy of thalamocortical/feed-forward connections via a nicotinic mechanism. This suggests that high levels of ACh should reduce centre/surround interactions of neurons in primary visual cortex, making cells more reliant on feed-forward information. In line with this hypothesis, I show in this chapter that local iontophoretic application of ACh in primate primary visual cortex reduces the extent of spatial integration, assessed by recording neuronal length tuning. When ACh was externally applied the preferred length shifted towards shorter bars, demonstrating reduced impact of the non-classical receptive field. I fitted a difference of Gaussians model and a ratio of Gaussians model to these data to determine the underlying mechanisms of this dynamic change in spatial integration. These models assume that overlapping summation and suppression areas, with different widths and gains, are responsible for spatial integration and size tuning. ACh significantly reduced the extent of the summation area, but had no significant effect on the extent of the suppression area. In line with previous studies I also found that applying ACh enhanced the response in the majority of cells, especially in the late (sustained) part of the response. The natural release of ACh is strongly linked with states of arousal and attention, and the effects of ACh presented here are similar to the effects of attention on neuronal activity. I therefore discuss these findings in terms of a possible neurobiological mechanism by which attention could dynamically control contextual modulation.

2.2.Introduction

There has been considerable interest in the effects and function of cortical acetylcholine (ACh). Early debate about the effect of cholinergic drugs on cortical cells mostly revolved around their effect on a cell's signal-to-noise ratio and tuning sharpness. Drachman had speculated that cholinergic drugs could amplify stimulus selection and processing, and optimise the separation between signal and noise (Drachman 1977). This proposal has been tested using *in vivo* iontophoresis to apply cholinergic drugs whilst simultaneously recording neuronal responses. Some studies demonstrated support for the hypothesis that ACh might sharpen tuning functions (Sillito and Kemp 1983; Sato et al. 1987; Sillito and Murphy 1987), while others did not (Habbicht and Vater 1996). The differences between results might be attributable to differences in anaesthetic regimes or biases towards different recording layers (Sato et al. 1987). The hypothesis that ACh might improve the signal-to-noise ratio has been generally supported by *in vivo* experiments (Sillito and Kemp 1983; Sato et al. 1987; Sillito and Murphy 1987). However, slice studies suggest that signal-to-noise ratio would deteriorate in the presence of ACh (McCormick and Prince 1986). Due to these inconsistencies in the literature, to date no clear conclusion can be reached as to whether or not ACh improves signal-to-noise ratio and sharpens tuning.

Cholinergic innervation in the mammalian central nervous system stems from two major sites: the basal forebrain and the brainstem. The basal forebrain innervates the neocortex, cingulate cortex and allocortical sites (hippocampus, amygdala and olfactory bulb), whereas cholinergic neurons originating from the brainstem principally innervate the thalamus (Sillito and Murphy 1987; Everitt and Robbins 1997; Sarter et al. 2001). Partly because of this anatomical separation it is proposed that the basal forebrain system mediates the more cognitive effects of ACh, whilst the brainstem system mediates lower-level systems such as sleep/wake cycles (Everitt and Robbins 1997; Sarter et al. 2001). Many early lesion experiments in both rodents and primates seemed to suggest that the nucleus basalis of Meynert (NBM) (an important cholinergic structure in the basal forebrain) was strongly involved in aspects of learning and memory, since its destruction profoundly impaired performance on almost every type of learning task (Dunnett et al. 1991; Sarter et al. 2003). However, these early studies used rather unselective methods of lesioning and so should be regarded with caution. Later studies, using methods which selectively

damaged only the cholinergic neurons in the NBM, failed to support the earlier finding (Everitt and Robbins 1997; Sarter et al. 2003); rather they suggested that disrupting cortical ACh by damaging the NBM impaired attentional functions.

The conclusion that NBM activation is related to attention rather than learning is necessarily qualified by the experimental protocols which have been used to test it. While studies employing classic learning and memory tasks (for example mazes and delayed match-to-sample tasks) failed to find an effect of NBM damage, studies using a multiple choice serial reaction-time task have found significant impairments (Everitt and Robbins 1997; Sarter et al. 2003). In the latter task, rats are trained to detect brief flashes of light presented randomly in one of several locations on a curved array. Responses are made by a nose-poke at the location of the flash. In correct trials the rat must then run to the opposite end of the test cage to collect a reward before returning rapidly to the array for the next stimulus presentation. Performance on this task is thought to demand a form of sustained attention (Arnold et al. 2002). The lesioned rat's impairment could be reduced by lengthening the stimulus duration, thereby reducing the attentional load, or by administration of an anti-cholinesterase (Muir et al. 1994). Micro-dialysis recordings have reported that performance on such a task is associated with increased ACh efflux into the cortex (Arnold et al. 2002). In their recent review of studies employing this and similar tasks, Sarter et al. (2005) focused on the animal's rates of hits, misses, false alarms and correct rejections (in tasks where the animal must also correctly identify the absence of a target stimulus). They report that the loss of cortical cholinergic input had a detrimental effect on an animal's hit rate but not on the animal's rate of correct rejection. This may be because correctly identifying the presence of a target (a hit) relies on thalamic input, while correctly identifying its absence (correct rejection) relies on the animal's internal representation of the world. This dichotomy is important given *in vitro* findings on the effects of ACh on the cortical network.

Hasselmo and Bower (1992) were the first to show that the effect of ACh on a particular synapse is critically dependent on the source of the synapse under study. In their experiment they took transverse slices from rat piriform cortex which preserved the laminar organisation. In these slices they could separately stimulate afferent fibres in layer 1a or intrinsic fibres in 1b, whilst recording from pyramidal cells in layer 2 which receive input from both types of synapses. When they applied cholinergic agonists (carbachol, muscarine or ACh combined with the

anticholinesterase neostigmine) responses elicited by stimulating intrinsic fibers were inhibited, whereas responses elicited by stimulating afferent fibers were largely unaffected. Assessment of the time course of intracellular responses suggested that the suppression of intracortical synapses was due to pre-synaptic mechanisms. Testing various combinations of cholinergic agents suggested that the M1 muscarinic receptor subtype was the responsible mechanism. Anatomical studies have shown that muscarinic receptors are primarily located pre-synaptically on intracortical synapses (Parkinson et al. 1988; Sahin et al. 1992; Lucas-Meunier et al. 2003). Since Hasselmo and Bower (1992), a number of other studies have supported their finding that ACh suppresses intracortical but not afferent synapses (Hsieh et al. 2000; Metherate and Hsieh 2004). Moreover, studies have also shown that ACh can facilitate thalamocortical synapses by a nicotinic mechanism (Gil et al. 1997; Gioanni et al. 1999). Nicotinic receptors are known to be found principally on the pre-synaptic membrane of thalamocortical synapses (Prusky et al. 1987; Parkinson et al. 1988; Sahin et al. 1992; Lavine et al. 1997; Gioanni et al. 1999; Disney and Aoki 2003; Lucas-Meunier et al. 2003). Suppressing intracortical transmission whilst leaving thalamocortical transmission unaffected, or enhanced, would rebalance the cortical network in favour of feed-forward activation, whilst suppressing the spread of lateral and feed-forward processing. This effect has been demonstrated using optical imaging in cortical slices (Kimura et al. 1999; Kimura 2000). Such a rebalancing of cortical processing may explain why rats lesioned in the NBM showed impaired hit rate but unaffected correct rejection rate. The loss of cholinergic input left cortical processing dominated by top-down inputs, which are necessary for reporting the absence of a target. The enhancement of bottom-up processing, necessary for reporting the presence of a briefly presented target, was not achieved.

In the visual cortex, thalamocortical synapses are thought to be responsible for a large part for the CRF input whilst intracortical synapses are thought to be the principal source of the nCRF input (Angelucci et al. 2002; Angelucci et al. 2002). The function of the nCRF is to provide neurons with access to a wider field of visual space than is afforded them by feed-forward inputs alone. Thus, responses to stimuli placed in the CRF can be modulated by the local stimulus context. In cluttered environments contextual information (the clutter) can hinder the detection of small objects. Moreover, contextual modulation may promote perceptual errors, as demonstrated in Chapter 1. Under natural vision it may therefore be necessary to

dynamically adjust the flow of feed-forward and lateral/feedback information; for example, to preferentially process information from a small area of visual space that is behaviourally relevant (Chelazzi 1995; Luck et al. 1997; Reynolds and Desimone 1999). The ability of ACh to selectively inhibit intracortical processing whilst enhancing thalamocortical transmission could be a mechanism by which such dynamic shifting between feed-forward and feedback processing is achieved. In the presence of high levels of ACh, the modulatory influence of the nCRF would be inhibited whilst the feed-forward CRF input would be facilitated. In the visual cortex neuronal responses would then be more strongly based on the CRF and less influenced by local context.

To test this hypothesis I investigated length tuning in V1 under conditions of externally applied and the absence of externally applied ACh. Length tuning is a classic demonstration of the nCRF influence and has several advantages over other stimulus paradigms that have been widely used to test the nCRF influence. Firstly, almost all cells can be expected to show both nCRF facilitation (i.e. the preferred length is typically longer than the CRF diameter (DeAngelis et al. 1994; Sceniak et al. 2001)) and nCRF inhibition (end-stopping). This is unlike centre/surround grating patches which often, although not always, only reveal nCRF inhibition (Cavanaugh et al. 2002). It is important that both facilitation and inhibition are present because there is evidence to suggest that the effect of ACh is stronger for excitatory synapses than for inhibitory synapses (Kimura and Baughman 1997). Second, bar length can be easily manipulated over a relatively small number of stimulus conditions. This is important since the drug application protocol requires many trials for each condition. Since length is a continuous variable, the data can be used to fit a model which allows subtle changes in tuning to be examined. Centre/surround patches or textured stimuli are usually either investigated only by centre and surround iso-oriented vs. cross-oriented stimuli (Knierim and Van Essen 1992), which do not give enough data points to fit a physiologically motivated model, or require a very large number of conditions to measure a full tuning curve (Jones et al. 2002). In this chapter I show that application of ACh caused a shift in a neuron's preferred length towards shorter bars and a decrease in its summation area, supporting the hypothesis that ACh rebalances lateral/feedback and feed-forward connections in favour of feed-forward activation.

2.3 Materials and Methods

All experiments were carried out in accordance with the European Communities Council Directive 1986 (86/609/EEC), the National Institutes of Health *Guidelines for the Care and Use of Animals for Experimental Procedures*, the Society for Neuroscience *Policies on the Use of Animals and Humans in Neuroscience Research*, and the UK Animals Scientific Procedures Act.

2.3.1 Animal preparation

We recorded extra-cellular responses of V1 neurons from four adult anaesthetised and paralysed marmosets (*callithrix jacchus*, 400-480g). Anaesthesia was induced by intramuscular injection of Saffan (Alphadalone/Alphaxalone acetate, 1.5ml/kg) and maintained by continuous intravenous injection of Propofol (0.8-1.5ml/kg/hour). Analgesia was provided by continuous injection of Alfentanil (156 μ g/kg/hour). Prior to paralysis, adequate depth of anaesthesia was ensured by repeatedly checking for absence of toe pinch withdrawal reflexes. Paralysis was induced and maintained by intravenous injection of vancuronium (Norcuron, 100 μ g/kg/hour). Level of anaesthesia following paralysis was monitored by means of heart rate and/or blood pressure changes following toe pinches. Animals were artificially ventilated at a rate of 30-70 strokes/min (3.5-5.5ml/stroke). End-tidal CO₂ was constantly monitored and maintained between 3.5-4.5%. In addition, arterial and venous blood pressure and electrocardiogram were continuously monitored and recorded. Animals received antibiotic injections every 12 hours (Cephuroxide, 125mg/kg). Eyes were protected with contact lenses and regularly irrigated with saline. Atropine eye drops were regularly applied to induce and maintain mydriasis and cycloplegia.

Once adequate depth of anaesthesia was ensured and prior to paralysis being induced the animals head was secured in a stereotaxic frame using ear bars, a mouth bar and eye bars. The skin overlaying the scalp was then cut open from just above the eyebrows as far as the back to the head. Additional support for the head achieved via dental acrylic attached to the skull and secured by stainless steel bone screws. This was then anchored to the stereotaxic frame. Once the dental acrylic has set, the eye bars could be removed. For recording access to the visual cortex a small (~5mm in diameter) craniotomy was made using an electric hand drill. Normally a new craniotomy was made for each recording penetration. At the end of the experiment

animals were culled by an overdose of Alfentanil. They were then perfused for histological analysis. The monkeys were perfused transcardially with 500ml of 0.9% saline, followed by 1,000ml of 4% paraformaldehyde in distilled water. The brains were removed and placed in 4% paraformaldehyde solution for 24h, after which they were transferred to 30% sucrose solution in distilled water.

Neuronal recordings made in anaesthetised animals can be problematic since anaesthetics often suppress neuronal activity. Moreover anaesthesia has been shown to suppress contextual modulation in primary visual cortex (Lamme et al. 1998). While the exact mechanism which produces anaesthesia is controversial, recent research has suggested that volatile anaesthetics such as halothane and isoflurane (as used in Lamme, Zipser et al. 1998) and gaseous anaesthetics (xenon and N₂O) inhibit neuronal nicotinic ACh receptor function (Mori et al. 2001; Tassonyi et al. 2002; Suzuki et al. 2003). In four pilot experiments, under otherwise near identical conditions, I had used halothane and N₂O to provide anaesthesia. I chose this regime because previous experiments using iontophoretic ACh application in cat visual cortex have used halothane and N₂O (Sillito et al. 1985; Sato et al. 1987), albeit at substantially lower levels (0.1-0.5%). In my pilot experiments using halothane (0.5-1%) and N₂O (30%) I was unable to detect any effect of ACh application on neuronal activity. Intravenous anaesthetics (barbiturates, Etomidate and Propofol) also disrupt nicotinic ACh receptors but only at doses higher than are necessary to produce adequate depth of anaesthesia (Tassonyi et al. 2002). Recent work suggests that Propofol exerts its major influence via a GABAergic mechanism (Alkire and Haier 2001) rather than nicotinic ACh mechanisms, although other work has shown that Propofol also inhibits signal transduction by M1-type muscarinic receptors (Nagase et al. 1999). These findings prompted me to switch to Propofol anaesthesia, since I reasoned that ACh application would be less influenced by this anaesthetic. Ultimately it will be necessary to perform similar experiments in awake animals in order to fully rule out the effects of anaesthetics (see Chapter 4).

2.3.2 Electrophysiological recording

At each recording location I attempted to achieve the best possible isolation of single unit activity by slowly moving the electrode forwards and backwards until the isolation improved no further. I then set the thresholds of a window-discriminating spike detector such that I could be reasonably confident that spikes

animals were culled by an overdose of Alfentanil. They were then perfused for histological analysis. The monkeys were perfused transcardially with 500ml of 0.9% saline, followed by 1,000ml of 4% paraformaldehyde in distilled water. The brains were removed and placed in 4% paraformaldehyde solution for 24h, after which they were transferred to 30% sucrose solution in distilled water.

Neuronal recordings made in anaesthetised animals can be problematic since anaesthetics often suppress neuronal activity. Moreover anaesthesia has been shown to suppress contextual modulation in primary visual cortex (Lamme et al. 1998). While the exact mechanism which produces anaesthesia is controversial, recent research has suggested that volatile anaesthetics such as halothane and isoflurane (as used in Lamme, Zipser et al. 1998) and gaseous anaesthetics (xenon and N₂O) inhibit neuronal nicotinic ACh receptor function (Mori et al. 2001; Tassonyi et al. 2002; Suzuki et al. 2003). In four pilot experiments, under otherwise near identical conditions, I had used halothane and N₂O to provide anaesthesia. I chose this regime because previous experiments using iontophoretic ACh application in cat visual cortex have used halothane and N₂O (Sillito et al. 1985; Sato et al. 1987), albeit at substantially lower levels (0.1-0.5%). In my pilot experiments using halothane (0.5-1%) and N₂O (30%) I was unable to detect any effect of ACh application on neuronal activity. Intravenous anaesthetics (barbiturates, Etomidate and Propofol) also disrupt nicotinic ACh receptors but only at doses higher than are necessary to produce adequate depth of anaesthesia (Tassonyi et al. 2002). Recent work suggests that Propofol exerts its major influence via a GABAergic mechanism (Alkire and Haier 2001) rather than nicotinic ACh mechanisms, although other work has shown that Propofol also inhibits signal transduction by M1-type muscarinic receptors (Nagase et al. 1999). These findings prompted me to switch to Propofol anaesthesia, since I reasoned that ACh application would be less influenced by this anaesthetic. Ultimately it will be necessary to perform similar experiments in awake animals in order to fully rule out the effects of anaesthetics (see Chapter 4).

2.3.2 Electrophysiological recording

At each recording location I attempted to achieve the best possible isolation of single unit activity by slowly moving the electrode forwards and backwards until the isolation improved no further. I then set the thresholds of a window-discriminating spike detector such that I could be reasonably confident that spikes

recorded within the window represented a single neuron, however, occasionally the isolation may have been such that multi-unit activity (2-3 cells) was recorded. To test for this I calculated the autocorrelation for each cell. Single unit recordings should show some evidence of the cell's refractory period. Recordings in which the bins immediately following the trigger spike (bins 1-3msec after the trigger) were almost or completely empty were counted as single units. Figure 2.1 shows examples of a single unit (top row) autocorrelation and multi-unit (bottom row) autocorrelation. The refractory period of the single unit example is clearly evident by the almost complete absence of spikes within three milliseconds of the trigger. By contrast, in the multi-unit autocorrelation spikes are most likely to occur in the first millisecond following the trigger. After the first millisecond the probability of a spike stays roughly constant. Also included in Figure 2.1 is an example of the cell's response profile. Apart from a higher firing rate in the multi-unit example, very little distinguishes the two. Response rate alone cannot be used to distinguish single units from multi-units since many single units in our sample actually had higher response rates than some multi-units.

Example of a single unit autocorrelation and a multi-unit autocorrelation

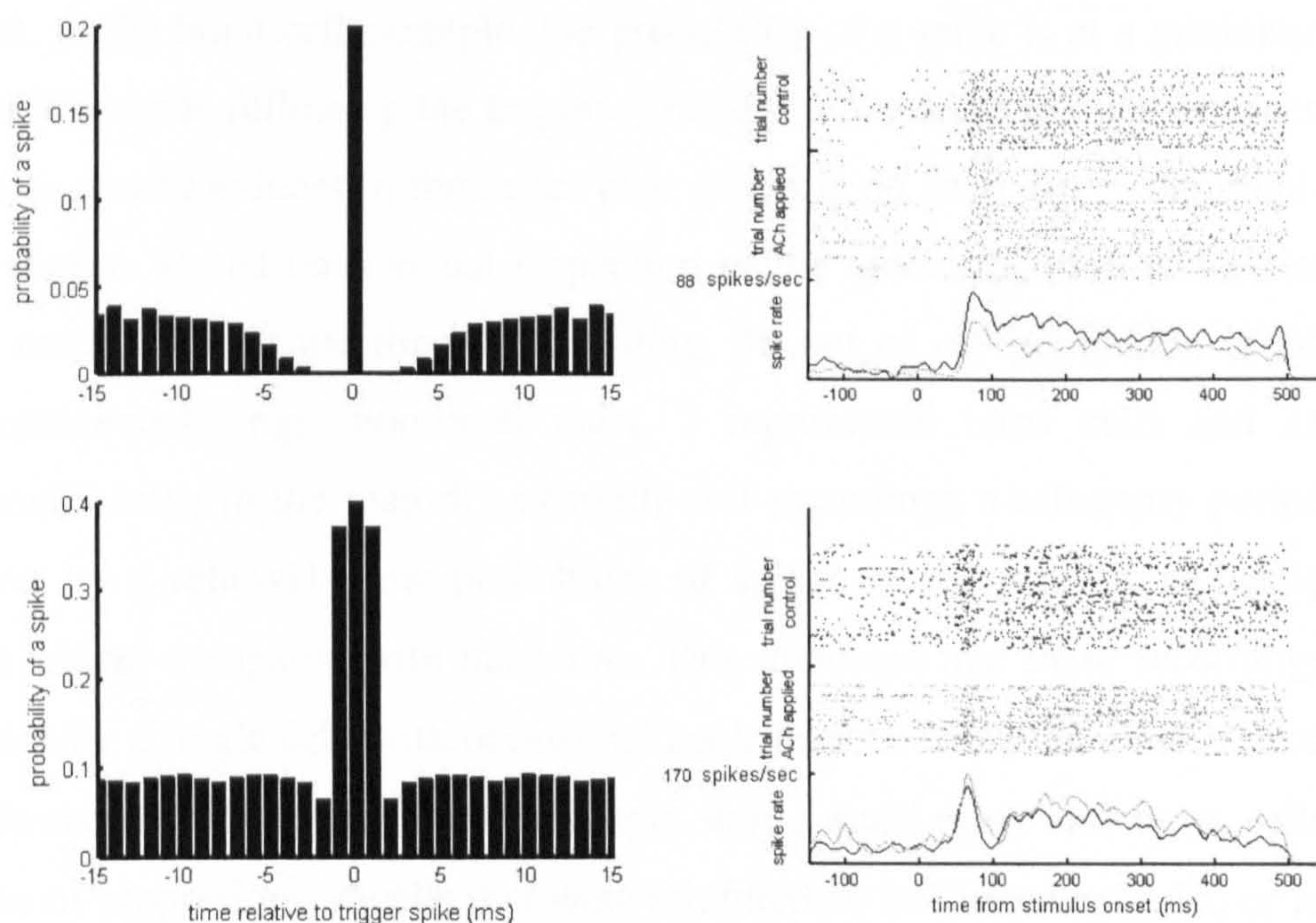


Figure 2.1 Example of autocorrelations for single unit (top row) and multi-unit (bottom row) activity. This analysis is done by making a histogram with 1msec time bins of each spike train relative to each spike in that train thus every spike in the train acts as the trigger. The central bin at 0msec always has a height of 1 (y-axis is truncated) because there is always a spike occurring at the time of the trigger

by definition. Bins to the left and right of the central bin are identical mirror images of each other. The height of the each bin shows the correlation, or probability of a spike occurring at that particular time before or after the trigger spike. The final plot in the row shows an example of the cell's response profile. Raster plots and histograms in grey show responses with ACh applied, plots in black show responses with ACh not applied. The x-axis shows the time following stimulus onset. The lower part of the y-axis shows firing rate in the histogram, the upper part shows trial number in the raster plots.

It might be argued that if the first bin following the trigger is not empty then the recording must be counted as a multi-unit. However, burst neurons can fire a second spike within 1.2-1.5msec and since I sampled at a rate of 1msec it was therefore likely that for these cells a second spike would occur within the first millisecond bin following the trigger. This could occur whenever the trigger spike occurred at the start of the first millisecond (e.g. 0.1msec after the bin onset). A second spike could occur up to 1.8msec later yet still be recorded in the bin nominally only 1msec following the trigger. I sorted burst cells from multi-units on the basis of a visual inspection of the raster plot, the overall shape of the autocorrelation within 100msec of the trigger, and according to notes taken at the time of the recording. Figure 2.2 shows examples of a burst cell autocorrelation and a multi-unit autocorrelation within 100msec of the trigger. In both examples spikes are highly likely to occur soon after the trigger, thus there is no evidence for a refractory period between individual spikes. The shapes of the autocorrelations are however quite different. In the burst cell example, the probability of a spike is at a minimum at 15 to 50 milliseconds following the trigger. This dip reflects the interval between bursts, which is clearly evident in the raster plot. There is no such dip in the multi-unit autocorrelation. Based on a visual inspection of the autocorrelation and raster plot, and on notes taken at the time of recording, 38 out of my population of 66 recordings represented single non-burst units, 7 represented burst cells and 21 represented multi-units. In the majority of multi-unit recordings a refractory period was evidenced by a relatively low probability of spikes in the bins immediately following the trigger compared with later bins. This indicated that these recordings were dominated by a single cell, with occasional contributions from a second or third cell. No differences were found between single units, multi-units and burst cells either in terms of proportions of cells that were inhibited or facilitated by ACh, or in terms of the effect of ACh on length tuning. Therefore no distinction is made between them for the remainder of the chapter.

Autocorrelation of a burst cell and a multi-unit

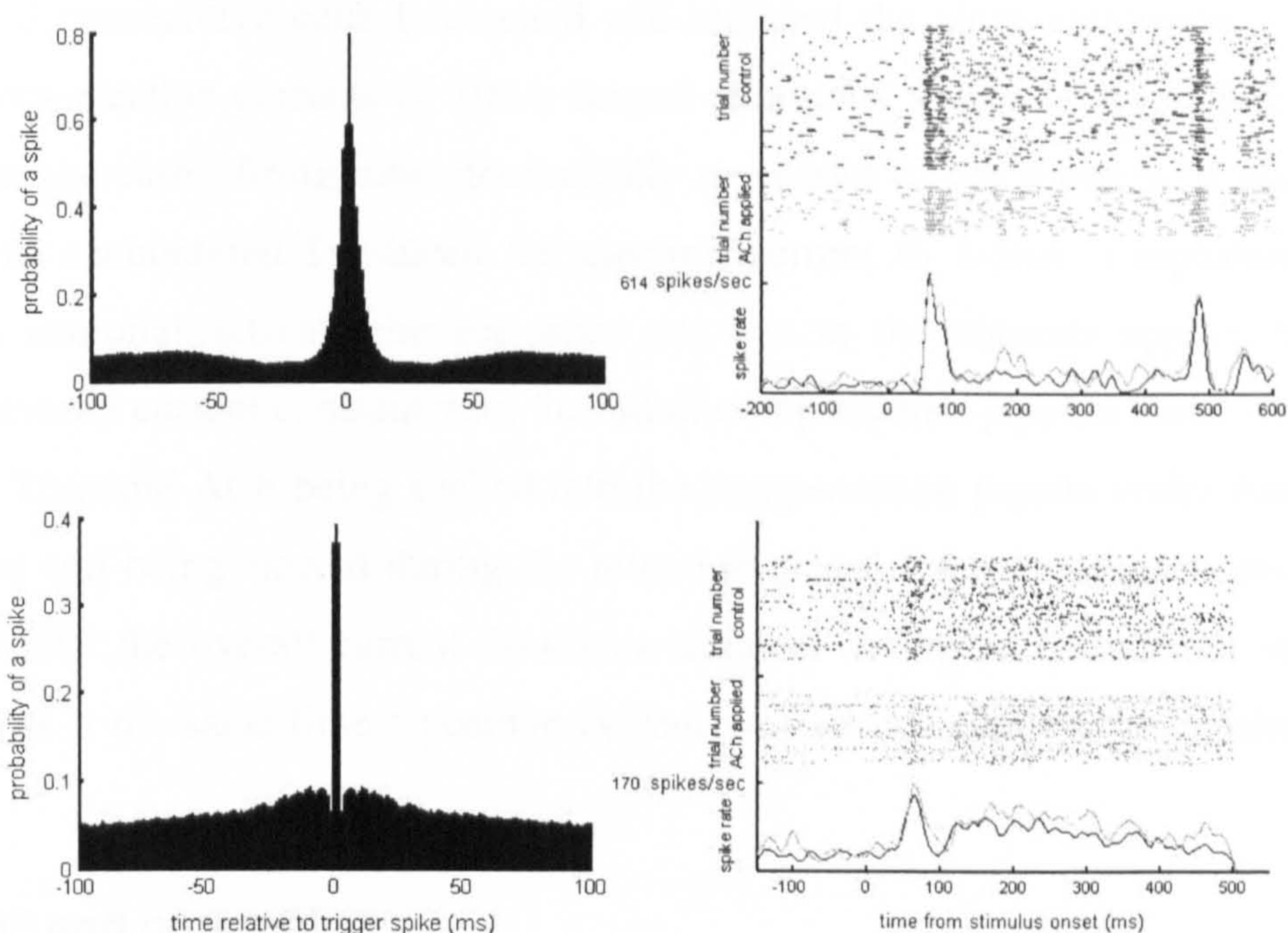


Figure 2.2 Autocorrelation and response profiles of a burst cell (top row of plots) and a multi-unit (bottom row). The multi-unit example is the same example shown in Figure 2.1. Notice that the maximum firing rate of the burst cell is much higher than the multi-unit example, demonstrating that firing rate alone cannot be used to distinguish multi-units from single units. The burst cell shown here was recorded as part of a separate experiment to the one reported in this chapter. In that experiment the effect of ACh application on the contrast tuning of V1 cells in a passively fixating alert macaque was investigated. I chose this example because the isolation of the cell was exceptionally good (a very high signal-to-noise ratio). Isolated burst cells were recorded in the marmoset experiments and are distinguishable on the basis of the autocorrelation and raster plots, however none were recorded with the exceptional quality of the isolation of the cell presented here.

2.3.3 Drug application

ACh was applied iontophoretically via a barrel pipette (5BBL W/FIL 1.2mm, World Precision Instruments, Inc.) onto which the recording electrode (Frederick Haer, FHC, 1-2M Ω) was mounted. The distance between the ACh pipette and electrode tips was 25 to 50 μ m. Pipette impedance was 10-30M Ω . ACh concentration was 0.8M (pH4.5). I applied retention currents of -10 to -5nA and ejection currents varied between +1nA and +100nA. Currents were applied by a Neurophore BH2 (Harvard Apparatus, Edenbridge, Kent, UK) device. I generally tried to adjust the ejection current depending on the strength of the effects of application. To do so I started with a relatively low ejection current (10-20nA), and monitored the effect on neuronal activity over time, while visual stimuli were presented. If the ejection current did not result in activity changes, I increased the current to 50-60nA and repeated the procedure. If no results were obtained using this application current, I

further increased the current to 80-100nA. If no ACh effects were obtained using this current strength I advanced the electrode/pipette to the next cell. If no effects were recorded for 3 consecutive cells I retracted and replaced the electrode/pipette. On some occasions ejection currents of 10nA caused enormous ACh effects, such that the cell either increased firing rates dramatically or ceased to fire entirely. If such behaviour was encountered I reduced the ejection current to 1-5nA. I repeatedly ensured that neuronal activity changes were not due to the currents applied by keeping the overall current constant with the aid of compensation pipettes filled with 0.9% saline. To avoid ACh being sucked into the compensation pipette under these circumstances and being ejected during the retention phase, I set the compensation currents such that the overall current flow was identical during ACh retention and ejection, whilst at the same time a positive current was always applied to the saline pipette.

2.3.4 Stimuli and protocol

Stimuli were displayed on a 20-inch analogue CRT monitor (75Hz, 1600x1200 pixels) positioned 57cm from the animal. They were presented on a grey background (24.6cd/m²). Stimuli were brighter or darker than the background, depending on cell preference (70% Michelson contrast). The receptive field borders (minimum response field, mRF) were mapped by moving a bar of adjustable size and orientation across the screen (Barlow et al. 1967; Maffei and Fiorentini 1976). mRF locations were within the central 10° for all neurons reported herein. mRF diameters ranged from 0.3° to 1.5°. After determining the cell's preferred orientation (at a resolution of 22.5°), bars of varying length and of the preferred orientation were presented centred over the mRF. Bar length was adjusted in 7 steps by multiples of the mRF diameter (0.5, 0.75, 1, 1.5, 2, 3, and 5 times mRF diameter in animals 1 and 2; 0.2, 0.4, 0.8, 1.6, 3.2, 6.4, 12.8 times mRF diameter in animals 3 and 4). Bar width was fixed at 0.15° for mRFs > 0.75°, and 0.05° for mRFs ≤ 0.75° diameter. To prevent adaptation of neuronal responses due to presentation of just one orientation, an additional four conditions were included in which bars orthogonal to the preferred orientation were presented (1.5, 2, 3, and 5 times mRF diameter in animals 1 and 2 and 1.6, 3.2, 6.4, 12.8 times mRF diameter in animals 3 and 4). I tested whether adaptation occurred by calculating a linear regression for each condition and recording (separately for initial, application, and control recording). I did find a very

small trend for negative regression slopes, i.e. decreasing activity as the experiment progressed (median slope: -0.0642, 25th percentile: -0.119, 75th percentile: 0.150). This means the median firing rate decreased very little over consecutive trials (less than 2% over 10 trials if the starting firing rate was 50 spikes/s), and if this decrease was due to adaptation it was unlikely to have influenced my general conclusions, because it was present for the initial recording, application and control. Additionally I inserted 3 to 5 minutes waiting times between recordings (initial recording, ACh application, recovery), which are also likely to be sufficient to eliminate adaptation between recordings. Stimuli were presented interleaved at least 15 times each. The presentation time of the stimuli was 500msec with 500msec pre- and 200msec post-stimulus time. Stimuli were presented and spike timings were collected with a sampling resolution of 1msec under the control of Remote Cortex 5.95 (Laboratory of Neuropsychology, National Institute of Mental Health, Bethesda). Recordings were performed during monocular stimulation. Spontaneous activity was calculated from the pre-stimulus time separately for ACh applied and ACh not applied.

2.3.5 Length tuning data

All stimulus-driven activity presented here was corrected for spontaneous activity. This was done to fulfill the assumption in the fitting models that the response is zero at zero bar length (no stimulus). I could have left responses uncorrected for spontaneous activity if I had included an additional 'offset' term to the fitting models. Length tuning was initially measured with no external ACh applied (control condition), at least once with ACh applied, and subsequently in at least one repeated control condition. Neuronal activity was compared across control (i.e. ACh not applied) conditions to ensure that full recovery following ACh application occurred ($p > 0.05$, 2-way Kruskal Wallis ANOVA). Cells that showed significant differences across control conditions ($p < 0.05$) were excluded from further analysis. This was done because cells that showed differences across control conditions may have been affected by some factor other than the drug application (drift of the tissue relative to the electrode, for example). Apparent differences between ACh-applied conditions and control conditions could then have been due to this additional factor rather than the drug application. Alternatively, differences between control conditions may have been due to a long-term drug effect persisting for many minutes after drug application had stopped. As there is no means to

discriminate drift effects from a long-term drug effect, these cells were discarded. For the remaining cells, data from control conditions were combined and compared with data obtained during ACh application. Only cells that showed a significant effect of drug application were included for further analysis. For a cell to be included it was sufficient either that the spontaneous activity was significantly affected by ACh, or that the response to the presentation of any of the bars of the preferred orientation was significantly affected by ACh application ($p < 0.05$, 2-way Kruskal-Wallis ANOVA). Cells that did not show a significant effect of ACh on firing rate were not included for further analysis.

2.3.6 Difference of Gaussian model

Length tuning data was fitted with a difference of Gaussians model (DOG) model, (Sceniak et al. 2001). In this model the narrower Gaussian represents the RF's excitatory centre whilst the broader Gaussian represents the inhibitory surround. Each Gaussian is described by a strength constant (gain) and a space constant, determining its height and width respectively. The response to a bar length is taken as the difference between the integrals of the area of each mechanism, up to the size of the stimulus (Figure 2.3). This function captures the shape of measured length tuning curves and it allows the relative contribution and size of excitation (summation) and inhibition areas to be separated. The fitted function is of the form:

$$m = K_e * (1 - \exp^{-(2x/a)^2}) - K_i * (1 - \exp^{-(2x/b)^2}) \quad (\text{Equation 2.1})$$

where 'm' corresponds to the model's response to a bar of length 'x', 'K_e' corresponds to the excitatory component amplitude (named 'summation gain' hereafter), 'a' corresponds to the size constant of excitatory area (named 'summation area'), 'K_i' corresponds to the inhibitory component amplitude (named 'inhibitory gain'), and 'b' is the size constant of the inhibitory area (named 'inhibitory area'). Separate examination of each parameter's contribution to the shape of the fitted function allows for a better understanding of the model. In Figure 2.3, for a hypothetical response curve I varied each of the four parameters separately to investigate their influences on the length tuning curve. All four parameters had an impact on the location of the peak of the function, however the impact of the

summation area was by far the greatest. Fits of the summation area and inhibitory area were constrained such that the inhibitory area was larger than the summation area. I constrained the maximum size of the inhibitory area to be 30 times the mRF diameter. I have tested different constraints, i.e. allowing these areas to become substantially larger (no constraints, size diameters 12.8 times and 20 times the mRF diameter) with the same general outcome, as described in section 2.4.2 *DOG fitting* and 2.4.3 *ROG fitting*.

Demonstration of the difference of Gaussians (DOG) model

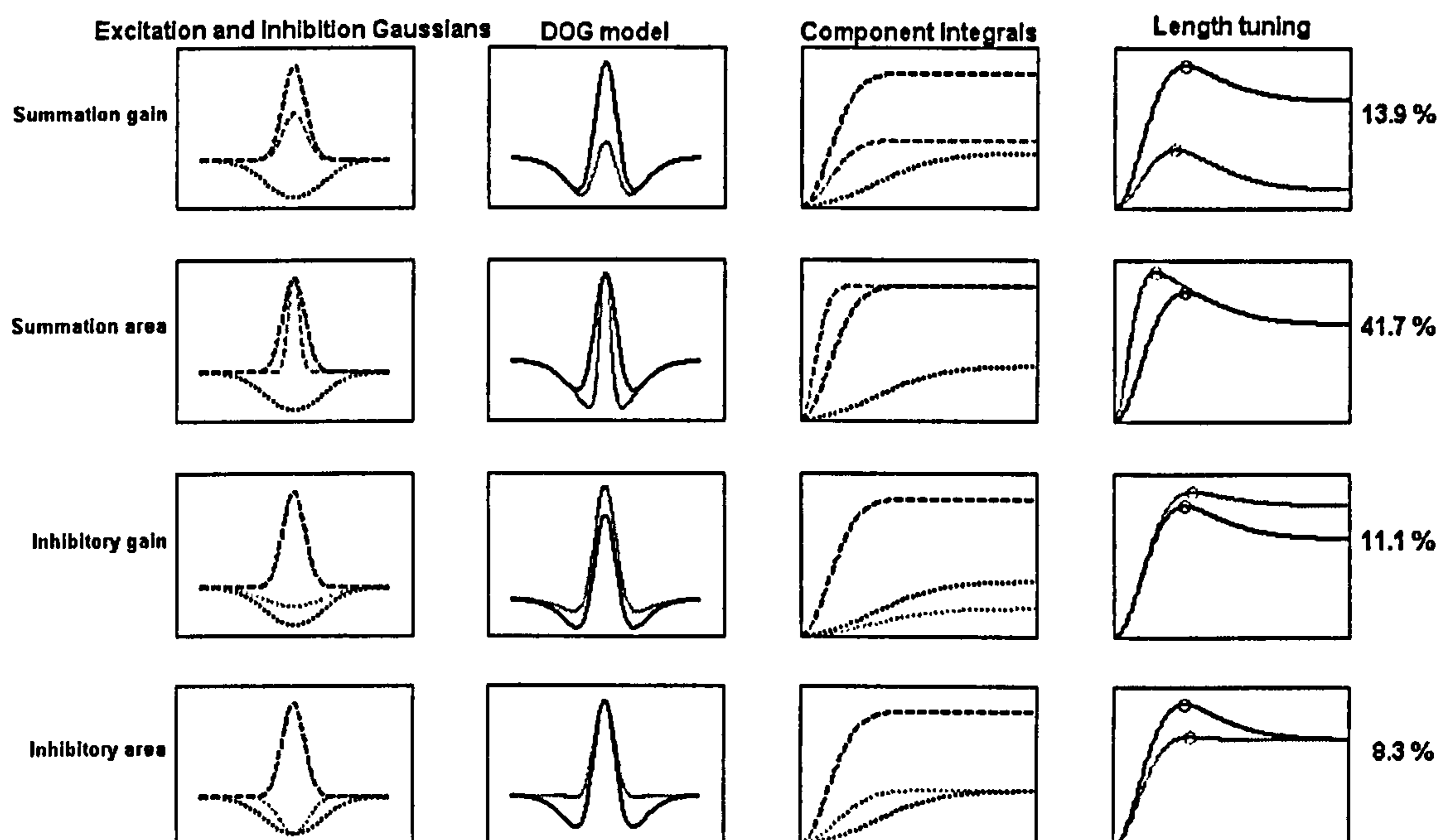


Figure 2.3 The influence of each fitting parameter in the DOG model on a hypothetical response curve. For each row of plots one parameter is varied (indicated at the left end of the row). The grey curve shows the model with the varied parameter set to half its value in the black curve. The first column of plots on the left shows separate excitatory (dashed lines) and inhibitory (dotted lines) Gaussians. The inhibitory Gaussian is inverted. The next column shows the difference between the excitatory and inhibitory Gaussians. This model represents the RF profile. Curves in the next column represent integrals of the separate components (excitatory in dashed line, inhibitory in dotted). Curves on the final column show the difference between the integrals. This curve is fitted to the length data. Preferred length (corresponding to the location of the peak) is marked with a circle on the curve. To the right of each plot is the percentage of horizontal peak shift associated with halving the specified parameter.

2.3.7 Ratio of Gaussians model:

An alternative description of spatial integration can be given by a ratio of Gaussians Model (ROG) (Sceniak et al. 2001; Cavanaugh et al. 2002). It is principally similar to the difference of Gaussians model, but instead of assuming a

linear combination of excitatory and inhibitory mechanisms, the ROG model assumes that the influence of the suppression area is a normalization:

$$m = \frac{K_e * (1 - \exp^{-(2x/a)^2})}{1 + K_i * (1 - \exp^{-(2x/b)^2})} \quad \text{(Equation 2.2)}$$

where again 'm' corresponds to the model's response to a bar of length 'x', 'K_e' corresponds to the summation gain, 'a' corresponds to the size of the summation area, 'K_i' corresponds to the inhibitory gain, and 'b' is the size of the inhibitory area. The influences of each parameter on the fitted function are different in the ROG model to the DOG model; most notably the only parameters to influence the location of the peak of the function are the summation area and the inhibitory gain. The summation gain and the size of the suppressive area have no influence (Figure 2.4) Compared with the DOG model, the influence of the summation area on the location of the peak is slightly weaker while the influence of the inhibitory gain is slightly stronger.

Demonstration of the ratio of Gaussians (ROG) model

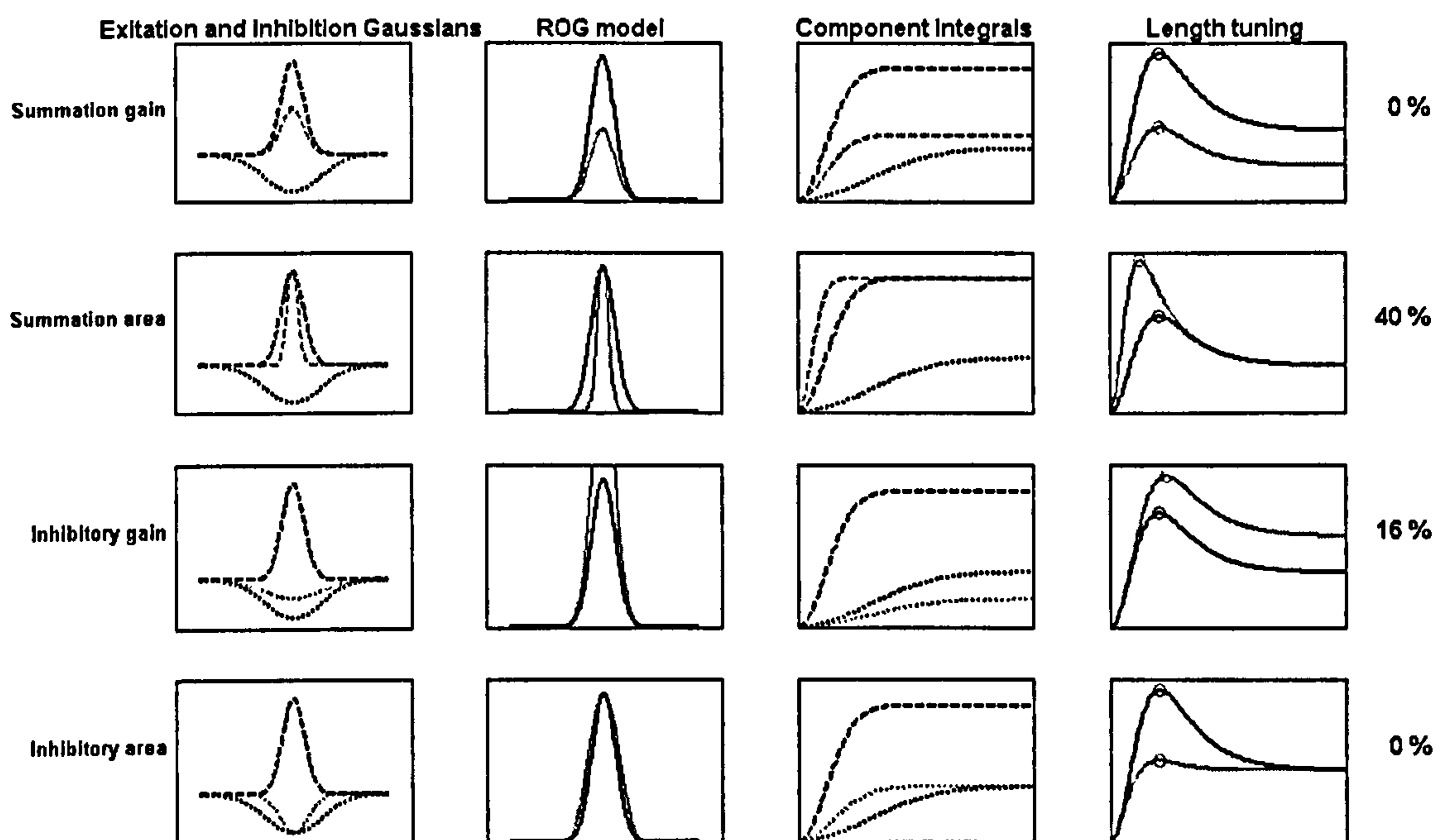


Figure 2.4 The influence of each fitting parameter in the ROG model on a hypothetical response curve. For each row of plots one parameter is varied (indicated at the left-hand end of the row). The grey curve shows the model with the varied parameter set to half its value in the black curve. The only parameters that influence the location of the peak length are the summation area and the inhibitory gain. As in the DOG model, the summation area has the largest effect. Halving the inhibitory gain has a slightly larger impact on the location of the peak in the ROG model than in the DOG model whilst halving the summation area has a slightly smaller impact in the ROG model than in the DOG model. The characteristic ‘Mexican hat’ shape seen in the DOG model is not present in the ROG. This is because once the excitatory mechanism falls to zero, dividing it by any value only produces zero.

2.3.8 Fit optimisation

I have used various optimising strategies to fit the models. I first fitted the data to minimise the summed squared error (SSE) between the model’s prediction and the mean of the recorded firing rates (spikes per second over 500msec) at each bar length. This method is fast and conceptually simple. Fitting to the mean alone however does not place any importance on the reliability of the data. To control for this I then optimised the fits to minimize the χ^2 error (Press et al. 2002) in which the error between the model and data at each bar length is weighted by the variance of the firing rate. Errors between the model and data are given greater weight where the variance is low. This method presents a challenge since the measured variance is only an estimate of the true variance and may be a rather poor estimate since I had a minimum of just 15 observations. I increased the confidence in my estimate of response variance by estimating the variance across the whole population of data. Since response variance is generally proportional to the firing rate (Carandini et al. 1997), I estimated the variance by fitting a polynomial function to the variance versus mean firing rate data separately for data from ACh-applied conditions and control conditions.

$$\text{var} = a * \text{mean}^b \quad \text{(Equation 2.3)}$$

The estimates for the parameters ‘a’ and ‘b’ were different for the two conditions (ACh not applied, $\text{var}=5.6328*\text{mean}^{1.1513}$; ACh applied, $\text{var}=12.9191*\text{mean}^{0.9505}$, see Figure 2.5). I used these fitted values to estimate the true variance for each cell at each bar length, based on the recorded mean activity. To avoid giving too much importance to data points with low firing rates I set all variance values less than 1 to be equal to 1.

Relationship between response mean and response variance

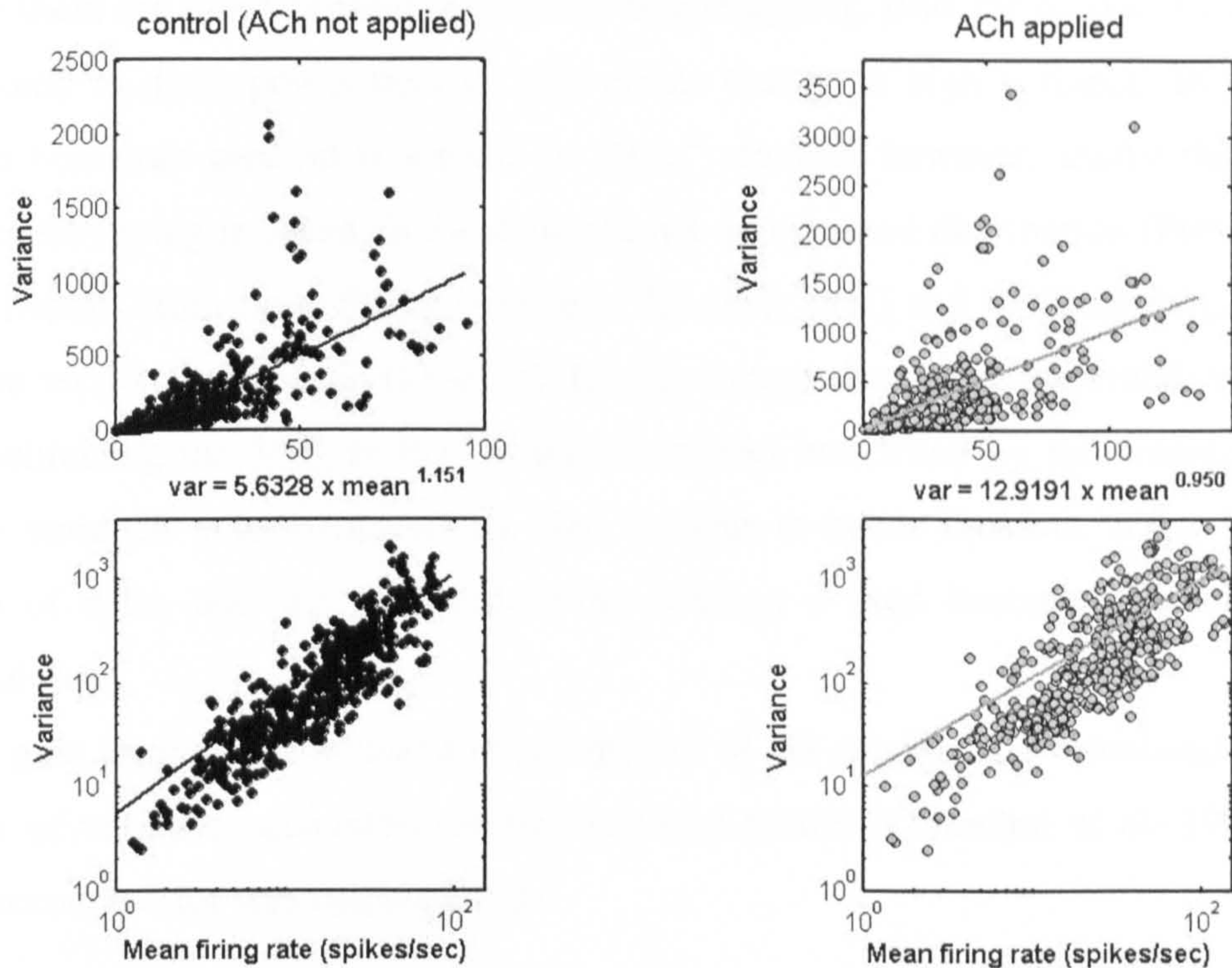


Figure 2.5 Relationship between response mean and response variance. Upper plots show data plotted on linear scales, lower plots show data plotted on a log-log scale; here variance is proportional to the mean. Data from ACh-applied conditions are shown in the right plots (grey points and grey line), data from conditions with ACh not applied are shown in the left plots (black points and black line). The solid line is the polynomial function used to estimate the true response variance based on the response mean. This estimate was used for the χ^2 fitting. The values of the fitted parameters are given in the middle of the figure on the left and the right for control condition and ACh-applied condition data respectively.

The χ^2 method presents an additional problem since measures of mean and variance assume that the underlying distribution of the data is a Gaussian. This may not be a valid assumption (consider, for example, a cell whose mean firing rate is low but has a relatively high variance: the estimated variance may place the lower bound below zero spikes per second). To get a better estimate of the true distribution based on the data, I fitted models to the data using a bootstrap method. To do this, for each stimulus condition I selected a set of 15-45 trials (depending on the number of repetitions measured for the respective cell) at random (random with replacement), and performed the model fitting by minimising the SSE between the model and the mean response across this selection of trials. The bootstrapping procedure was performed 100 times for each cell when ACh was applied and 100 times for when it was not applied, thus resulting in 100 different estimates of preferred length for each condition, and 100 estimates of each of the four fitting parameters with ACh applied

and with ACh not applied for each cell recorded. Data points that have less variance attached to them are more constant across the bootstrapping, thus the output is more closely related to these points than to data points that have high variance. In this respect the bootstrap method is similar to the χ^2 method, however, unlike the χ^2 method, bootstrapping is based on the data and not an assumed distribution (Press et al. 2002). Results from three fitting strategies, for both DOG and ROG models, are presented in section 2.4 *Results*: in the first fitting strategy the model was fitted to the data by minimising the SSE, in the second the model was fitted by minimising χ^2 where the variance was estimated by the variance-to-mean function across the population of cells, and for the third fitting strategy I used bootstrap fitting as described above.

To gain an intuitive measure of the quality of the model fit, I calculated the percentage of variance accounted for by the fitted model (Carandini et al. 1997). Variance accounted for was calculated as:

$$\% \text{Variance} = 100 \times \left(1 - \frac{D(m,r)}{D(R,r)} \right) \quad (\text{Equation 2.4})$$

where ‘D(m,r)’ corresponds to the mean squared difference between the model predicted response (‘m’, see Equations 2.1 and 2.2) and the observed mean firing rate (‘r’) at each bar length with and without ACh application, and ‘D(R,r)’ corresponds to the mean squared difference between the grand mean firing rate (‘R’, calculated across bar lengths with and without ACh application) and mean firing rate at each stimulus, separately for both the ACh-applied conditions and control conditions. Thus ‘D(m,r)’ corresponds to the difference between the model prediction and the data and ‘D(R,r)’ corresponds to the variance of mean responses across stimulus and drug application conditions. I calculated D(m,r) and D(R,r) as:

$$D(m,r) = \frac{1}{N} \sum_s |m_s - r_s|^2, \quad (\text{Equation 2.5})$$

$$D(R,r) = \frac{1}{N} \sum_s |R - r_s|^2, \quad (\text{Equation 2.6})$$

In both cases the sum is over the range of stimuli and conditions 's'; 'N' is the number of stimuli multiplied by two (ACh-applied conditions and control conditions). To give an example, if the mean difference between the model prediction and the observed data is small (e.g. $D(m,r) = 10$ spikes/sec) and the variance in the mean responses to each bar length and between the attend-RF and attend-away conditions is large (e.g. $D(R,r) = 100$ spikes/sec) then the percentage of variance that is accounted for by the model is large (in this example 90%).

In order to increase the probability that my fitting routine would yield small error values (and thus good fits), I initially fitted the models with a set of 24 different starting positions for the different parameters. The starting parameters that resulted in the smallest error were used for the final optimization. Empirical evidence showed that starting parameters needed to be different for the DOG and the ROG models to produce adequate fits with small errors, and were thus different for the two models.

2.3.9 Tonic index

To determine whether ACh changed the response profile of a cell, I calculated a 'tonic index' ('TI') as the mean firing rate during the late response period (' R_{late} ', 250-500msec after stimulus onset) divided by the firing rate during the early response period (' R_{early} ', 30-250msec after stimulus onset).

$$TI = \frac{R_{late}}{R_{early}} \quad (\text{Equation 2.7})$$

High values of this index indicate a tonic (sustained) response profile whilst low values indicate a phasic response. I calculated TI from responses recorded in the presence of externally-applied ACh and from responses recorded with no ACh applied.

2.4 Results

We recorded the length tuning of a total of 120 neurons. Of these, 66 units showed a significant effect of externally-applied ACh on firing rate ($p < 0.05$, 2-way Kruskal Wallis ANOVA), and a return to baseline following recovery. How many of the remaining 54 neurons were unaffected by ACh is impossible to say, because the pipette may either have leaked occasionally causing high ambient ACh levels

throughout individual recordings, or it may have been blocked despite current flow across the tip. Due to these difficulties I did not attempt to quantify the number of neurons that were susceptible to ACh application. Application of ACh caused a facilitation of responses in 41 out of 66 (62.1%) units and suppression in 25 out of 66 units (37.9%) compared to control conditions. This number is comparable with reports from earlier studies (Sillito and Kemp 1983; Sato et al. 1987; Sillito and Murphy 1987; Murphy and Sillito 1991).

To determine the preferred length, the summation area, the inhibition area, and the excitatory and inhibitory gains, I fitted the data with a difference of Gaussians (DOG) model and with a ratio of Gaussians (ROG) model using three fitting strategies (see methods). These models capture length tuning properties and provide independent estimates of the relative strength and size of the summation and inhibitory areas (Sceniak et al. 1999; Cavanaugh et al. 2002). Both models provided good fits to the data (the median variance accounted for was >90% for both models under all fitting strategies, see Table 2.1). Across the population the ROG model yielded marginally better fits under all fitting strategies, demonstrated by lower residual error values (Figure 2.6) and a higher percentage variance accounted for (Table 2.1). Comparing the residual errors between the ROG and DOG models in a pair-wise fashion (i.e. errors after fitting the two models to the same data) showed that the reduction in errors was only significant for the SSE fitting. The difference between the DOG and ROG models was not significant in the χ^2 and bootstrapping strategies, suggesting that the ROG model loses its superiority once the variance in the data is taken into account (although errors were still on average lower in the DOG model). Based on these marginal differences between the quality of fits for the DOG and ROG model I do not attempt to determine which of the two is a better descriptor of V1 spatial integration. The important finding is that the two models yielded similar results regarding the effects of ACh application on length tuning, as detailed below.

Comparison of fit quality from DOG and ROG models

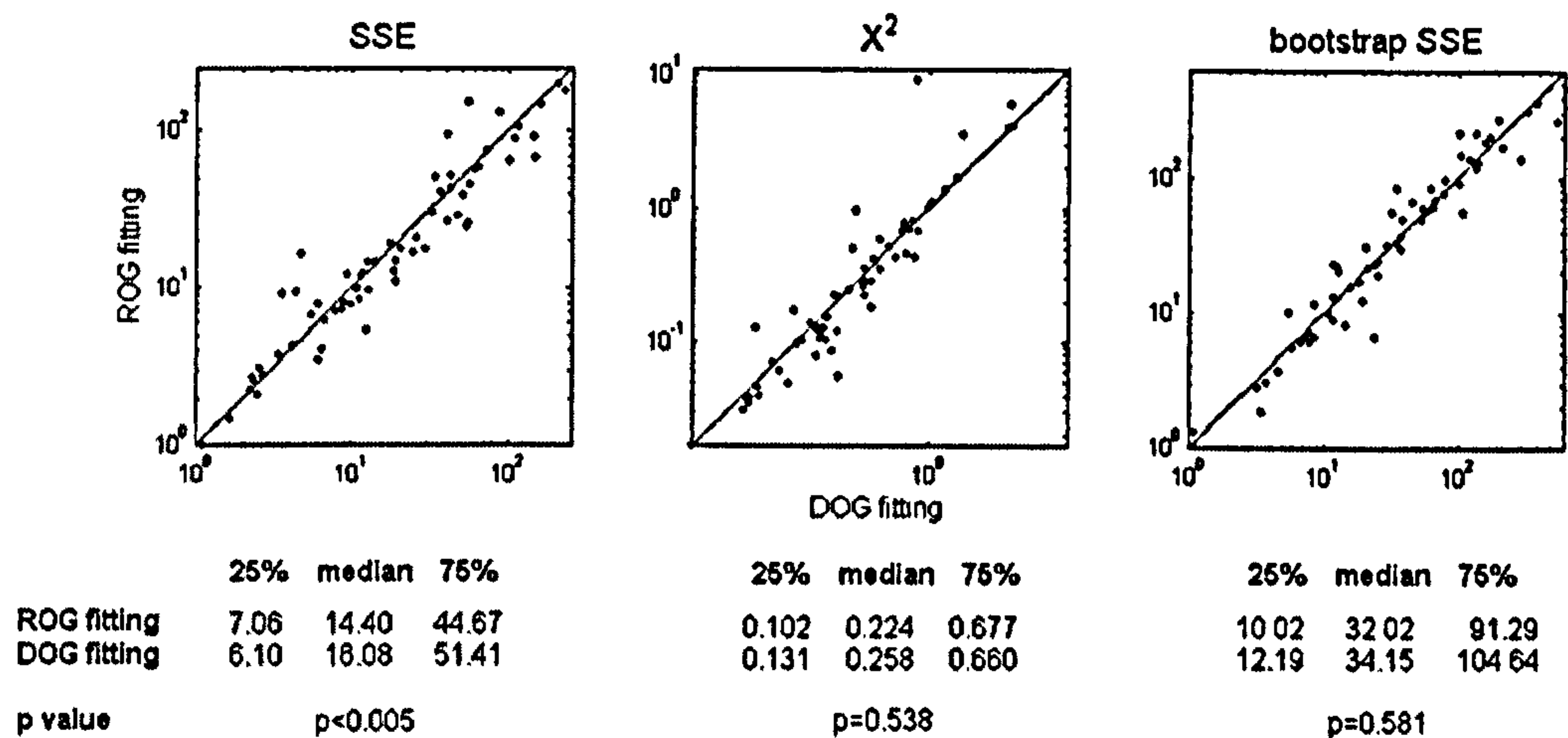


Figure 2.6. Comparison of residual errors between ROG and DOG models using the three fitting strategies. For each cell the residual error from fitting the ROG model is plotted on the y-axis and the residual error from fitting the DOG model is plotted on the x-axis. Residual error in each case refers to the value which is minimised in the fitting strategy. In the bootstrap fitting, the plotted value is the median summed squared error (SSE) taken across the bootstrapping. Below each plot are the 25, 50 and 75th percentile residual errors. The p-value tests for a difference in the residual error between the two models (signed rank test).

Comparison of fit quality from DOG and ROG models using three fitting strategies

DOG	25%	50%	75%		ROG	25%	50%	75%
SSE fit	91.6	96.2	98.4		SSE fit	92.3	96.6	98.6
χ^2 fit	87.5	94.1	97.9		χ^2 fit	90	94.6	97.8
bootstrap	91.9	95.3	98.8		bootstrap	90.8	95.6	98.2

Table 2.1. Median (50%), upper (75%) and lower (25%) quartiles of percentage variance explained by fitted models. Table to the left shows data from the DOG model under the three fitting strategies. Table on the right shows data from the ROG model under the three fitting strategies.

2.4.1 Length tuning

For the majority of cells (69.7%), the highest activity with ACh absent occurred at bar lengths greater than the diameter of the minimum response field (mRF), demonstrating that the area surrounding the mRF facilitated the response to long bars of the preferred orientation. With ACh present the preferred length tended to shift towards shorter bars (Figure 2.7), suggesting that ACh reduced modulation from outside the mRF. To quantify this effect I fitted the data with a DOG and a ROG model using three different fitting strategies (see methods). Preferred length

was taken as the peak of the fitted curve. The finding that preferred length was reduced during ACh application was supported by both models in all three fitting strategies (Figures 2.8 and 2.9 left column, Tables 2.2 and 2.3 in Appendix), thus the reduction in preferred length was a highly robust finding. The effects of ACh on the model fitting parameters were somewhat dependent on the model and the fitting strategy used. Since I find a reduction of preferred length in facilitated and inhibited cells (Tables 2.2 and 2.3 in Appendix), the result is unlikely to be due to response saturation. Interestingly I found that the preferred length of cells inhibited by ACh tended to be somewhat longer than the preferred length of cells facilitated by ACh (cells inhibited: median preferred length = 3.15 times mRF diameter, 25th percentile = 0.94, 75th percentile = 5.0; cells facilitated: median preferred length = 1.65 times mRF diameter, 25th percentile = 0.9, 75th percentile = 3.87), although the difference was not significant ($p=0.13$, 2-sample t-test).

Examples of the effect of ACh application on length tuning in facilitated and inhibited cells

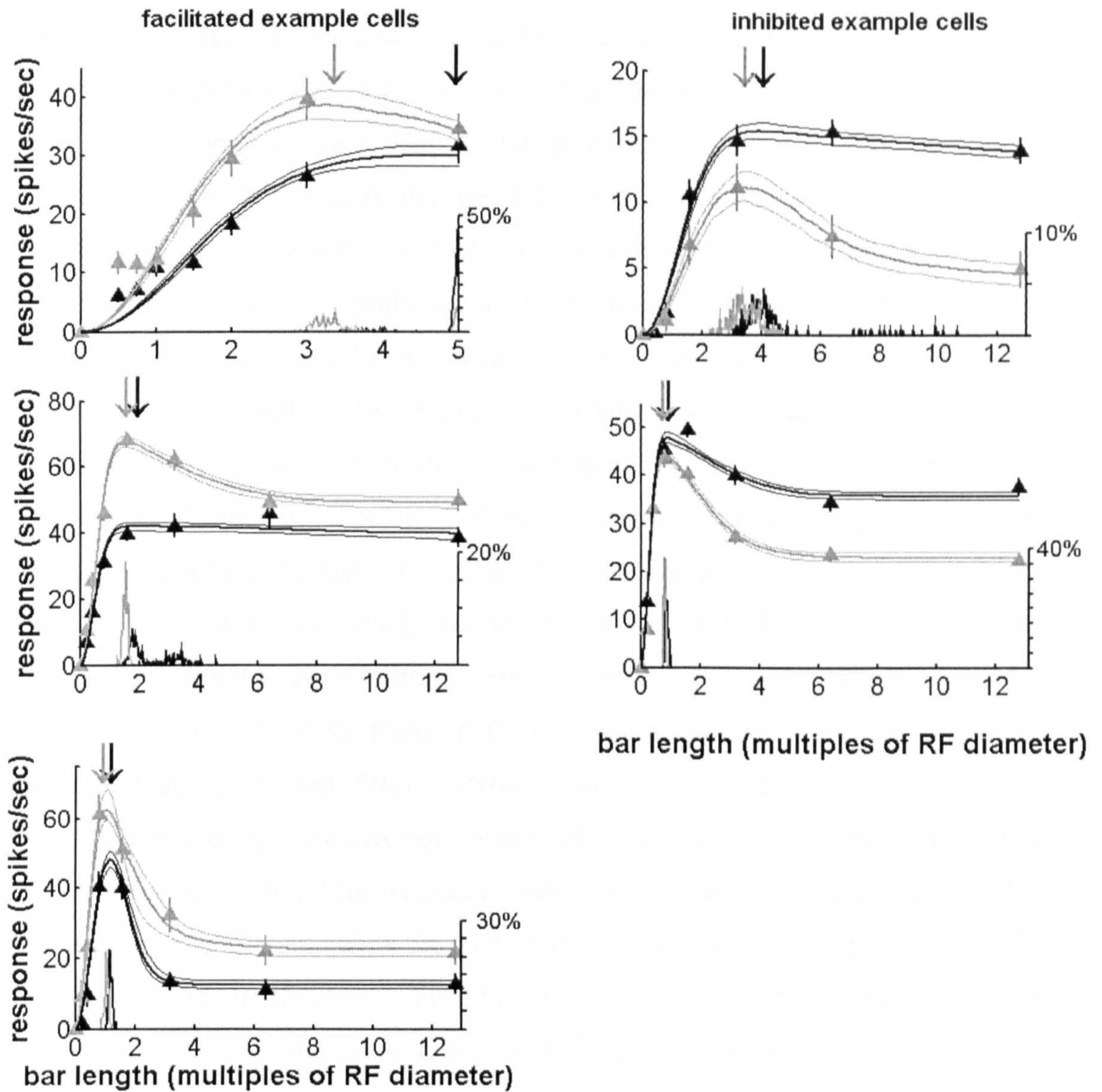


Figure 2.7 Single cell examples of the effect of ACh application on length tuning. Mean stimulus-driven response to seven stimuli of varying length during ACh application (grey) and during control conditions (black). Triangles show the mean response, error bars show standard error. The heavy line fitted to the data shows the median fitted DOG model from the bootstrap procedure, narrow lines fitted to the data show the upper and lower quartiles. In the three examples on the left of the figure, responses were stronger for all stimuli during ACh application (especially for the shortest stimuli). In the two examples on the right, responses were inhibited for all stimuli but especially for the longest stimuli. Vertical arrows mark the preferred length, taken as the median peak of the fitted curve across the bootstrapping. The preferred length was shortened with ACh present. The histograms at the base of the graphs show the distribution of preferred length obtained by the bootstrap method during ACh application (grey) and during control conditions (black). The height of the histogram is shown on the right of each plot.

2.4.2 DOG fitting

I used a DOG model and a ROG model to quantify how ACh application affected length tuning. The reduction of preferred length was largely due to a decrease of the summation area (Figure 2.8 and Table 2.2 in Appendix). This was found to be reduced under all three fitting strategies. The trend was not significant below the 0.05 level in the χ^2 fitting strategy ($p=0.099$) but was significant in the SSE ($p=0.041$) and bootstrap fitting ($p=0.019$). Separately examining cells facilitated by ACh and cells inhibited by ACh (Table 2.2) showed that the reduction in summation area was only significant for facilitated cells (SSE $p=0.02$, χ^2 $p=0.009$, bootstrap $p=0.026$) and not for inhibited cells (SSE $p=0.946$, χ^2 $p=0.527$, bootstrap $p=0.353$). This is unlikely to be due to the small sample size of the inhibited population, since the p-value for the whole population of cells is larger than the p-value for the facilitated population alone, indicating that including the inhibited population weakened the trend for reduced summation area. There was a trend for increased summation gain which was significant in the SSE and bootstrap fitting strategies but absent in the χ^2 fitting ($p=0.513$). Summation gain was not affected in cells inhibited by ACh (SSE fitting $p=0.51$, bootstrap $p=0.412$) but was significant among facilitated cells (SSE fitting $p=0.041$, bootstrap $p=0.033$).

The inhibitory area was not consistently affected by ACh under any fitting strategy. There was a trend for increased inhibitory gain during ACh application. The trend was only significant below the 0.05 level in the bootstrap fitting ($p=0.022$). The trend approached significance in the SSE fitting ($p=0.075$) and was absent from the χ^2 fitting ($p=0.333$). When facilitated and inhibited cells were examined separately the trend was not significant for either population, although it approached significance for inhibited cells in the χ^2 fitting ($p=0.058$) and for facilitated cells in the bootstrap fitting ($p=0.088$).

To summarise the DOG fitting: the most consistent finding was a reduction in preferred length during ACh application. For facilitated cells the reduction in preferred length was largely mediated by a reduction in the summation area. For inhibited cells the reduction in preferred length must have been mediated by a combination of changes in different fitting parameters in different cells, since no parameter was consistently affected across the population by ACh application.

Effect of ACh on DOG fitting parameters

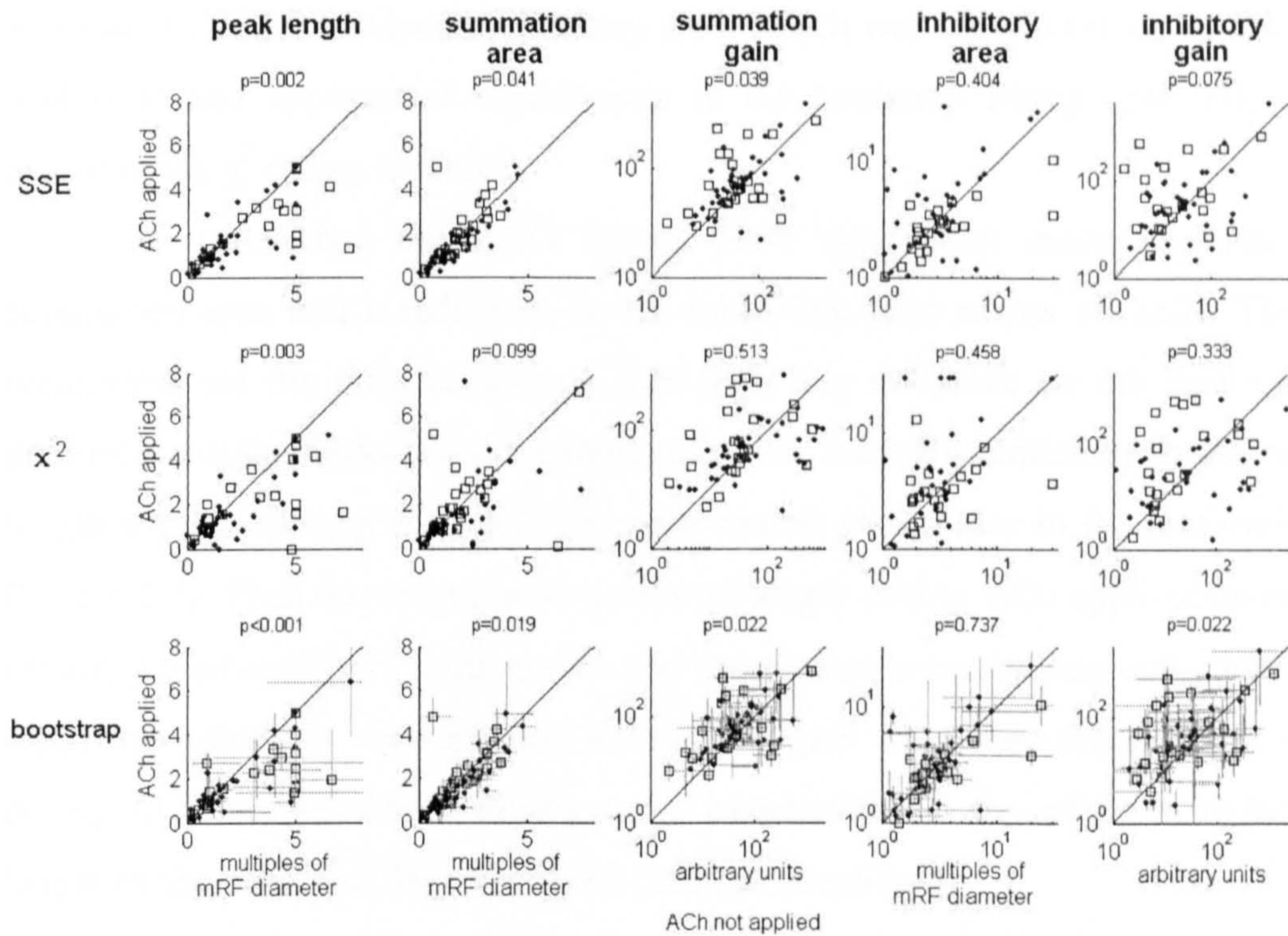


Figure 2.8 Preferred length and fitting parameters as a function of ACh application, extracted from the difference of Gaussians model (DOG) using three different fitting strategies. The first row shows the model's output when fitted to minimise the summed squared error (SSE) between the model and the mean response. The second row shows the output when the model was fitted to minimise the χ^2 error. The third row shows the median (circle or square) and upper and lower quartiles (error bars) of the model's output when fitted using a bootstrap procedure. In each plot, cells inhibited by ACh are marked with an open square, and facilitated cells are marked with a filled circle. The value of the parameter of interest (column titles) without ACh applied is shown on the x-axes, and the value with ACh applied is shown on the y-axes. Cells in which the parameter of interest was reduced by ACh application appear below the diagonal. Above each plot, the p-value gives the significance of differences in the parameter of interest between ACh-applied conditions and control conditions across the population (signed rank test).

2.4.3 ROG fitting

In the ROG model the reduction in preferred length was largely due to a reduction in the summation area. Unlike in the DOG model, the trend was highly significant both for facilitated and inhibited cells (Table 2.3 in Appendix). Also contrary to the DOG model, there was a trend towards reduced summation gain across the population. This trend was absent in cells facilitated by ACh (SSE $p=0.354$, χ^2 $p=0.069$, bootstrap $p=0.35$); for cells inhibited by ACh the trend was highly significant in the SSE and bootstrap fitting (SSE $p<0.005$, bootstrap $p<0.005$), but not significant in the χ^2 fitting ($p=0.058$). There was a trend for reduced inhibitory gain across the population, which was significant for all three fitting strategies (SSE $p=0.035$, χ^2 $p=0.016$, bootstrap $p=0.016$). The trend was evident

amongst both facilitated and inhibited cells (Table 2.3). Among inhibited cells there was also a trend for reduced inhibitory area, which was significant in the SSE fitting ($p=0.014$) and approached significance in the bootstrap fitting ($p=0.05$), but was absent in the χ^2 fitting ($p=0.33$).

To summarise the ROG fitting: ACh application caused a reduction in summation area and a reduction in the inhibitory gain across all cells. These two parameters are the only parameters that have any influence on the location of the preferred length. Reducing the summation area causes a reduction in the preferred length whilst reducing the inhibitory gain causes an increase in the preferred length (Figure 2.4). Thus the reduction in preferred length during ACh application is almost certainly mediated by a reduction in the summation area. Among cells inhibited by ACh, the inhibitory area and the summation gain were also significantly reduced during ACh application. Reducing these parameters has the effect of reducing the height of the peak, but does not affect the peak location.

Effect of ACh on ROG fitting parameters

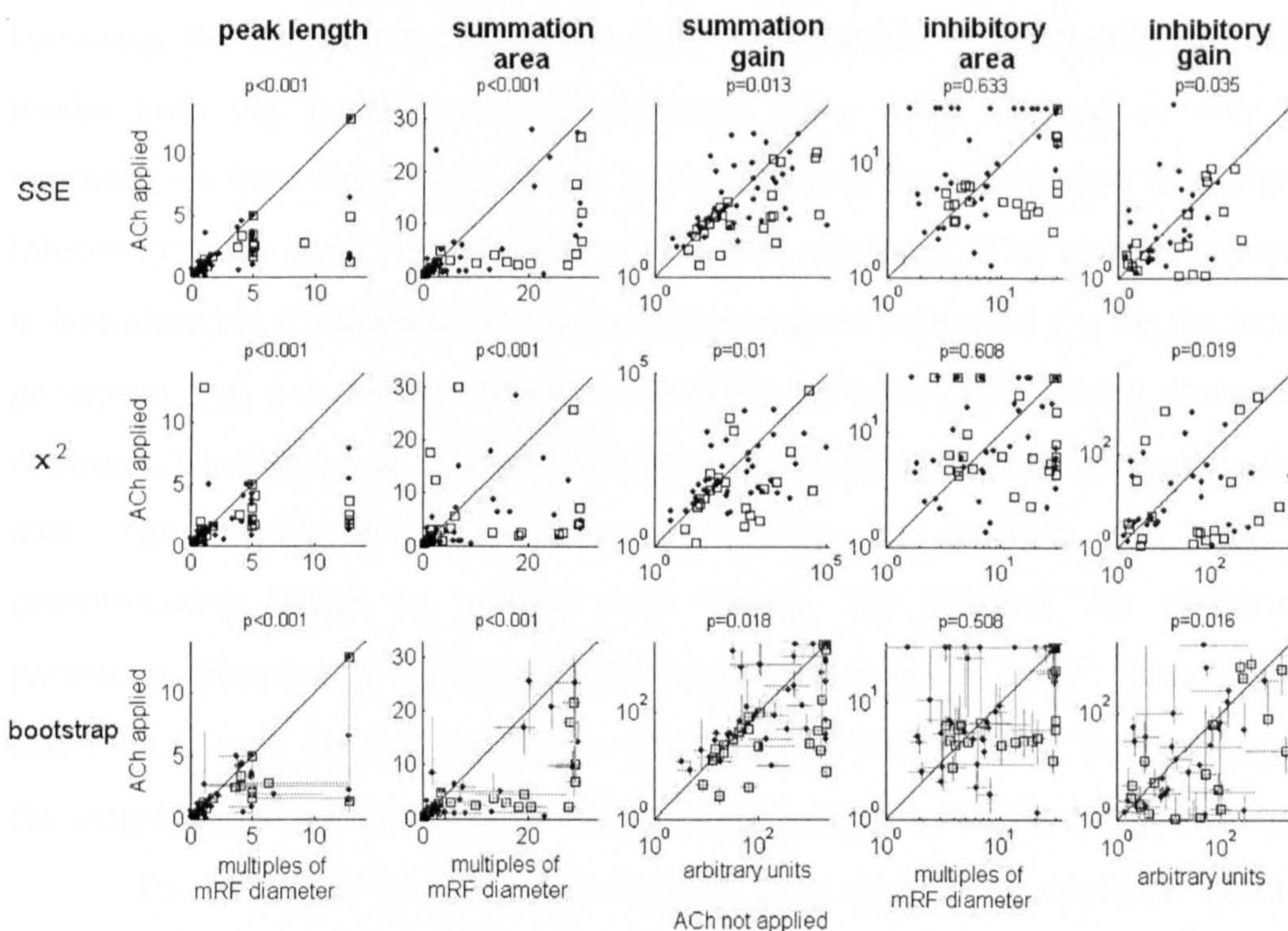


Figure 2.9 Preferred length and fitting parameters as a function of ACh application, extracted from ratio of Gaussian model (ROG) using three different fitting strategies. The first row shows the model's output when fitted to minimise the summed squared error (SSE) between the model and the mean response. The second row shows the output when the model was fitted to minimise the χ^2 error. The third row shows the median (square or circle) and upper and lower quartiles (error bars) of the model's output when fitted using a bootstrap procedure. In each plot, cells inhibited by ACh are marked with an open square, and facilitated cells are marked with a filled circle. The value of the parameter of interest (column titles) without ACh applied is shown on the x-axes, and the value with

ACh applied is shown on the y-axes. Cells in which the parameter of interest was reduced by ACh application appear below the diagonal. Above each plot, the p-value gives the significance of differences in the parameter of interest between ACh-applied conditions and control conditions across the population (signed rank test).

2.4.2 Mechanism for reduced preferred length

In a recent paper, Cavanaugh et al. (2002) have argued that contrast-induced changes in size tuning were not due to changes in the size of the summation or suppression area, but rather due to changes in the gain of these mechanisms. They fitted the ratio of Gaussians model (ROG) to ‘families’ of data, where a ‘family’ is one cell’s size tuning curve at several different stimulus contrasts. To test the importance of each of the fitting parameters they used different forms of the model in which various parameters could either be free to vary between contrasts, or could be fixed to be the same across contrasts but optimised to fit the family. The authors compared χ^2 , normalised by the degrees of freedom (number of data points minus the number of fitting parameters, χ^2_N), across three forms of their model. In their ‘uniform’ model only the summation gain parameter was permitted to vary between contrasts; the other three parameters were optimised to fit the family. In their ‘gain’ model both the summation and inhibitory gains were allowed to vary between contrasts. In their final ‘size’ model both gains and the summation area (but not the inhibitory area) were permitted to vary across contrasts. The authors reasoned that unless allowing a parameter to vary across contrasts improved χ^2_N for the family, that parameter was not relevant to the mechanism by which size tuning changed across contrasts. Cavanaugh et al. report that all three models provided acceptable fits to the data. They report that χ^2_N improved between the uniform and gain models, demonstrating better fit quality even taking into account the additional free parameter. However χ^2_N deteriorated between the gain and ‘size’ models suggesting that even though the size model provided better fits to the data than the gain model, the magnitude of the reduction in error did not justify including the extra parameter.

To determine whether the effect of drug application could be described by changes in response gain alone, I fitted the data using three forms of the DOG and ROG models. In the ‘gain’ model the two space constants (summation area and inhibitory area) were forced to take the same values in the ACh-applied and control conditions, while excitatory gain and inhibitory gains were free to vary. In the ‘size’ model the two gain parameters and the summation area, but not the inhibitory area,

were allowed to vary between ACh-applied and control. The 'full' model was the model as detailed above, in which all four parameters were allowed to vary with ACh application. All models were fitted to optimise χ^2 . The percentage of variance accounted for by the fits demonstrated that all three forms of both the DOG and ROG models provided acceptable fits to the data (Table 2.4).

Figure 2.10 shows a three-way comparison of χ^2_N between the three forms of the DOG and ROG models. In the DOG model the gain and size models performed more or less equally as well as each other and performed marginally better than the full model. This is shown by the large numbers of data points falling into the 'gain' and 'size' sectors whilst very few points fall in the sector for the 'full' model. This suggests that allowing the summation area to vary between the ACh-applied and control conditions was justified by the reduction in error in a large proportion of the population, however, allowing the inhibitory area to vary was not justified by the improvement in fit quality for the majority of cells. One can test for the significance of these patterns by testing whether the distribution of points is significantly away from the centre along each of the three dimensions. This analysis shows that the distribution is not significantly away from the centre along the 'gain' axis ($p=0.94$, 2-tailed t-test) but was significantly above the centre along the 'full' axis ($p<0.05$, 1-tailed t-test) and significantly below the centre along the 'size' axis ($p<0.001$, 1-tailed t-test). Thus the 'size' model was significantly better than the 'gain' and 'full' forms of the DOG model across the population. These fits indicate that the changes in length tuning I observed during ACh application were unlikely to have occurred due to gain changes alone. Thus in the DOG model the main effect of ACh application was to change the size of the summation area, rather than (or in addition to) causing changes to the gains of facilitation and inhibition.

In the ROG model, the 'gain' form performed marginally better than the other two forms, as demonstrated by the high numbers of points in the gain sector. The distribution of points was significantly away from the centre along all three axes (gain axis $p<0.05$, size axis $p<0.05$, full axis $p<0.001$, 2-tailed t-test). It was significantly above the centre along the 'full' axis ($p<0.001$, 1-tailed t-test) and significantly below the centre along both the size axis ($p<0.05$, 1-tailed t-test) and the gain axis ($p<0.001$, 1-tailed t-test). Thus both the 'gain' and the 'size' forms of the ROG model were significantly better than the 'full' form of the model. The great majority of points fell within the 'gain' sector of the plot, demonstrating that the gain

model produced the lowest χ^2_N of the three forms of the ROG model, and was thus the most parsimonious description of the data.

Comparison of fit quality between three forms of the DOG and ROG models

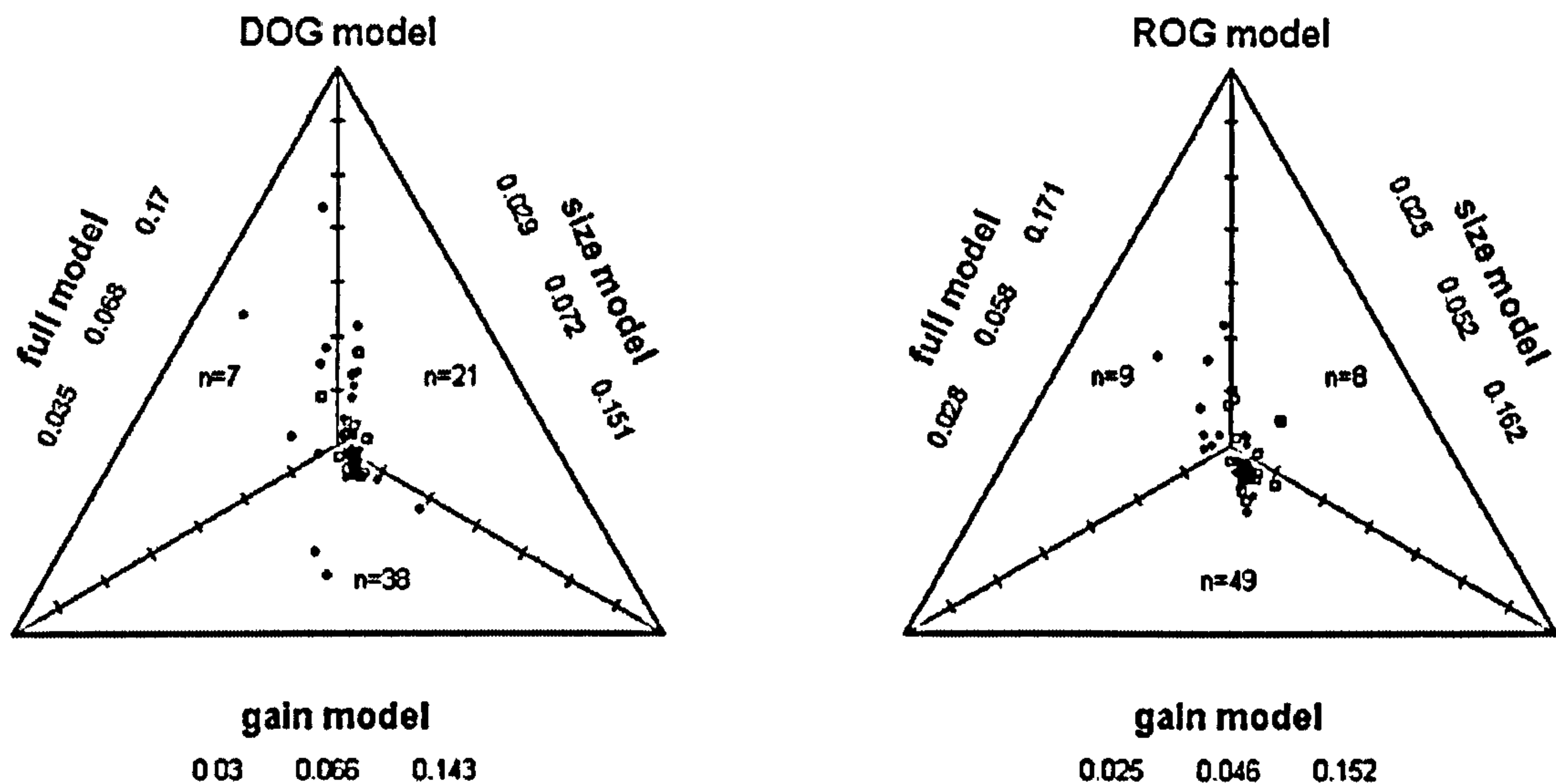


Figure 2.10 Three-way comparison of χ^2_N across three forms of the DOG (left) and ROG (right) models. In the 'gain' form only the excitatory and inhibitory gain mechanisms were permitted to vary between ACh-applied and control conditions. In the 'size' form the summation area was also allowed to vary between ACh-applied and control recordings. In the 'full' form all four parameters were allowed to vary. Axes units are normalised to make the total χ^2_N for each point equal to 1. The centre of the figure marks the point at which χ^2_N is equal in all three forms of the model. Increasing the χ^2_N for any one of the three forms drags a data point away from the centre towards the corner opposite to the edge marked with the form name (i.e. high χ^2_N in the gain model moves data points towards the top corner). The distance towards the corner corresponds to the percentage of the difference between the three factors accounted for by that factor. Tick marks along each axis mark increments of 6.66% (10% of the distance between the centre and 100%) from 33.33% (centre) to 73.3% at the edge. Reducing the χ^2_N for any one of the three forms drags a data point towards the edge marked by the form's name. The three inner axes mark out three sectors of the plot. The name of each sector is given by the name of the adjacent edge. The number of points within each sector (n) corresponds to the number of cells for which χ^2_N is smallest for that form of the model. The median, upper, and lower percentiles of χ^2_N in each form of the model are written along the corresponding edge. Cells facilitated by ACh are marked with a filled circle and cells inhibited by ACh are marked with an empty square.

Comparison of fit quality from three forms of the DOG and ROG models

DOG	25%	50%	75%
full model	87.5	94.1	97.9
size model	85.2	93.7	96.8
gain model	83.2	93.5	95.8

ROG	25%	50%	75%
full model	90	94.6	97.8
size model	87.9	94.2	96.8
gain model	86.7	94	95.9

Table 2.4 Median (50%), upper (75%), and lower (25%) quartiles of percentage variance explained by the three forms of the DOG (left table) and the ROG (right table) models.

Figure 2.11 compares peak length and fitting parameters extracted from the three forms of the ROG model. My main finding, that preferred length shifts towards shorter bars during ACh application, was evident in the full model and in the size model but absent in the gain model. Also, it was interesting to note that in the full model there was a significant reduction in the summation and inhibitory gains; this pattern was absent in the size model and was reversed in the gain model. Since the gain model was unable to account for my main finding, I conclude that the effect of ACh application on length tuning cannot be explained by gain changes alone (despite the low χ^2_N for the gain model), and that the reduction in preferred length was mediated principally by the reduction in summation area.

Effect of ACh on fitting parameters in three forms of the ROG model

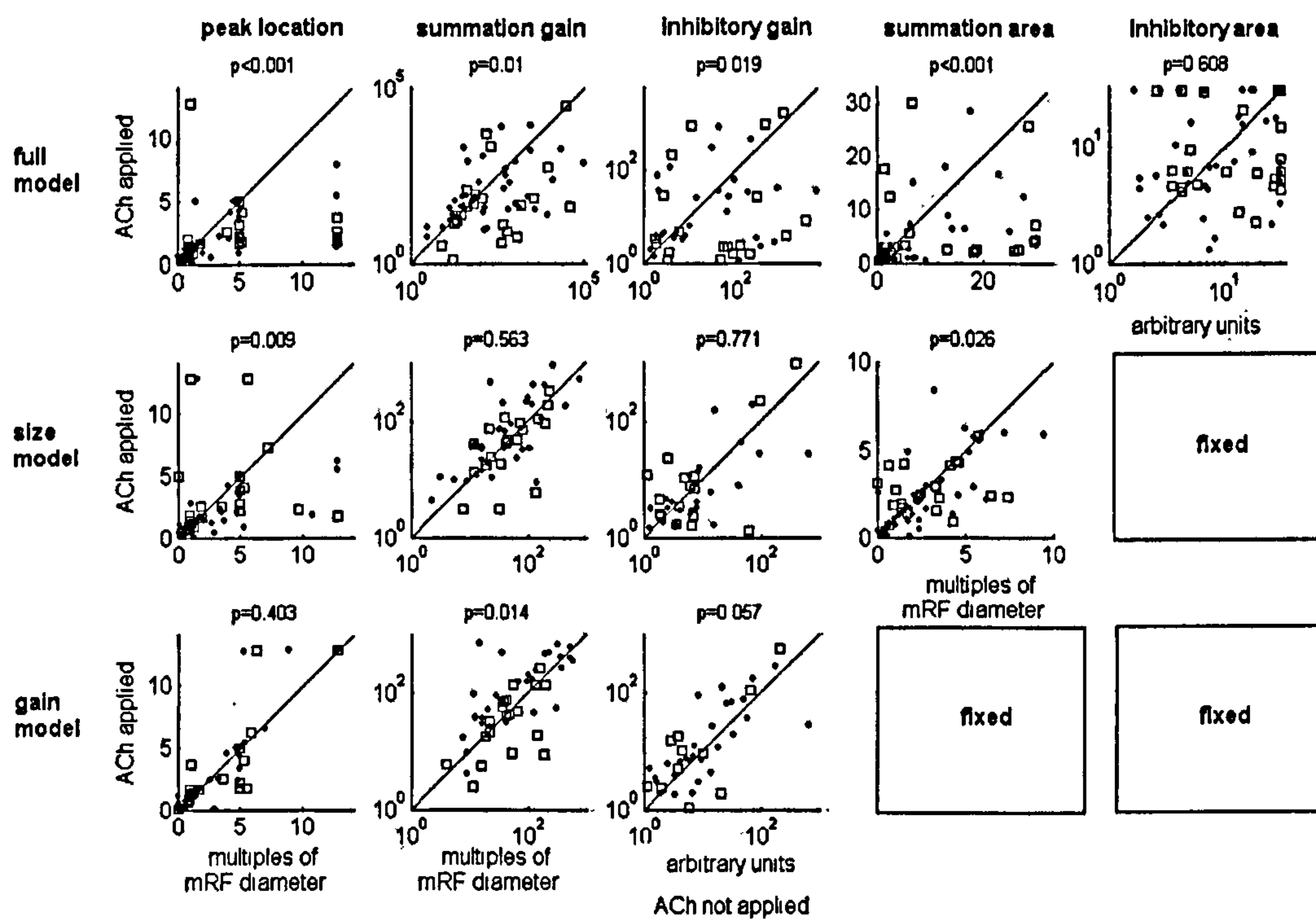


Figure 2.11 Preferred length and fitting parameters as a function of ACh application, extracted from three forms of the ROG model. The first row shows the output of the full model where all four fitting parameters were free to vary between ACh-applied and control conditions. The second row shows the output of the size model, where the inhibitory area was forced to have the same value under both ACh-applied and control conditions. The third row shows the output of the gain model where only the summation and inhibition gains were able to vary between ACh-applied and control conditions. In each plot, cells inhibited by ACh are marked with an open square and facilitated cells are marked with a filled circle. The value of the parameter of interest (column titles) without ACh applied is shown on the x-axes, and the value with ACh applied is shown on the y-axes. Cells in which the parameter of interest was reduced by ACh application appear below the diagonal. Above each plot, the p-value gives the significance of differences in the parameter of interest between ACh-applied conditions and control conditions across the population (signed rank test). All fits were optimised to minimise the χ^2 error. Preferred length (peak location) and the two area parameters are in units of multiples of mRF diameter, the gain parameters are in arbitrary units.

2.4.3 Effect of ACh on the time course and evolution of length tuning

Neuronal responses generally became more sustained during ACh application (see next section, *2.4.4 Response Profile*). To investigate the time course of length tuning and how it was affected by ACh application, I fitted DOG and ROG models to response profiles. To do this I took 10msec bin histograms of neuronal response from 30msec after stimulus onset, and fitted the DOG and ROG models in each bin. I fitted the data using the bootstrapping strategy as described above (i.e. taking a random selection of single trial histograms). This method allowed fits to be optimised whilst taking the reliability of responses in each bin into account. A χ^2 method would have been difficult to implement since estimates of variance from 10msec bins would be extremely unreliable. Using an estimated variance taken from the whole response period would also be unreliable, since it is known that the relationship of mean against variance alters over the time course of a response (Robinson and Harsch 2002). Figures 2.12 and 2.13 show the mean of the preferred length and fitting parameters as a function of time and ACh application for facilitated and inhibited cells, fitted with a DOG (Figure 2.12) or ROG (Figure 2.13) model. In both models, preferred length showed quite a degree of temporal dynamics over the response period. Cells preferred relatively long bars during the earliest part of the response (50 to 100ms). Following this early period, preferred length reduced substantially and reached a minimum at 120msec, after which preferred length increased again. In both models the temporal dynamics of the summation area showed a high correspondence with that of the preferred length. In the DOG model the inhibitory area has a similar time course to the preferred length, although the dynamic range was reduced. In the ROG model the inhibitory area was relatively constant across time. In both models the gain parameters were also very dynamic. The shape of these curves however showed little correspondence with the shape of the peak length time course.

During ACh application cells preferred shorter bars from shortly after stimulus onset, however, the difference in preferred length became particularly pronounced from ~200msec after stimulus onset. Cells facilitated by ACh and cells inhibited by ACh both showed very similar dynamics, although the early reduction in preferred length was somewhat more pronounced in the facilitated population, and the late reduction was somewhat larger among inhibited cells. The effect of ACh on the dynamics of the summation area was very similar in both cell groups. The

dynamics of the inhibition area was not systematically affected by ACh application in either the DOG or ROG model.

In the DOG model the summation gain in facilitated cells was particularly enhanced during the late part of the response (from ~200msec). The summation gain among inhibited cells was particularly reduced during the early part of the response. This pattern is very similar to ACh-induced changes to the response profile, which are described in the next section (2.4.4 *Response profile*). The temporal profile of the inhibitory gain was not systematically affected among cells facilitated by ACh. Among cells inhibited by ACh, the inhibitory gain was strongly reduced during the early transient peak of the function. In the ROG model, the variance of the dynamics of both the inhibitory gain and summation gain was very high, therefore the patterns should be regarded with caution. Among cells facilitated by ACh, the summation gain was enhanced by ACh across most of the response period, but especially from ~100msec after stimulus onset. The inhibitory gain was enhanced by ACh application particularly during the early part of the response. Among cells inhibited by ACh, the summation gain was reduced by ACh application, particularly during the late part of the response. The inhibitory gain was enhanced particularly at the start and at the end of the response period.

Time course of length tuning (DOG model)

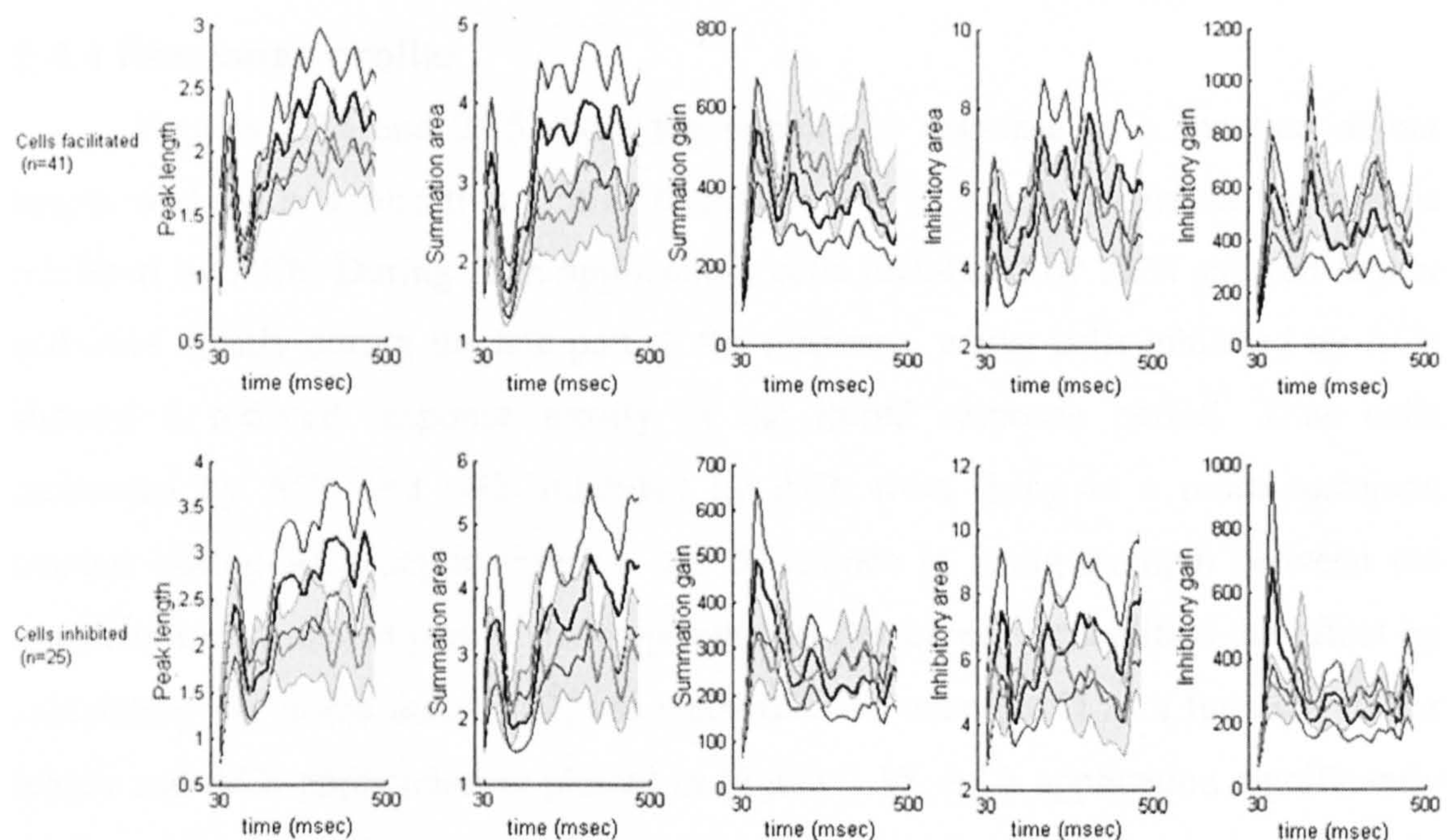


Figure 2.12 Preferred length and fitting parameters extracted from the DOG model as a function of time following stimulus onset for cells facilitated by ACh (top row) and cells inhibited by ACh

(bottom row). Fits from data in the ACh-applied condition are shown in grey (thick grey line shows mean, grey shaded area shows standard error) and fits from data in the control condition are in black (thick black line shows mean, flanking narrower lines show standard error). Peak length, summation area and inhibitory area are in units of multiples of mRF diameter. Summation and inhibitory gains are in arbitrary units.

Time course of length tuning (ROG model)

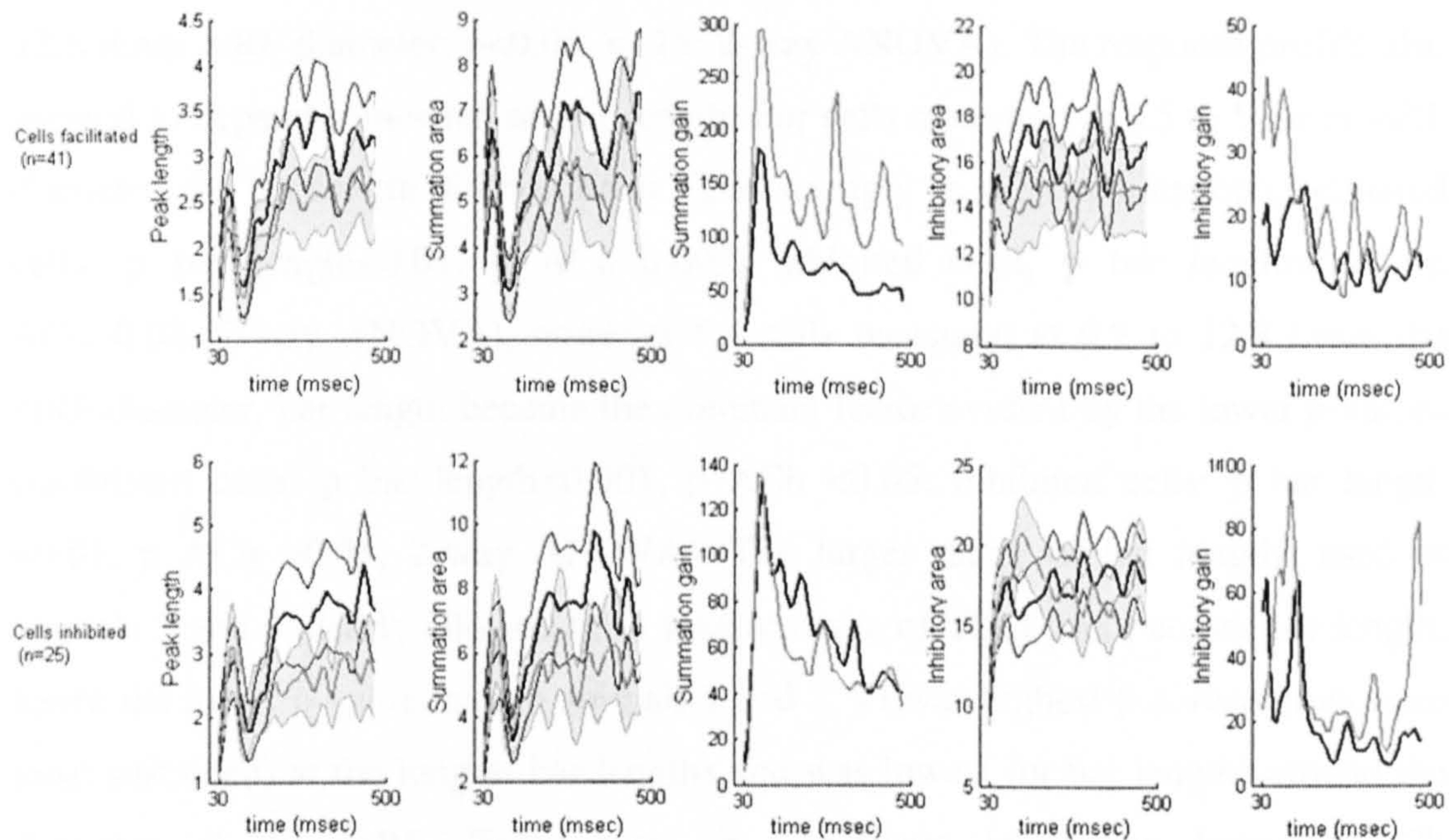


Figure 2.13 Preferred length and fitting parameters extracted from the ROG model as a function of time following stimulus onset for cells facilitated by ACh (top row) and cells inhibited by ACh (bottom row). Data are displayed in the same format as in Figure 2.12. The standard errors in the gain parameters were so large that including them obscured the pattern in the mean; hence they have been omitted. These data should therefore be regarded with caution.

2.4.4 Response profile

Figures 2.14 and 2.15 show the population response as a function of bar length and ACh application. Cells facilitated by ACh are separated from cells inhibited by ACh. During ACh application, cells facilitated by ACh showed higher activities mostly during the late part of the response, whilst cells inhibited by ACh showed a reduced response mostly in the initial response period. Thus cells facilitated by ACh and cells inhibited by ACh were firing in a more sustained manner during ACh application, i.e. the difference in firing strength between the transient and sustained part of the response was decreased. I quantified the effect by calculating the ‘tonic index’ (TI, see methods); the average TI as a function of bar length and ACh application is plotted in Figure 2.16. ACh application significantly increased TI, i.e. cell responses became more sustained. This effect was significant for cells facilitated by ACh (cells measured at 0.5-5 times mRF diameter: $p < 0.001$,

n=19; cells measured at 0.2-12.8 times mRF diameter: $p < 0.05$, n=22; 2-way ANOVA (factor 1: treatment, factor 2: bar length)). The trend also occurred for cells inhibited by ACh, although it did not reach significance for cells measured with bar lengths 0.5-5 times the diameter of the mRF, probably due to the small sample size (cells measured at 0.5-5 times mRF diameter: $p = 0.08$, n=10; cells measured at 0.2-12.8 times mRF diameter: $p < 0.05$, n=15; 2-way ANOVA). The response profile also seemed to depend somewhat on bar length. For cells measured at 0.5 to 5 times mRF diameter, the bar length did not affect TI as strongly as ACh application (facilitated cells: $p_{\text{bar length}} < 0.01$, $p_{\text{ACh}} < 0.001$; inhibited cells, $p_{\text{bar length}} = 0.41$, $p_{\text{ACh}} = 0.08$; 2-way ANOVA), however for cells measured at 0.2 to 12.8 times the mRF diameter, bar length became the dominant factor evident by the lower p-values (facilitated cells: $p_{\text{bar length}} < 0.001$, $p_{\text{ACh}} < 0.05$; inhibited cells: $p_{\text{bar length}} = 0.01$, $p_{\text{ACh}} = 0.05$; 2-way ANOVA). The larger range of bar lengths used in animals 3 and 4 clearly allowed for a greater range of TI to occur across bar length, hence the lower p-value than in animals 1 and 2. TI was highest (i.e. responses were most sustained) at the longest bar lengths and was lowest for bar lengths around the diameter of the mRF. There was no significant interaction between ACh presence/absence and bar length for any of these measurements, i.e. the effects of ACh presence/absence did not depend on what length was present. These results show that ACh application changed the response profile to be more sustained; increasing the bar length had a similar effect.

It may seem puzzling that facilitated and inhibited cells showed such similar dynamics of preferred length (Figure 2.12 and 2.13) despite their response profiles being affected in quite different manners. From Figure 2.16 it is clear that the reduction in peak length among cells facilitated by ACh was due to a larger increase in the response to short bars than to long bars. Cells inhibited by ACh show the opposite pattern, that is, a larger decrease in the response to long bars than for short ones. Thus in both cases the response is higher for short bars than for long ones. This pattern is evident across the whole response period.

Population responses from animals 1 and 2 (bar lengths 0.5 to 5 times mRF diameter)

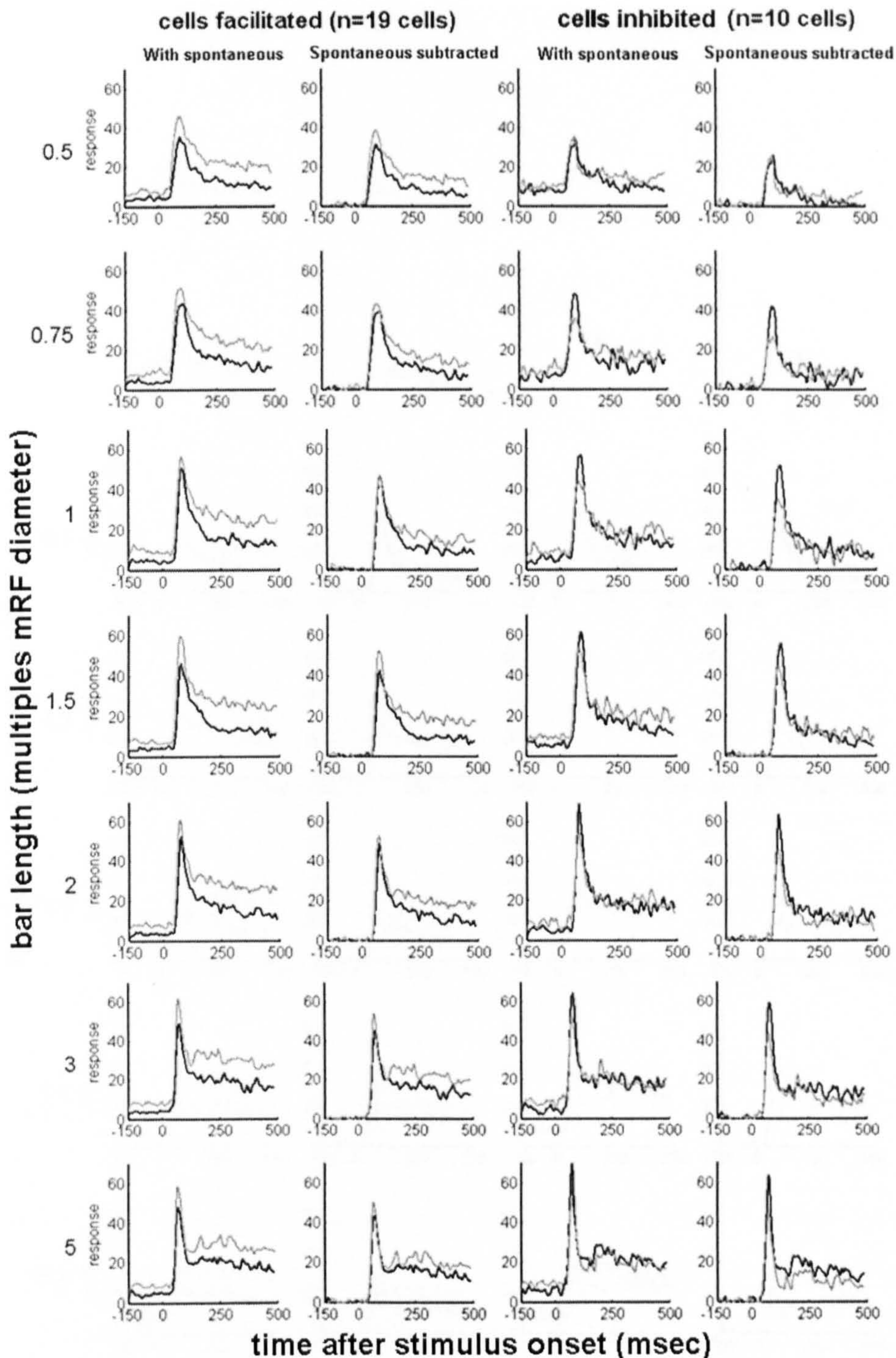


Figure 2.14 normalised population activity. Cells facilitated by ACh are shown in the two left-hand columns with and without spontaneous activity. Population activity from cells inhibited by ACh is shown in the two right-hand columns. Activity during ACh application is shown in grey; activity in the control condition is shown in black. Rows of plots show different bar lengths (left-hand label). Responses from each cell were normalised to the highest response for that cell before being added to the population, thus each cell contributes equally to the mean responses shown here.

Population response from animals 3 and 4 (bar lengths 0.2 to 12.8 times mRF diameter)

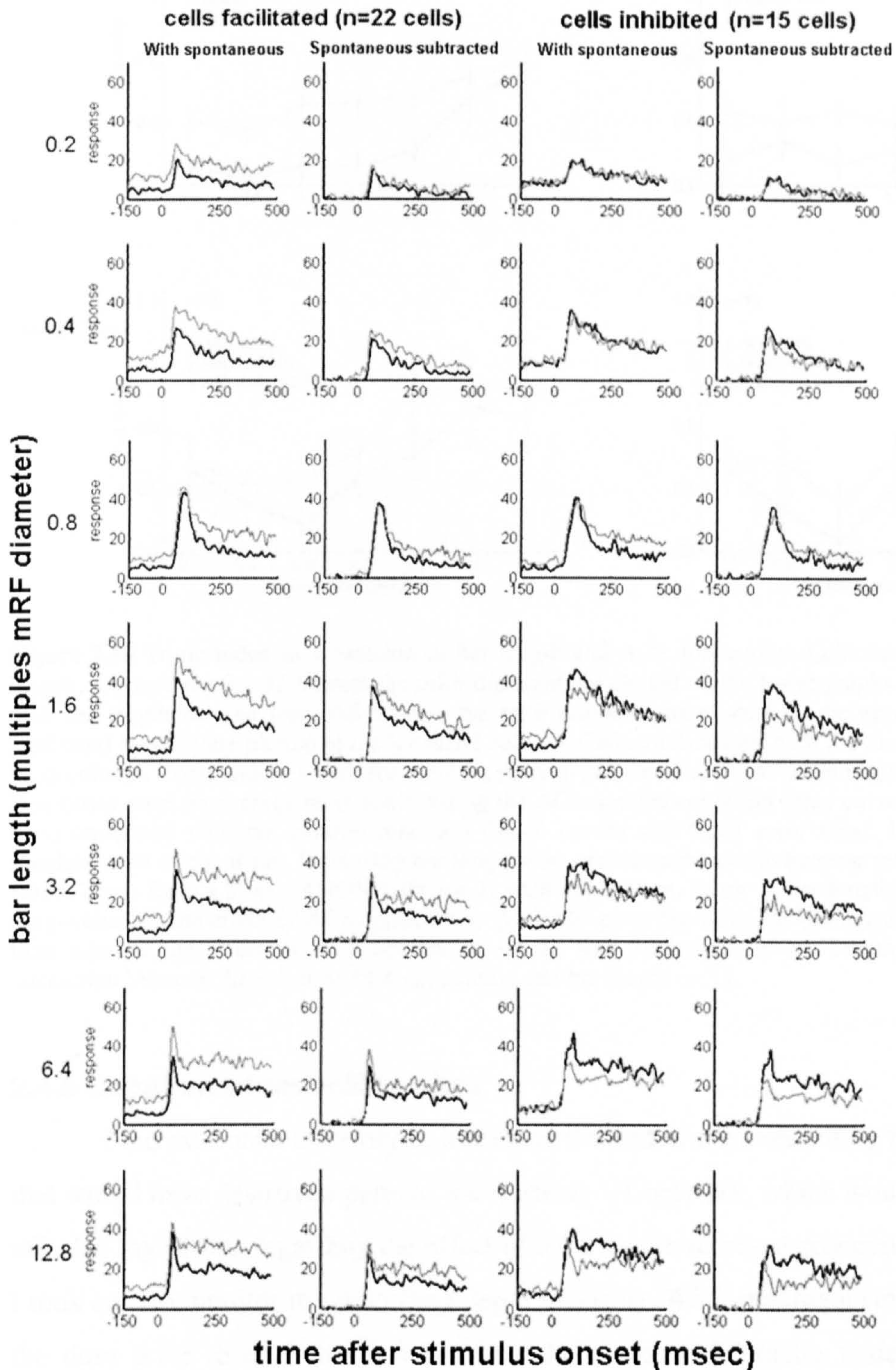


Figure 2.15 normalised population activity. Cells facilitated by ACh are shown in the two left-hand columns with and without spontaneous activity. Population activity from cells inhibited by ACh is shown in the two right-hand columns. Activity during ACh application is shown in grey; activity in the control condition is shown in black. Rows of plots show different bar lengths (left-hand label). Responses from each cell were normalised to the highest response for that cell before being added to the population, thus each cell contributes equally to the mean responses shown here.

Effect of ACh on the tonic index

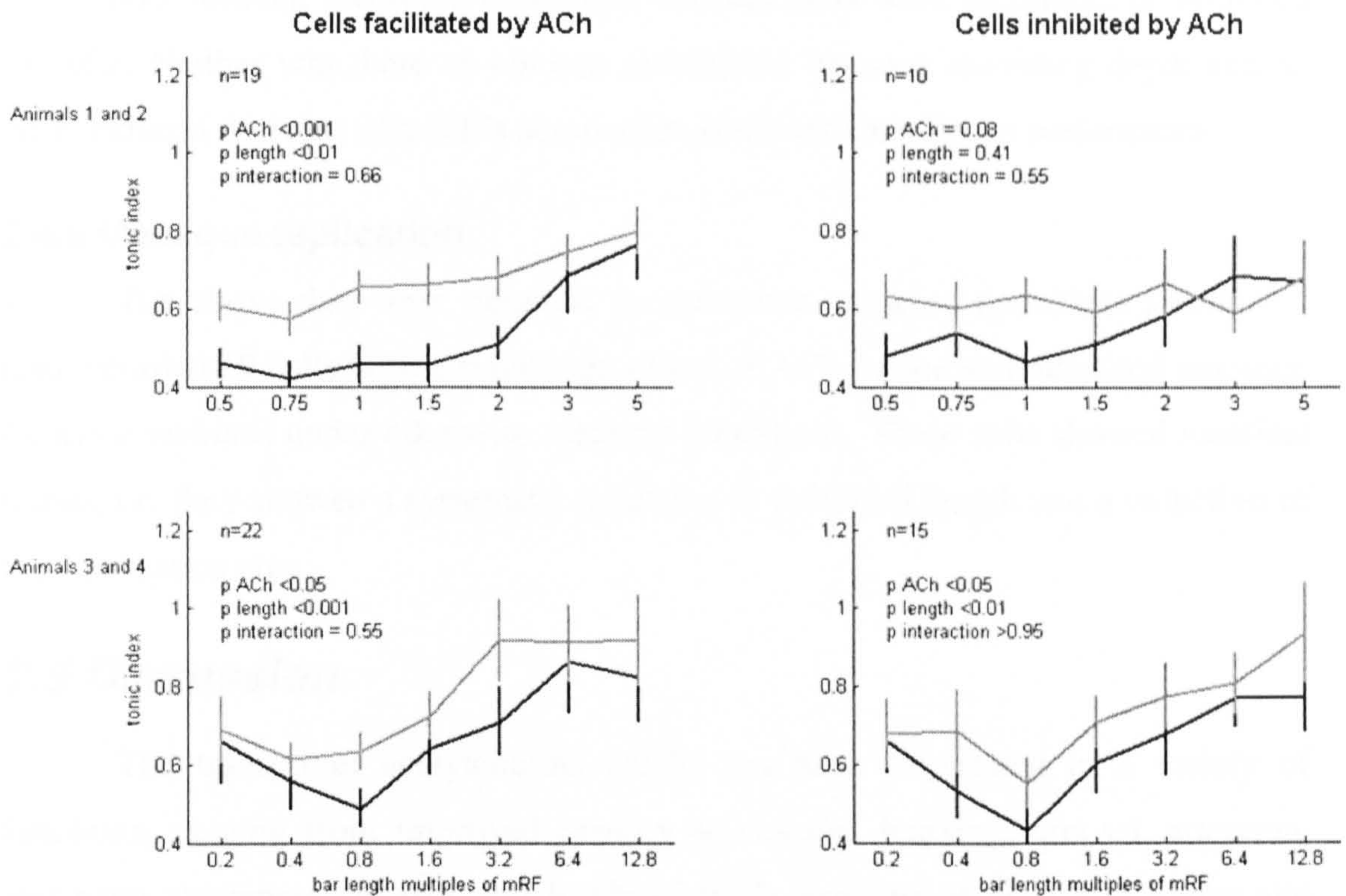


Figure 2.16 Tonic index as a function of bar length and ACh application. Cells measured with bar length ranging from 0.2-12.8 times the mRF diameter are plotted on the lower graphs. Cells measured with bar length ranging from 0.5-5 times the mRF diameter are plotted on the upper graphs. Cells facilitated by ACh are plotted in the left-hand column. Cells inhibited by ACh are plotted in the right-hand column. Tonic index is high for tonic (sustained) responses and low when responses are phasic. Responses were on average more tonic during the ACh-applied condition (grey curves and grey error bars) compared with the control condition (black curves and black error bars). Error bars show standard error of the mean. Increasing bar length also caused responses to become more sustained. P-values come from a 2-way ANOVA (factor 1: ACh application, factor 2: bar length). ‘p ACh’ gives the p-value for the effect of ACh application, ‘p length’ gives the value for bar length, ‘p interaction’ tests whether the effect of ACh application on TI was influenced by bar length. There was no interaction between the effect of ACh application and bar length on TI.

2.4.5 Location of recording sites

I did not make electrolytic lesions at the end of each recording track, because that would have destroyed parts of the intrinsic V1 network, which would likely have affected my results regarding the effect of ACh on intracortical processing. However, I took care to monitor my recording depth precisely. After making a small incision in the dura prior to each track, I positioned the electrode/pipette under microscope guidance such that the zero depth registration corresponded to the location where the pipette tip just touched the cortical surface. I attempted to make penetrations perpendicular to the cortical surface, thereby hoping to be able to reconstruct the depth (and potentially the layers cells were recorded from) with reasonable precision.

From these measurements I reconstructed the recording depth. There was no obvious correlation between recording depth and whether cells were facilitated or inhibited by ACh. Neither was there an obvious correlation between recording depth and an ACh-induced decrease of a cell's summation area (and thus length preference).

2.4.6 Macaque replication

The above data were obtained in marmoset monkeys (*callithrix jacchus*). I also recorded 19 cells with a significant effect of ACh in one anaesthetised macaque (*macaca mulatta*) under otherwise identical conditions. These cells showed identical trends, i.e. they showed a systematic reduction in preferred length and a reduction of the summation area.

2.5 Discussion

The transmitter acetylcholine (ACh) has been implicated in a variety of functions, ranging from improved sensory processing, learning, arousal, attention, and even awareness (Everitt and Robbins 1997; Robbins et al. 1997; Sarter and Bruno 1997; Sarter and Parikh 2005). Moreover, deficits in cortical cholinergic functions often cause substantial cognitive deficits (Sarter and Bruno 1998; Perry et al. 1999). Despite its wide implication in various functions, the precise effects of ACh on cortical processing remain unknown. Several recent *in vitro* studies suggest that a key function of cortical ACh may be to control the flow of neuronal information by selectively suppressing lateral intracortical synapses whilst leaving thalamocortical/feed-forward synapses unaffected (Hasselmo and Bower 1992; Habbicht and Vater 1996; Kimura et al. 1999), or even increasing their efficacy (Gil et al. 1997; Hsieh et al. 2000). In the visual cortex, these two types of synapses separately influence nCRF modulation and CRF activation (Angelucci et al. 2002; Angelucci et al. 2002). Thus, high levels of ACh should attenuate nCRF interactions whilst potentially facilitating the CRF response. In line with this proposal I show that during ACh application, cells shift their length preference towards shorter bars, demonstrating reduced summation from outside the classical receptive field. Fitting the length tuning data with a difference of Gaussians (DOG) or ratio of Gaussians (ROG) model showed that ACh reduced the size of the summation area. Despite reduced spatial summation, most cells responded more strongly in the presence of ACh, suggesting that CRF activation was also boosted. I did not find significant

changes in the size of the suppression area under conditions of increased ACh. This potentially reflects the fact that inhibitory synapses are less affected by ACh than excitatory synapses (Kimura and Baughman 1997).

ACh facilitated the response of the majority of cells, and one might therefore argue that the shift of length preference towards shorter bar lengths might have been due to response saturation, i.e. in the presence of ACh neurons fired at their maximum level when relatively short bars were presented, and therefore firing rate could not increase further when longer bars were presented, although synaptic activity might still have increased (which could only be determined through intracellular recordings). Contrary to this argument, I also found a shift in length tuning towards shorter bars in neurons inhibited under conditions of high ACh, arguing against an explanation based on response saturation.

A recent study has reported a similar effect in rat somatosensory 'barrel' cortex. In this cortical area, thalamic inputs representing a single whisker target an individual barrel. Stimulation of this 'primary' whisker only can elicit responses from neurons within its related barrel; all other whiskers hardly elicit a response. Thus the primary whisker would seem to be the somatosensory equivalent of the CRF in the visual cortex. Whiskers adjacent to the primary whisker would therefore seem to be the equivalent of the nCRF, because stimulation of these whiskers can modulate responses to the primary whisker. The modulation by adjacent whiskers is mediated by horizontal connections between adjacent barrels. Olford and Castro-Alamancos (2003) show that increasing the level of ACh in the barrel cortex, either by exogenous application via a micro-dialysis probe or by application of physostigmine, enhanced the response to the primary whisker and inhibited the modulatory influence of adjacent whiskers. Thus ACh was shown to boost the feed-forward input whilst suppressing contextual modulation mediated by lateral connections. My finding that ACh reduces contextual modulation is therefore not specific to the visual cortex, and may be a common feature of cortical processing.

In this study I mapped the spatial diameter of the receptive field by means of the minimum response field (mRF) (Barlow et al. 1967; Blasdel and Fitzpatrick 1984), the area within which presentation of a small stimulus elicits an extracellular response. The term classical receptive field (CRF) is often used as a synonym (Knierim and Van Essen 1992) for the mRF. Surrounding the CRF/mRF is an area that can modulate the response to stimuli presented within the CRF/mRF, and this

modulation can be facilitatory or inhibitory. The excitatory and inhibitory parts of the receptive field are usually assumed to extend over the CRF *and* the nCRF. The excitatory area is continuous in the sense that within its spatial sampling range, visual stimuli elicit EPSPs, but the number of EPSPs elicited and/or efficacy of changing the membrane potential near the axon hillock decreases as the stimulus is moved away from the centre of the receptive field (Sillito 1977; Orban et al. 1979). The CRF can be well modeled with a Gaussian envelope (Jones and Palmer 1987). According to the difference of Gaussians model (DeAngelis et al. 1994), the CRF is surrounded by an excitatory fringe, which is continuous with the CRF and contributes to spatial summation (Sceniak et al. 1999; Cavanaugh et al. 2002). DeAngelis et al. (1992) argue that a cell's excitatory receptive field is best described as the region of space within which a stimulus can either elicit an excitatory response or add to the response elicited by another stimulus. By having used the mRF technique to determine the RF size, the mapping stimulus was likely to only elicit subthreshold responses in the insensitive excitatory RF fringes. The presentation of a longer bar therefore caused changes in suprathreshold responses. As a result, the preferred bar length was almost always larger than the mRF (the median preferred length in the absence of ACh was 1.33 times the mRF size). The suppressive area seems to be organized slightly differently and subdivided into two systems. One acts in the RF centre and is only weakly orientation tuned, and the other is responsible for end and side inhibition, is orientation tuned, and originates from outside the excitatory RF, although it can overlap with it (DeAngelis et al. 1994). Although the source of inputs to the excitatory fringe surrounding the CRF is not precisely known, my finding of a reduced influence of this fringe (a reduced summation area) when ACh was applied suggests that the inputs to this fringe are predominantly intracortical synapses, which are inhibited possibly by a muscarinic mechanism upon ACh application (Kimura and Baughman 1997). Interestingly, I did not find a systematic influence of ACh on the size or gain of the inhibitory area. If the surround suppression was largely mediated by feedback projections, as suggested by Hupe et al. (1998) and Bair et al. (2003), this could suggest that feed-back connections are affected by ACh in a different manner to that of lateral connections. Future intracellular *in vivo* studies are necessary to determine the sources of these interactions and how they are affected by neuromodulators.

Previous experiments have demonstrated that the relative strength and size of the summation and suppression areas can change according to stimulus parameters and context (Kapadia et al. 1999; Sceniak et al. 1999; Kapadia et al. 2000). The mechanism behind this change is still debated. While Sceniak et al. (2001) suggest that different stimulus contrasts can cause a change in the size of the summation area, Cavanaugh et al. (2002) argue that these changes are better explained by gain changes alone. My findings are in agreement with both claims. In the DOG model (as used by Sceniak et al.) a three-way comparison of χ^2_N showed that the changes in the summation area between the ACh-applied and control conditions were necessary to account for the data. In the ROG model (as used by Cavanaugh et al.), χ^2_N values were smallest when the size parameters were not allowed to vary between ACh-applied and control conditions, suggesting that in this model, gain changes alone could account for the data (Figure 2.10). Despite this finding I argue that changes in the summation area best explain the ACh-mediated reduction in preferred length. This assertion is supported firstly by the highly-consistent reduction in summation area during ACh application, demonstrated in the 'full' model in which all four parameters were allowed to vary between ACh and control conditions (Figure 2.11), and secondly by the strong correspondence between the time course of length tuning and of the summation area (Figure 2.13). Moreover I show that gain changes alone (the gain model) could not account for the reduction in preferred length (Figure 2.11) despite giving acceptable fits to the data (χ^2_N). My argument is not necessarily contrary to Cavanaugh et al.'s reports, since different mechanisms are likely to be involved in the two phenomena. Whilst changes in stimulus contrast are likely to involve contrast normalization (Heeger 1992), possibly mediated by GABAergic mechanisms (Thiele et al. 2004) or synaptic depression (Abbott et al. 1997; Carandini et al. 2002), ACh acts through a variety of pre-synaptic and post-synaptic mechanisms and receptors (Gil et al. 1997; Kimura and Baughman 1997; Kimura et al. 1999; Kimura 2000); thus the different findings are not necessarily contradictory.

A recent paper (Ozeki et al. 2004) showed that applying the GABA_a receptor antagonist bicuculline methiodide (BMI) to cat V1 cells only slightly widened the cells' size tuning, whilst at the same time surround suppression did not become unselective. Based on this, they argued that size tuning does not arise from intracortical interactions but is more likely to arise from size-tuned cells in the lateral geniculate nucleus. My data do not support this proposal, but rather argue for cortical

mechanisms of spatial integration. There are a few problems with the BMI argument as proposed by Ozeki. Application of BMI does not affect excitatory connections within the cortex, and thus does not address whether spatial summation is mediated intracortically. Moreover, BMI application only affects GABA_a receptors, leaving GABA_b receptors unaffected; i.e. GABAergic inhibition was only partly affected by BMI injection.

My finding of changes in the spatial integration of cortical neurons upon ACh application is contrary to reports from cat LGN. Receptive fields of relay cells in this area mainly show increases in gain, with small increases of receptive field size (summation area) (Fjeld et al. 2002). ACh in the LGN excites relay cells (Sillito et al. 1983; Eysel et al. 1986), seems to have an inhibitory effect on inhibitory interneurons (McCormick and Pape 1988) and inhibits perigeniculate neurons, which in turn inhibit relay cells (McCormick and Prince 1987). The network involved is thus different from the cortical network (Gil et al. 1997; Kimura and Baughman 1997; Kimura et al. 1999; Kimura 2000), and therefore these differences of ACh action are not necessarily surprising.

In this chapter I have shown that cortical RF integration can be dynamically modulated by internal factors, such as the neuromodulator ACh. Since the natural release of ACh is bound to states of arousal and attention (Everitt and Robbins 1997; Sarter and Bruno 1997; Sarter et al. 2003), ACh may be involved in dynamic RF changes (Connor et al. 1997; Treue and Trujillo 1999; Li et al. 2004; Thiele 2004) and reduction in contextual influence (Chapter 1; Ito et al. 1998) associated with spatial attention. It has been suggested that the function of the nCRF is to allow visual neurons to code natural scenes more efficiently by exploiting redundancies in the scene (Young 2000). Coding more efficiently by this mechanism relies on inference about the visual world (Young 2000), and may therefore come at the cost of an increased error rate (Dayan and Yu 2001; Yu and Dayan 2002). By reducing the power of the nCRF, the presence of ACh may cause cells to process stimuli within its CRF more accurately without modulation from the wider context, thereby increasing local information processing and potentially reducing errors due to contextual influence. One parallel between the effects of attentional modulation and the results presented in this chapter is that response enhancement by attention is generally stronger during the late part of the response (Motter 1994; Roelfsema et al. 1998; McAdams and Maunsell 1999; Seidemann et al. 1999; Reynolds et al. 2000;

Fries et al. 2001; Roelfsema and Spekreijse 2001; Treue 2001). It might be argued that the cholinergic system lacks the speed and spatial precision to mediate the effects of spatial attention which operate rapidly with high spatial resolution. Recent experiments show that spatial/regional specificity of ACh release is higher than originally thought (Fournier et al. 2004). Additionally it might be argued that the speed and spatial specificity of spatial attention is mediated by an interaction of cholinergic input and feedback (synapto/synaptic) connection. This would, however, imply that ACh affects feedback projections in a manner different to its effects on lateral connections; something which future experiments will have to determine.

2.6 Conclusion

In this chapter I have demonstrated that the application of ACh to cells in primate V1 can significantly change the cell's length tuning. This result is compatible with the hypothesis that the effect of cortical ACh is to control the flow of neuronal information, such that the efficacy of information arriving from the senses is boosted relative to information from within the cortex. Various earlier lines of evidence have contributed to this hypothesis; however this is the first study to test it directly *in vivo* in the primate. A number of features of my data are strikingly similar to data from studies investigating the effects of spatial attention on neuronal processing. For example my data resembles data from an attention experiment which showed that neuronal response profiles become more tonic during attentive states (Motter 1994; Roelfsema et al. 1998; McAdams and Maunsell 1999; Seidemann et al. 1999; Reynolds et al. 2000; Fries et al. 2001; Roelfsema and Spekreijse 2001; Treue 2001). Perhaps more striking is the finding that spatial attention reduces contextual influences (Ito and Gilbert 1999) in a manner similar to my demonstration of the application of ACh reducing contextual influences. To what extent neuronal effects of attention are similar to, and may be explained by, the action of cortical ACh is explored in Chapters 3 and 4.

Chapter 3: The Interaction of Attention, Contrast and Eccentricity in the Dynamic Control of Spatial Integration in Alert Macaque Primary Visual Cortex

3.1 Abstract

In this chapter I investigate how attention affects spatial integration in V1 neurons. I recorded neuronal activity from two alert macaques engaged in a task which required attention to be directed either towards or away from the receptive field (RF) of the neuron under study. The effect of attention on spatial integration was assessed by measuring length tuning in the presence and absence of directed visual attention. Stimuli were dark bars of varying length set to the cell's preferred orientation; the contrast of the bars was set to between ~5% and 100%. Results showed that in the majority of cells, attention enhanced neuronal activity at the attended location. Contrary to previous reports, I often found response enhancement from early on after stimulus onset, although the largest effects generally occurred later on in the response. Moreover, I found that in the majority of cells attention altered length tuning, causing a shift in preferred length towards shorter bars. This shortening of preferred length demonstrates a reduction in the impact of the non-classical receptive field. This effect was not evident when the stimulus was presented at a contrast of less than ~8%. Fitting a difference of Gaussians model to the data suggested that the shift in preferred length was due to a reduction in the cell's spatial summation area. The size of the inhibitory area was unaffected by attention.

The finding that attention reduces the impact of the non-classical RF in V1 suggests a possible neuronal substrate for the observed reduction in contextual influence in human orientation perception, as reported in Chapter 1. In addition to this, my findings on the effect of attention on length tuning, and the temporal profile of response enhancement by attention, match the effect of external acetylcholine (ACh) application reported in Chapter 2. Thus, the current findings fully support my general hypothesis that attention reduces contextual processing, possibly by the action of ACh.

3.2 Introduction

In Chapter 1 I described how local context influenced the perception of orientation in human subjects. These experiments showed that contextual influences were weaker under conditions of full attention than under conditions of reduced attention. Chapter 2 put forward a possible pharmacological mechanism for this attention-mediated reduction in contextual influence. I showed that the application of acetylcholine (ACh) reduced contextual influences in V1 neurons, evidenced by a reduction in preferred length. I suggested that ACh mediated the reduction in contextual influence by causing a reduction in the efficacy of lateral and feedback connections (Hasselmo and Bower 1992; Kimura et al. 1999; Hsieh et al. 2000; Kimura 2000) and an increase in the efficacy of feed-forward inputs (Gil et al. 1997), in line with a number of *in vitro* reports. Since the natural release of ACh is associated with attentive states (Blokland 1995; Everitt and Robbins 1997; Sarter and Bruno 1997), an ACh-mediated reduction in surround modulation could potentially explain the psychophysical findings of Chapter 1. In this chapter I test the hypothesis that the effect of attention on spatial integration in V1 neurons is similar to the effect of external ACh application.

Previous studies on the effects of attention in visual cortex have consistently demonstrated that directing attention towards stimuli presented within the receptive field (RF) of a neuron generally increases the responsiveness of the cell. Recently it has emerged that the effect of attention on neuronal responses is generally greater when multiple stimuli are presented within the attended location (Luck et al. 1997; Treue and Maunsell 1999). Moreover, attention influences the way in which multiple stimuli interact with each other in the neuronal response (Moran and Desimone 1985; Desimone and Duncan 1995; Luck et al. 1997; Reynolds et al. 1999; Treue and Maunsell 1999; Reynolds and Desimone 2003). Two stimuli presented in a single RF apparently compete for representation in the neuronal response. In the absence of attention, a non-preferred stimulus presented together with a preferred stimulus results in a response somewhere between the responses to each stimulus presented in isolation. When attention is directed to either of the pair, the effect is to bias the competition in favour of the attended stimulus: attending to the preferred stimulus enhances the response to the pair, whilst attending to the non-preferred stimulus suppresses the response to the pair (Moran and Desimone 1985; Desimone and

Duncan 1995; Luck et al. 1997; Reynolds et al. 1999; Treue and Maunsell 1999; Reynolds and Desimone 2003). Thus it seems that one function of attention is to bias cortical processing in favour of behaviourally relevant stimuli whilst filtering out the response to behaviourally irrelevant stimuli. Competing stimuli may often occur within the large RFs of V4 and MT neurons but it is more difficult for two separate stimuli to appear within the small RF of a V1 cell. This, nevertheless, does not exclude the possibility of competition in V1.

V1 neuronal responses are influenced both by stimuli within the classical receptive field (CRF) and by stimuli in the area surrounding the CRF, known as the non-classical receptive field (nCRF). Stimuli presented within the nCRF typically suppress the neuronal response to the stimuli presented within the CRF, although facilitation can also occur (Knierim and Van Essen 1992; Kapadia et al. 1995; Fitzpatrick 2000; Kapadia et al. 2000; Angelucci et al. 2002; Cavanaugh et al. 2002; Cavanaugh et al. 2002; Jones et al. 2002; Bair et al. 2003; Series et al. 2003; Ozeki et al. 2004). The geometric arrangement and relative contrast of stimuli within the CRF and nCRF determine the strength and sign (whether it is facilitatory or inhibitory) of nCRF modulation (Levitt and Lund 1997; Polat et al. 1998; Sceniak et al. 1999; Dragoi and Sur 2000; Angelucci et al. 2002). In this way, V1 responses can reflect stimuli that are presented within the nCRF as well as stimuli presented within the CRF. The extent to which the response is controlled by stimuli within the CRF versus stimuli within the nCRF may be similar to the competition between stimuli that are presented simultaneously within the large RFs of higher cortical areas. The effect of attention on the interaction between stimuli presented in the classical and non-classical parts of V1 RFs may also be similar to the effect of attention reported in higher areas, i.e. biasing the competition between the CRF and nCRF. In line with this proposal, the effects of attention on V1 responses are reported to be larger when the CRF is stimulated in conjunction with the nCRF than when the CRF is stimulated in isolation (Ito and Gilbert 1999), just as the effect of attention in higher areas is reported to be larger when multiple stimuli are presented in the RF (Luck et al. 1997; Treue and Maunsell 1999).

The effect of attention on the interaction between central and surrounding stimuli has previously been investigated psychophysically (Ito et al. 1998; Zenger et al. 2000; Roberts and Thiele 2005). These studies reported that directing attention towards a central target stimulus reduced the influence of surrounding stimuli on the

perception of the target. Ito and Gilbert (1999) followed up their psychophysical study by recording from V1 neurons in two alert macaques using parameters identical to those in their psychophysics study. The monkey either focused attention towards the location of the RF of the neuron under study, or distributed its attention over the whole visual field. Stimuli were either isolated bars presented in the CRF, or a bar in the CRF combined with a collinear flanker in the nCRF. Thus the effect of the flanker on the response to the bar in the CRF was measured under conditions of both focused and distributed attention. Unfortunately, the results of this study concerning the interaction of attention and contextual influences were inconsistent between the two monkeys. In one monkey contextual facilitation was stronger in the distributed attention condition than in the focused attention condition, in line with their human psychophysical findings. However in the second monkey the effect was reversed: there was increased surround facilitation in the focal attention condition. Due to this inconsistency, the precise effect of attention on contextual modulation of V1 neuronal responses remains to be determined.

In my psychophysical study, presented in Chapter 1 (Roberts and Thiele 2005), I suggested a possible pharmacological basis for the observed reduction in contextual modulation with attention. High levels of attention are associated with increased ACh release into the cortex (Everitt and Robbins 1997; Sarter and Bruno 1997). Several *in vitro* studies have suggested that an important function of ACh is to selectively suppress the efficacy of intracortical synapses whilst leaving thalamocortical synapses unaffected (Hasselmo and Bower 1992; Kimura et al. 1999; Hsieh et al. 2000; Kimura 2000), or even enhanced (Gil et al. 1997). Thus the action of ACh might be to bias cortical processing in favour of the feed-forward input (Kimura 2000). In primary visual cortex, feed-back and lateral connections are thought to underlie the nCRF influence, whilst feed-forward connections from the LGN are likely to be the major source of CRF activation (Hupe et al. 1998; Lamme and Roelfsema 2000; Hupe et al. 2001; Angelucci et al. 2002; Angelucci et al. 2002; Li 2003; Lund et al. 2003). Thus in primary visual cortex, ACh would be expected to reduce nCRF modulation and enhance CRF activation by suppressing the efficacy of intracortical connections and boosting the efficacy of feed-forward connections.

I addressed this proposal directly in Chapter 2 (Roberts et al. 2005), where I showed that iontophoretic application of ACh into primate primary visual cortex reduced contextual modulation, demonstrated by a reduction in preferred length in

the presence of applied ACh. In this chapter I investigate whether directing visual attention towards the RF of the cell under study would lead to similar effects on preferred length. Length tuning is a classic demonstration of non-classical receptive field (nCRF) modulation (DeAngelis et al. 1994). For almost all cells in primary visual cortex, the presentation of a bar longer than the diameter of the classical receptive field (CRF) results in a higher response than the presentation of a bar equal to the CRF diameter. This effect demonstrates the presence of an excitatory inner-fringe of the nCRF (DeAngelis et al. 1994; Sceniak et al. 2001; Angelucci et al. 2002; Angelucci and Bullier 2003). Stimulation of this inner fringe alone does not cause the cell to respond, therefore it is generally not thought to be part of the CRF. The extent of the CRF together with the excitatory inner fringe of the nCRF describes the cell's summation area. Increasing stimulus length up to the limit of the summation area will cause an increase in response. The stimulus length that yields the highest responses corresponds to the cell's preferred length. Beyond the limit of the summation area, the nCRF is typically suppressive (DeAngelis et al. 1994; Sceniak et al. 2001; Angelucci et al. 2002; Angelucci and Bullier 2003); thus when stimuli extend beyond the summation area the neuronal response is reduced. The amount by which the response can be suppressed, and the area over which increased stimulus length causes increased response suppression reveal the strength and spatial extent of the inhibitory parts of the nCRF. Thus, length tuning is a good method to assess the impact of the nCRF, because both excitatory and inhibitory interactions can be explored. Moreover, since length is a continuous variable, the data can be used to fit a model which allows subtle changes in tuning to be examined. In the current chapter I found that in the near-foveal visual field (eccentricity $\sim 2^\circ$), directing attention towards the RF caused a shift in the cell's preferred length towards shorter bars, matching the effect of ACh application presented in Chapter 2. Such a reduction in preferred length reflects a reduction in nCRF (contextual) modulation, demonstrating a possible neuronal substrate for the psychophysical effects presented in Chapter 1.

I used a range of stimulus contrasts in my experiment and found that the reduction in preferred length occurred for both saturating and non-saturating stimuli. However, I found no attentional effect on length tuning for low contrast (<8%) stimuli. Interestingly, I also found that the effect of attention on preferred length was reversed when stimuli were presented in the periphery of the visual field ($5^\circ - 9^\circ$

eccentricity). This reversal could potentially be explained by differences in surround modulation across the visual field (Xing and Heeger 2000; Petrov et al. 2004; Petrov et al. 2005) and so does not necessarily contradict my argument that attention reduces contextual modulation.

3.3 Methods

All experiments were carried out in accordance with the European Communities Council Directive 1986 (86/609/EEC), the National Institutes of Health *Guidelines for the Care and Use of Animals for Experimental Procedures*, the Society for Neuroscience *Policies on the Use of Animals and Humans in Neuroscience Research*, and the UK Animals Scientific Procedures Act.

3.3.1 Initial animal training

The subjects were two macaques (*macaca mulatta*); I refer to them as monkey B and monkey D. Before implantation the monkeys were trained to sit calmly in a primate chair for up to four hours and to perform a simple task. In this task, the monkeys initiated a trial by holding a touch bar. A dark or light square was then presented on a computer screen in front of them. After a variable random time interval the luminance of the square would change. The monkey's task was to hold the touch bar until the stimulus changed luminance. Once the change had occurred the monkey had to release the touch bar within a limited time period to gain a juice reward. Since both the stimulus and the luminance change were small, I could be sure that the monkey was fixating the stimulus in order to solve the task. I could use this task to calibrate the eye tracker on a daily basis once fixation training began.

3.3.2 Surgical preparation

The monkeys were implanted for chronic awake electrophysiological recordings. Implants consisted of one head post placed at the top of the head, and two to three recording chambers of which at least one was above primary visual cortex. These were held in place by dental acrylic (Griptm cement, DENTSPLY Caulk, Delaware), which was secured to the skull by three T-shaped trans-cranial screws. Gaps in the bone surrounding the trans-cranial screws were filled with Biobon (Merck biomedical). Additional support for the implant was provided by a number of ceramic bone screws (7 in monkey B, 6 in monkey D; S14 2.7mm cortex screws Thomas Recording). The recording chambers, head post and trans-cranial screws

were made of peek plastic (Tecapeak GF 30 Ensinger). Ferrous and paramagnetic materials were avoided to make the implant MRI compatible. In addition, an eye-coil was implanted between the conjunctiva and the sclera in one eye to allow for the recording of eye position. The coil surgery closely followed the description in Judge et al. (Judge et al. 1980). In particular, the coil was implanted above the rectus muscles and was not sutured to the sclera, as described in earlier methods (Fuchs and Robinson 1966). The surgery differed from that described by Judge et al. (1980) in that the incision around the limbus was made with fine scissors whilst holding the eye still, rather than by rotating the eye beneath a stationary held scalpel blade. Moreover, in addition to the pouch created between Tenon's capsule and the conjunctiva (in the subconjunctival space), a second pouch was created in the skin at the temple. Loops of wire were placed into both pouches to prevent mechanical interference during eye movements. The eye-coil was made of thin stainless steel wire coated in silicone (code AS632 Cooner Wire, CA). The impedance of the coil ranged from 40Ω - 80Ω . All surgeries were performed under general anaesthesia and sterile conditions. Drugs used for anaesthesia were ketamine (0.1ml/kg) to sedate the animal, followed by bolus intravenous (i.v.) injections of Propofol whilst the animal was intubated to allow for artificial ventilation during surgery. Anaesthesia during surgery was maintained by a gaseous anaesthetic (sevoflurane or isoflurane, 1-3%) combined with alfentanil ($156\mu\text{g}/\text{kg}/\text{hour}$ i.v.). Antibiotics were also administered (1ml Ceporex). The animal's rectal temperature, heart rate, blood oxygenation (SpO_2) and expired CO_2 were monitored and recorded during surgery. Antibiotics (Ceporex 0.5ml/kg or Synulox 0.25ml/kg) and analgesics (Metacam 0.1ml/kg) were given for 3 to 5 days after surgery.

3.3.3 Care after surgery

After implantation the monkeys continued working without head restraint for a few months, to allow for adequate implant stability. The animals were then trained to accept head restraint for several hours at a time, and to fixate accurately (to within $\pm 0.5^\circ$) on a small stimulus for up to 4 seconds. Once this was achieved I began to train the animal on my main experimental task, in which attention could be directed either towards or away from the receptive field (RF) of the neuron under study.

I cleaned the implant surface, the wound margin and the inside of any chambers that had a craniotomy with betadine solution at the beginning and end of

every recording or training session. Hair around the wound margin was regularly clipped. Moreover, to reduce the problem of dural scarring leading to tough impenetrable tissue, I applied 5-fluoro-uracil for 5 to 10 minutes three times per week once recording started (Spinks et al. 2003). Despite this treatment it was still necessary to scrape away fibrous tissue covering the dura, usually every 6 to 8 weeks, to allow for continued access to the cortex. This was done under surgical conditions as described above. In monkey B it became necessary to remove and re-implant the V1 recording chamber due to reduced recording stability. I was thus able to record at two retinal locations from this monkey. One recording location had cell RFs with eccentricities of $\sim 2^\circ$, the other had cell RFs with eccentricities of $\sim 7^\circ$. In monkey D all RFs were at an eccentricity of $\sim 2^\circ$ (see Figure 3.22).

3.3.4 Receptive field mapping

Receptive fields were assessed using an automated mapping procedure under passive viewing conditions. For this, a 0.1° black (100% contrast) square was presented at pseudo-random locations on a 10×10 grid (thus mapping a 1 degree^2 area). At each location the square was presented for 100msec with a 100msec inter-stimulus interval. Each location was stimulated five times during the mapping procedure. To prevent the monkey from attributing a 'special status' to the RF location, an identical stimulus was presented in the opposite hemifield simultaneously. The mean response at each stimulus location (spikes occurring from 30msec after stimulus onset until stimulus offset) was represented as a 2D coloured surface. To find the centre of the RF I normalised the mean response across space (so that the highest response was equal to 1) and fitted a 2D Gaussian to the surface. The RF centre was taken as the location of the peak of the fitted Gaussian. If there was a large discrepancy between the fitted centre and the location of the highest mean response, I took the location of the highest mean response as the RF centre. The form of the fitted 2D Gaussian was:

$$m(x, y) = (\exp^{-2 \times (x - x_{\mu}) / \sigma})^2 \times (\exp^{-2 \times (y - y_{\mu}) / \sigma})^2 \quad (\text{Equation 3.1})$$

where 'm(x,y)' is the predicted response at the location 'x' and 'y' degrees from fixation, 'x μ ' is the location of the fitted peak in the 'x' dimension, 'y μ ' is the location of the fitted peak in the y dimension and 'sigma' is the width of the fitted

Gaussian, which was symmetrical in x and y dimensions. The peak of the fitted function is always equal to 1, and since it was fitted to normalised data there is no need for a gain parameter.

To assess the size of the RF I counted the number of locations where the response was not significantly below the maximum response. I took $p > 0.05$ as my threshold for inclusion into the RF area (1-tailed 2-sample t-test).

Example of raw data from RF mapping

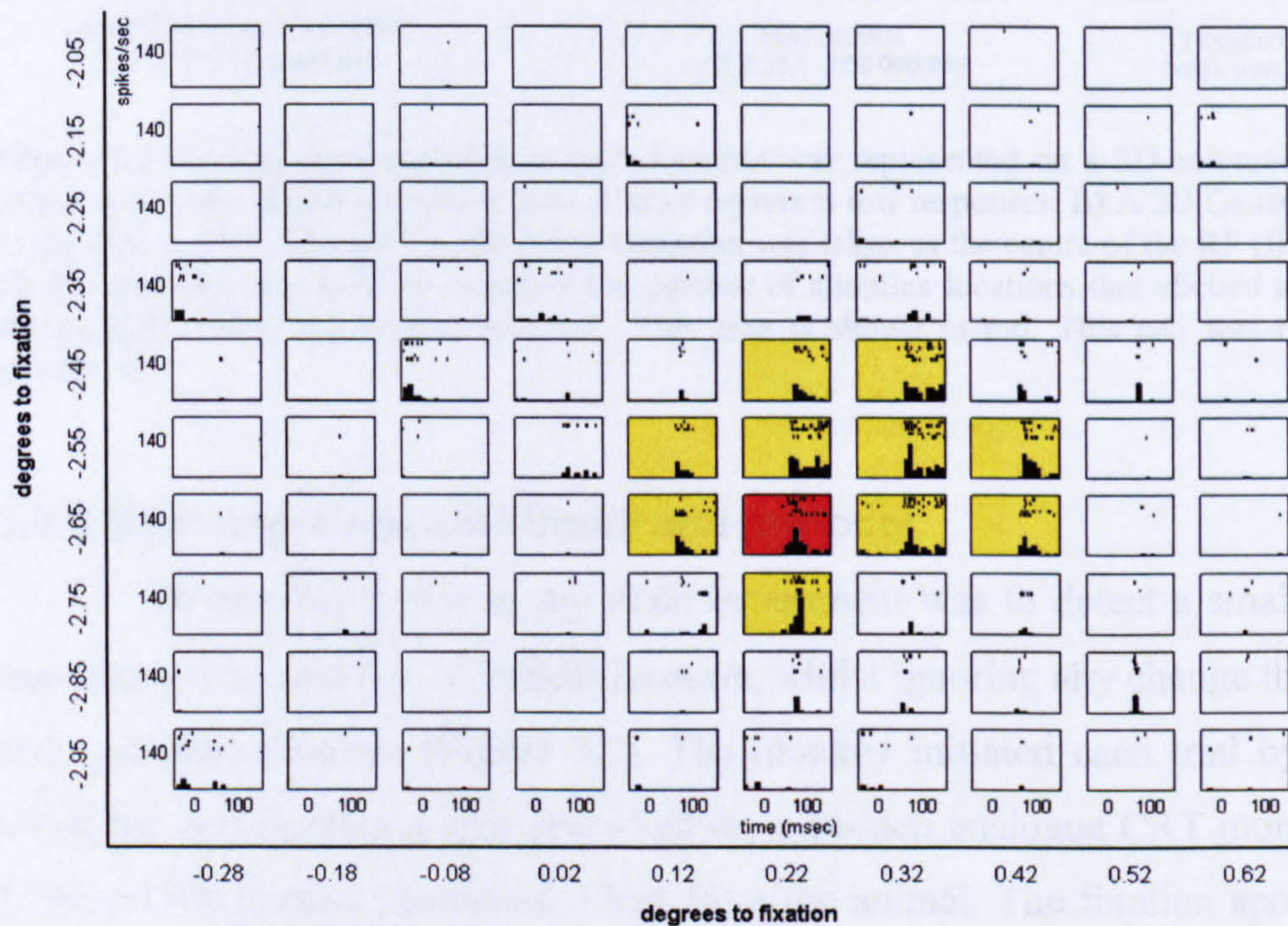


Figure 3.1 Raw data from automated RF mapping. 1 degree² of visual space was mapped by presenting 0.1° squares at 100 locations on a 10x10 grid. This grid is represented by the small plots in the figure. The stimulus was presented for 100msec at each location. Each small plot in the figure shows the neuronal response (raster plots and histograms) to the presentation of the stimulus at the corresponding location (large x- and y-axes). The plot marked in red shows the location of the highest mean response. Plots marked in yellow show locations where the response was not significantly below the highest response (1-tailed, 2-sample t-test, $p > 0.05$). The RF size was taken as the sum of the areas where the response was not significantly below the highest response (here 0.11 degree²). This cell was recorded from monkey B.

Processed RF mapping data

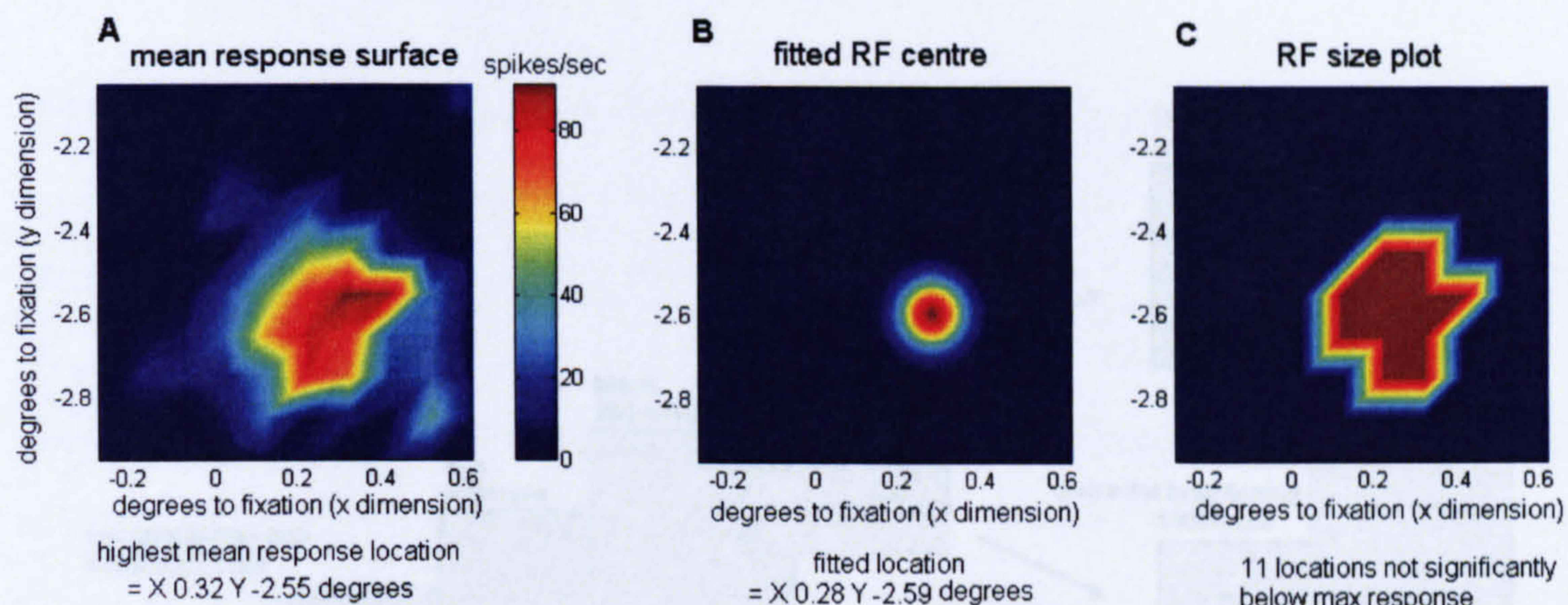


Figure 3.2 **A)** The mean response at each location was represented on a 3D coloured surface; red colours represent higher responses, blue colours represent low responses. **B)** A 2D Gaussian was fitted to the data surface. The peak of the fitted Gaussian was taken as the centre of the RF (fitted location). **C)** RF area was measured by counting the number of stimulus locations that elicited a response not significantly below the highest response. This area is shown in red. This cell was recorded from monkey B.

3.3.5 Main experimental stimuli and protocol

The monkey's task in my main experiment was to detect a small change in luminance at a cued (i.e. attended) location, whilst ignoring any change that occurred at a non-cued location (Figure 3.3). The monkey initiated each trial by holding a touch bar and fixating a spot presented on a 20-inch analogue CRT monitor (75Hz, 1600 x 1200 pixels) positioned 57cm from the animal. The fixation spot was a red circle or annulus (0.1° to 0.05° diameter) on a grey background (21.0cd/m^2). Once the trial was initiated, a cue (a blue annulus, 0.24° diameter) was presented for 400msec on one side of the fixation spot. The location of the cue indicated the location to which the monkey had to attend. The cue was presented displaced along the axis connecting the fixation spot and the RF location by one quarter of the eccentricity of the RF of the neuron under study, thus the cue never infringed even remotely on the RF. It could be displaced either towards or away from the RF, to indicate whether attention should be directed towards or away from the stimulus presented in the RF. After the cue was extinguished there was a 250msec interval during which the monkey continued fixating and continued to hold the touch bar. By spatially and temporally separating the cue from the test stimuli, I ensured that the presentation of the cue would have no direct effect on the neuronal response to the test stimulus. At the end of this interval two identical stimuli were presented (test

PAGE: 129.

MISSING

IN

ORIGINAL

Representation of main experimental task

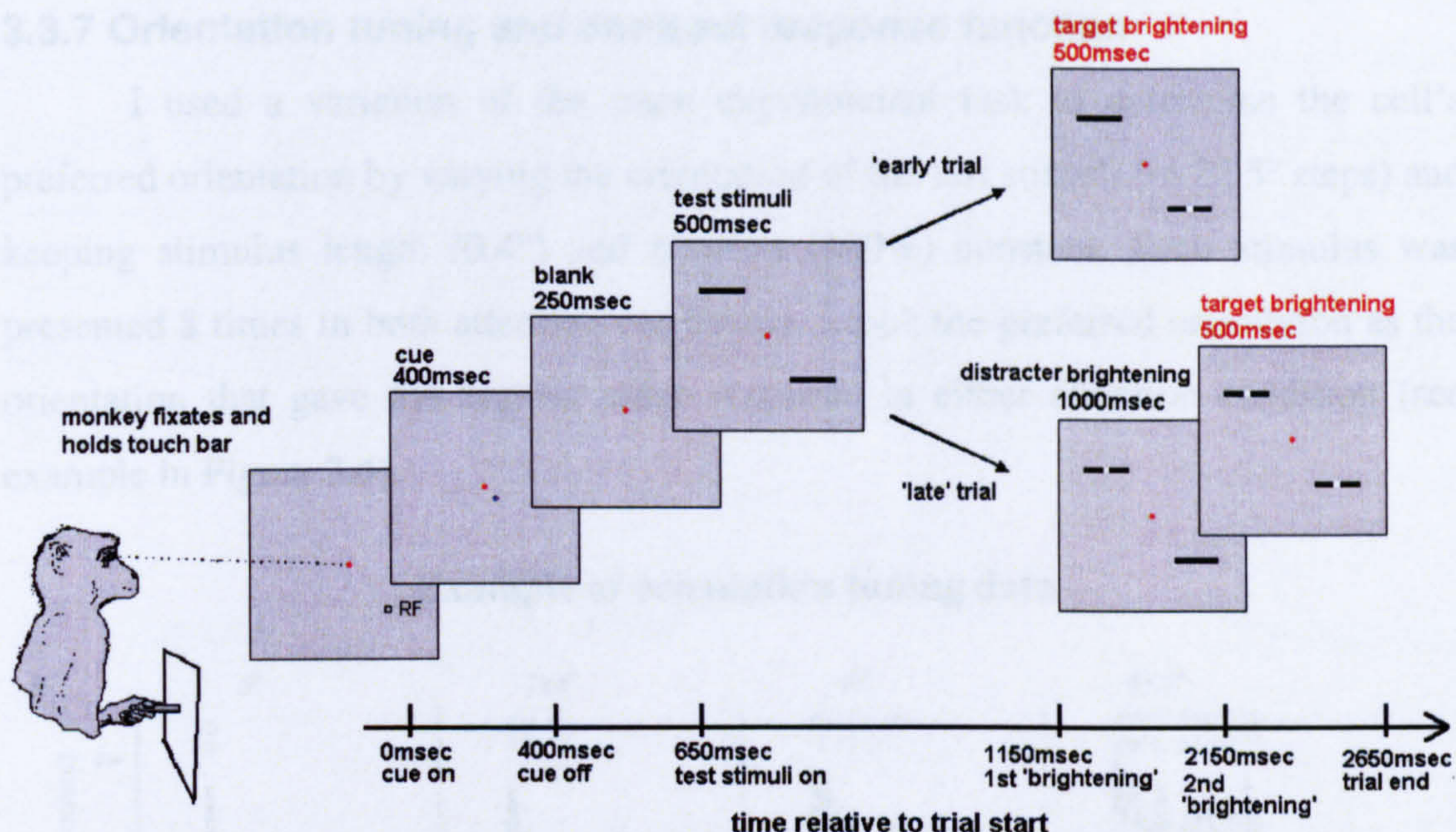


Figure 3.3 Representation of the main experimental task. The timing of relevant events relative to the start of the trial is marked along the bottom axis. Above the each frame is written the duration for which it is presented. The monkey initiated the trial by fixating centrally (red dot) and holding a touch-bar. At the start of the trial a cue (blue dot) pointed towards the location to which the monkey should attend. The cue was spatially and temporally separated from the stimulus. In the current example the cue points towards the RF of the neuron under study. Test stimuli were two identical bars, one presented at the RF of the neuron under study and one in the opposite hemifield. The monkey's task was to detect an increase in luminance over the central 0.1° of a cued bar, referred to as a 'brightening'. The first 'brightening' occurred 500msec after bar appearance. In an 'early' target trial the first brightening was presented at the cued (target) location. The monkey then had 500msec to respond by releasing the touch bar to receive a juice reward. In a 'late' target trial the first brightening was presented at the un-cued location. The target brightening occurred at the cued location 1000msec after the presentation of the distracter brightening at the un-cued location. The monkey then had 500msec to respond correctly.

3.3.6 Experimental design

I used a two-block design: cueing towards and cueing away from the RF. Within each block bar length was varied in six steps (0.1° 0.2° 0.4° 0.8° 1.6° and 2.4°). For each bar length the target occurred once before the distracter (early target) and once after the distracter (late target) within each block. Thus blocks lasted for 12 correct trials (i.e. 6 bar lengths each for early and for late targets in random order). If the monkey made an error the condition would be repeated later in the block. The two blocks occurred alternately in random order. For sessions in which I varied contrast as well as bar length, I used a four-block design: cued-towards and cued-away from the RF at both higher and lower contrast. I only included cells for further

analysis if the monkey worked for long enough to record at least 8 trials per condition (i.e. at least 4 repeats of each block).

3.3.7 Orientation tuning and contrast response function

I used a variation of the main experimental task to determine the cell's preferred orientation by varying the orientation of the test stimuli (in 22.5° steps) and keeping stimulus length (0.4°) and contrast (100%) constant. Each stimulus was presented 8 times in both attention conditions. I took the preferred orientation as the orientation that gave the highest mean response in either attention condition (see example in Figure 3.4).

Example of orientation tuning data

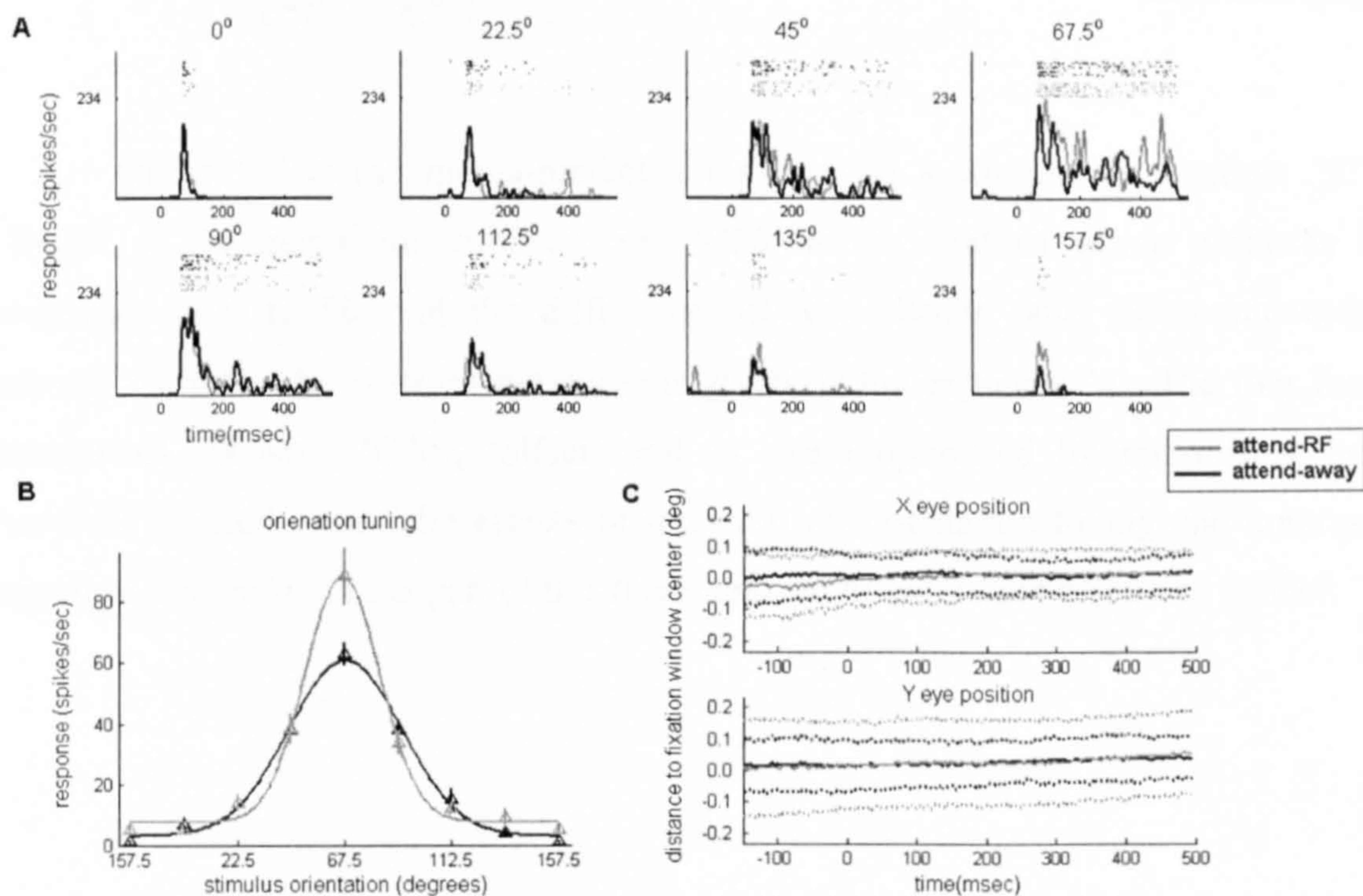


Figure 3.4 Example of orientation tuning data. **A)** Neuronal responses to eight stimuli of varying orientation (see plot titles). At the base of each plot responses are shown as histograms, and at the top of each plot responses are shown as raster plots. Responses in the attend-away condition are shown in black, responses in the attend-RF condition are shown in grey. **B)** Orientation tuning: triangles show mean response to each stimulus orientation, error bars show standard error. Smooth curves show fitted Gaussians. Triangles, error bars and curves in black correspond to the attend-away condition; those in grey correspond to the attend-RF condition. The distribution is centred over the highest mean response, corresponding to the preferred orientation (here 67.5°). **C)** X and Y eye position (upper and lower plots respectively) during the trial. In each plot, the x-axis shows time relative to stimulus onset. The y-axis in each plot shows the eye position in degrees relative to the centre of the fixation window. Solid lines show the median eye position, and dashed lines show the 25th and 75th percentiles. Black lines show eye position in the attend-away condition, grey lines show eye position in the attend-RF condition. This cell was recorded from monkey B.

I measured the contrast response function either under passive viewing conditions using flashed bars of different contrasts, or by using a variation of the main experimental task in which the contrast of the test bar was varied in 8 steps. The bar was set to the preferred orientation of the cell, and had a length of 0.4°. Each stimulus was presented 8 times in both attention conditions. A Naka-Rushton contrast response function was fitted to the mean response at each contrast. This function was used to choose two contrast values that I predicted would give significantly different responses (see example in Figure 3.5). The form of the fitted function was:

$$Y = \left(R_{\max} \times \frac{X^n}{c50^n + X^n} \right) + \text{offset} \quad (\text{Equation 3.2})$$

where 'Y' is the model-predicted response to a stimulus of contrast 'X', 'Rmax' is the maximum response, and 'C50' is the contrast which produces a response equal to 50% of the difference between 'Rmax' and the spontaneous activity 'offset'. The slope of the curve is given by the exponent 'n'. The four free parameters, 'Rmax', 'C50', 'offset' and 'n' were optimised by minimising the summed squared error. The effects of attention on orientation tuning and contrast response functions are not part of this thesis and are therefore not discussed further.

Example of contrast response function

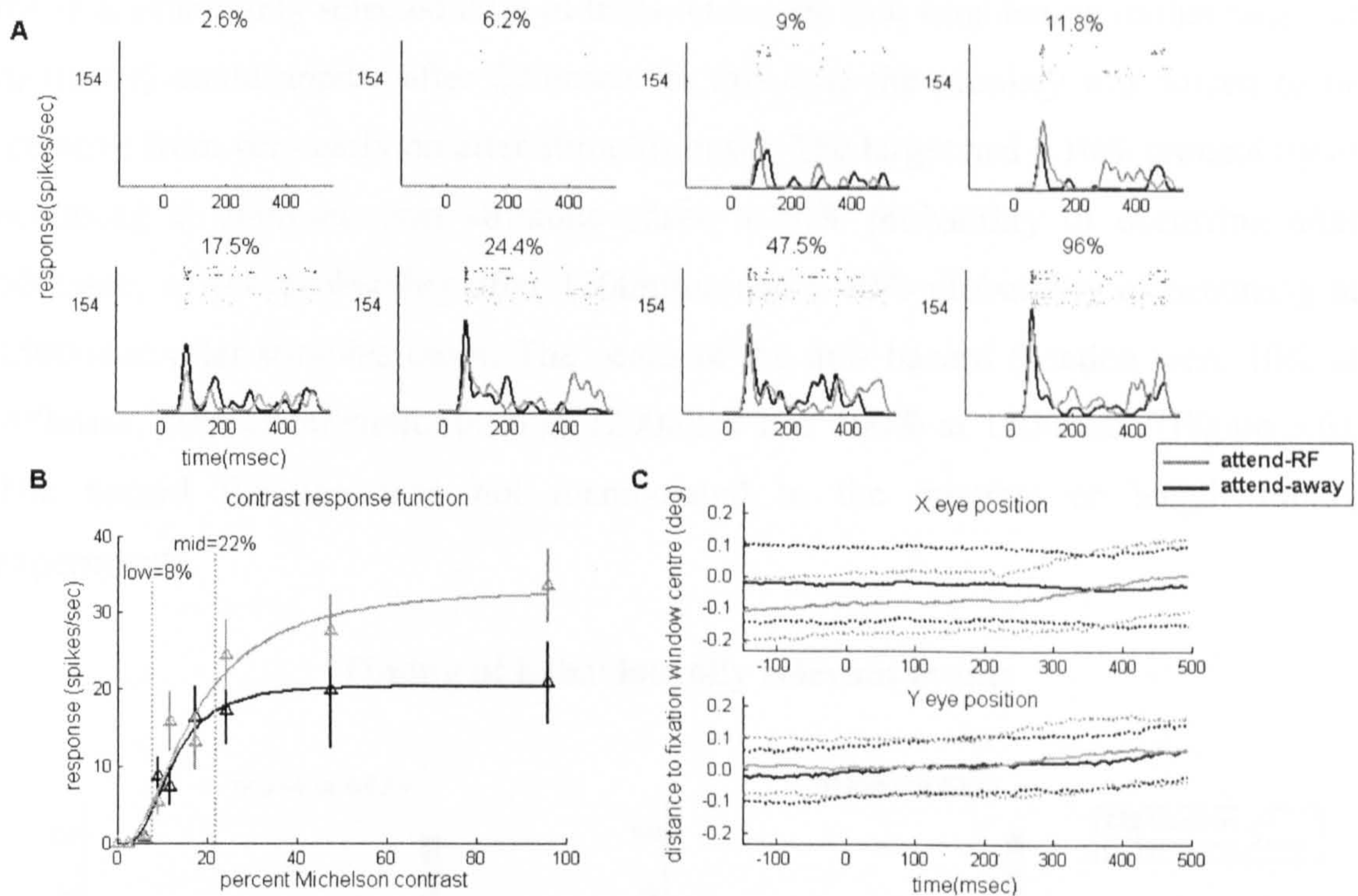


Figure 3.5 Example of contrast response data. **A)** Neuronal responses to eight stimuli of varying Michelson contrast (see plot titles). At the base of each plot responses are shown as histograms, at the top of each plot responses are shown as raster plots. Responses in the attend-away condition are shown in black, responses in the attend-RF condition are shown in grey. **B)** Contrast response function: triangles show mean response to each stimulus contrast, error bars show standard error. Smooth curves show fitted Naka-Rushton function. Triangles, error bars and curves in black correspond to the attend-away condition, those in grey correspond to the attend-RF condition. Vertical dotted lines show contrasts to be used for low and medium (mid) contrast recordings in the length tuning experiment. **C)** X and Y eye position are shown in the same format as in figure 3.4. This cell was recorded from monkey B.

3.3.8 Assessing the impact of the hazard function

The hazard function describes the temporal distribution of behaviourally relevant events (e.g. the appearance of the target brightening) during a trial. It is calculated as the probability that such an event will occur given that it has not already occurred during a trial. Thus, the hazard function is the cumulative probability of the target being presented in each time interval.

In my main task the target had a 50% probability of occurring at 500msec post stimulus onset and a 50% probability of occurring at 1500msec after stimulus onset. Thus the hazard function had one peak at 500msec after stimulus onset where the hazard was 50%, and a second peak at 1500msec where the hazard was 100%. Under these conditions the monkey may have been inattentive for the first several hundred milliseconds. To test whether the hazard function was reflected in the temporal profile of attentional modulation of neuronal responses, I modified monkey

B's orientation tuning task after ~8 months of recording. In the modified version of the task I randomly selected 20% of trials where the first brightening (either target or distracter) could appear after 200msec. In this case the monkey was forced to be attentive from very early on after stimulus onset. The target had a 10% probability of occurring at 200msec post stimulus onset, a 40% probability of occurring after 500msec, a 10% probability after 1200msec and a 40% probability of occurring at 1500msec after stimulus onset. The peaks of the new hazard function were 10% at 200msec, 50% at 500msec, 60% at 1200msec and 100% at 1500msec (Figure 3.6). The hazard function was not manipulated in the contrast or length tuning experiments.

Timing of behaviourally relevant events

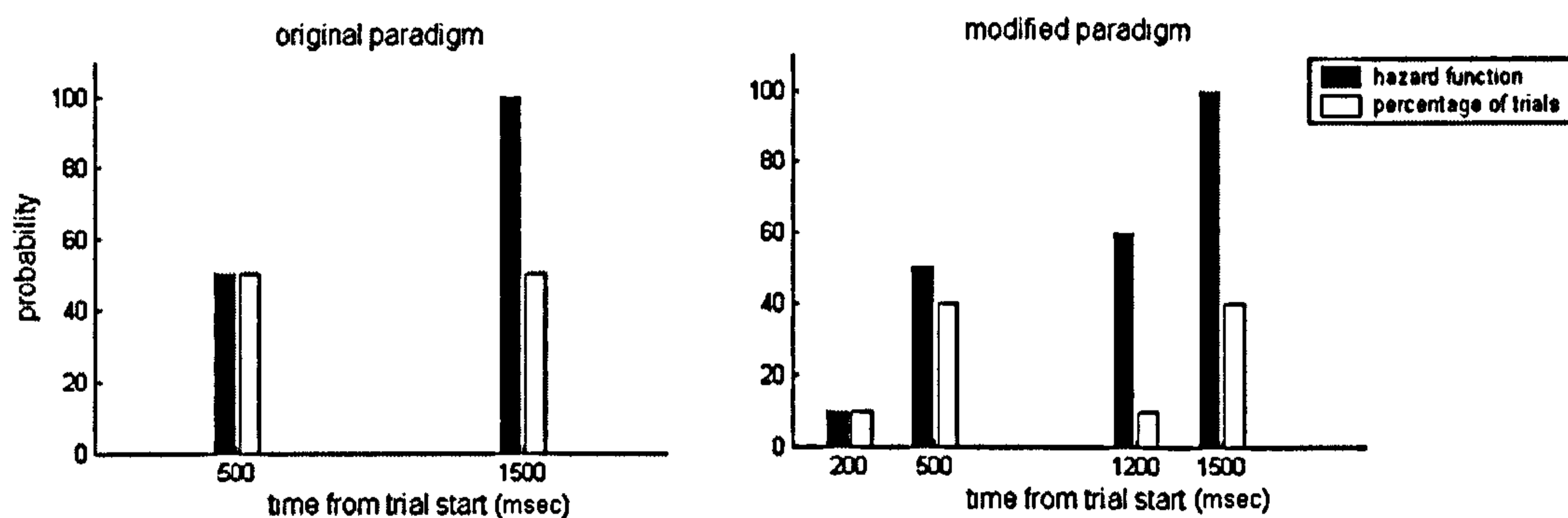


Figure 3.6 The timing of behaviourally relevant events (the target) in the original and modified paradigms. White bars show the percentage of trials in which the target was presented at each possible time. Black bars show the hazard function; the probability that the target will be presented at each possible time, given that it has not occurred at a previous time.

3.3.9 Electrophysiological recordings

Once the monkeys were able to perform the task reliably a craniotomy was made to allow electrode access to V1. Extracellular responses were recorded either by tungsten-in-glass micro-electrodes (pulled with a Narishege PE-21 puller, 0.5-1.5M Ω , Harvard apparatus LTD borosilicate glass capillaries 1mm outer diameter, 0.58mm inner diameter holding one sharpened tungsten wire 0.125mm diameter) or by tungsten-in-epoxy micro-electrodes (Frederick Haer, FHC, 1-2M Ω). Recordings were usually taken from just one site per day. After penetrating the dura and entering the cortex I allowed the tissue to 'settle' for between 5 and 30 minutes. I then attempted to achieve the best possible isolation of single unit activity by slowly moving the electrode forwards or backwards until good isolation was achieved. Because I attempt to isolated units as soon as the cortex had been entered and the

tissue had settled, my recordings were mostly from the supra-granular layers. Stimuli were presented and spike timings were collected with a sampling resolution of 1msec under the control of Remote Cortex 5.95 (Laboratory of Neuropsychology, National Institute for Mental Health, Bethesda). I set the thresholds of my window-discriminating spike detector such that I could be reasonably confident that spikes recorded represented a single neuron, however, occasionally the isolation may have been such that multi-unit activity (2-3 cells) was recorded.

3.3.10 Recording protocol

For each cell I first mapped the RF (see example in figure 3.1 and 3.2), then measured the orientation tuning (see example in Figure 3.4), followed by the contrast response function for most cells (see example in Figure 3.5) and finally the length tuning (see example in Figure 3.8). To test the interaction between attention, contrast and bar length I compiled data sets of three contrast categories: high contrast, medium contrast and low contrast. In recordings using high contrast stimuli (named 'high contrast recordings' hereafter) the test bar contrast was always 100% relative to the background and therefore the cell's response may have been saturated. In recordings defined as 'medium contrast' a lower contrast was used and the cell's response was demonstrably not saturated (i.e. the highest response to a medium contrast stimulus was significantly lower than the highest response to any high (100%) contrast stimulus ($p < 0.05$, 1-tailed t-test). In recordings defined as 'low contrast' the cell's response was significantly lower than any medium contrast response ($p < 0.05$, 1-tailed t-test). Data obtained using stimuli from these contrast categories are referred to as 'high contrast data', 'medium contrast data' and 'low contrast data' respectively throughout the text. I used the measured contrast response function to determine which contrasts to use for the medium and low contrast categories on a cell-by-cell basis. Depending on the training and motivational status of the monkey I measured the effect of attention on length tuning at either one contrast level (either high or medium contrast) or at two (high and medium contrast or medium and low contrast). In some cases I included a single high contrast stimulus, interleaved with medium and low contrast length tuning recordings, as an additional test for the saturation response. In cases where I tested two contrasts, but found no significant reduction in the response to the lower of the two contrasts

($p > 0.05$, 1-tailed t-test), I accepted the responses to the higher contrast stimuli for further analysis and discarded the responses to the lower contrast stimuli.

3.3.11 Cell sample selection

Not every cell recorded was included for further analysis. I excluded cells where eye-position was substantially different between the attend-RF and attend-away conditions (mean difference in eye position $> 0.1^\circ$). Furthermore, since I had mapped the RF using 0.1° high contrast squares, I excluded cells where there was no response to high contrast bars of 0.1° length (response not significantly different from spontaneous activity, t-test $p > 0.05$). No response to the 0.1° bar suggested that the stimulus had been presented outside of the RF. Finally I excluded cells in which the length tuning was poorly described by the fitted model (percentage variance accounted for $< 80\%$). Based on these criteria I excluded 19 recordings from my sample (12 from monkey B and 7 from monkey D) out of a total of 218 recordings (146 from monkey B, 72 from monkey D).

3.3.12 Calculating stimulus-driven responses

I measured the neuronal response to each bar length in the attend-RF and attend-away conditions. In monkey B I calculated the mean response from 30msec after test bar onset to 500msec after test bar onset (i.e. up to the time of the appearance of the first brightening). In monkey D I calculated the response over the first 30 to 200msec after bar onset. I was forced to restrict the analysis in this way because the monkey made a stereotyped saccade of around 0.1° to 0.2° towards the cued location at around 200msec after bar onset, despite a fixation window of only $\pm 0.3^\circ$ to $\pm 0.55^\circ$. It is likely that the saccade was made in response to the onset of the test stimuli, as 200msec is approximately the latency of a stimulus-triggered saccade (Carpenter 2004). The effect of the saccade was often evident in the response rate of the neuron under study, thus the effect of attention on the response rate was confounded by the eye-position (Figure 3.7). To test whether differences between results from monkey B and D were accounted for by the different time intervals I re-analysed monkey B's data only including spikes up to 200msec after stimulus onset.

Spontaneous firing rate was calculated separately for the two attention conditions from responses during the 250msec preceding the presentation of the test stimuli. All stimulus-driven activity presented in this chapter was corrected for

spontaneous activity (i.e. spontaneous activity subtracted). This was done to fulfill the assumption in the fitting model that response is zero at zero bar length (no stimulus). Responses could have been left uncorrected for spontaneous activity only if an additional ‘offset’ term had been included into the fitting models (see next section *3.3.13 Length tuning analysis and fitting*).

Examples of the stereotyped saccade made by monkey D and its effect on neuronal responses

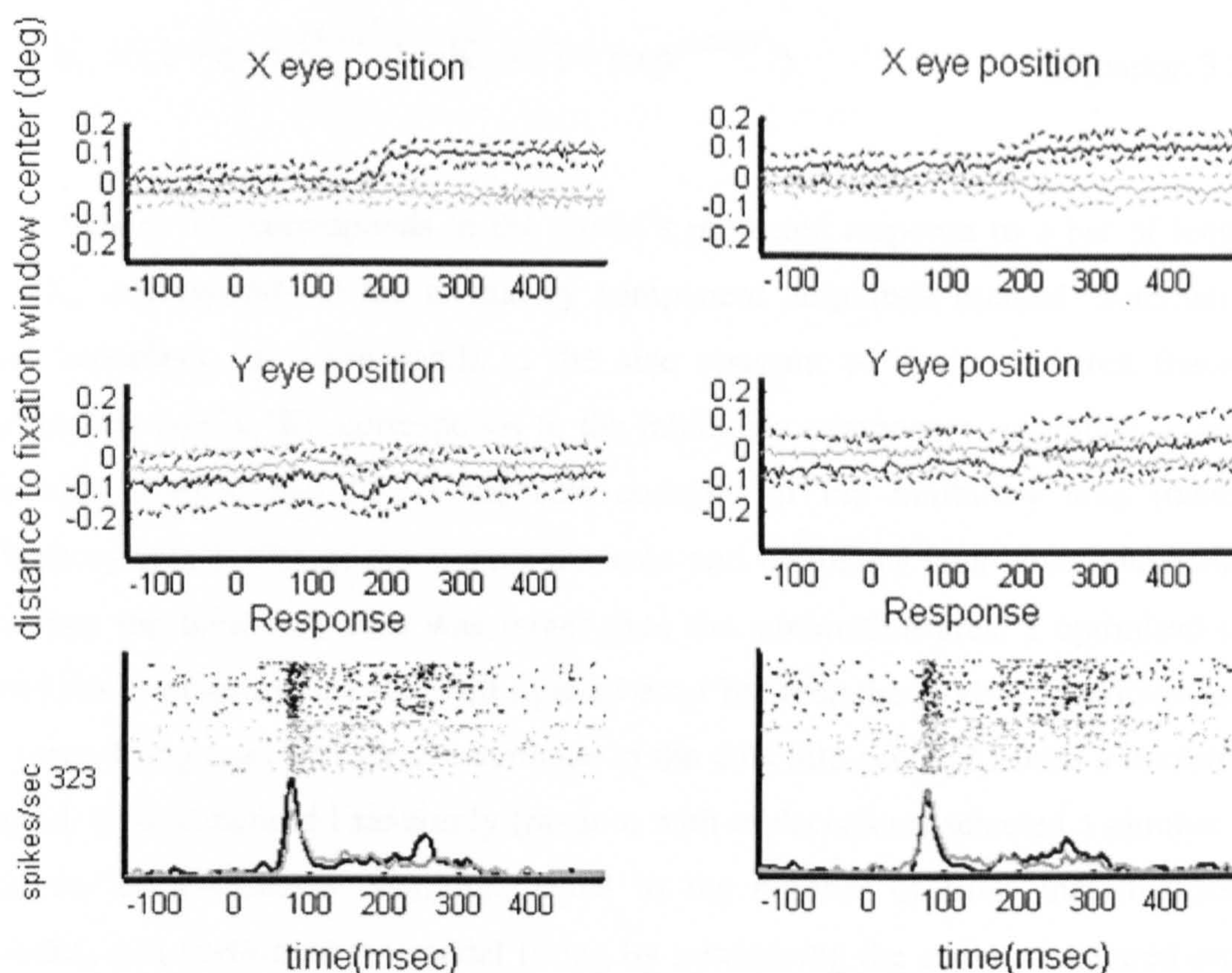


Figure 3.7 Two examples from the same cell where monkey D’s stereotyped saccade had a clear influence on response strength. Eye position in X and Y co-ordinates relative to the centre of the fixation window is shown in the upper plots. Solid lines show the median eye position, dashed lines show the 25th and 75th percentiles. Black lines show eye position in the attend-away condition, grey lines show eye position in the attend-RF condition. The saccade occurred in the attend-away condition at ~200msec after stimulus onset and is clearly evident in the X eye position in both examples. The bottom plots show the neuronal response as raster plots and histograms. Data from the attend-away condition is shown in black, data from the attend-RF condition in grey. Response was enhanced shortly after the saccade in the attend-away condition. This is likely to reflect a relative shift in the position of the stimulus within the RF.

3.3.13 Length tuning analysis and fitting

Length tuning data (mean response at each bar length corrected for spontaneous activity) was fitted with a difference of Gaussians (DOG) model (Sceniak et al. 2001). In this model the narrower Gaussian represents the RF’s

excitatory centre whilst the broader Gaussian represents the inhibitory surround. Each Gaussian is described by a strength constant (gain) and a space constant, determining its height and width respectively. The response to any bar length is modelled by the difference between the integrals of the area of each mechanism covered by the stimulus. This function captures the shape of measured length tuning curves and it allows the relative strength and size of excitation (summation) and inhibition areas to be separated. The fitted function is of the form:

$$m = K_e \times (1 - \exp^{-(2x/a)^2}) - K_i \times (1 - \exp^{-(2x/b)^2}) \quad (\text{Equation 3.3})$$

where 'm' corresponds to the model's predicted response to a bar of length 'x', 'K_e' corresponds to the excitatory component amplitude (named 'summation gain' hereafter), 'a' corresponds to the size constant of excitatory area (named 'summation area'), 'K_i' corresponds to the inhibitory component amplitude (named 'inhibitory gain'), and 'b' is the size constant of the inhibitory area (named 'inhibitory area'). Fits of the summation area and inhibitory area were constrained such that the inhibitory area was larger than the summation area. I optimised the model fits to minimise the summed squared error between the model's prediction and the mean firing rate. To take the variance in the data into account I used a bootstrap method. In this method I randomly (random with replacement) selected a number of trials for each stimulus condition, equal to the number of trials that had been recorded, and performed the model fitting by minimising the summed squared error between the model and the mean response across this selection of trials. The bootstrapping procedure was performed 100 times for each cell for data from the attend-RF condition and 100 times for data from the attend-away condition, thus resulting in 100 different estimates of preferred length for each condition, and 100 estimates for each condition of the four fitting parameters for each cell recorded. In order to increase the probability that the fitting routine yielded small error values (and thus good fits), I initially fitted the data with a set of 24 different starting positions for the different parameters. The starting parameters that resulted in the smallest error were used for the final optimization.

To gain an intuitive measure of the quality of the model fit, I calculated the percentage of variance accounted for by the fitted model (Carandini et al. 1997) calculated as:

$$\% \text{variance} = 100 \times \left(1 - \frac{D(m,r)}{D(R,r)}\right) \quad (\text{Equation 3.4})$$

where ‘D(m,r)’ corresponds to the mean squared difference between the model-predicted response (‘m’, Equation 3.3) and the observed mean firing rate (‘r’) at each bar length in the attend-RF and attend-away conditions, ‘D(R,r)’ corresponds to the mean squared difference between the grand mean firing rate (‘R’, calculated across all bar lengths and across the two attention conditions) and mean firing rate for each stimulus, separately for the two attention conditions. Thus ‘D(m,r)’ corresponds to the difference between the model prediction and the data and ‘D(R,r)’ corresponds to the variance of mean responses across stimulus and attention conditions. I calculated D(m,r) and D(R,r) as:

$$D(m,r) = \frac{1}{N} \sum_s |m_s - r_s|^2, \quad (\text{Equation 3.5})$$

$$D(R,r) = \frac{1}{N} \sum_s |R - r_s|^2, \quad (\text{Equation 3.6})$$

In both cases, the sum is over the range of stimuli and conditions ‘s’; ‘N’ is the number of stimuli multiplied by 2 (the number of attention conditions). To give an example of the calculation, if the mean difference between the model prediction and the observed data is small (e.g. D(m,r) = 10 spikes/sec) and the variance in the mean responses to each bar length and between the attend-RF and attend-away conditions is large (e.g. D(R,r) = 100 spikes/sec), then the percentage of the variance that is accounted for by the model is large (in this case 90%).

I optimised the fitted model using a bootstrap method, resulting in 100 model fits for both attention conditions. I calculated the percentage of variance accounted for by the median fitted model, i.e. the model prediction ‘m’ in Equation 3.4 was calculated as the median prediction obtained from the bootstrap procedure.

Example of length tuning data

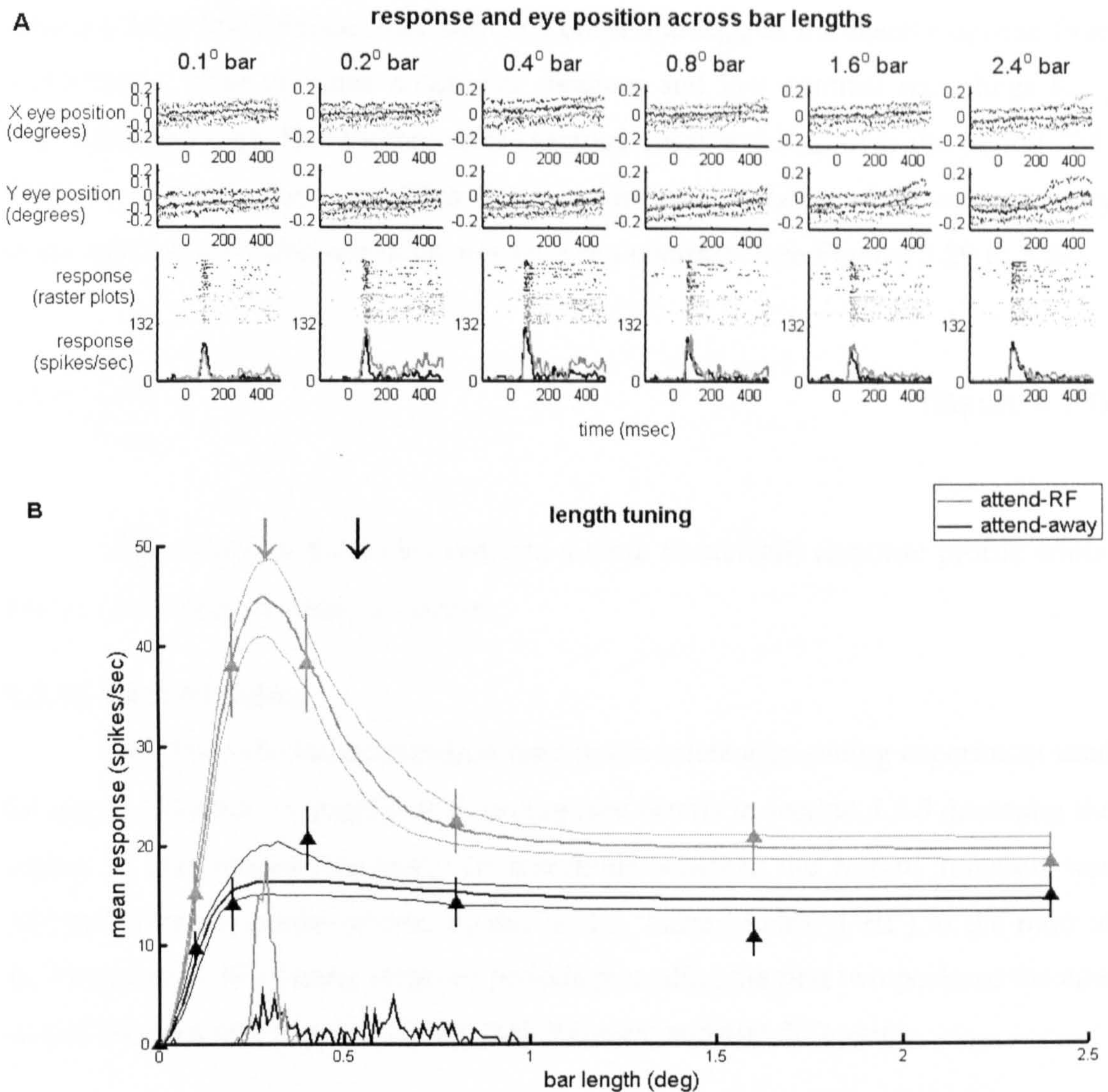


Figure 3.8 Example of length tuning data. **A**) Neuronal response and eye position at each bar length. X and Y eye position over time (relative to stimulus onset) is shown in degrees relative to the centre of the fixation window. Solid lines show the median eye position, dashed lines show the 25th and 75th percentiles. Black lines show eye position in the attend-away condition, grey lines show eye position in the attend-RF condition. The neuronal response relative to stimulus onset is shown as raster plots and histograms. Data from the attend-away condition is shown in black, data from the attend-RF condition is in grey. **B**) Length tuning. Triangles show mean response at each bar length, error bars show standard error. Bold line fitted to the data shows the median DOG model fit from the bootstrap procedure, flanking upper and lower narrow lines show the 75th and 25th percentile fits. Curves at the base of each plot show the distribution of preferred lengths taken from 100 iterations of the bootstrap procedure. Values in the histogram are normalised such that units have the same size on the y-axis as spikes/sec, thus units on the y-axis give spikes/sec and frequency in the histogram. The median preferred length is marked with the downwards-pointing arrow. Grey triangles, lines and arrows show data from the attend-RF condition, black triangles, lines and arrows show data from the attend-away condition. This cell was recorded from monkey B.

3.3.14 Tonic index

To determine whether attention influenced the shape of the response profile, I calculated a ‘tonic index’ (‘TI’) defined as the firing rate during the second half

response period ('R_{late}'), divided by the firing rate during the first half of the response period ('R_{early}'). For high contrast recordings I calculated R_{early} as the mean response from 30-235msec after stimulus onset and R_{late} as the mean response from 235-500msec after stimulus onset. For medium and low contrast recordings R_{early} was calculated over 50-225msec after stimulus onset and R_{late} over the period 225-500msec after stimulus onset. This difference in the calculation of TI was necessary to account for the difference in latency between contrasts (see Figures 3.29 to 3.32).

$$TI = \frac{R_{late}}{R_{early}} \quad (\text{Equation 3.7})$$

High values of this index indicate a tonic (sustained) response profile whilst low values indicate a phasic response.

3.3.15 Hazard index

I modified the hazard function used in the orientation tuning experiment used for monkey B after ~8 months of recording (see details in section 3.3.8 *Assessing the impact of the hazard function*). To determine whether the hazard function was reflected in the response profile, I calculated a 'hazard index' ('HI') as the ratio of the firing rates ('R') during 100msec periods preceding the first two peaks of the new hazard function (see Figure 3.6), i.e. 100-200msec and 400-500msec.

$$HI = \frac{R_{400\text{msec to }500\text{msec}}}{R_{100\text{msec to }200\text{msec}}} \quad (\text{Equation 3.8})$$

The HI was compared between the attend-RF and attend-away conditions. An increase in HI with attention indicated that attention enhanced the response more strongly in the 400-500msec post stimulus onset period than during the 100-200msec post stimulus onset period. No change in HI, despite a change in the mean firing rate over whole response period (30-500msec post stimulus onset), indicated that attention enhanced the response by the same amount in both periods.

3.3.16 Receiver operating characteristic (ROC) analysis

In addition to calculating absolute changes in firing rate between the two attention conditions, I calculated receiver operating characteristic (ROC) curves to assess by how much attention affected the response. The ROC is a measure of the overlap between the distributions of responses in the attend-RF condition and the attend-away condition. The ROC value represents the ability of an ideal observer to correctly identify the attend-RF condition based on the firing rate from an individual trial (Celebrini and Newsome 1994; Britten et al. 1996; Roelfsema and Spekreijse 2001). Unlike a parametric test (e.g. a t-test) the ROC method does not depend on assumptions about the variance or shape of the two distributions.

Each point along the y-axis of the ROC curve is calculated as the probability that responses in the attend-RF condition are greater than a set response criterion (Figure 3.9). The corresponding point on the x-axis is calculated as the probability that responses in the attend-away condition are greater than the criterion (Vogels and Orban 1990). The range of criteria used was equal to the range of the cell's responses recorded for each bar length in both attention conditions. The ROC value is calculated as the area beneath the ROC curve. If the distributions perfectly overlap, then there will be an approximately equal probability that responses from the attend-RF or attend-away condition will be above the criterion, thus the ROC value will be 0.5. If attention facilitates the response, then the probability that a response from the attend-RF condition is above the criterion will be larger than the probability that a response from the attend-away condition is above the criterion, thus the ROC value will be greater than 0.5. If attention inhibits the response, then the probability that a response from the attend-RF condition is above the criterion will be lower than the probability that a response from the attend-away condition is higher than the criterion, making the ROC value less than 0.5.

To assess the effect of attention on test response rates I calculated ROC curves for each cell at each bar length. I then tested whether the distribution of ROC values from across the population was significantly different from 0.5. I also used ROC values to test whether the magnitude of the attentional effect was dependent on stimulus length and stimulus contrast.

Explanation of ROC analysis

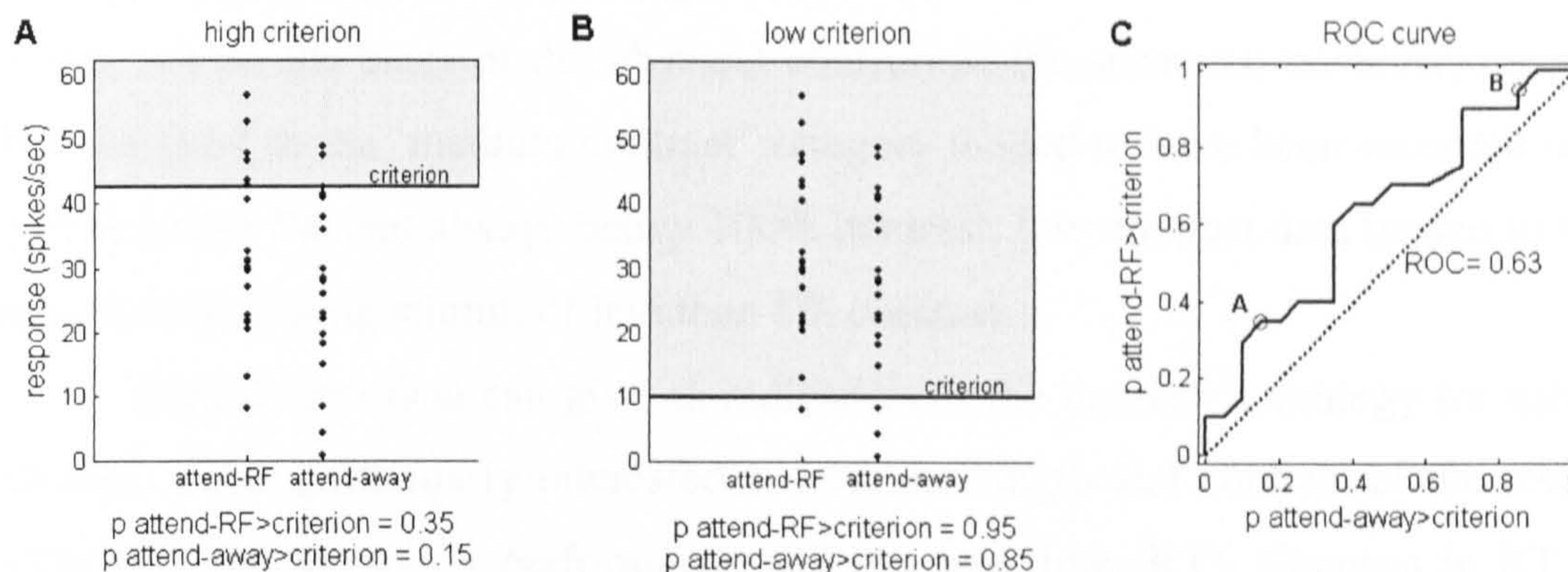


Figure 3.9 To calculate the receiver operating characteristic (ROC) a range of criteria was used. **A)** and **B)** Model responses from individual trials in both attention conditions are marked by a black dot ($n = 20$ in both conditions). The criterion is marked with a solid black line. For both a high (**A**) and a low (**B**) criterion there are more trials from the attend-RF condition above the criterion than there are trials from the attend-away condition. **C)** For each criterion, the probability that responses from the attend-RF condition are above the criterion gives the y-axis value of the ROC curve (black line). The corresponding point on the x-axis shows the probability that responses from the attend-away condition are greater than the criterion. Results from parts **A** and **B** are marked with circles along the curve. If responses in the attend-RF condition are generally higher than in the attend-away condition (as in the figure) then data from the attend-RF condition will be generally more likely above the criterion than data from the attend-away condition, therefore the area beneath the ROC curve will be greater than 0.5.

3.4 Results

3.4.1 Monkeys' behavioural performance

To determine the monkeys' behavioural performance I analysed trials from all sessions in which the monkey worked for at least 4 cycles of each block (8 trials per bar length) while neuronal data was recorded, however behavioural data has been included from recording sessions where neuronal data may be excluded from the analyses below, for example, due to poor recording conditions. Data was included from 79 sessions from monkey B and 42 sessions from monkey D. In many of these sessions stimuli of two different contrasts were presented. Data was divided into three contrast categories, depending on the contrast of the test stimulus. The 'high contrast' category represents data from conditions where the bar was at 100% contrast. The 'medium contrast' category represents data where the contrast of the bar was below 100% but above 8%. The 'low contrast' category represents data where the contrast of the bar was at or below 8%. The medium and low contrast categories are approximately equivalent to the medium and low contrast categories

used to analyse the neuronal data. They are not exactly equivalent because neuronal data were assigned to contrast categories on the basis of the cell's individual contrast tuning, not on the basis of the physical contrast of the stimulus; however, neuronal data assigned to the 'medium contrast' category tended to have been recorded using stimuli above 8% and always below 100% contrast; low contrast data tended to have been recorded using stimuli of less than 8% contrast.

Behavioural data can give an indication of the monkey's strategy for solving the task. I was particularly interested in how the length and contrast of the test bar influenced the monkey's performance and reaction time (RT). Changes in RT and performance could indicate differences in task demands between stimulus conditions. Since changing task demands are associated with different levels of attentional modulation (Spitzer et al. 1988; Seidemann and Newsome 1999), different task demands between the stimulus conditions could have influenced the degree of attentional modulation of neuronal responses between stimuli, and thus influenced the effect of attention on neuronal tuning functions. It was also interesting to investigate how the monkey's performance and RT were influenced by the cued location, the time of the target brightening and the amount of training. Furthermore, I investigated whether the monkey directed attention according to the cue or according to a 'blocked' strategy in which attention was directed to a particular location for as long as that location produced rewards. These alternative strategies could have had implications for the level of alertness of the monkey and the general state of the attentional network.

3.4.1.1 Reaction time and bar length

To calculate RT across bar lengths I first separated trials according to the location of the cue and the time of the target brightening. Thus, data were separated into four conditions; cued downwards (towards the RF), cued upwards (away from the RF), for both 'early' trials (target brightening presented at 500msec after test stimulus onset) and 'late' trials (target brightening presented at 1500msec after test stimulus onset, see Figure 3.3).

For high and medium contrast stimuli, both monkeys had RTs that were slower for shorter bars than for longer bars. For monkey B the fastest RT was for the longest bar length, for monkey D the fastest RT was for the 0.8° bar. The effect of bar length on RT was highly significant in all cases for high and medium contrast

stimuli ($p < 0.001$, 1-way ANOVA). For low contrast stimuli, monkey D showed a similar dependence of RT on bar length in 'early' trials ($p < 0.01$ in both cued up and cued down conditions), but no significant effect of bar length on RT in 'late' trials (cued down $p = 0.65$, cued up $p = 0.49$, 1-way ANOVA). In monkey B, low contrast stimuli were used only with stimuli presented at $\sim 7^\circ$ eccentricity. The data were similar to that of monkey D, RT was slower for short stimuli than for long stimuli in the early trials, and there was no clear trend in the late trials. The effect of bar length on RT was however, not significant in the early trials. It is likely that the effect of bar length on RT indicates that the bar aided the detection of the target brightening. This was unsurprising, since the contrast of the target brightening relative to the bar was greater than the contrast of the brightening relative to the background. These results show that there was a significant difference in RT across bar lengths, which might indicate that the task was harder with short bars than with long bars. An increase in RT alone does not however necessarily mean that the task was harder in the associated condition, since the animal may have traded speed for accuracy. That this was not the case is shown in the next section (*3.4.1.2 Performance and bar length*).

Effect of bar length on RT

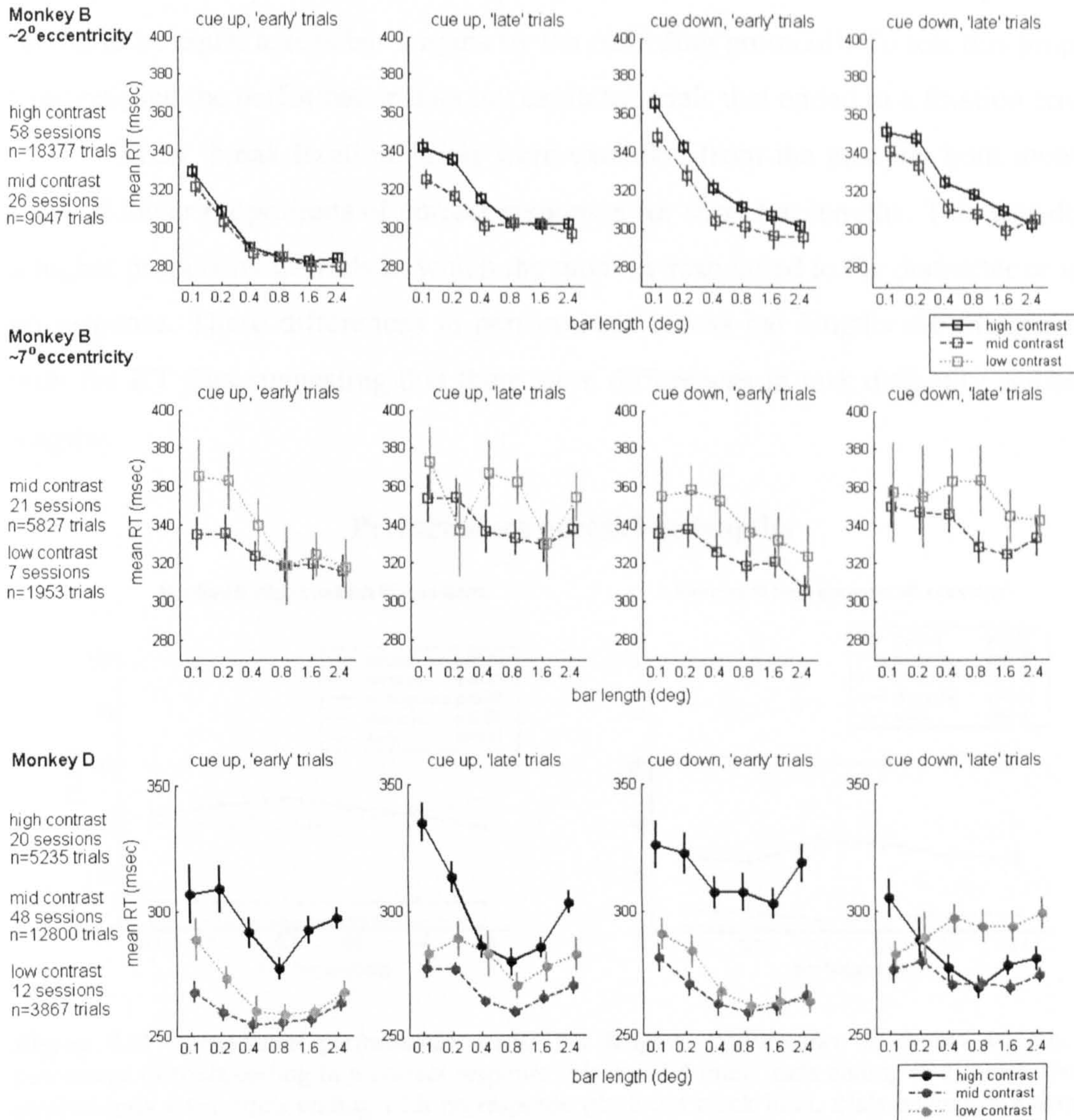


Figure 3.10 Reaction time as a function of bar length for high (black solid lines), medium (dark grey dashed lines) and low (light grey dotted lines) contrast stimuli. Points show mean RT, error bars show standard error. Here and throughout the chapter, data from monkey B is shown with open squares and data from monkey D is shown with filled circles.

3.4.1.2 Performance and bar length

To further address the possibility that task difficulty was dependent on bar length, I calculated the monkey's performance across bar lengths. Both monkeys showed the highest proportion of correct responses at the 0.4° bar length. Monkey B showed the lowest proportion of correct responses for the longest bar length. Monkey D showed approximately equal proportions of correct responses for the longest and shortest bar lengths. For both monkeys the pattern in proportions of correct responses across bar length was mirrored by differences in the proportions of fixation errors

across bar length, suggesting that fixation errors accounted for most of the variance in proportion correct across bar length. (N.B. the number of correct responses was forced to be equal across bar lengths by the recording protocol). To test this proposal I re-analysed the performance data but excluded trials that ended in a fixation error.

When ‘break fixation’ trials were excluded from the analysis both monkeys showed lower proportions of correct responses for short bar lengths. This was due to a higher proportion of trials in which the monkey responded to the distracter or made no response. These differences in performance across bar lengths are in agreement with the RT data suggesting that there were differences in task difficulty across bar lengths.

Performance across bar lengths

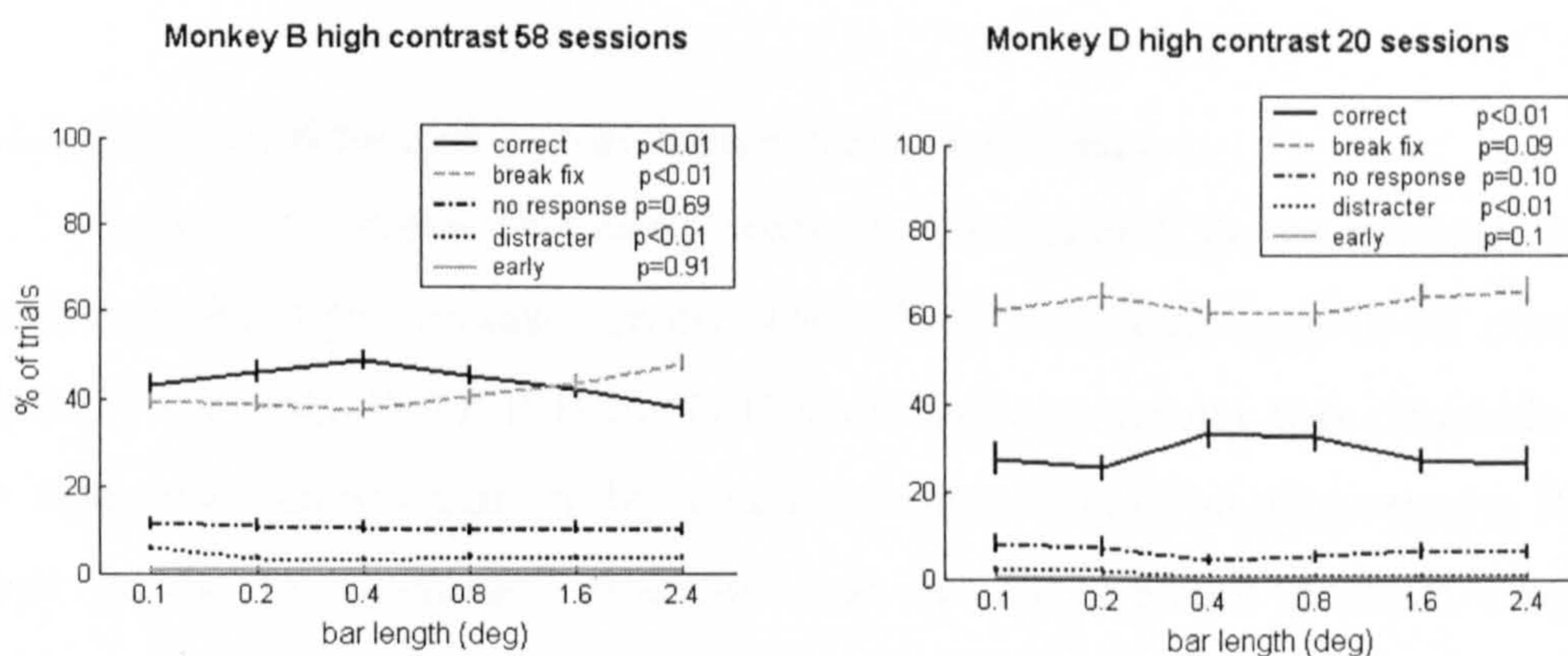


Figure 3.11 Behavioural performance across bar lengths. Performance is shown as: the mean percentage of trials ending in a correct response (black solid line), trials ending in a ‘break fixation’ (dashed grey line), trials ending with no response (dash-dot black line), trials ending in a distracter response (dotted black line) and percentage of trials ending in an early response (solid grey line; touch bar released before the first brightening). The data was calculated as the mean performance across sessions, error bars show standard error. The figure shows only data from trials using high contrast stimuli for both monkeys. At other contrasts the pattern is similar, although absolute values were different. P-values included in the legend show the significance of differences in the respective parameter across bar lengths (1-way ANOVA).

Performance across bar lengths, excluding fixation error trials

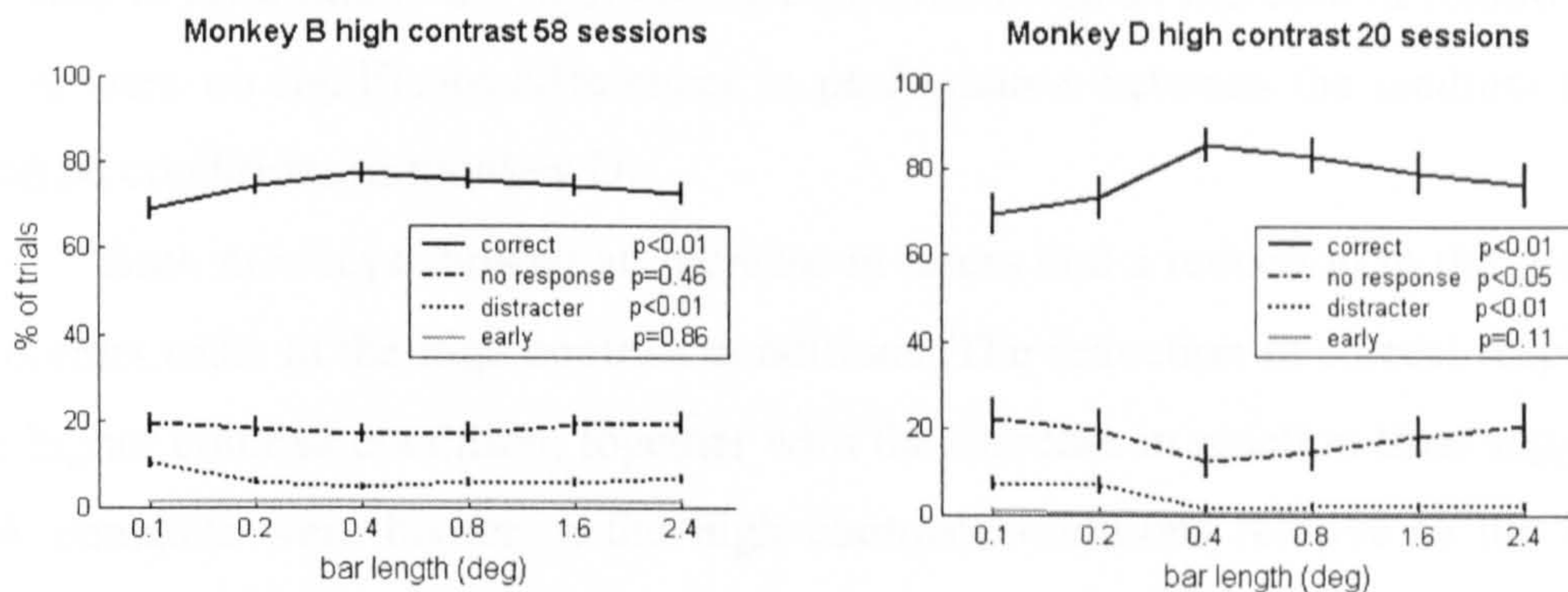


Figure 3.12 To assess the importance of trials ended due to a fixation break, data shown in Figure 3.11 were re-calculated excluding trials which ended in a fixation error. This analysis highlights the importance of changes across bar lengths in the percentage of trials ending in a distracter release or with no response. Data are shown in the same format as for Figure 3.11.

3.4.1.3 Reaction time and performance across contrasts

Figure 3.10 shows that both monkeys had faster RTs for medium contrast stimuli than for high contrast stimuli. This effect was significant in all conditions ($p < 0.01$, 2-way ANOVA). It is likely that this reflects greater task demands in the high contrast condition than in the medium contrast condition. Conversely, RT was slower in the low contrast condition than in the medium contrast condition, indicating that task demands were also greater in the low contrast condition compared with the medium contrast condition. To investigate this further I calculated performance in the different contrast conditions (Figure 3.13).

I found that the proportion of correct responses was generally higher in the medium and low contrast conditions than in the high contrast condition. In monkey B, the lower proportion of correct responses in the high contrast condition was accounted for by a higher proportion of trials in which the monkey made no response, or responded to the distracter. The monkey was also more likely to make an early response in the high contrast condition, but only when cued downwards. Between the medium and low contrast conditions ($\sim 7^\circ$ eccentricity presentation), the monkey was more likely to make an error in the low contrast condition than in the medium contrast condition. This caused a slight increase in the proportion of correct responses for the medium contrast condition, which was only significant when the monkey was cued downwards. In monkey D all types of error were somewhat more likely in the high contrast condition than in the medium contrast condition, with the

exception of 'no response' errors when the monkey was cued up. The largest increase in error rate in the high contrast condition was an increase in fixation errors. There were no significant differences in performance between the medium and low contrast conditions in monkey D.

Both monkeys showed an increase in errors and a reduction in the proportion of correct trials in the high contrast conditions. The reduction in correct responses at the higher contrast condition, together with the increase in reaction time suggest that task demands were higher in the high contrast conditions relative to the medium contrast condition. This is a surprising finding because analysis of reaction time and performance across bar lengths suggested that the test bar aided the detection of the target brightening. Thus it would be expected that a higher contrast bar would give the highest benefit. This apparent paradox can be explained by the fact that, in order to keep the luminance difference between the test bar and the brightening approximately constant ($7.3 \pm 2\text{cd/m}^2$) across contrast conditions, the luminance of the brightening patch was higher in the medium and low contrast conditions (patch luminance = 24.9cd/m^2) than in the high contrast condition (patch luminance = 7.3cd/m^2). Changing the luminance of the brightening in this way resulted in a target that was brighter than the background in the medium and low contrast conditions (mean Michelson contrast = 8.4%), but darker than the background in the high contrast conditions (mean Michelson contrast = -48.5%). This may have resulted in the brightening having higher salience in the medium and low contrast conditions than in the high contrast condition, since the test bars (test stimuli) were darker than the background.

The hypothesis that performance was enhanced in the medium contrast condition because of the change in luminance of the target brightening, rather than the test stimulus (the bar), is supported by the finding that bar length did not moderate the amount by which the contrast affected RT (p interaction >0.05 , 2-way ANOVA). If the luminance of the test stimulus were an important factor, I would have expected a larger contrast influence on RTs to the longest bar.

RT was slower in the low contrast condition than in the medium contrast condition, but tended to be faster in the low contrast condition than in the high contrast condition (the latter comparison can only be made in monkey D, since high and low contrast stimuli were presented at different eccentricities in monkey B). This indicates that the benefit of the test stimulus on RT and the benefit of making the

target brighter than the background acted independently on the RT. In the low contrast condition, the RT was faster than in the high contrast condition because of raising the luminance of the target brightening. However, lowering the contrast of the test bars reduced their beneficial effect on RT, causing RT to slow down relative to the medium contrast conditions.

Performance as a function of contrast and trial type

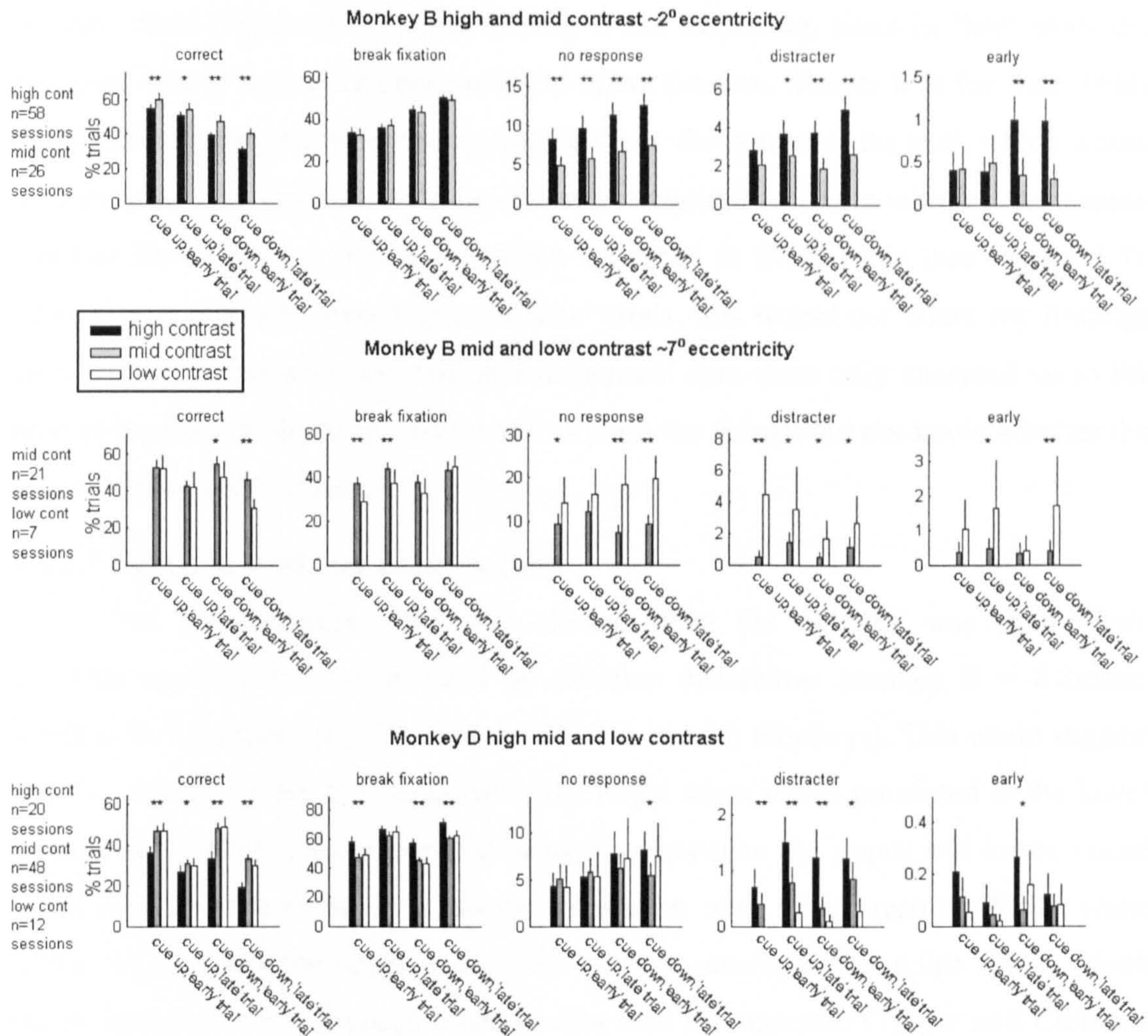


Figure 3.13 Monkeys' performance across contrasts. Performance was calculated as the mean percentage of trials ending in a correct response, a fixation error, no touch bar response, a distracter response or an early (touch bar released before the first brightening) response (see plot titles). Mean percentages are calculated across sessions. Error bars show standard error. Performance was calculated separately for 'early' and 'late' trials (target presented at 500msec and 1500msec respectively) and trials in which the monkey was cued up or down. Black bars show performance in the high contrast condition, grey bars show performance in the medium (mid) contrast condition and white bars show performance in the low contrast condition. Asterisks above each bar chart indicate the significance of differences between the contrast conditions. A single asterisk indicates $p < 0.05$, a double asterisk indicates $p < 0.01$ (1-way ANOVA).

3.4.1.4 Reaction time and time of target brightening

In the previous analyses I separately analysed data from 'early' and 'late' trials. For monkey B, and for most cases in monkey D, RT was faster for 'early' target conditions than for 'late' target trials. The only exception in monkey D's data was in the high contrast condition when the cue was up, where RTs were faster in 'late' trials. I also found that performance (proportion of correct trials) was poorer in 'late' trials for both monkeys. This was mostly due to higher rates of fixation errors in 'late' trials (Figure 3.13). This finding is not surprising, since in 'late' trials the monkeys clearly had more opportunity to break fixation. Slower RTs for 'late' trials could reflect the monkey becoming fatigued over the course of the trial, which would be unsurprising given that the monkeys were required to fixate within a very small window for 2150msec before the target appeared in these trials (see Figure 3.3). Even if task demands were higher in 'late' trials, this would not affect my findings on the effect of attention on neuronal responses: data were only analysed up to the time of the first brightening, and up to this point the animal did not know whether the trial would be early or late.

3.4.1.5 Reaction time and cued location

For both monkeys, RT was slower when the monkey was cued down (towards the RF) than when cued up (median difference: monkey B = 8.8msec, monkey D = 6.9msec; $p < 0.01$, 2-way ANOVA in both monkeys). This could suggest that the monkeys were less sensitive to the target when it was presented in the lower visual field. Differences in contrast sensitivity between the upper and lower visual fields have been reported by a number of studies with mixed results. Whilst some studies suggest that the upper visual field is more sensitive (Skrandies 1985), which could account for my finding, other studies find the opposite (Talgar and Carrasco 2002). It is possible that in the monkeys used in this experiment, lower sensitivity in the lower visual field could have arisen due to some small damage of the cortex at the recording location. I investigated this possibility by comparing RT and performance from sessions soon after recording started, with data from later sessions (see section 3.4.1.6 *Training and practice effects*).

3.4.1.6 Training and practice effects

For monkey D the reduction in RT and error trials with reduced contrast could reflect improved performance with training, since most of the high contrast

data was recorded prior to most of the medium and low contrast data. However, it is difficult to investigate practice effects in monkey D's data, since I have little data with comparable contrasts from early and late sessions.

In monkey B, high contrast data was collected over a much longer period than in monkey D. Monkey B's data from sessions 1-32 (early sessions) were examined separately from sessions 33-64 (late sessions). Session 64 was the last session recorded with high contrast stimuli placed at $\sim 2^\circ$ eccentricity. RT was faster in sessions 33-64 compared with sessions 1-32 in trials where the monkey was cued up (away from the recorded RF location). This was significant for 'early' target trials ($p < 0.001$, 2-way ANOVA) but not for 'late' target trials ($p = 0.06$). It is likely that this improvement in RT is due to the additional training. In trials where the monkey was cued down (towards the location of the recorded RF), and where the target appeared at 500msec post stimulus onset ('early' target trials), RT was significantly slower in sessions 33-64 compared with sessions 1-32. This pattern could indicate that repeatedly penetrating the cortex for recording caused some damage, impairing the monkey's performance. The same pattern was not found in 'late' target cued-down trials. For these conditions RT was improved (i.e. faster) in sessions 33-64, but only for short bar lengths (effect of practice $p < 0.001$, bar length and practice interaction $p < 0.001$, 2-way ANOVA). Performance in 'late' target trials does not depend on sensory input to the same extent as performance in 'early' target trials since the hazard function is 100% for the late period. As long as the monkey knows that the target has not already occurred, a response could have been made on the basis of timing alone.

Monkey B, RT in early and late sessions (high contrast stimuli)

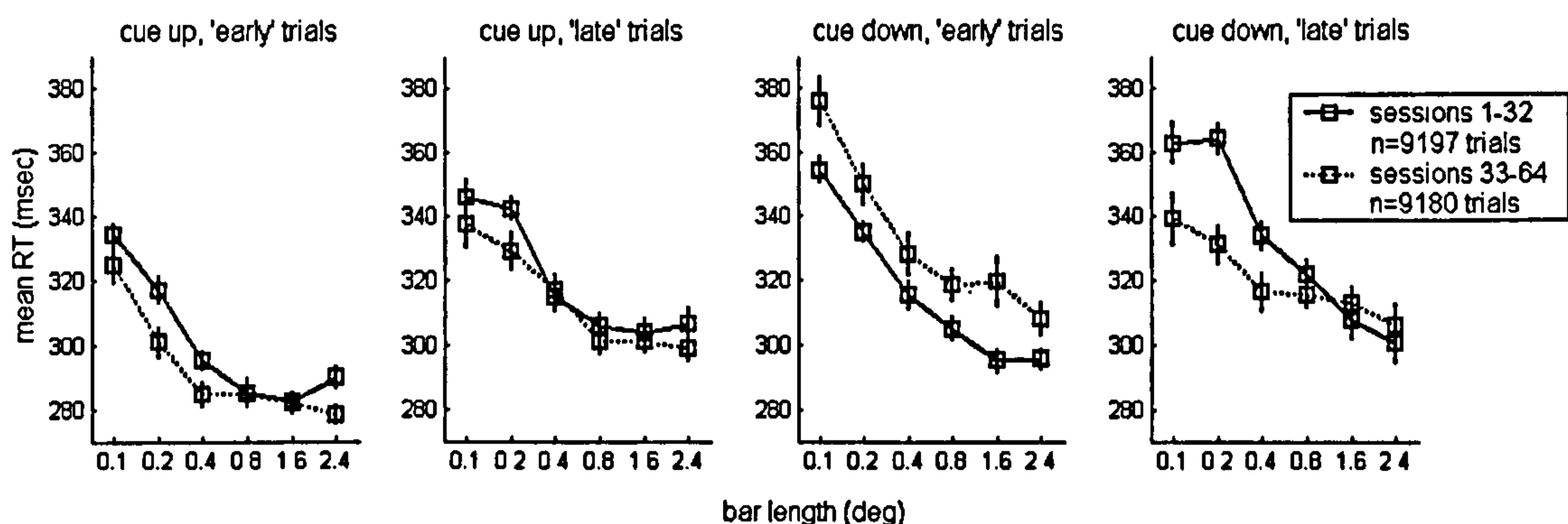


Figure 3.14 RT for high contrast test stimuli as a function of bar length and time of recording. Data from early sessions (sessions 1-32 after recording began) are shown in solid lines. Dotted lines show data from late sessions (33-64). Points show mean RT, error bars show standard error.

The analysis of the performance data shows that monkey B performed the task with a high level of accuracy from the start of recording, demonstrated by the low proportion of distracter releases in the early sessions (high contrast; distracter release = 6% of trials). Additional practice nevertheless improved the monkey's performance as demonstrated by the reduction in the proportion of distracter releases in the late sessions. However there was also a significant reduction in the proportion of correct responses between early and late sessions. This reduction reflects the large increase in the number of fixation errors between early and late sessions, most likely due to a reduction of the size of the fixation window in later sessions.

Monkey B, performance in early and late sessions (high contrast stimuli)

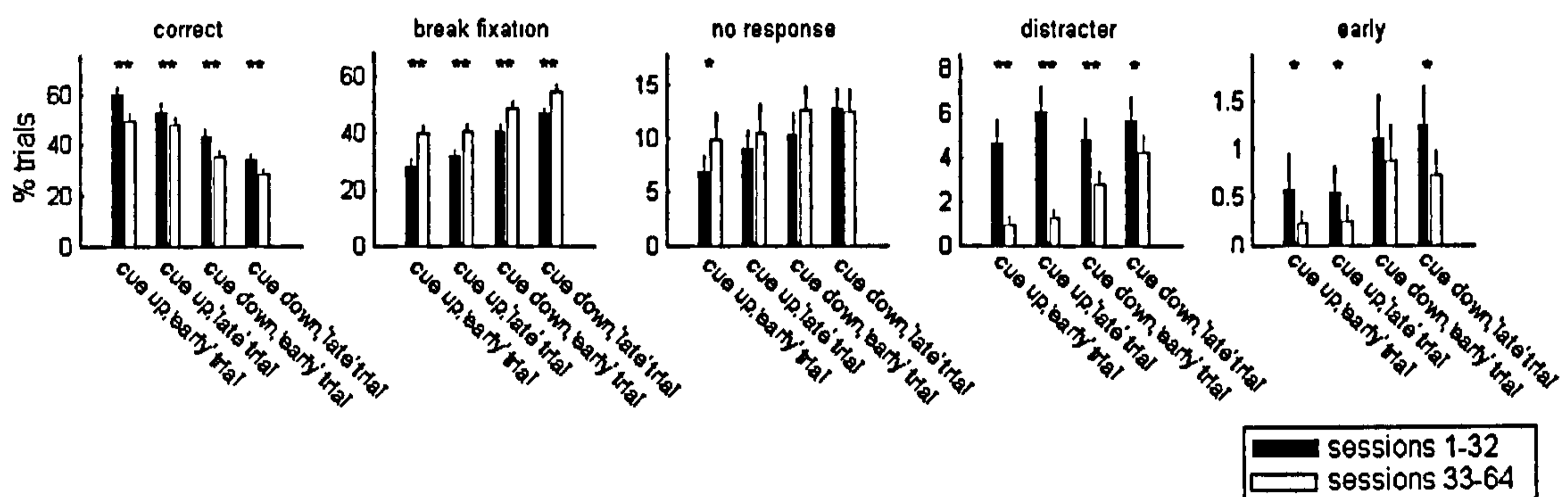


Figure 3.15 Performance in sessions 1-32 (early sessions) and sessions 33-64 (late sessions). Performance was calculated as percentages of trials ending in a correct response, a fixation error, no touch bar response, a distracter response, or an early response (plot titles). Error bars show standard error. Performance was calculated separately for early and late trials (target presented at 500msec and 1500msec respectively) and trials in which the monkey was cued up or down. Black bars show performance in sessions 1-32, white bars show performance in sessions 33-64. Asterisks above each bar chart indicate the significance of differences between the contrast conditions. A single asterisk indicates $p < 0.05$, a double asterisk indicates $p < 0.01$ (1-way ANOVA).

3.4.1.7 Performance and reaction time on block change trials

Of particular interest regarding the monkey's strategy was whether the monkeys were directed by the cue on each trial or whether they switched attended location only when their responses failed to yield rewards. In the latter strategy I would expect to see a high proportion of responses to the presentation of the distracter brightening ('distracter release') following a change in the cued location. To test for this, I analysed the performance data separately for trials at the start of a block (when the cued location changed) and compared this with the performance data across all trials. Figure 3.16 shows this comparison for the high contrast data from monkey B and medium contrast data from monkey D. These data sets were chosen because they included the largest numbers of block change trials for each

monkey. There was very little difference in the performance of monkey D on block change trials compared with all trials. In monkey B however, the proportion of distracter responses on block change trials was larger than on other trials. This indicates that monkey D acted in response to the cue on every trial whilst monkey B heeded the cue somewhat less.

The proportion of distracter releases on block change trials was higher in monkey B when the cue was down than when it was up. This could reflect poorer sensitivity in the lower visual field (i.e. the monkey was more likely not to see the cue), consistent with the monkey's slower reaction times when cued down (see Figure 3.10). It should be noted that despite a larger number of distracter releases on block change trials (17%), the correct responses on these trials were still more than twice as likely (38%). This demonstrates that the monkey did not entirely ignore the cue.

Comparison between performance in block change trials and performance in all trials

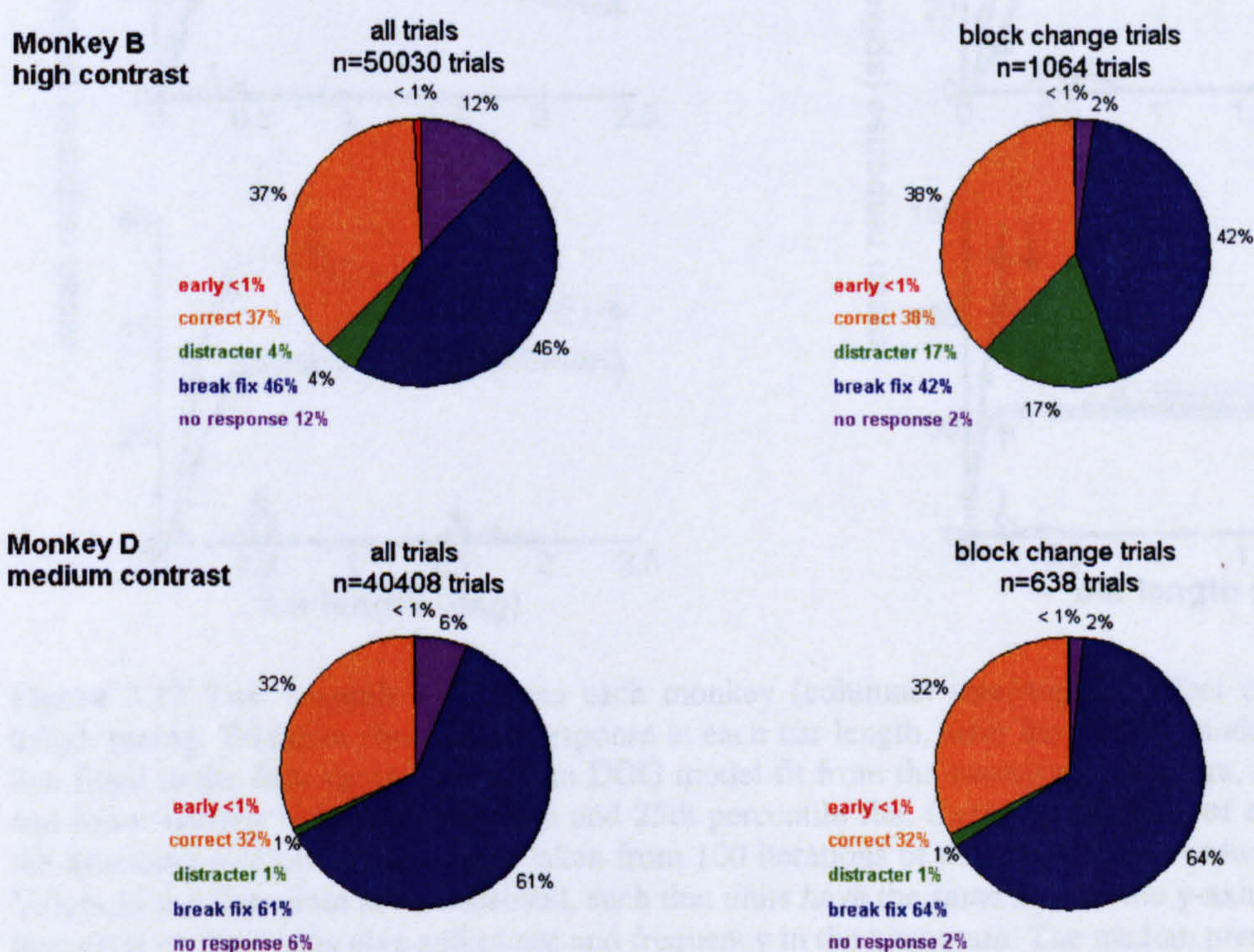


Figure 3.16 Comparison of performance in trials where the cued location changed from the previous trial (block change trials) with performance in all trials. Performance is shown as percentages of trials ending in an early response (red), a correct response (orange), a distracter response (green), a fixation error (break fix, blue) or ending with no response (purple). Data is shown for the high contrast condition for monkey B (upper row) and the medium contrast condition for monkey D (lower row). These were the conditions where most data points were available for each monkey. Because of the

relatively small number of block change trials, I did not divide between cued-up and cued-down trials or between early and late trials.

3.4.2 Effects of attention on neuronal length tuning

Length tuning is a classic demonstration of non-classical receptive field (nCRF) modulation (DeAngelis et al. 1994). In this study I measured length tuning under conditions where the monkey was cued to attend towards the RF of the neuron under study (attend-RF condition), and when the monkey was cued to attend towards a location in the opposite hemifield of the RF of the neuron under study (attend-away condition). I found that cells' preferred length tended to occur at shorter bars when attention was directed towards the RF (Figure 3.17).

Examples of the effect of attention on length tuning

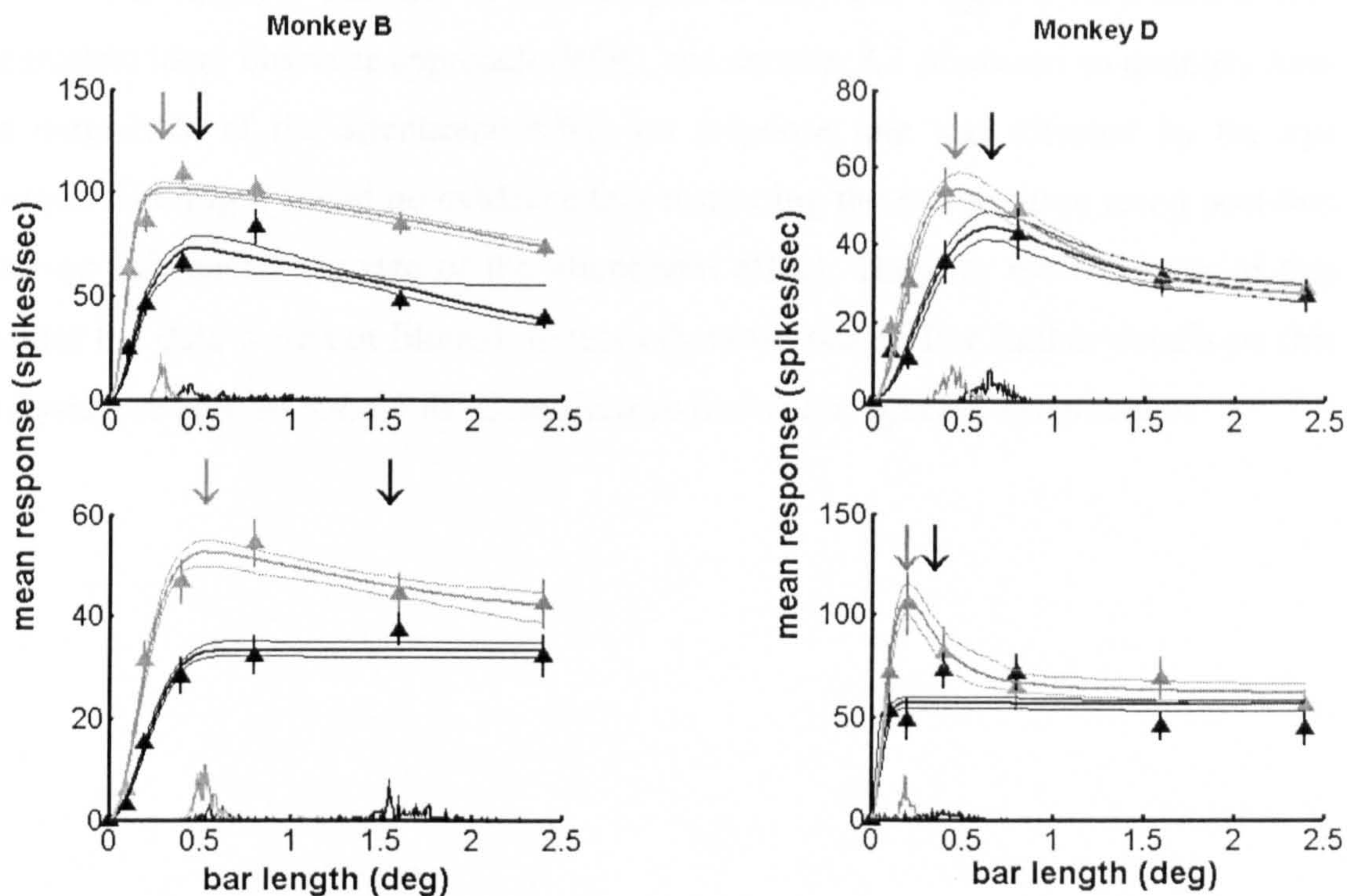


Figure 3.17 Two example cells from each monkey (columns) showing the effect of attention on length tuning. Triangles show mean response at each bar length, error bars show standard error. Bold line fitted to the data shows the median DOG model fit from the bootstrap procedure, flanking upper and lower narrow lines show the 75th and 25th percentile fits. Curves at the base of each plot show the distribution of preferred lengths taken from 100 iterations of the bootstrap procedure (0.01° bins). Values in the histogram are normalised, such that units have the same size on the y-axis as spikes/sec; thus units on the y-axis give spikes/sec and frequency in the histogram. The median preferred length is marked with the downwards-pointing arrow. Grey triangles, lines and arrows show data from the attend-RF condition; black triangles, lines and arrows show data from the attend-away condition. All examples are from the high contrast condition.

The influence of eye position was a critical factor to test for, since the test stimuli and the RFs were both small. To examine whether small differences in eye

position between the two attention conditions could contribute to the observed effects on firing rate, and thus length tuning, I used a post-hoc eye position filter which allowed me to examine data with the smallest difference in eye position between the two attention conditions. For this analysis I first calculated the eye position between 0-500msec (or 200msec in monkey D) post stimulus onset, averaged over all trials in the recording. I then set a new eye position threshold that was even more restrictive than the already small fixation window allowed during the recording. Any trial in which the eye position deviated from the mean position by more than the threshold allowed was excluded from further analysis. Thus I selected only those trials with minimal eye position difference between the two attention conditions. I used various threshold settings to examine the effect of attention at increasingly restrictive eye position filtering. An example of this analysis is shown in Figure 3.18. I used a non-parametric ideal observer approach (ROC, see section 3.3 *Methods*) to quantify how the magnitude of the attentional effect on response rate was affected by the eye position filtering. I found no evidence that restricting the eye position using post-hoc filtering influenced the size of the attentional effect. Thus for the remainder of this chapter the data were not filtered, unless otherwise stated. For further details on this analysis, see section 3.4.4.3 *ROC analysis to assess the effect of eye position*.

Effect of restricting eye position on attentional modulation

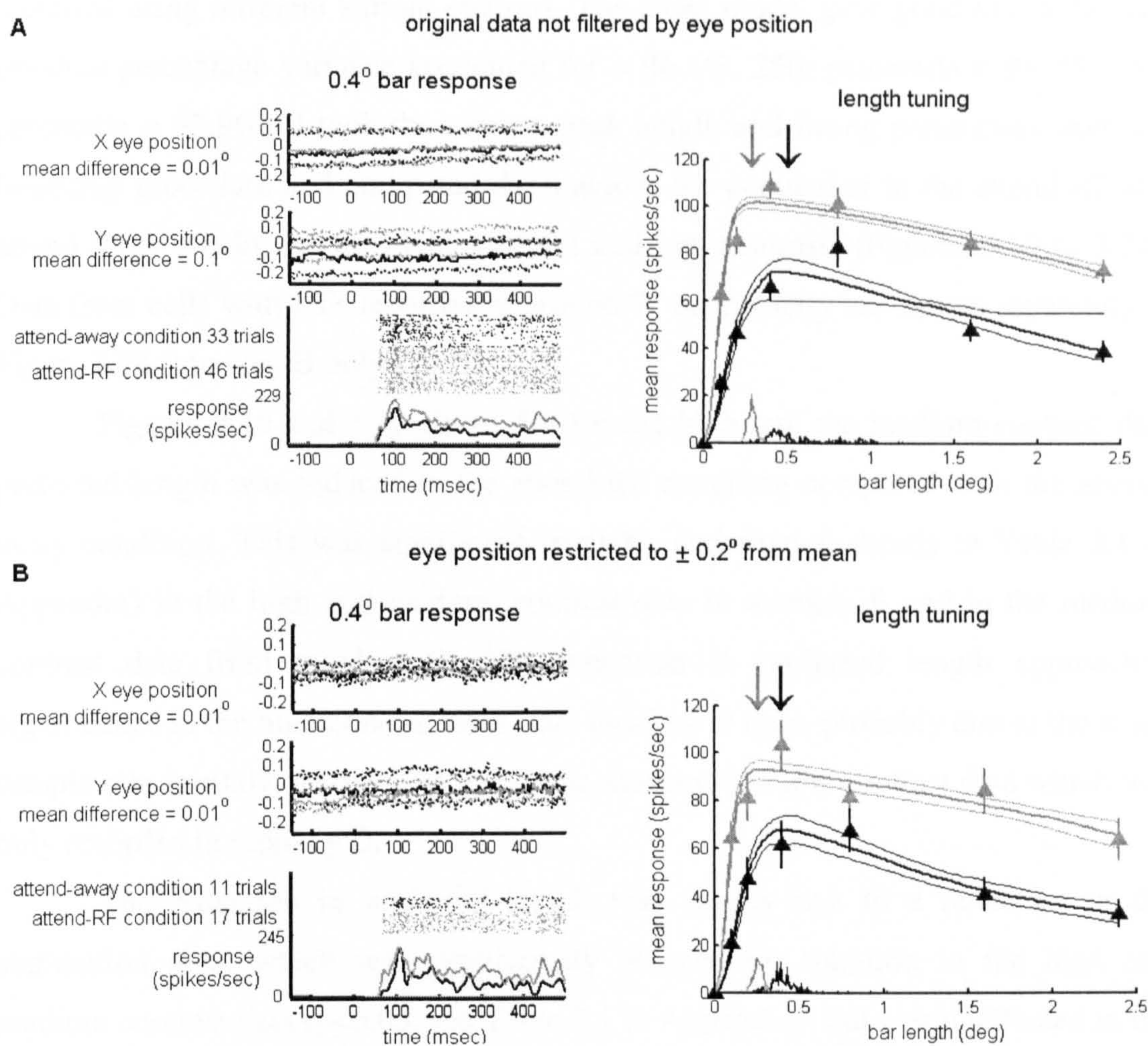


Figure 3.18 The effect of restricting eye position on attentional modulation on neuronal responses and length tuning. **A)** data is not filtered by eye position, and **B)** trials where the eye position was more than 0.2° from the mean eye position were excluded from the analysis. Plots on the left show eye position and neuronal response to the stimulus for which the largest effect of attention was recorded for this cell (0.4°). Solid lines in eye position plots show the median eye position relative to the centre of the fixation window; dotted lines show the 25th and 75th percentiles. Responses are shown as histograms and raster plots. Time is relative to stimulus onset. Data in grey corresponds to the attend-RF condition; data in black corresponds to the attend-away condition. Plots on the right show length tuning. Triangles show mean responses at each bar length, error bars show standard errors. Bold line fitted to the data shows the median DOG model fit from the bootstrap procedure, and flanking upper and lower narrow lines show the 75th and 25th percentile fits. Curves at the base of each plot show the distribution of preferred lengths taken from 100 iterations of the bootstrap procedure. Values in the histogram are normalised such that units have the same size on the y-axis as spikes/sec; thus units on the y-axis give spikes/sec and frequency in the histogram. The median preferred length is marked with the downwards-pointing arrow. Grey triangles, lines and arrows show data from the attend-RF condition; black triangles, lines and arrows show data from the attend-away condition. This cell was recorded from monkey B using high contrast stimuli.

3.4.2.1 Difference of Gaussians model, population analysis

Length tuning was assessed by repeatedly fitting a difference of Gaussians (DOG) model to bootstrapped data samples (see Methods and Chapter 2). This was

done separately for the attend-RF and attend-away conditions and for conditions recorded using different stimuli contrast. The DOG model gave good fits to the data (median percentage variance accounted for = 96.1%, 25th percentile = 93.2%, 75th percentile = 97.9%). I took the median peak length and fitting parameters from the bootstrap procedure and compared them across the population in the attend-RF and attend-away conditions for high, medium and low contrasts (Figures 3.19 to 3.21). Data from cells with RFs recorded at around 7° eccentricity are shown separately in Figure 3.24 (monkey B only).

Figures 3.19 and 3.20 show that for the high and the medium contrast data preferred length was reduced in the attend-RF condition compared with the attend-away condition. This was significant ($p < 0.05$, quantitative details in Table 3.1 in Appendix) in the high and medium contrast data in monkey B and in the medium contrast data from monkey D. The reduction in preferred length approached significance in the high contrast data from monkey D only, probably due to the small sample size ($p = 0.07$, $n = 16$). The trend was absent in the low contrast data which was only recorded in monkey D.

The reduction in preferred length was largely due to a reduction in the summation area, which was significantly reduced by attention in the high and medium contrast data ($p < 0.05$, see Table 3.1 in Appendix), but was unaffected in the low contrast data. The summation gain was significantly enhanced by attention in the high contrast data from monkey B ($p < 0.001$) but not from monkey D ($p = 0.16$). In the medium and low contrast data the summation gain was unaffected. The inhibitory area and the inhibitory gain were not consistently affected by attention at any contrast level (see values in Table 3.1 in Appendix).

The effect of attention on length tuning at high contrast

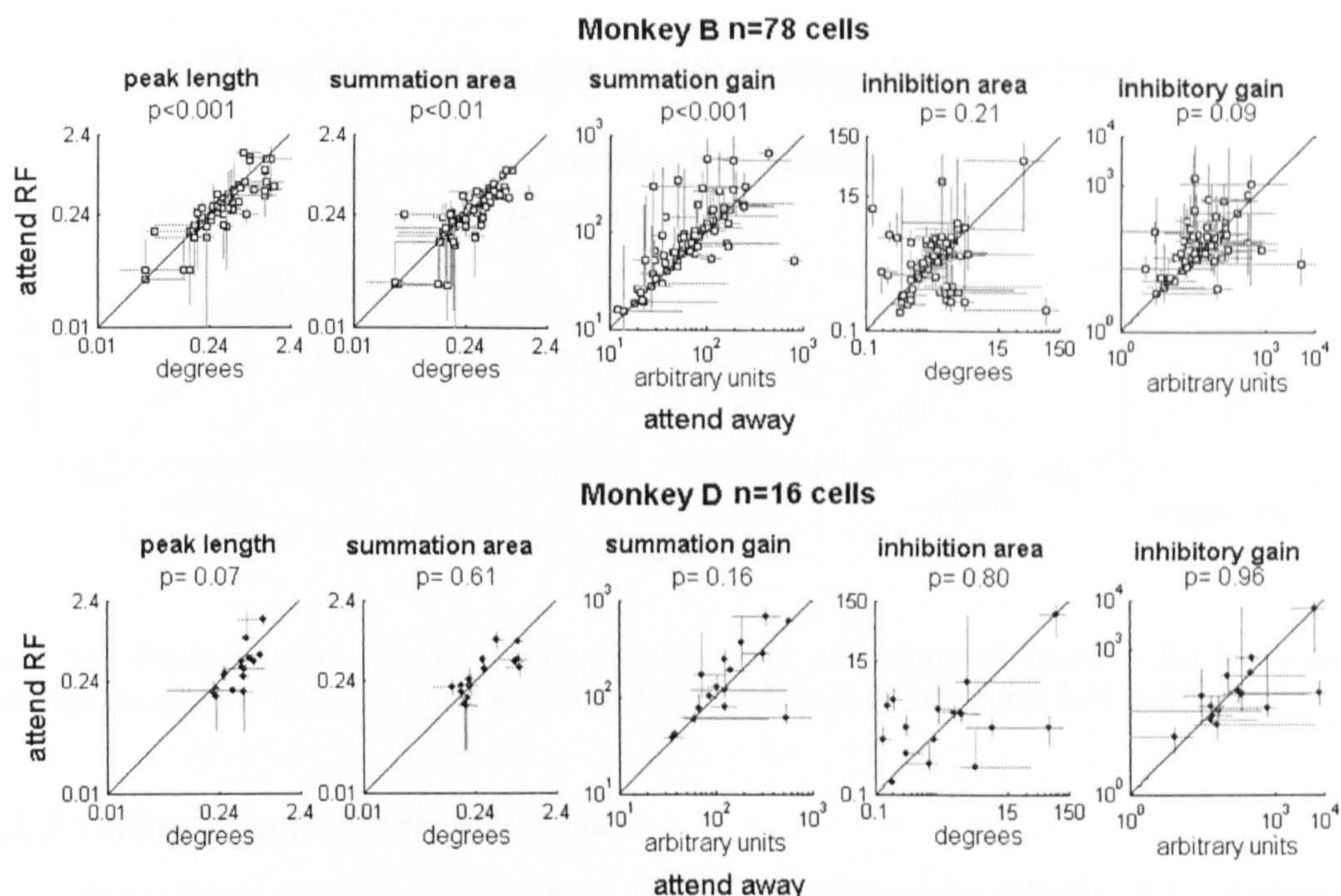


Figure 3.19 Peak location and DOG fitting parameter as a function of attention for high contrast recordings. Each point marks the median value of the respective parameter (column headings) taken from the bootstrap procedure for a given cell; error bars show 75th and 25th percentiles. Points above the diagonal indicate that the parameter of interest was increased in the attend-RF (y-axis) condition. Points below the diagonal indicate that the parameter of interest was reduced in the attend-RF condition. Above each plot, p-values show the significance of differences across the whole population between the attend-RF and attend-away conditions (signed rank test). Axes are in logarithmic units.

The effect of attention on length tuning at medium contrast

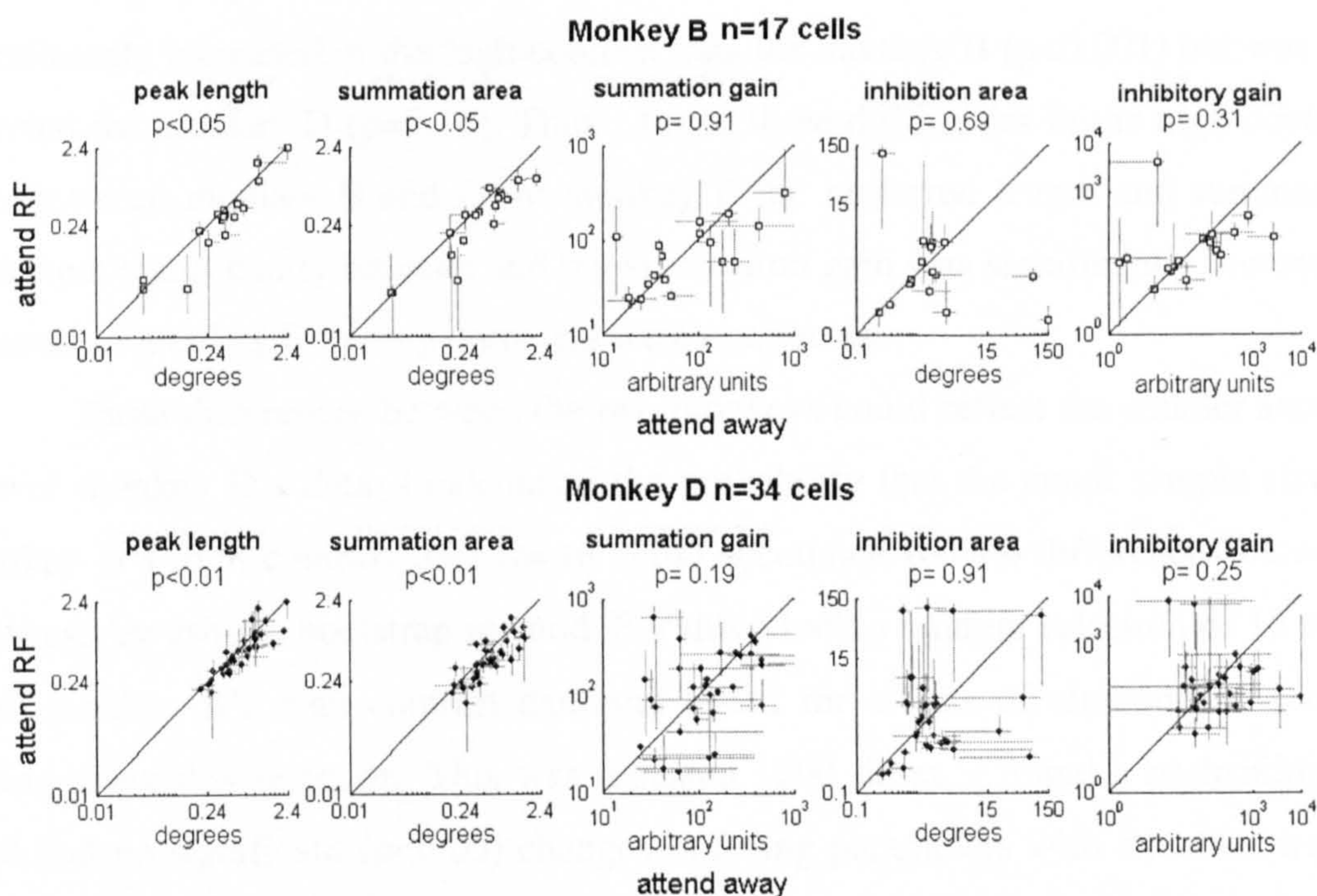


Figure 3.20 Peak location and DOG fitting parameter as a function of attention for medium contrast recordings. Data are shown in the same format as in Figure 3.19.

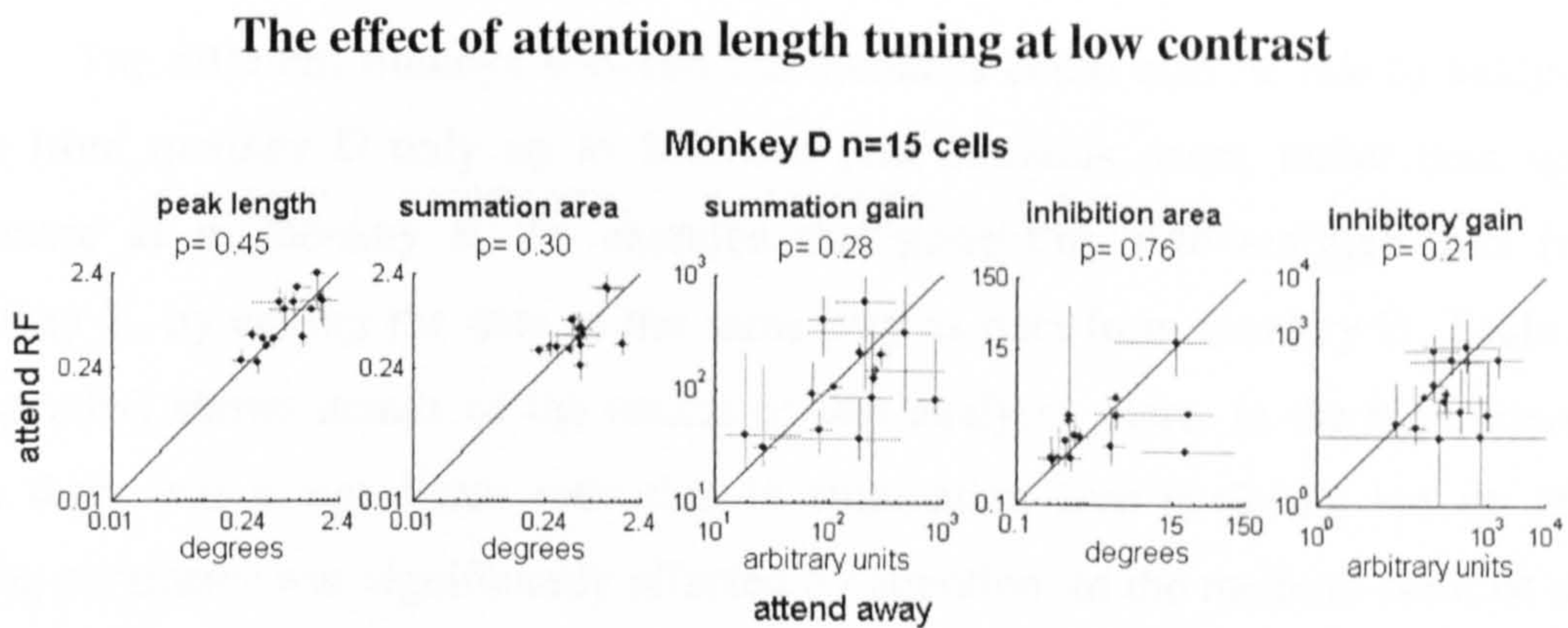


Figure 3.21 Peak location and DOG fitting parameter as a function of attention for low contrast recordings (monkey D only). Data are shown in the same format as in Figures 3.19 and 3.20.

3.4.2.2 Differences between monkeys

Examining data from monkey B and D separately (Table 3.1, Appendix) shows that preferred length was significantly reduced in the attend-RF condition for both monkeys in the medium contrast data. The result was also significant for monkey B in the high contrast data, but only approached significance in the high contrast data for monkey D. Reductions in summation area occurred for both monkeys in medium contrast data (values in Table 3.1, Appendix) but was not significant for high contrast stimuli in monkey D ($p=0.61$). The summation gain was significantly increased in the high contrast data for monkey B ($p<0.001$) but was not affected for monkey D ($p=0.16$). Thus I found three differences in the high contrast data between monkey B and D: in monkey B the preferred length and summation area were significantly reduced and the summation gain was significantly increased, whereas in monkey D these parameters were unaffected.

These differences between the two monkeys could reflect the smaller sample size of monkey D's data. I calculated the probability that the small sample size in monkey D's high contrast data ($n=16$ cells) accounted for the differences between monkeys by using a bootstrap method. For this I took a random selection of 16 cells from monkey B's high contrast data and tested for effects of attention on length tuning using this selection. This was repeated 1000 times. I found a probability of 0.24 that no significant ($p<0.05$) changes in fitting parameters with attention would be found in a population of 16 units. Thus, there was a relatively high probability ($p=0.24$) that I found no significant effects of attention on length tuning in monkey

D's high contrast data because of the small sample size and not because of a genuine difference between the two monkeys.

The different findings between the monkeys could also be due to analysing data from monkey D only up to 200msec post stimulus onset, rather than up to 500msec as in monkey B. To examine this possibility I re-analysed data from monkey B, by cutting the data in the same way as data from monkey D. Table 3.2 (Appendix) shows details of the results of this analysis. Here, in the high contrast data there was a significant reduction in summation area ($p < 0.01$), but no other fitting parameter was significantly affected by attention. In the medium contrast data the reduction in peak length and the reduction in summation area were both significant ($p < 0.01$). This matches the pattern in the medium contrast data from monkey D, where the peak length and summation area were significantly reduced. However in monkey D's high contrast data no significant changes were found. I used the bootstrap method described above to test whether a significant reduction in summation area was found in the first 200msec of monkey B's data, but not in monkey D's data, because of the larger sample size in monkey B. Here I found a probability of 0.738 that no significant effects would be found in a sample of 16 cells. Thus, differences between monkey B and D shown in Table 3.1 (Appendix) are likely to reflect the differences in the time intervals for analysis in the two monkeys as well as the smaller sample size in data from monkey D, rather than necessarily reflecting a genuine difference between the two monkeys.

3.4.3 Data recorded at greater retinal eccentricity

Due to reduced recording stability in monkey B it became necessary to remove the recording chamber and re-implant at a new location. Thus I collected data from two locations from this monkey. Figure 3.22 shows the eccentricity and RF size of cells recorded in both locations. In the first recording location, RFs were at an eccentricity of around 2° ; in the second recording location, RFs were at an eccentricity of around 7° . RFs were significantly larger in the $\sim 7^\circ$ eccentricity sample than in the $\sim 2^\circ$ eccentricity sample ($p < 0.001$, 2-sample t-test).

I analysed data from cells recorded at the new location separately from cells recorded at the original location. 22 cells were recorded for the current study at the $\sim 7^\circ$ location. For these cells I used a medium contrast (median contrast used = 22.4%, minimum = 8.1%, maximum = 41.5%). For 17 cells in this sample I

interleaved a lower contrast stimulus (median contrast = 10.9%, minimum = 7.2%, maximum = 21.4%), for which responses were significantly lower ($p < 0.05$, 2-way ANOVA) than responses to the medium contrast stimulus.

The distribution of RF size and eccentricity

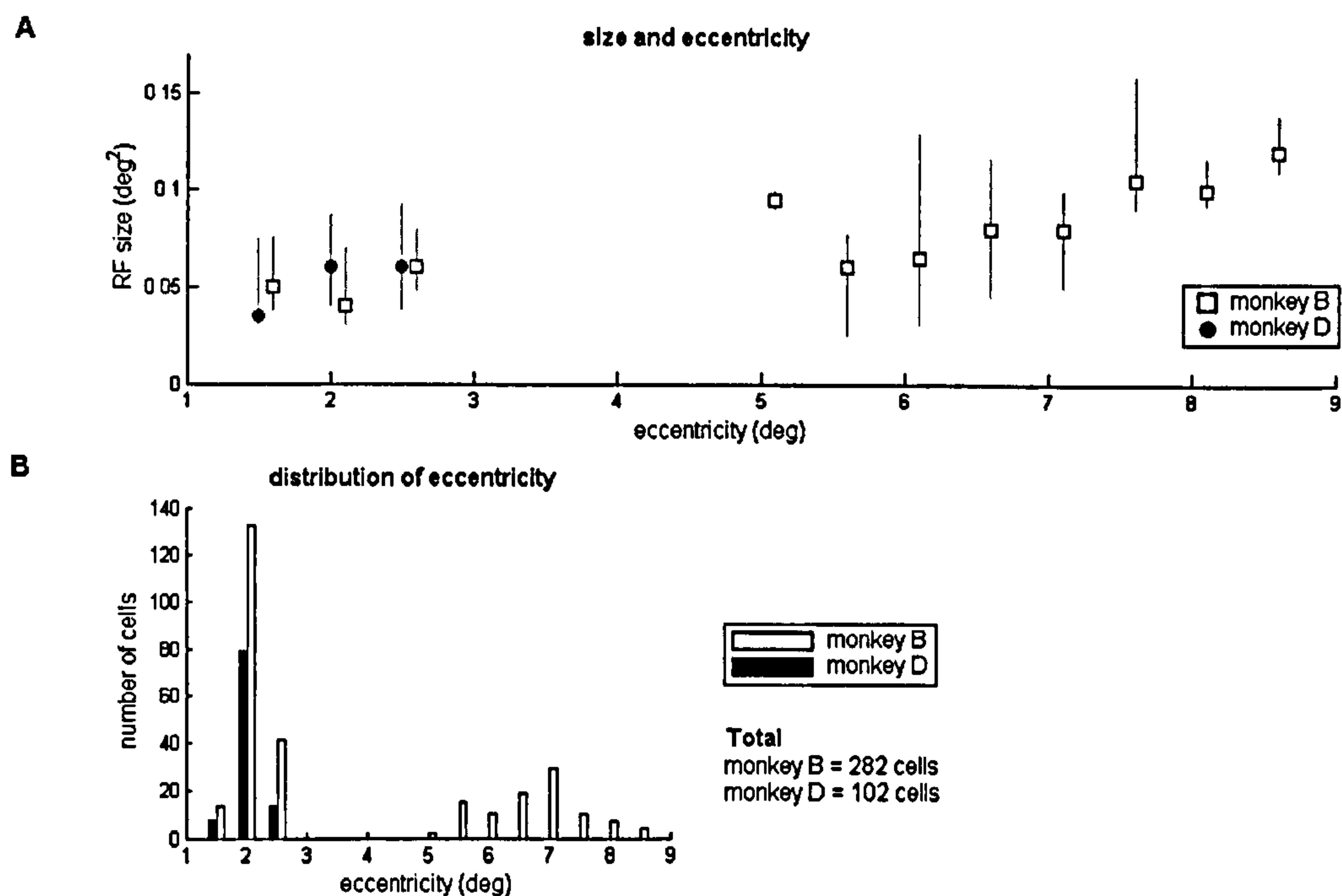


Figure 3.22 Distributions of RF size and retinal eccentricity for monkey B (white symbols and bars) and monkey D (black symbols and bars). **A)** Symbols mark median RF size across eccentricity in 0.5° bins. Error bars show 25th and 75th percentiles. RFs were mapped using a 10×10 grid of 0.1 degree^2 stimuli. RF size was taken as the number of 0.1 degree^2 stimulus locations that gave a response not significantly below the maximum response. Symbols are aligned with the start of each bin. Symbols for monkey B and D are displaced from one another. **B)** Histogram showing number of cells at different retinal locations in 0.5° bins.

3.4.3.1 Effects of attention on length tuning at a greater retinal eccentricity

In the $\sim 7^\circ$ eccentricity sample (Figures 3.23 and 3.24) the effect of attention on length tuning for medium contrast stimuli was the reverse of the effect at $\sim 2^\circ$ eccentricity (Figures 3.20), i.e. the preferred bar length was increased in the attend-RF condition ($p < 0.05$). There was also a significant increase of the summation area in the attend-RF condition ($p < 0.05$). Other fitting parameters were not significantly affected by attention in the $\sim 7^\circ$ eccentricity sample, which is consistent with the medium contrast data from the $\sim 2^\circ$ eccentricity sample. There was no consistent effect of attention on peak length or any fitting parameter for low contrast stimuli in

the $\sim 7^\circ$ eccentricity sample. The exact values of changes in fitting parameters are shown in detail in Table 3.3 (Appendix).

Examples of the effect of attention on length tuning at $\sim 7^\circ$ eccentricity

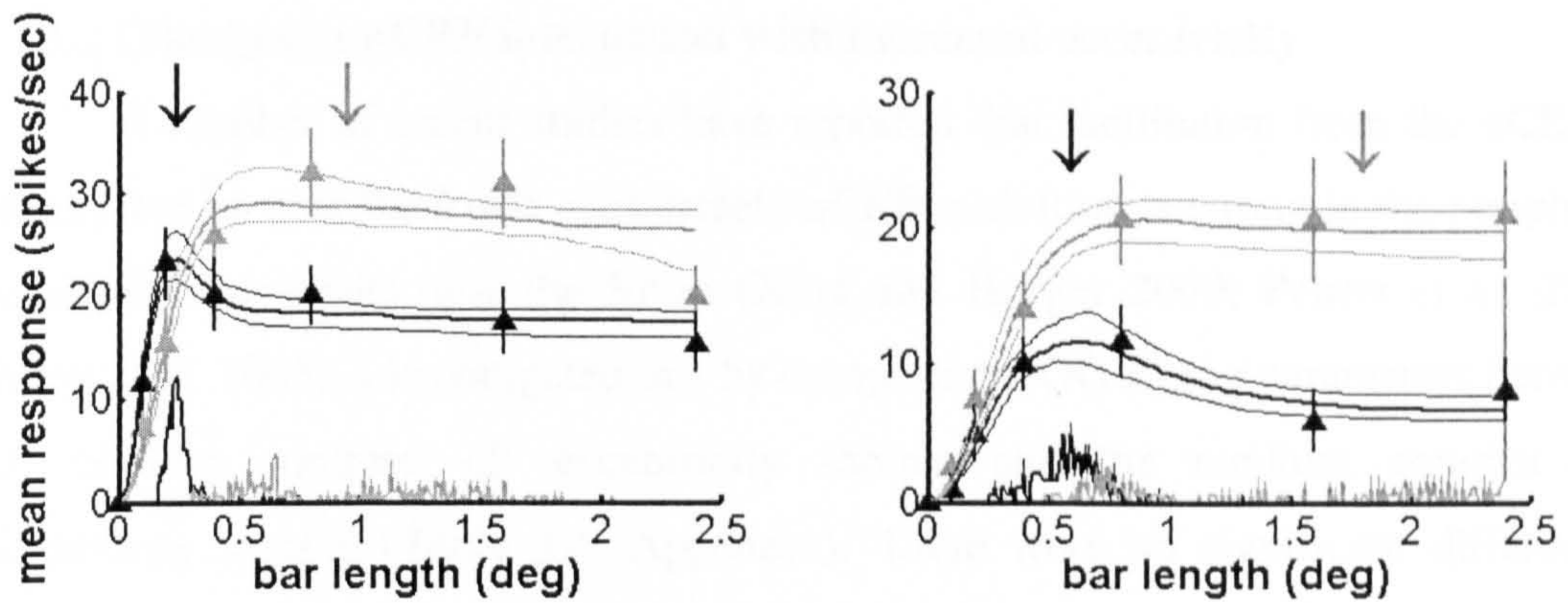


Figure 3.23 Two example cells with RFs at an eccentricity of $\sim 7^\circ$ demonstrate the effect of attention on length tuning. Triangles show mean response at each bar length, error bars show standard error. Bold line fitted to the data shows the median DOG model fit from the bootstrap procedure, and flanking upper and lower narrow lines show the 75th and 25th percentile fits. Curves at the base of each plot show the distribution of preferred lengths taken from 100 iterations of the bootstrap procedure. Values in the histogram are normalised such that units have the same size on the y-axis as spikes/sec; thus units on the y-axis give spikes/sec and frequency in the histogram. The median preferred length is marked with the downwards-pointing arrow. Grey triangles, lines and arrows show data from the attend-RF condition; black triangles, lines and arrows show data from the attend-away condition. Both examples were recorded using medium contrast stimuli.

The effect of attention on length tuning across the population at $\sim 7^\circ$ eccentricity

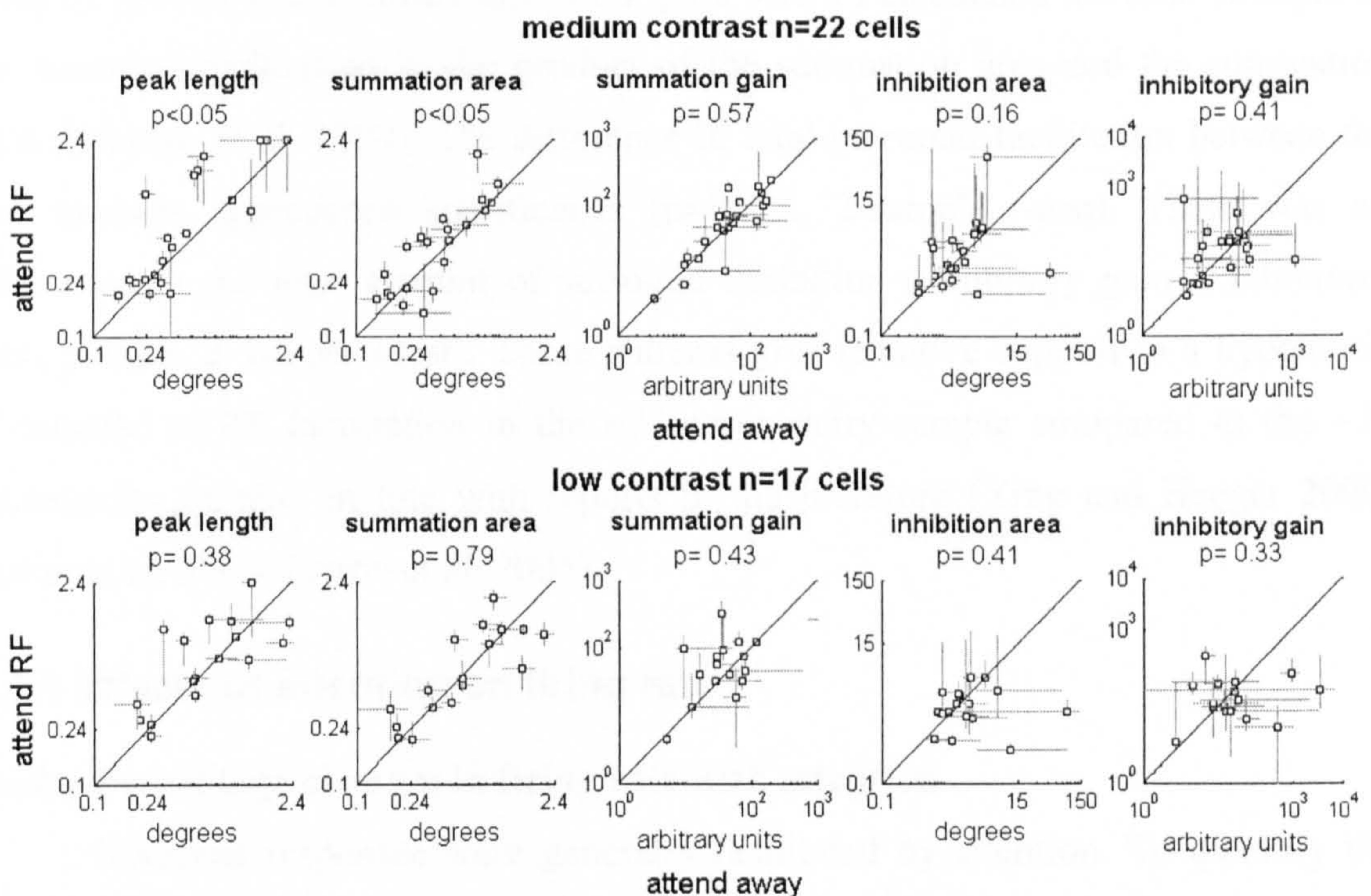


Figure 3.24 Peak location and DOG fitting parameters as a function of attention condition for the $\sim 7^\circ$ eccentricity sample. Each point marks the median value of the respective parameter (column headings) taken from the bootstrap procedure for a given cell; error bars show 75th and 25th

percentiles. Points above the diagonal indicate that the parameter of interest was increased in the attend-RF (y-axis) condition, points below the diagonal indicate that the parameter of interest was reduced in the attend-RF condition. Above each plot, p-values show the significance of differences across the whole population between the attend-RF and attend-away conditions (signed rank test). Axes are in logarithmic units.

3.4.3.2 Changes in nCRF interaction with increased eccentricity

A number of recent studies have reported that facilitation from the nCRF is strongest at or near the fovea. Conversely nCRF inhibition is strong in the periphery, but absent (or weak) near the fovea (Xing and Heeger 2000; Petrov et al. 2004; Petrov et al. 2005). I investigated this by comparing DOG fitting parameters between the medium contrast $\sim 2^\circ$ eccentricity sample and the medium contrast $\sim 7^\circ$ eccentricity sample (Table 3.4, Appendix). There were no significant differences between the two populations (2-sample t-test), which is unsurprising given that the sample sizes were relatively small and there was substantial within-sample variation. There were, however, two interesting patterns which approached significance. First, in the attend-away condition summation gain tended to be lower in the $\sim 7^\circ$ eccentricity sample than in the $\sim 2^\circ$ eccentricity sample ($p=0.11$, 2-sample t-test). More remarkably, in the attend-away condition the summation area tended to be smaller in the $\sim 7^\circ$ eccentricity sample than in the $\sim 2^\circ$ eccentricity sample ($p=0.18$, 2-sample t-test) despite the significant increase in the mapped RF area between the two samples ($p<0.001$, 2-sample t-test; see Figure 3.22). I calculated the total strength of the surround facilitation as the product of the summation area and the summation gain (Sceniak et al. 1999). The difference in total surround facilitation between the two samples approached significance ($p=0.088$, 2-sample t-test). There was no difference in the total amount of surround inhibition (inhibitory gain x inhibitory area, $p=0.25$, 2-sample t-test). These patterns give tentative support to a hypothesis of reduced nCRF facilitation in the $\sim 7^\circ$ eccentricity sample compared to the $\sim 2^\circ$ eccentricity sample, in line with reports in the literature (Xing and Heeger 2000; Petrov et al. 2004; Petrov et al. 2005).

3.4.4 Effects of attention on firing rate

3.4.4.1 Percentage changes in firing rate with attention

Neuronal responses were generally facilitated by attention. To quantify the facilitation of the response I first calculated the percentage change in firing rate between the two attention conditions. In monkey B, when stimuli were presented at

~2° eccentricity the median change in firing rate in the high contrast condition was a 21.3% increase during the attend-RF condition, whilst for medium contrast stimuli the median change was a 22.8% increase in firing rate. For these samples, the percentage of response enhancement was significantly greater for short bar lengths ($p < 0.05$ 1-way ANOVA). When stimuli were presented at ~7° the median percentage enhancement was 8.4% for medium contrast stimuli and 5.4% for low contrast stimuli. There was a trend towards higher percentage enhancement for long bars, however this was not significant (mid contrast $p = 0.61$, low contrast $p = 0.76$, 1-way ANOVA).

In monkey D the effect of attention on firing rate was significantly lower than in monkey B ($p < 0.01$, 2-way ANOVA). The median percentage enhancement was 14.6% for high contrast stimuli, 3.7% for medium contrast stimuli whilst responses to low contrast stimuli were suppressed by a median value of 3%. Bar length did not influence the percentage change at any contrast (high contrast $p = 0.42$, mid contrast $p = 0.16$, low contrast $p = 0.94$, 1-way ANOVA).

The percentage change in firing rate is a rather crude measure of firing rate changes. For example, the highest percentage change recorded was a change of almost 6000%, from a firing rate of 0.06 spikes/sec in the attend-away condition to a rate of 3.6 spikes/sec in the attend-RF condition. Moreover, the percentage change gives no information about the overlap of the distributions of data. For these reasons I used ROC analysis, a non-parametric method, to assess firing rate changes as described below.

Percentage change in firing rate across bar length and contrast

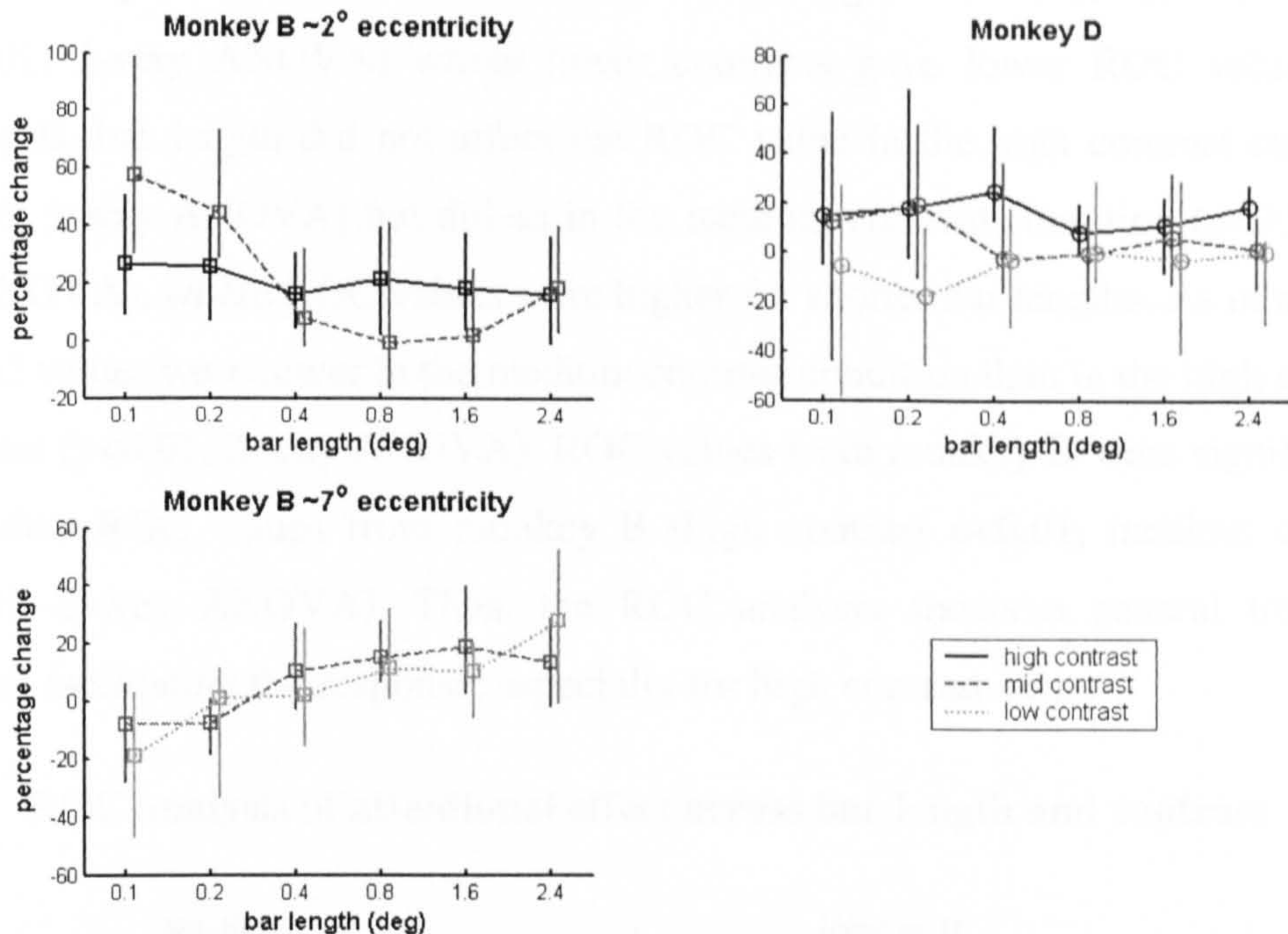


Figure 3.25 Percentage changes in firing rate. Points show median percentage change in firing rate from the attend-away condition to the attend-RF condition. Error bars show the inter-quartile range. Data from the high contrast condition is shown in black, dark grey dashed lines show medium contrast data, and light grey dotted lines show low contrast data.

3.4.4.2 Ideal observer approach to assess attentional effects of firing rate

The receiver operating characteristic (ROC) is a non-parametric, ideal observer approach to determine by how much two distributions differ from each other (see section 3.3 *Methods*). ROC values above 0.5 indicate that the responses were enhanced by attention whilst values below 0.5 indicate that responses were suppressed by attention. Across all stimulus conditions the median ROC values was 0.54 (25th percentile=0.47; 75th percentile=0.64). The distribution was significantly greater than 0.5 ($p < 0.001$, 1-tailed t-test) indicating that responses were generally enhanced in the attend-RF condition. When analysed separately for each monkey and each stimulus contrast, I found that in monkey B ROC values were significantly greater than 0.5 for all contrasts (Table 3.5). For monkey D, ROC values were significantly greater than 0.5 in the high contrast condition and significantly less than 0.5 in the low contrast condition. ROCs were not significantly different from 0.5 in the medium contrast condition.

Figure 3.26 shows ROC values at each bar length separately for high, medium and low contrast for each monkey. For monkey D, bar length had no effect

on the ROC at any contrast (high contrast $p=0.95$, mid contrast $p=0.55$, low contrast $p=0.73$, 1-way ANOVA). Stimulus contrast had a significant effect on ROC values ($p<0.001$, 1-way ANOVA) where lower contrasts gave lower ROC values. For monkey B, bar length did not affect the ROC value in the high contrast condition ($p=0.16$, 1-way ANOVA) but did so in the medium contrast condition ($p<0.005$, 2-way ANOVA), where ROC values were higher for shorter bar lengths. As in monkey D, ROC values were lower in the medium contrast condition than in the high contrast condition ($p<0.01$, 2-way ANOVA). ROC values from monkey D were significantly lower than ROC values from monkey B (high contrast $p<0.01$, medium contrast $p<0.001$, 2-way ANOVA). Thus, the ROC analysis shows a general trend for attention facilitating the response, especially for high contrast stimuli.

ROC analysis of attentional effect across bar length and contrast

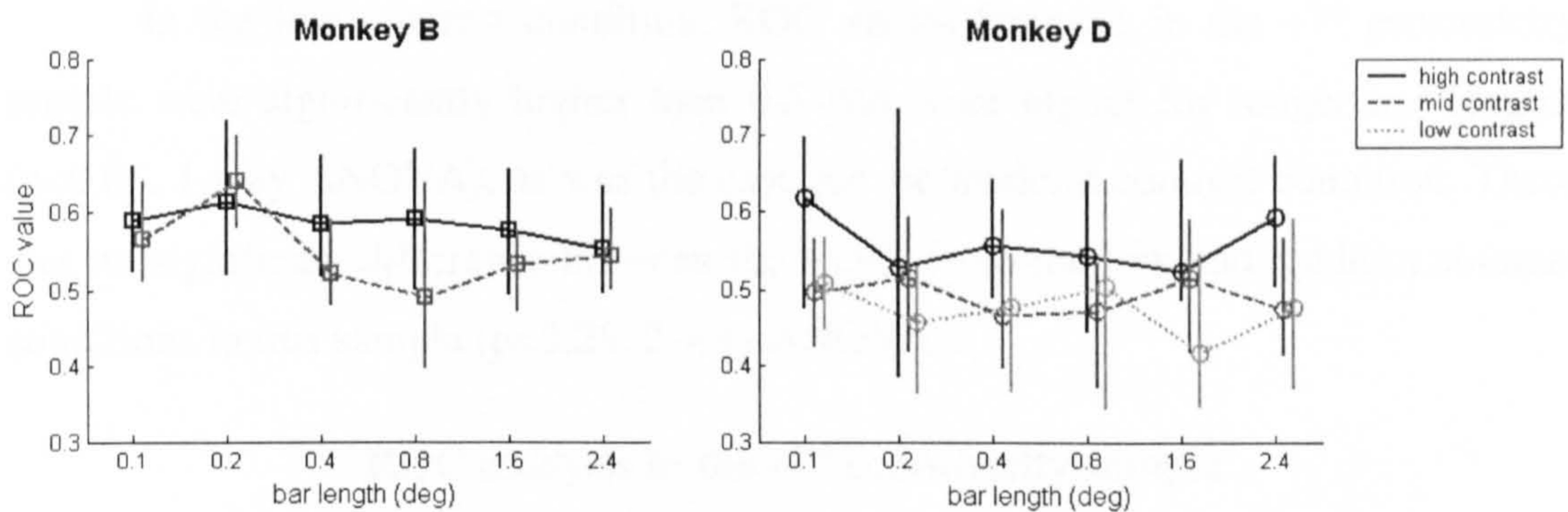


Figure 3.26 ROC values across bar length and contrast for monkey B ($\sim 2^\circ$ eccentricity) and monkey D. Points show median ROC value; error bars show inter-quartile range. Solid black lines show data from the high contrast condition, dark grey dashed lines show data from the medium contrast condition, and light grey dotted lines show data from the low contrast condition.

Comparison of ROC values across contrasts

Monkey	Contrast	25th	50 percentile	75th	ROC \neq 0.5
B	high $\sim 2^\circ$	0.5	0.59	0.67	$P<0.001$
	mid ~ 2	0.48	0.55	0.64	$P<0.001$
	mid ~ 7	0.47	0.52	0.61	$P<0.005$
	low $\sim 7^\circ$	0.44	0.51	0.59	$P<0.05$
D	high	0.48	0.56	0.68	$P<0.001$
	mid	0.41	0.49	0.57	$P= 0.1$
	low	0.36	0.48	0.56	$P<0.05$

Table 3.5 Median, 25th percentile, and 75th percentile ROC values for each monkey at each contrast (separated by eccentricity in monkey B). The final column shows significance of the difference in the ROC value from 0.5 (2-tailed t-test).

3.4.4.3 ROC analysis in the $\sim 7^\circ$ eccentricity sample

Figure 3.27 shows the ROC values for cells from monkey B in the $\sim 2^\circ$ and $\sim 7^\circ$ eccentricity samples recorded with medium contrast stimuli. In both populations ROC values were significantly greater than 0.5 (Table 3.5). Taken across all bar lengths there was no significant difference between the ROC values from the two populations ($p=0.13$, 2-sample t-test), demonstrating that the magnitude of the attentional effect was approximately equal at both eccentricities. However, in the $\sim 7^\circ$ eccentricity sample values of ROC, values were higher for longer bar lengths ($p<0.001$, 1-way ANOVA), whilst for the $\sim 2^\circ$ eccentricity sample ROC values were higher for shorter bars ($p<0.005$, 1-way ANOVA). This demonstrates that the dependency of attentional enhancement on stimulus length was reversed between the $\sim 2^\circ$ eccentricity sample and $\sim 7^\circ$ eccentricity sample, in line with the above findings concerning length tuning.

In the low contrast condition, ROC values for cells in the $\sim 7^\circ$ eccentricity sample were significantly higher than 0.5 and were higher for longer bar lengths ($p<0.05$, 1-way ANOVA), as was the case for the medium contrast condition. There was no significant difference between the ROCs from the low and medium contrast conditions in this sample ($p=0.28$, 2-way ANOVA).

ROC analysis in the $\sim 7^\circ$ eccentricity sample

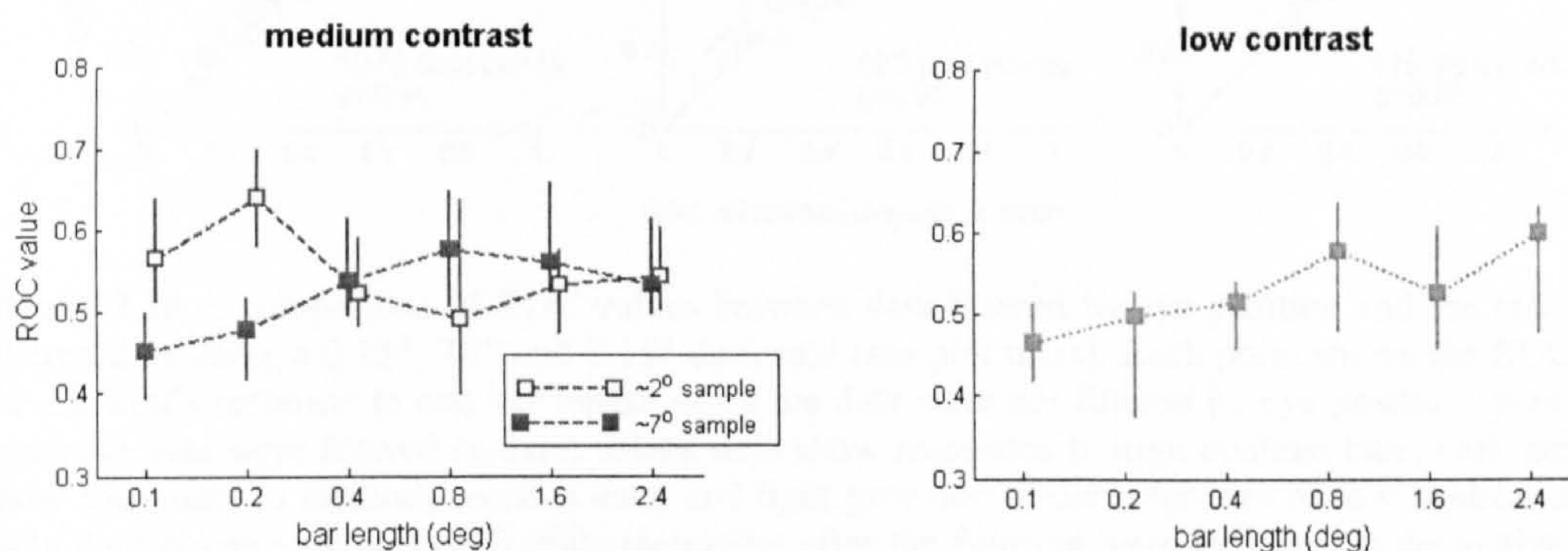


Figure 3.27 ROC values across bar length and contrast for data recorded for data recorded at $\sim 7^\circ$ eccentricity (filled squares). Data from the medium contrast condition recorded at $\sim 2^\circ$ eccentricity is included for comparison (open squares). Points show the median ROC value, error bars show the 25th and 75th percentiles.

3.4.4.4 ROC analysis to assess the effect of eye position

The influence of eye position was a critical factor to test for, since the stimuli and the RF sizes were both small. To examine the effect of eye position on neuronal

data, I used a post-hoc filtering to restrict the eye position window, which allowed me to take selections of trials where there were especially small differences in eye position between the two attention conditions. For this analysis I first calculated the mean eye position during the analysis period (i.e. 30-500msec post stimulus onset in monkey B or from 30-200msec post stimulus onset in monkey D) from all recorded trials. I then set a threshold to excluded trials in which the eye position deviated from the mean position by more than the threshold allowed. I tested whether filtering the eye position in this way affected the magnitude of attentional modulation of neuronal responses using ROC analysis on data filtered with increasingly restrictive thresholds.

I found no significant difference in ROC values between filtered and unfiltered data at any threshold level (Figure 3.28), demonstrating that eye position differences did not contribute to the difference in response between the two attention conditions.

Comparison of ROC values in raw data and data filtered by eye position

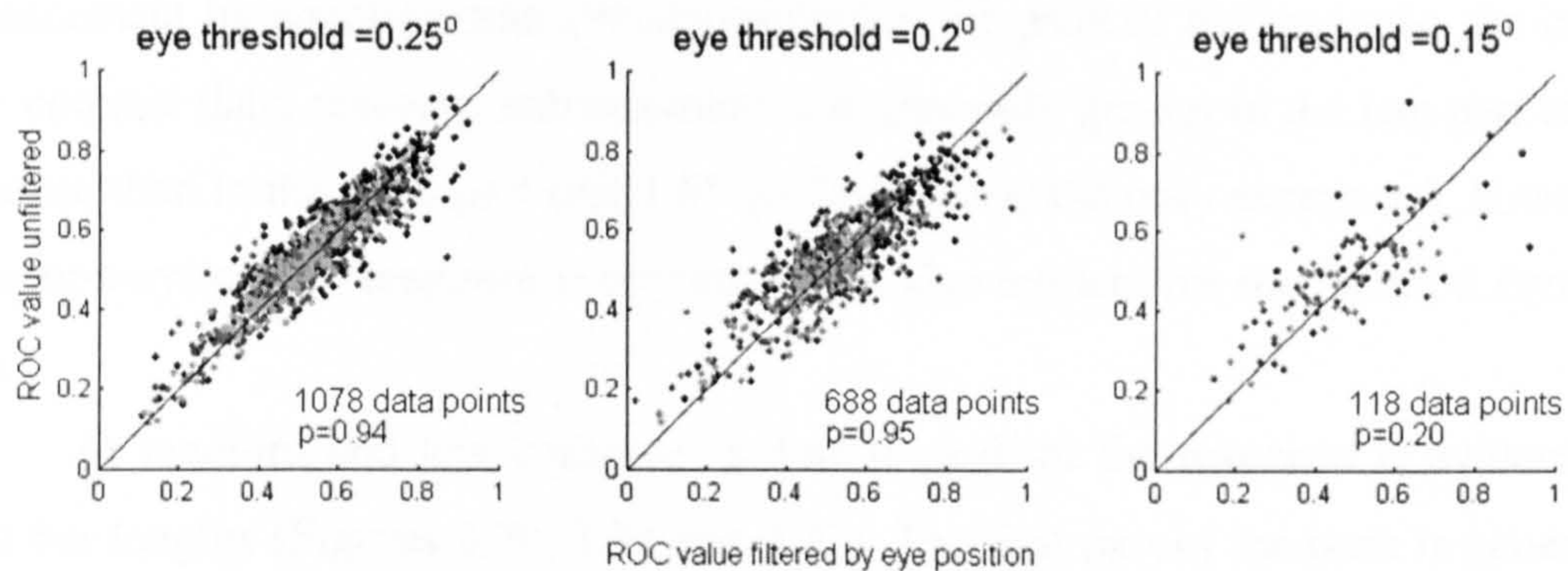


Figure 3.28 A comparison of ROC values between data filtered by eye position and the raw data. I filtered data using a 0.25° , 0.2° and 0.15° threshold (see plot titles). Each point shows the ROC value for one cell's response to one bar length when the data were not filtered by eye position (y-axis) and when the data were filtered (x-axis). Black dots show responses to high contrast bars, dark grey dots show responses to medium contrast bars, and light grey dots show responses to low contrast stimuli. Only data points with at least 8 trials remaining after the filtering were included in the analysis. The number of data points in the analysis is shown on the lower right corner of each plot. The p-values show the significance of differences between the filtered and unfiltered ROC values (paired t-test).

3.4.4.5 Temporal profile of the response enhancement

A feature of attentional enhancement that has been consistently reported in the literature is that responses are more strongly enhanced by attention in the late part of the response than in the early part, making responses more tonic (Motter 1994; Roelfsema et al. 1998; McAdams and Maunsell 1999; Seidemann and Newsome

1999; Reynolds et al. 2000; Roelfsema and Spekreijse 2001; Treue 2001). To investigate this effect I calculated population histograms and a tonic index (TI Equation 3.7) for responses during the attend-RF and attend-away conditions. These analyses were only carried out for monkey B, since the stereotyped saccade made by monkey D at 200msec post stimulus onset caused data in the late part of the response to be affected by small but systematic eye-movements.

In the high contrast data from monkey B, I found response enhancement by attention from response onset. There was a sharp drop in response enhancement at the peak of the response. After the response peak, enhancement by attention increased with time somewhat monotonically for most bar lengths. Responses to shorter bars were enhanced more strongly than responses to longer bars. This difference was most evident towards the end of the response.

Attentional enhancement in the medium contrast condition was less well defined than in the high contrast data, possibly due to the smaller sample size. A notable difference between the high and medium contrast data was that for the shortest bar lengths (0.1° and 0.2°) in the medium contrast condition, response enhancement by attention was already evident at the peak of the response. As in the high contrast data, response enhancement was generally greater in the late part of the response than in the early part (the 1.6° bar length was the only exception), however, some non-systematic response suppression was also evident for the medium contrast data.

At medium and low contrasts, a double peak of the response is evident for most bar lengths (Figures 3.30, 3.31 and 3.32). The first part of the peak is generally higher than the later part and is very transient. The later part of the peak is lower and somewhat more sustained. A similar pattern is present in the medium and low contrast data from the $\sim 7^\circ$ eccentricity sample. The double peak represents two distinct cell types with different response profiles. The sharp early peak of the population histogram comes from a small group of cells (~ 3 cells in the medium contrast data) with a very regular and high response onset. In some of these cells, the early onset is followed by a second peak that is shallower and more sustained. The second group of cells contributes to the second peak in the population histogram. These cells have a later, lower and more sustained peak in their response profile. There were 10 cells with an early transient response peak present in the high contrast data population. However, their peak is masked in the population histogram, because

the latency of the second group of cells (those with a later and more sustained peak response) was shorter for high contrast stimuli and so a gap between the peaks of the two cell types is less evident.

In the $\sim 7^\circ$ eccentricity sample the overall response was suppressed by attention for the two shortest bar lengths at both medium and low contrast conditions (Figure 3.27). This suppression of the response occurred shortly after, but not directly at, the response peak. There was no clear effect of attention in the late part of the response for these bar lengths. For longer bar lengths of both medium and high contrast, attention enhanced the overall response. This enhancement of the response was most evident during the late part of the response.

The effect of attention on response profiles to high contrast stimuli ($\sim 2^\circ$ eccentricity, $n=78$ cells)

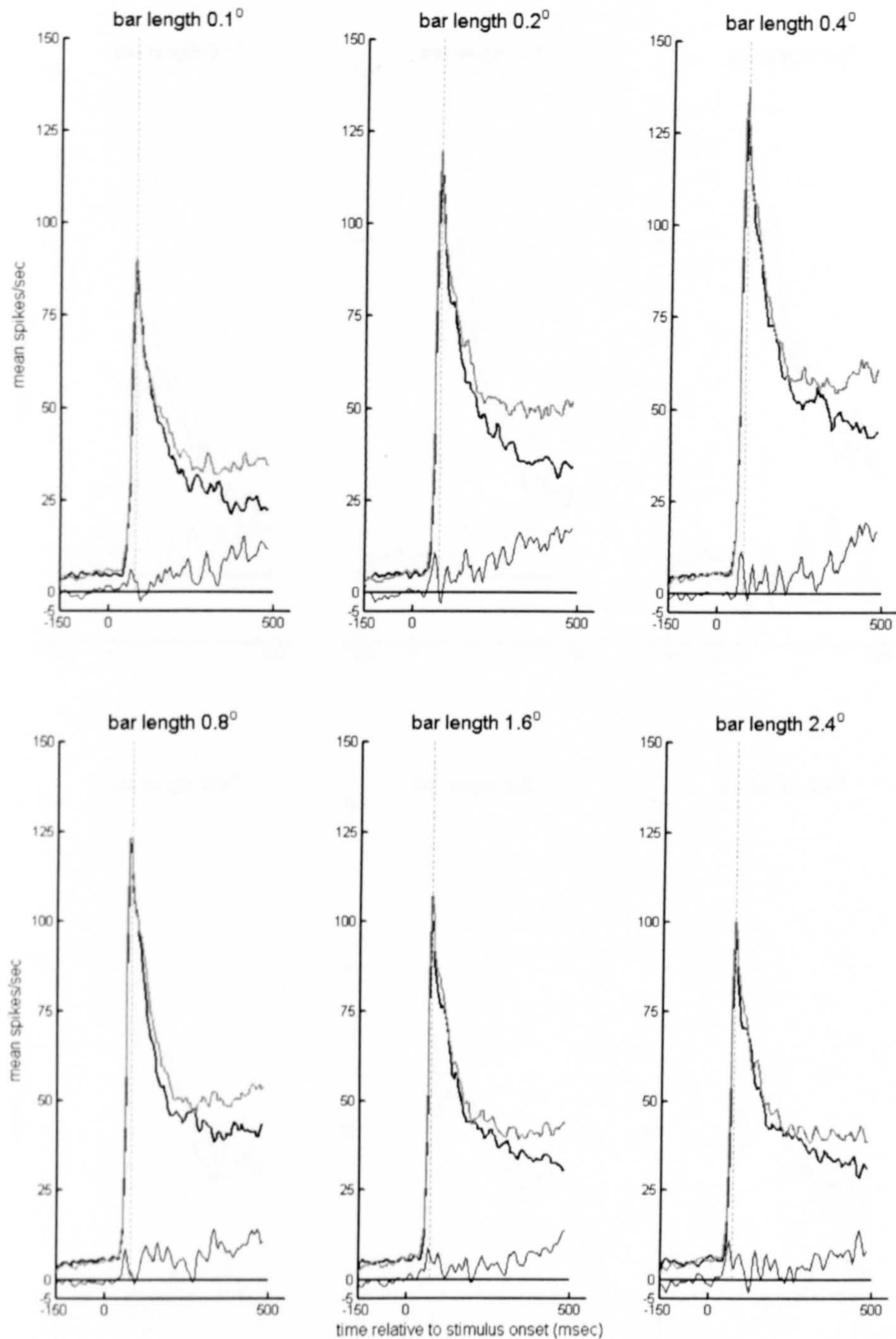


Figure 3.29 Mean response profiles to high contrast stimuli ($\sim 2^\circ$ eccentricity). Thick black curves show the mean response histogram in the attend-away condition for the relevant bar length (see plot titles). Grey curves show the response in the attend-RF condition. Thin black lines at the base of the plots show the difference between the attend-away and attend-RF responses. The vertical dotted line marks the time of the peak response.

The effect of attention on response profiles to medium contrast stimuli ($\sim 2^\circ$ eccentricity, $n=17$ cells)

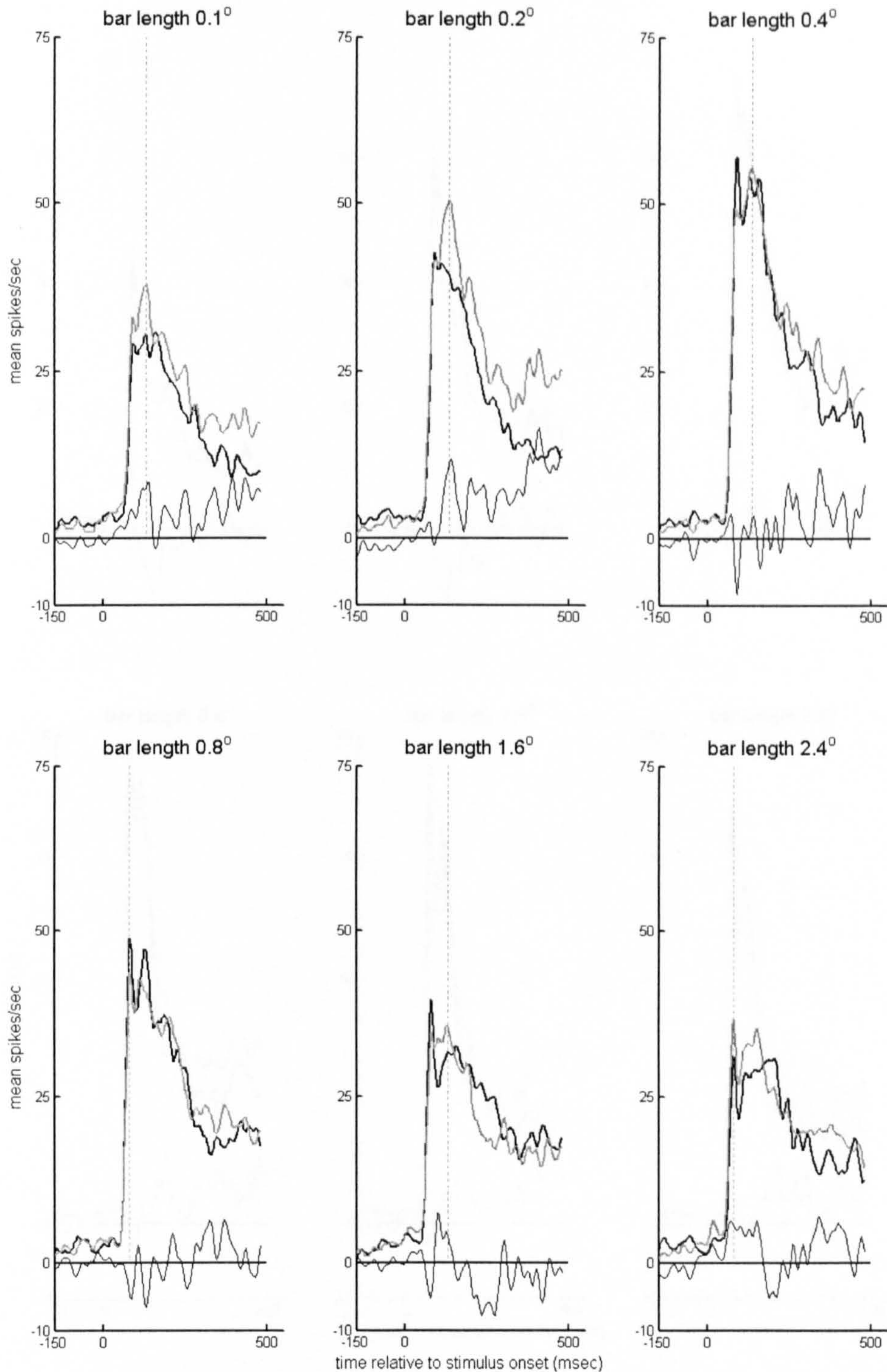


Figure 3.30 Mean response profiles to medium contrast stimuli ($\sim 2^\circ$ eccentricity). Thick black curves show the mean response histogram in the attend-away condition for the relevant bar length (see plot titles). Grey curves show the response in the attend-RF condition. Thin black lines at the base of the plots show the difference between the attend-away and attend-RF responses. The vertical dotted line marks the time of the peak response in the attend-RF condition.

The effect of attention on response profiles to medium contrast stimuli ($\sim 7^\circ$ eccentricity, $n=22$ cells)

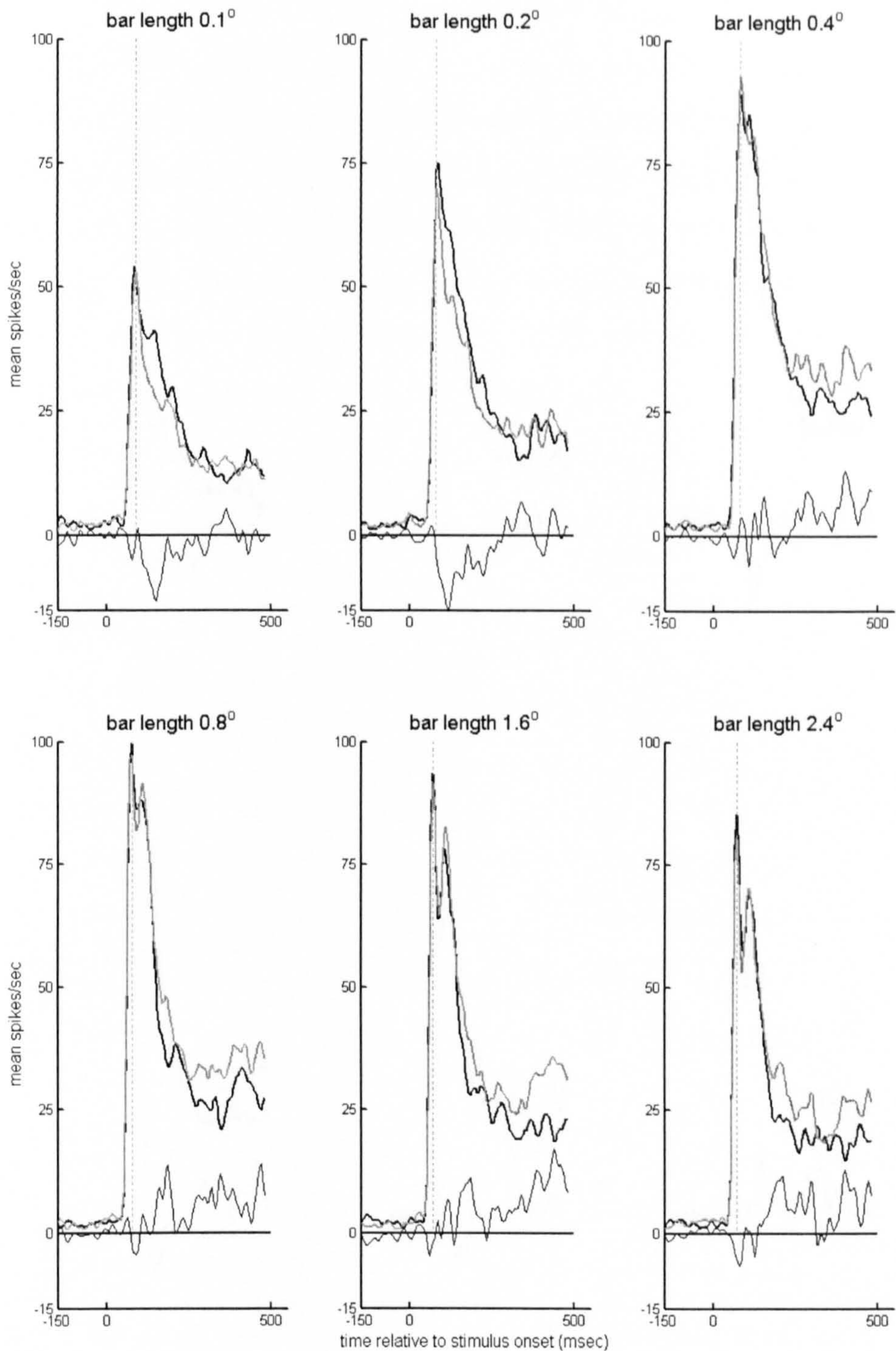


Figure 3.31 Mean response profiles to medium contrast stimuli ($\sim 7^\circ$ eccentricity). Thick black curves show the mean response histogram in the attend-away condition for the relevant bar length (see plot titles). Grey curves show the response in the attend-RF condition. Thin black lines at the base of the plots show the difference between the attend-away and attend-RF responses. The vertical dotted line marks the time of the peak response in the attend-RF condition.

The effect of attention on response profiles to low contrast stimuli ($\sim 7^\circ$ eccentricity, $n=17$ cells)

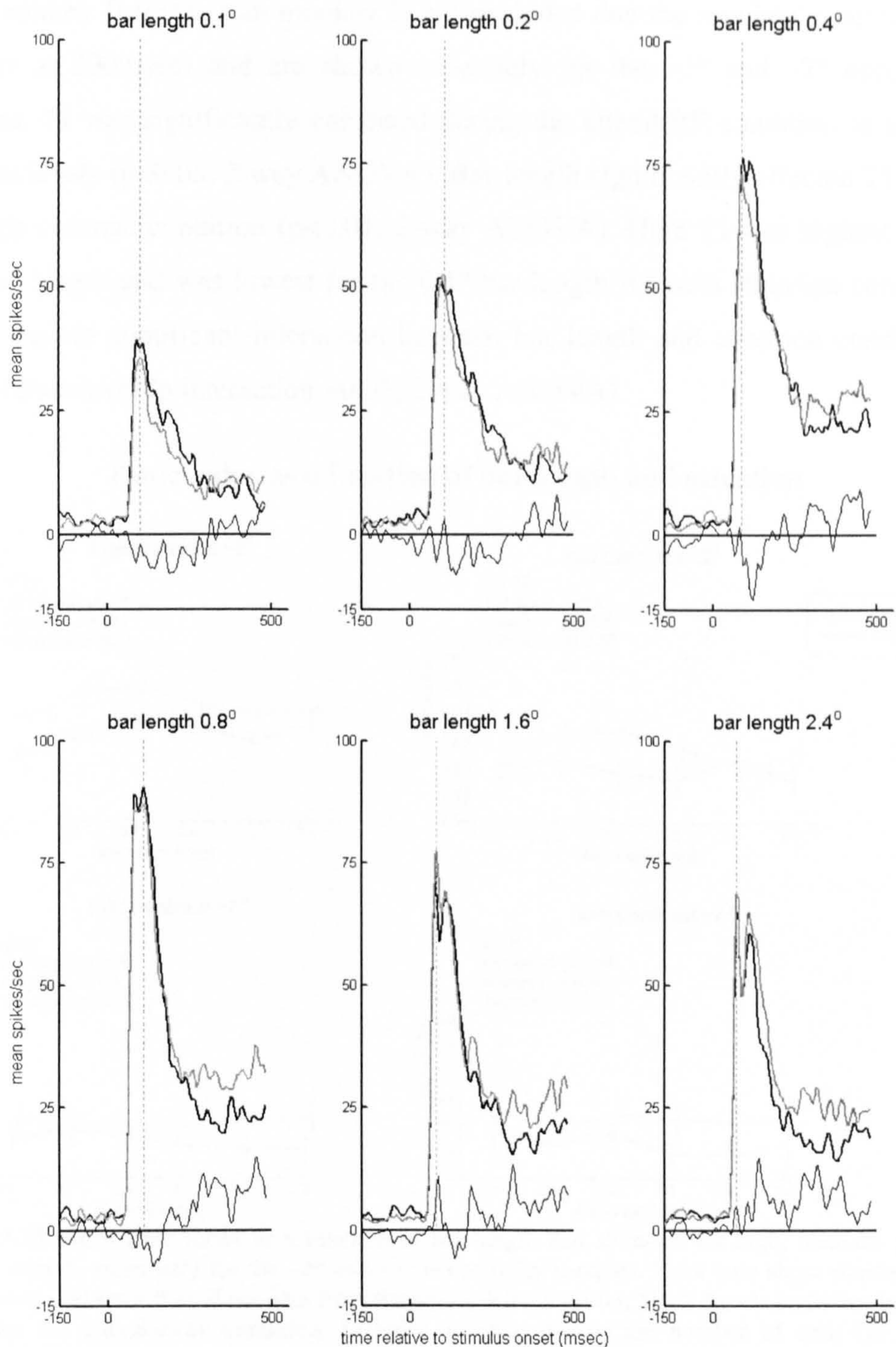


Figure 3.32 Mean population response to low contrast stimuli ($\sim 7^\circ$ eccentricity). Thick black curves show the mean response histogram in the attend-away condition for the relevant bar length (see plot titles). Grey curves show the response in the attend-RF condition. Thin black lines at the base of the plots show the difference between the attend-away and attend-RF responses. The vertical dotted line marks the time of the peak response in the attend-RF condition.

To quantify how the response profile was changed by attention I calculated a tonic index (TI). Figure 3.33 shows TI as a function of attention and bar length for neuronal responses to high, medium and low contrast stimuli. Data are only included from monkey B (data from monkey D are excluded due the monkey's stereotypical saccade at 200msec) and are shown separately for the $\sim 2^\circ$ and $\sim 7^\circ$ eccentricity samples. TI was significantly enhanced during the attend-RF condition at all three contrast levels ($p < 0.05$, 2-way ANOVA). Bar length significantly affected TI only in the high contrast condition ($p < 0.01$, 2-way ANOVA). Here TI was highest for the 0.4° bar length and was lowest for the 0.1° bar length for both attention conditions. There was no significant interaction between bar length and attention condition at any contrast level (p interaction > 0.05 , 2-way ANOVA).

Tonic index as a function of bar length and attention

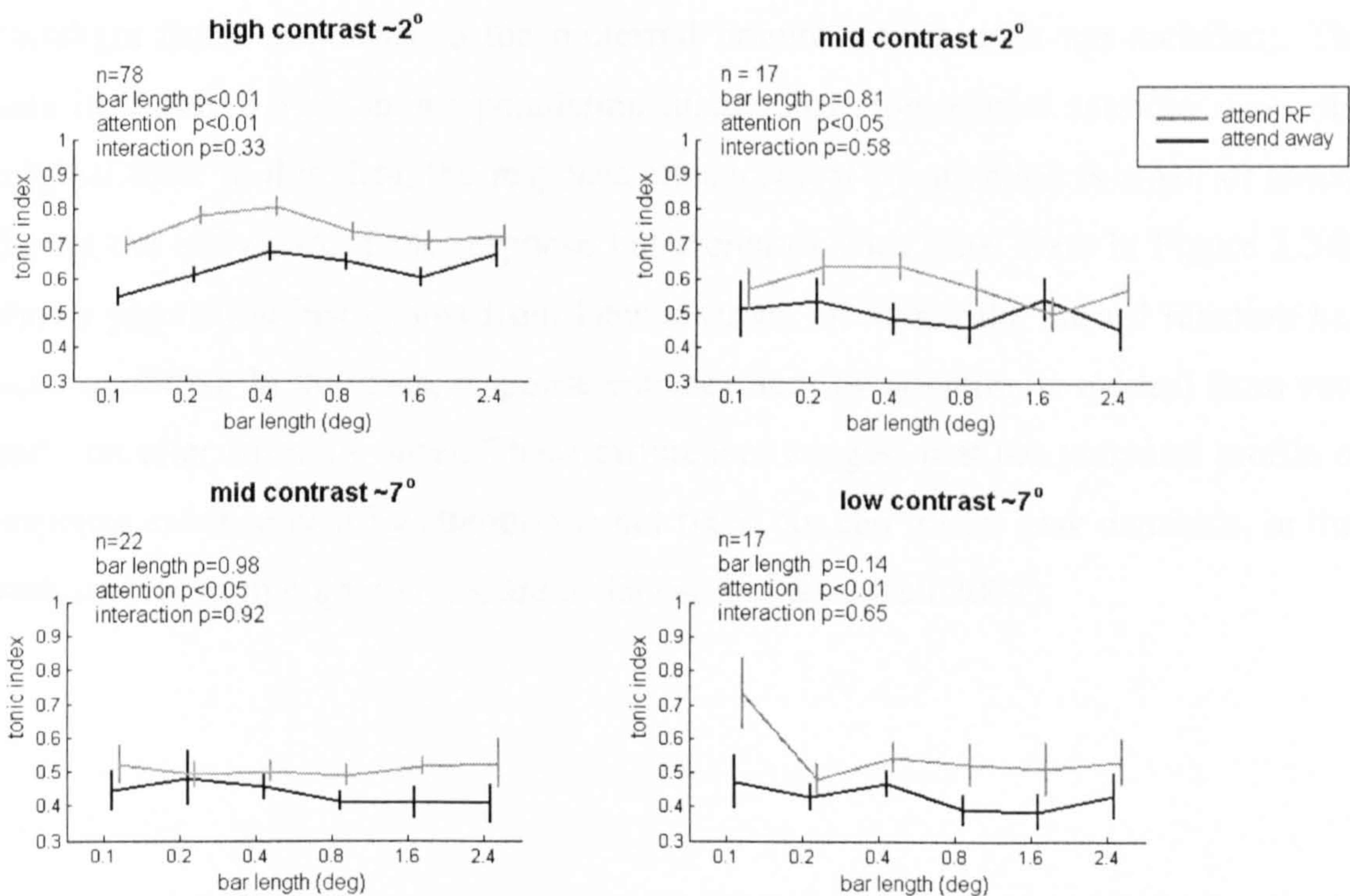


Figure 3.33 Mean tonic index as a function of bar length and attention for high, medium, and low contrast stimuli, separately for the $\sim 2^\circ$ and $\sim 7^\circ$ eccentricity samples. Error bars show standard error. Grey curves and error bars show data from the attend-RF condition; black curves and error bars show data from the attend-away condition. Included in each plot is the number of cells (n) and the significance of difference in TI across bar lengths, attention conditions and the interaction between bar length and attention condition (2-way ANOVA).

3.4.4.6 Response enhancement and the hazard function

The hazard function describes when behaviourally relevant events (the appearance of the target brightening) are likely to occur during a trial. To test

whether the hazard function was reflected in the temporal profile of attentional enhancement I modified the hazard function in the orientation tuning experiment used for monkey B after ~8 months of recording (see section 3.3 *Methods*). In its original form, the task was identical to the task used in the length tuning experiment, except that the test stimuli varied in orientation and had constant length (0.4°). Initially, the target brightening had a 50% probability of occurring at 500msec post stimulus onset and a 50% probability of occurring at 1500msec post stimulus onset. In the modified version of the task I randomly selected 20% of trials in which the first brightening (target or distracter) occurred after 200msec. Thus the target brightening had a 10% probability of occurring at 200msec, a 40% probability of occurring at 500msec, a 10% probability of occurring at 1200msec and a 40% probability of occurring at 1500msec.

Figure 3.34 shows population histograms from the orientation tuning paradigm (only responses to the preferred orientation stimulus are included). The data in Figure 3.34A shows population histograms from earlier sessions using the original task. In this data, the response enhancement by attention is small or absent during the early part of the response but increases with time. Data in Figure 3.34B shows population histograms from later sessions, in which the hazard function had been modified. In this data, response enhancement by attention is evident from very early on after stimulus onset. These differences suggest that the temporal profile of response enhancement by attention is not fixed but can follow task demands, in line with reports from higher visual areas (Ghose and Maunsell 2002).

The effect of task demands on response profile

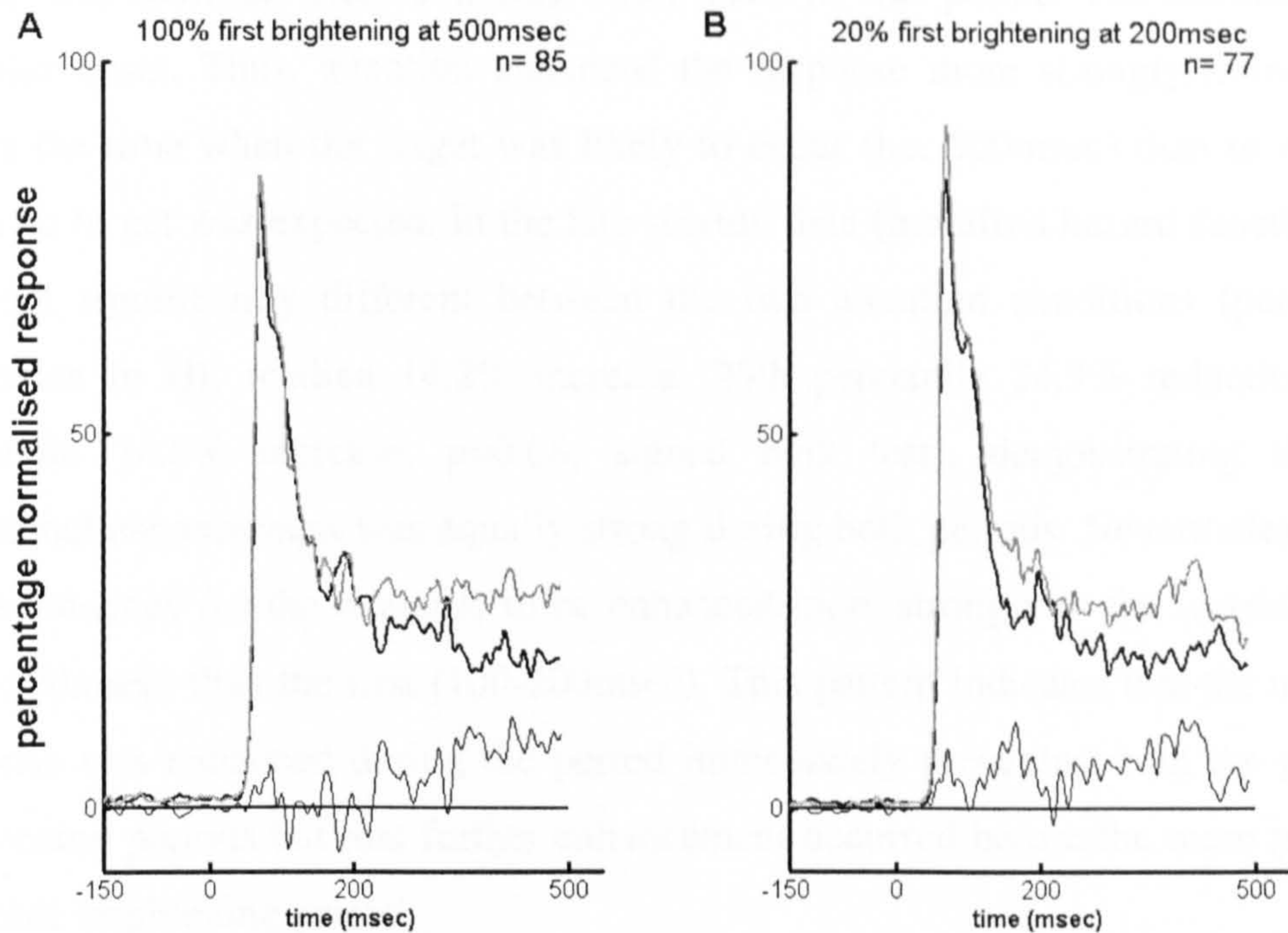


Figure 3.34 Normalised population response to a 0.4° long bar of the preferred orientation, **A**) under standard task conditions and **B**) under conditions of modified hazard function. Thick black curves show responses in the attend-away condition, grey curves show responses in the attend-RF condition. Thin black lines at the base of the plots show the difference between the attend-away and the attend-RF responses. Responses from each cell were normalised to the highest response for that cell before being added to the population, thus each cell contributes equally to the mean responses shown here.

To quantify how task demands influenced the temporal profile of neuronal responses, I calculated a ‘hazard index’ (HI, see Equation 3.8) as the ratio of the mean firing rate from 400-500msec after stimulus onset to the mean firing rate from 100-200msec after stimulus onset, i.e. the ratio of firing rates preceding the first two periods when a target may occur in the modified task. I compared HI between the attend-RF and attend-away conditions. An increase in HI with attention would indicate that attention affected the response more strongly in the period preceding the 500msec brightening than in the period preceding the 200msec brightening. No change in HI would indicate that attention affected the response by the same amount in both periods.

I calculated the effect of attention on HI in data from the early sessions where I had used the original hazard function, and in the late sessions where the hazard function had been modified. HI was significantly increased by attention in the early session data (percentage difference in HI: median 36.9% increase, 25th percentile 6.6% increase, 75th percentile 112.6% increase, $p < 0.001$, signed rank test) indicating

that the neuronal response had been enhanced by attention more strongly in the period 400-500msec after stimulus onset than in the period 100-200msec after stimulus onset. Thus, attention enhanced the response more strongly immediately before the time when the target was likely to occur (i.e. 500msec) than in a period when no target was expected. In the late session data (modified hazard function), HI was not significantly different between the two attention conditions (percentage difference in HI: median 14.2% increase, 25th percentile 24.9% reduction, 75th percentile 74.8% increase, $p=0.08$, signed rank test), demonstrating that the attentional enhancement was equally strong during both periods. Nevertheless, there was a tendency for the response to be enhanced more strongly in the second period (400-500msec) than the first (100-200msec). This pattern indicates that the neuronal response was enhanced during the period immediately preceding both the possible brightening periods but that further enhancement occurred before the more probable 500msec brightening period.

3.4.5 The interaction of contrast and attention on length tuning

For 58 cells I measured the effect of attention on length tuning at two contrasts. Figure 3.35 shows two cell examples of the effects of contrast and attention on length tuning. The effect of contrast on the length tuning across the population is shown in Figure 3.36 and 3.37. Lowering the contrast (either between high and medium contrast or between medium and low contrast) caused a significant ($p<0.01$) increase in the cell's preferred length in most cases, during both the attend-away and attend-RF conditions. The increase in preferred length with reduced contrast was mediated by an increase in the summation area, which was the only fitting parameter to be significantly affected by lowering the contrast. The exact values and significances of these changes are shown in Tables 3.6 and 3.7 in the Appendix.

Cell examples of the effect of contrast and attention on length tuning

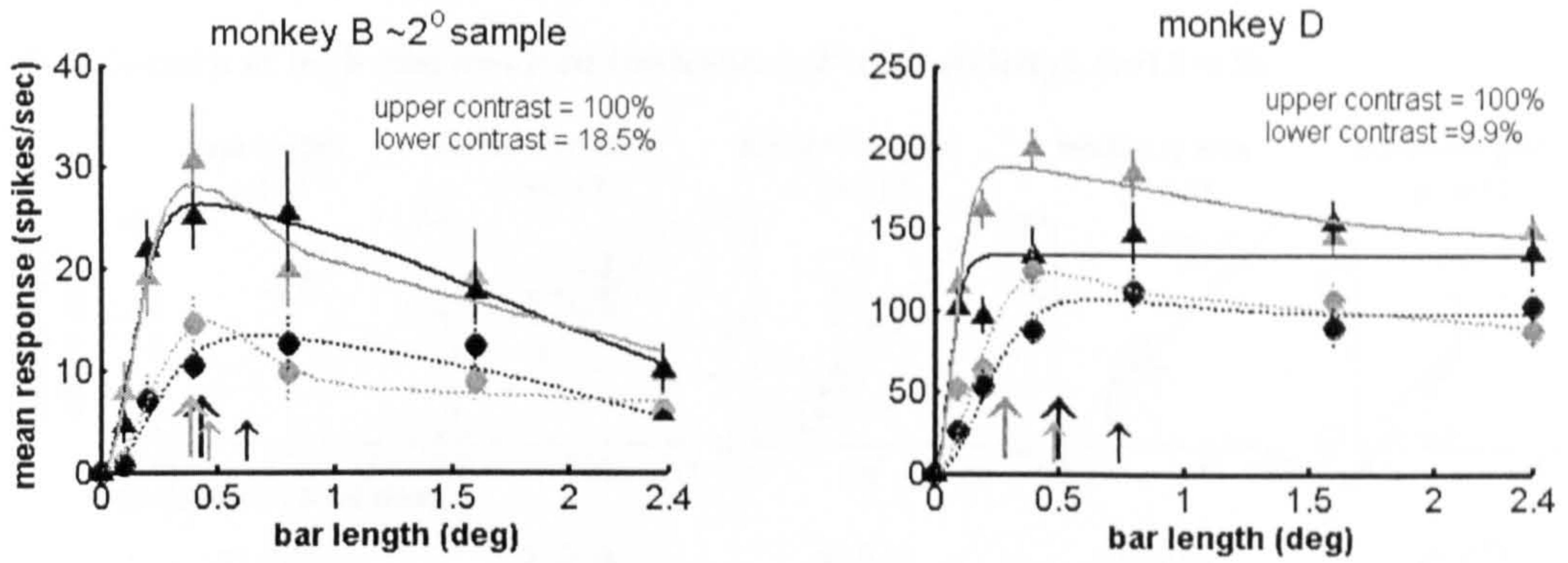
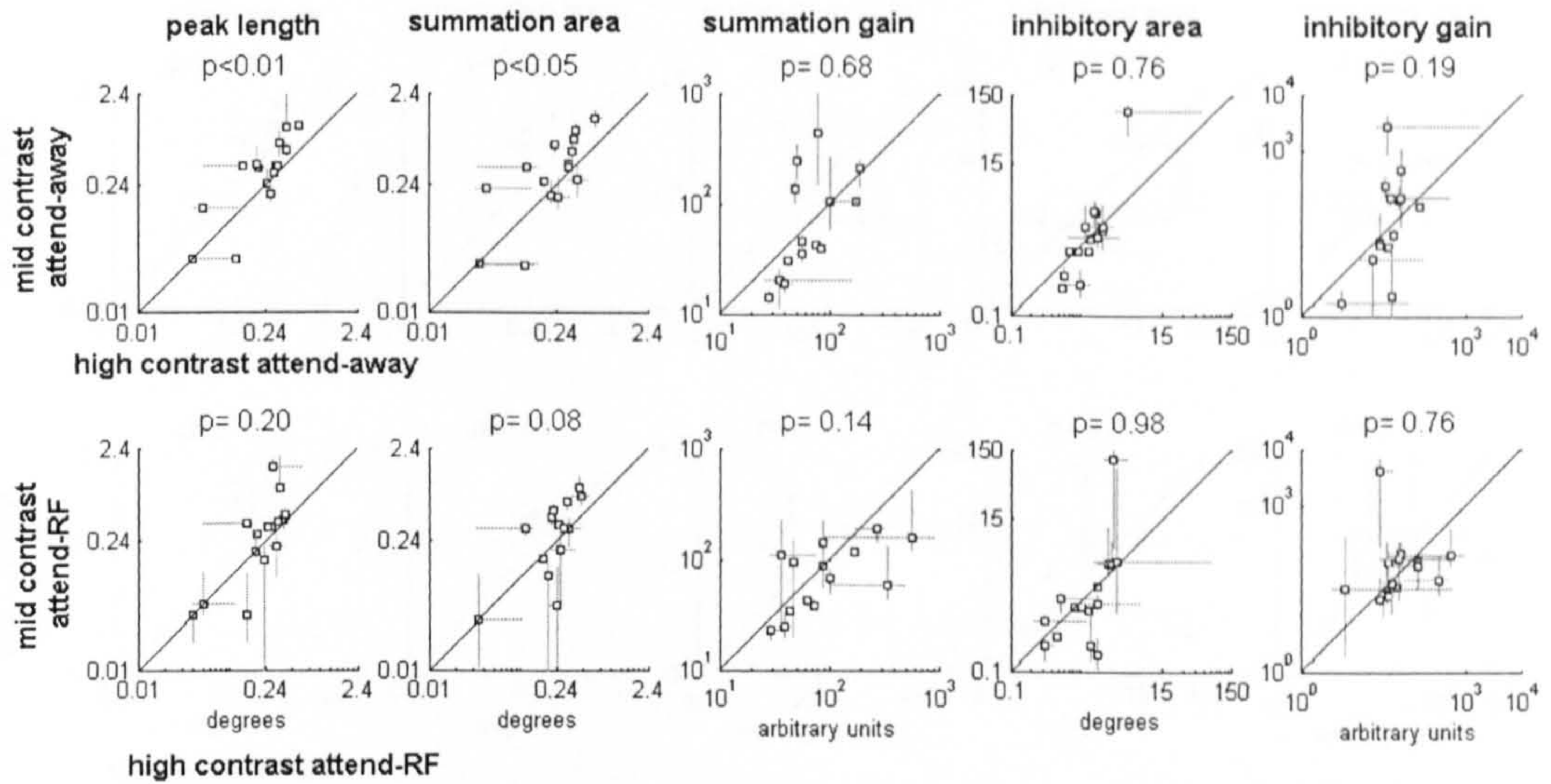


Figure 3.35 Two example cells showing the effect of attention on length tuning at two contrasts. Upwards-pointing triangles show mean response at each high contrast bar length. Circles show mean response at each lower contrast bar length; error bars show standard error. Curves fitted to the data show the median DOG model fit from the bootstrap procedure. Solid curves are fitted to the high contrast data; dotted curves are fitted to the lower contrast data. The median preferred length is marked with upwards-pointing arrows. Large arrows correspond to the peak of the high contrast length tuning; smaller arrows mark the peak of the lower contrast length tuning. Grey triangles, circles, lines and arrows show data from the attend-RF condition; black triangles, lines and arrows show data from the attend-away condition. The distribution of peak lengths and the upper and lower quartiles of the fitted curves, which have been shown in previous figures, are not shown here for simplification.

The effect of contrast on length tuning in monkey B

A) Comparison of high and medium contrasts ($\sim 2^\circ$ eccentricity), $n=15$ cells



B) Comparison of medium and low contrasts ($\sim 7^\circ$ eccentricity), $n=17$ cells

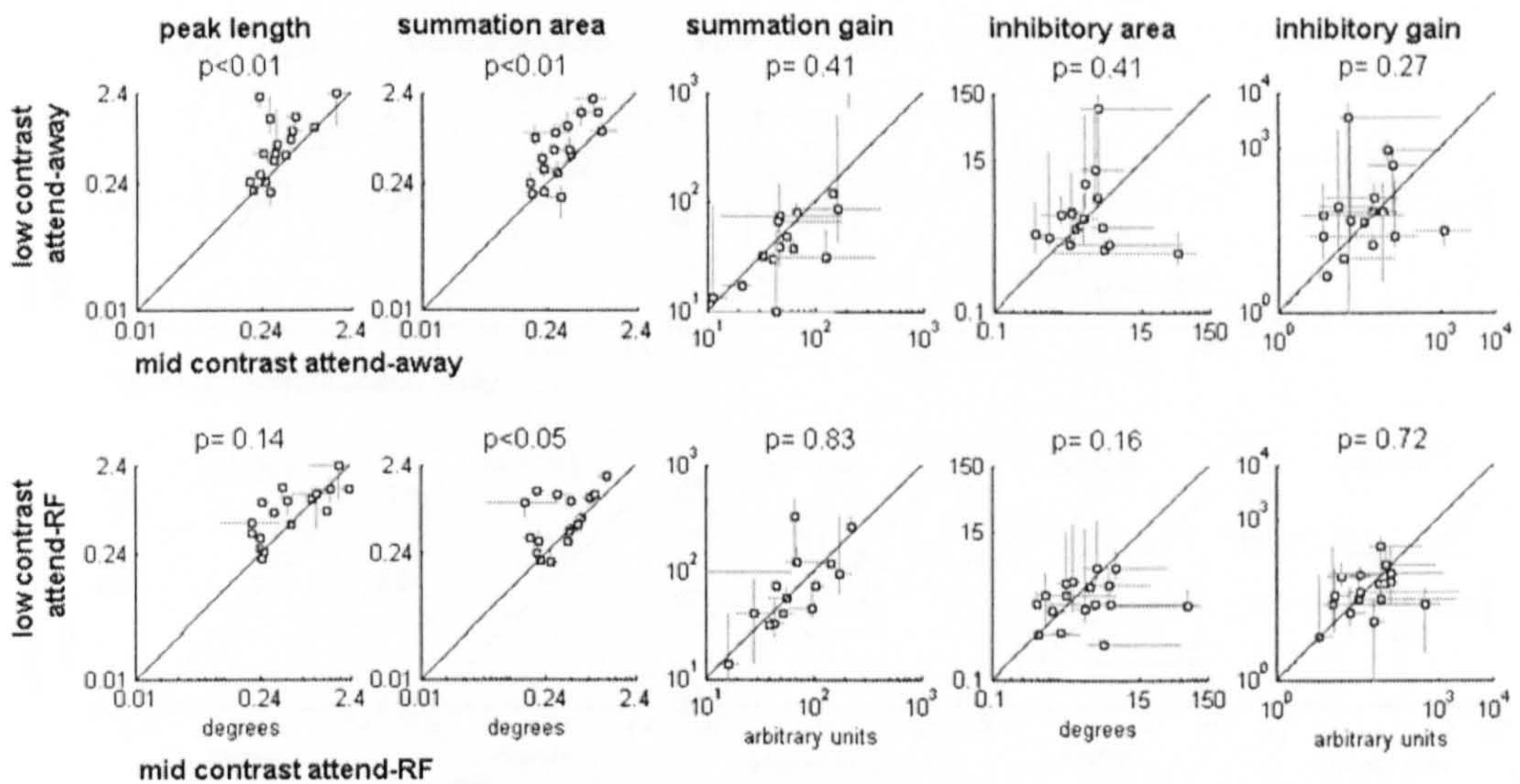
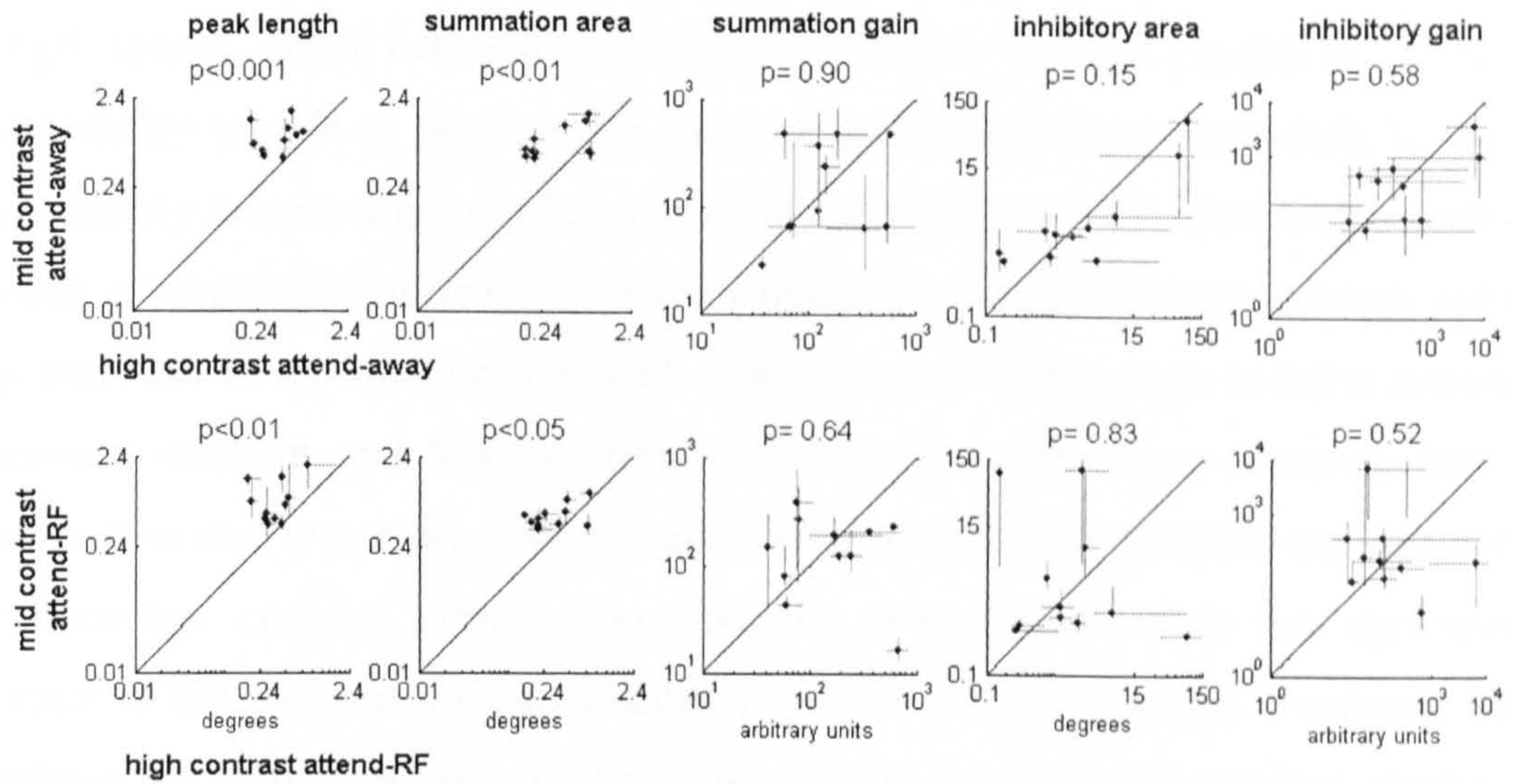


Figure 3.36 Preferred length and DOG fitting parameters as a function of contrast in both attention conditions, **A)** for cells recorded at both high and medium contrast ($\sim 2^\circ$ eccentricity) and **B)** for cells recorded at both medium and low contrast ($\sim 7^\circ$ eccentricity), from monkey B. Each point marks the median value of the respective parameter (see column headings) for a given cell in each attention and contrast condition (x- and y-axis labels). Points above the diagonal indicate that the parameter of interest was increased in the lower contrast condition. Above each plot, the p-value shows the significance of differences as a function of contrast across the population (signed rank test).

The effect of contrast on length tuning in monkey D

A Comparison of high and medium contrasts n=11 cells



B Comparison of medium and low contrasts n=15 cells

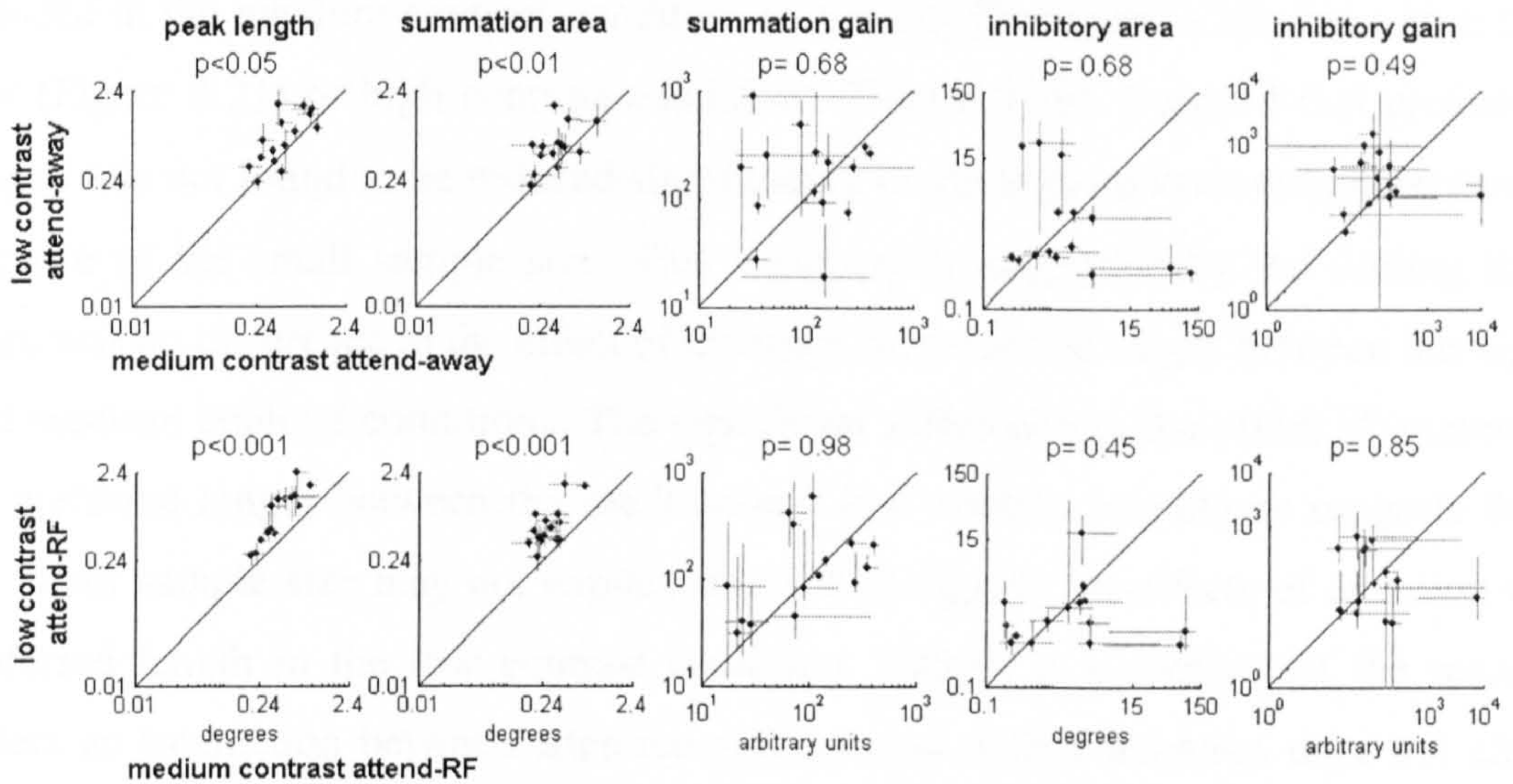


Figure 3.37 Preferred length and DOG fitting parameters as a function of contrast in both attention conditions, **A**) for cells recorded at both high and medium contrast and **B**) for cells recorded at both medium and low contrast, from monkey D. Each point marks the median value of the respective parameter (see column headings) for a given cell in each attention and contrast condition (x- and y-axis labels). Points above the diagonal indicate that the parameter of interest was increased in the lower contrast condition. Above each plot, the p-value shows the significance of differences as a function of contrast across the population (signed rank test).

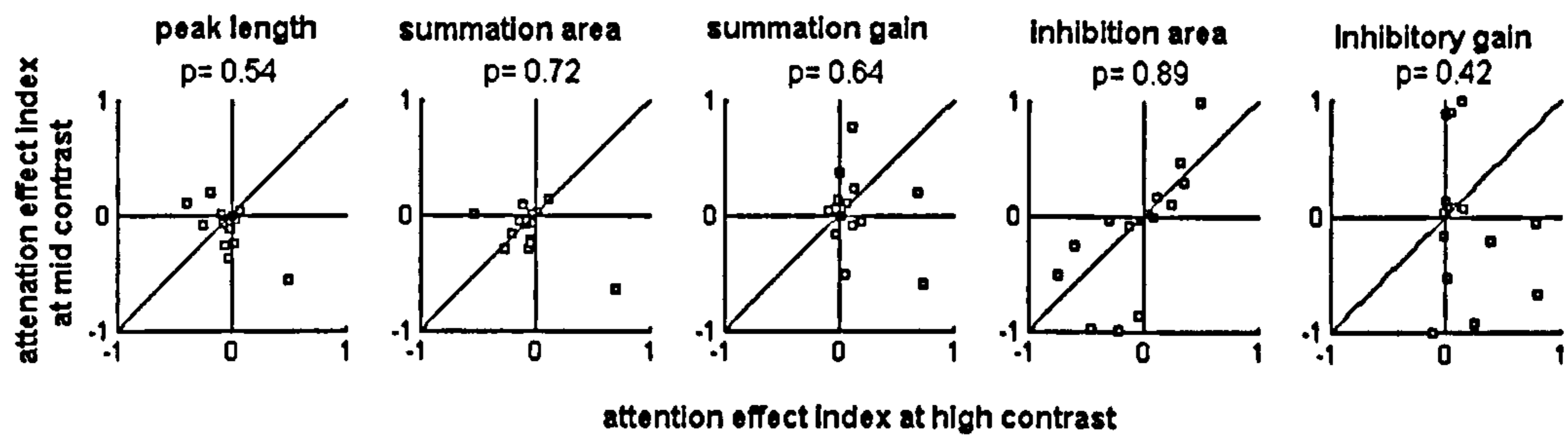
To test for an interaction between attention and contrast I compared the effect of attention on length tuning at different contrast levels. I calculated the effect of attention length tuning parameters as the difference between the parameter of interest in the two attention conditions divided by the sum. This index gives a value of

between -1 and 1, where negative values indicate that the parameter was reduced in the attend-RF condition.

In monkey B, I found no significant differences in the effect of attention on length tuning, either between the high and medium contrast conditions in the $\sim 2^\circ$ eccentricity sample or between the medium and low contrast conditions in the $\sim 7^\circ$ eccentricity sample (Figure 3.38). For monkey D (Figure 3.39) there was a tendency, which approached significance, for the summation area to be more strongly reduced by attention in the medium contrast condition than in the high contrast condition. Between medium and low contrast conditions the effect was reversed; here the summation area was more strongly reduced by attention for medium contrast stimuli than for low contrast stimuli. The reduction in preferred length was significantly greater in the medium contrast condition than in the low contrast condition. These findings are consistent with the findings presented earlier, where it was shown that preferred length and summation area with attention were found to be significantly reduced in the medium contrast condition in monkey D (Figure 3.20), but not in the low (Figure 3.21) or high contrast conditions (Figure 3.19). I argued that preferred length was not found to be reduced significantly in the high contrast condition partly because of the small sample size. This argument is supported by the finding that there was no difference in the effect of attention on preferred length between the high and medium contrast conditions. The significant difference in the effect of attention on preferred length between the medium and low contrast conditions suggests that the small sample size may not explain the lack of significant effects of attention on preferred length in the low contrast condition. Rather, it is likely that the results reflect an interaction between attention and contrast, where attention does not alter spatial summation at low contrasts.

The interaction of attention and contrast on length tuning (monkey B)

A Monkey B: the effect of attention at high and medium contrast ($\sim 2^\circ$ eccentricity) $n=15$



B Monkey B: the effect of attention at medium and low contrast ($\sim 7^\circ$ eccentricity) $n=17$

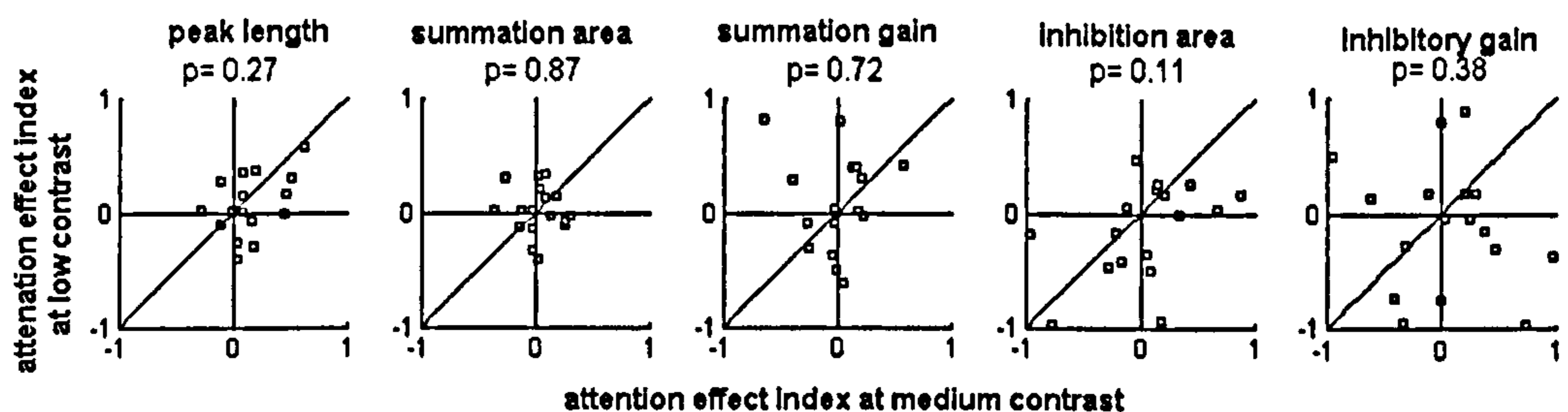


Figure 3.38 Comparison of the effect of attention on peak length and DOG fitting parameters at two contrasts in monkey B. Each point shows the attention effect index for each contrast (see axis labels). **A)** Cells recorded using high and medium contrast stimuli ($\sim 2^\circ$ eccentricity sample). **B)** Cells recorded using medium and low contrast stimuli ($\sim 7^\circ$ eccentricity sample). The attention effect index is calculated for each parameter as the difference in the parameter between the two attention conditions divided by the sum. The value of the parameter of interest is taken as the median value from the bootstrap procedure. Negative values indicate that the parameter was reduced in the attend-RF condition. For positive values, points above the diagonal indicate that the attention effect index was higher in the lower contrast (mid contrast in A, low contrast in B) condition. For negative values points below the diagonal indicate that the effect was higher in the lower contrast condition.

The interaction of attention and contrast on length tuning (monkey D)

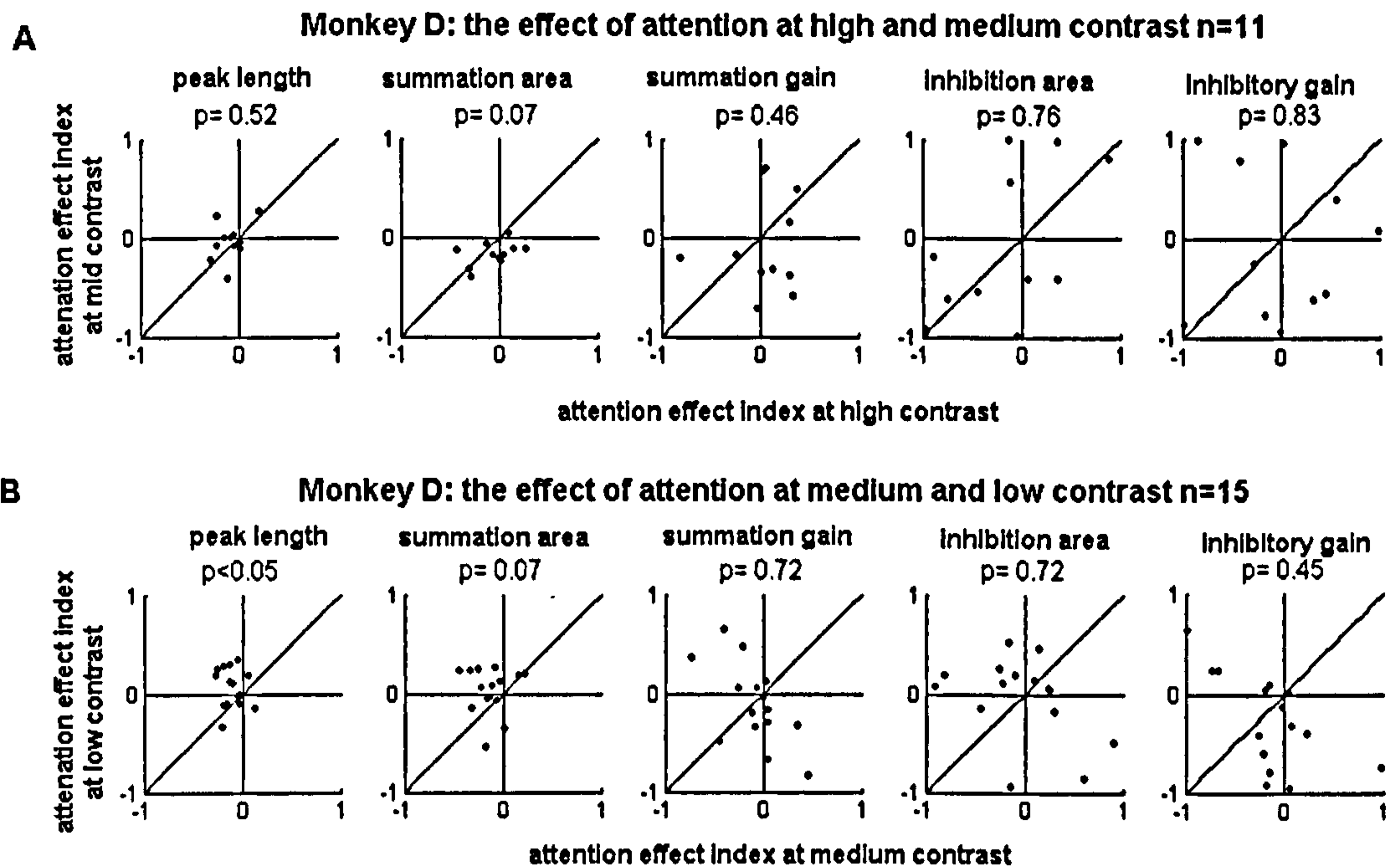


Figure 3.39 Comparison of the effect of attention on peak length and DOG fitting parameters at two contrasts in monkey D. Each point shows the attention effect index for each contrast (see axis labels). **A)** Cells recorded using high and medium contrast stimuli. **B)** Cells recorded using medium and low contrast stimuli. The attention effect index is calculated for each parameter as the difference in the parameter between the two attention conditions divided by the sum. The value of the parameter of interest is taken as the median value from the bootstrap procedure. Negative values indicate that the parameter was reduced in the attend-RF condition. For positive values, points above the diagonal indicate that the attention effect index was higher in the lower contrast (mid contrast in A, low contrast in B) condition. For negative values points below the diagonal indicate that the effect was higher in the lower contrast condition.

3.4.6 Results summary

My main finding is that attention caused a reduction in preferred length for cells with RF eccentricities of $\sim 2^\circ$. For cells with eccentricities of $\sim 7^\circ$ attention caused an increase in preferred length. These effects were evident for stimuli of high and medium contrast but were absent for stimuli with contrasts of less than $\sim 8\%$. Lowering stimulus contrast caused a significant increase in preferred length at both eccentricities. I found an interaction between attention and contrast whereby attention did not affect length tuning at low contrasts.

Attention was also found to increase firing rates. This increase was present from response onset but was generally stronger during the late part of the response. However, I also showed that the temporal profile of response enhancement by attention reflected task demands, since strong attentional enhancement occurred earlier in the response when behaviourally relevant events were likely to occur early

in the trial. Stimulus contrast also affected attentional modulation, with a larger effect of attention for high contrast stimuli than for medium or low contrast stimuli.

3.5 Discussion

In this chapter I investigated the effects of attention on spatial integration in primate primary visual cortex. I found that in the majority of the cell sample, attention caused a shift in the preferred length towards shorter stimuli. This shift reflects a reduction in spatial integration, demonstrating a reduced influence from the nCRF. Fitting a difference of Gaussians (DOG) model to the data suggested that the reduction in preferred length was mediated by a reduction of the summation area. Inhibitory interactions were not significantly affected by attention. These effects match the main findings from my experiments investigating the effects of external acetylcholine (ACh) application on length tuning, as presented in Chapter 2. Thus, the current findings support the central hypothesis of the study: that attention affects the spatial properties of V1 neurons in a similar manner to the application of ACh. The reduced nCRF influence suggests a neural substrate for my psychophysical findings from Chapter 1. Taken together, all these findings support the hypothesis that attention reduces contextual modulation in visual processing, possibly through the action of ACh.

3.5.1 Potential confounds with task difficulty

Length and contrasts of the test stimulus influenced the monkey's RT and performance. The percentage of correct responses was lower and RT was slower when the test stimulus was presented at high contrast than when it was presented at medium or low contrasts. This indicates greater task demands in the high contrast condition. I also found that the monkey's RT was slowest for the shortest bar length. This indicates that the task was hardest for the shortest bar lengths. Greater task difficulty may be expected to lead to greater attentional modulation (Spitzer et al. 1988; Seidemann and Newsome 1999). It could therefore be argued that the differences in the strength of attentional modulation observed across stimulus length and contrast were due to differences in task difficulty rather than to stimulus features *per se*. This argument fails to account for the shift in length tuning observed in the $\sim 7^\circ$ eccentricity sample. Here the RT was highest for the shortest bar length, as in the $\sim 2^\circ$ eccentricity sample; however, attention caused the greatest enhancement in the

responses to longer bar lengths. Moreover, although I found that the effect of bar length on RT was significantly reduced from high to medium contrasts, there was no significant difference in the reduction of preferred length with attention. Thus the pattern of attentional modulation across bar length was not directly related to the changes in RT across bar length. It cannot therefore be argued that the effects of attention on length tuning I observed are simply the result of changes in task difficulty between bar lengths.

It is more difficult to argue against the idea that a reduction in task demands was the cause of smaller attentional modulation in responses to lower contrast stimuli. In many ways, this argument is more compelling than the previous argument that changing task demands could explain the effects on length tuning: different bar lengths were randomly interleaved on a trial-by-trial basis, whilst contrasts were grouped into blocks. It is therefore more likely that the monkeys might switch between high and low effort strategies between contrast blocks than switch between bar lengths on a trial-by-trial basis, as this would require high frequency, unpredictable switching. Because of the potential confound of changing task demands between contrast conditions I do not make strong claims about how contrast affects the degree of attentional modulation. It is clear, however, that a simple contrast gain mechanism for attentional enhancement as suggested by some authors (Reynolds et al. 2000; Reynolds and Desimone 2003) does not account for my findings, since the contrast gain model predicts no enhancement when high contrast stimuli are attended (Reynolds and Desimone 2003; Huang and Dobkins 2005), whilst I find substantial enhancement for high contrast stimuli.

When I have presented this work at conferences (Roberts and Thiele 2004), it has sometimes been suggested that the reduction in preferred length with attention is more likely to reflect the nature of the monkey's task, rather than a general attentional effect. It was argued that since the monkeys were required to detect a small target presented at the centre of the test stimulus, it made sense that neurons integrated over a smaller area in the attend-RF condition. This argument is based on the idea that it would be advantageous to exclude the background in order to solve the task. The argument is contradictory to the behavioural data where I find the fastest RTs for the longest bar lengths, indicating that the background (the test stimulus) *aids* the detection of the target. It seems therefore that it would not be advantageous to exclude the background to solve the task. Given this it seems that by

reducing the impact of the surround, attention actually reduces the ability of neurons to detect the target. This suggestion is in line with a study by Yeshurun and Carrasco (1998). They reported that attention could reduce as well as improve performance in a texture segregation task, according to whether or not the increased spatial resolution associated with attention was advantageous for solving the task. Thus, some effects of attention are not necessarily task dependent, but may occur even in situations where they are disadvantageous. My finding for reduced spatial integration may be one example of this.

3.5.2 Attention and neuronal tuning functions

A number of reports have demonstrated that attention does not alter neuronal tuning functions (McAdams and Maunsell 1999; Treue and Martinez-Trujillo 1999; Talgar et al. 2003). My finding that length tuning is altered by attention is at odds with these reports, but tuning to stimulus length may be a special case. This is reflected by the fact that length tuning is influenced by stimulus contrast, as demonstrated here and by others (Sceniak et al. 1999; Cavanaugh et al. 2002), whilst many other forms of tuning are contrast invariant (Hammett et al. 2003; Alitto and Usrey 2004); but see (Sceniak et al. 2002; Pack et al. 2005). Cortical neuronal tuning arises through a combination of feed-forward and lateral processes (Grinvald et al. 1994; Douglas et al. 1995; Ferster et al. 1996; Angelucci et al. 2002; Crook et al. 2002; Shapley et al. 2003). As stimulus length is varied, the extent of the cortical network stimulated by it changes. Thus, the relative contribution of the feed-forward and lateral/feed-back connections varies with stimulus length. Lowering stimulus contrast reduces the strength of the feed-forward input and increases pooling among cortical neurons (Lund et al. 2003). Thus, at low contrast the influence of the CRF is reduced whilst the influence of the nCRF is enhanced, causing a shift in preferred length towards longer bars.

I suggest that attention causes a facilitation of feed-forward inputs and a suppression of feedback/lateral connections. Because the relative importance of feed-forward and feedback/lateral inputs changes with stimulus length, the influence of attention also varies with stimulus length. Small stimuli presented in the CRF of a cell elicit mostly feed-forward inputs to that cell; thus, the response to small stimuli is boosted by attention. Large stimuli elicit both feed-forward and lateral inputs. In cases where the lateral input is facilitatory, attention will suppress this facilitation.

The overall response to large stimuli may still be boosted by attention due to enhancement of the feed-forward input; however, this enhancement will be weaker than the enhancement of responses generated by purely feed-forward mechanisms, because of the reduction in nCRF facilitation. If the lateral input is inhibitory, attention could relieve this inhibition. Thus, responses to large stimuli might be enhanced by attention more strongly than responses to short stimuli because of a combination of enhanced feed-forward input with reduced surround suppression. In this way, length tuning is altered by attention irrespective of whether the lateral input is facilitatory or suppressive.

3.5.3 Retinal eccentricity

I found that the effect of attention on length tuning was dependent on retinal eccentricity. Attention caused a reduction in preferred length in the majority of the sample of cells when the RF eccentricity was $\sim 2^\circ$. Attention caused an increase in preferred length in a subset of the sample when the RF eccentricity was $\sim 7^\circ$. The discrepancy between the $\sim 2^\circ$ and $\sim 7^\circ$ eccentricity samples may be explained by differences in centre/surround interactions across eccentricity. A number of recent studies have reported that facilitation from the nCRF is strongest in, or even restricted to, regions of visual space at or near the fovea, whilst nCRF suppression is strongest in the periphery (Xing and Heeger 2000; Petrov et al. 2004; Petrov et al. 2005). In line with these findings, I found that the summation area and summation gain tended to be somewhat smaller in the $\sim 7^\circ$ than in the $\sim 2^\circ$ eccentricity sample (although the differences did not reach significance). This tendency indicates that, because CRFs in the $\sim 7^\circ$ eccentricity sample were significantly larger than in the $\sim 2^\circ$ eccentricity sample, the proportion of the summation area accounted for by the facilitatory zone of the nCRF was considerably smaller in the $\sim 7^\circ$ eccentricity sample.

Length tuning arises from a combination of nCRF facilitation and inhibition. Strong nCRF facilitation increases preferred length beyond the CRF boundary, whilst strong nCRF inhibition reduces the preferred length to within the CRF boundary. If attention reduces surround modulation independent of the sign of the modulation (i.e. whether it is facilitatory or inhibitory), as suggested by my psychophysical studies (Chapter 1, Roberts and Thiele 2005), preferred length is expected to be reduced when the nCRF is dominated by facilitation (e.g. near-foveal). However, preferred

length is expected to be increased when the nCRF is dominated by inhibition (e.g. in the periphery). This expected pattern matches my findings, and so the reduction in preferred length in the $\sim 2^\circ$ eccentricity sample and the increase in preferred length in the $\sim 7^\circ$ eccentricity sample during the attend-RF condition are both consistent with attention causing a reduction in CRF modulation.

My finding on the importance of eccentricity has interesting implications for the results of a previous study. Ito et al. (1999) followed up their psychophysical study (1998) with a parallel electrophysiology and psychophysics study, using two alert macaques. In one of the monkeys (monkey SA) they found reduced psychophysical and physiological nCRF facilitation under conditions of focused attention. In the second monkey (monkey UM) they report increased psychophysical and physiological surround facilitation under conditions of focused attention. Reduced facilitation from the nCRF in the focused attention condition would be expected to reduce preferred length, had they used this measure, and so data from monkey SA is compatible with my data from the $\sim 2^\circ$ eccentricity sample. Increased nCRF facilitation in the focused attention would be expected to cause increased preferred length condition, and so data from monkey UM is compatible with my data from the $\sim 7^\circ$ eccentricity sample. The authors suggest that the opposite effects observed between the two monkeys can be explained by differences in the amount of training the two monkeys had received at the time of recording and by differences in the monkey's strategy. However there were also differences in the RF eccentricity between the two monkeys. Monkey SA, whose data were compatible with my $\sim 2^\circ$ eccentricity sample, had RFs with eccentricities in the range of 1.85° to 3.22° . Monkey UM, whose data were compatible with my $\sim 7^\circ$ eccentricity sample, had RFs with eccentricities in the range of 3.68° to 5.25° (personal communication with M. Ito, see Appendix). The difference in eccentricity between the two monkeys is not as large as between my two samples; however, the pattern of focused attention causing reduced integration closer to the fovea but increased integration further towards the periphery matches my finding. My findings suggest that the inconsistency in Ito and Gilbert's data may be explained by differences in eccentricity rather than, or in addition to, differences in training and strategy.

3.5.4 Temporal profile of attentional enhancement

A much-reported aspect of attentional modulation on neuronal responses has been that enhancement tends to be stronger in the late part of the response than in the early part (Motter 1994; Roelfsema et al. 1998; McAdams and Maunsell 1999; Seidemann and Newsome 1999; Reynolds et al. 2000; Roelfsema and Spekreijse 2001; Treue 2001). I have confirmed this finding in the current study; however, I also highlighted the importance of the timing of behaviourally relevant events (the hazard function). In the main experimental task the first behaviourally relevant event (the target brightening) occurred 500msec after stimulus onset. The monkeys could thus be relatively inattentive for the initial part of the stimulus presentation, which may account for the low degree of attentional modulation during this period. To investigate this possibility I altered the hazard function by including trials where the first target could appear after 200msec. In this case the monkey was forced to be attentive from early on in the trial. I found that altering the task in this way caused attentional enhancement to be stronger from earlier on after stimulus onset. Thus, the temporal structure of behaviourally relevant events influenced the temporal profile of response enhancement by attention. Based on these findings it seems possible that many of the studies reporting that attentional enhancement was absent from the early part of the response (Luck et al. 1997; McAdams and Maunsell 1999; Seidemann and Newsome 1999; Treue and Maunsell 1999) may underestimate the importance of the subject's anticipation of the timing of behaviourally relevant events (Ghose and Maunsell 2002).

3.5.5 Potential pharmacological substrate

States of attention are known to be related to the release of ACh into the cortex (Everitt and Robbins 1997; Sarter and Bruno 1997; Sarter et al. 2001). In Chapter 2, I presented a study in which I tested the effect of iontophoretic application of ACh on length tuning among primate V1 cells. I found that the application of ACh caused a significant reduction in preferred length across the population of cells. Since for the majority of cells in the population the preferred length in the absence of applied ACh occurred beyond the CRF boundary, a reduction in preferred length indicated a reduction in nCRF modulation. Fitting the data with a DOG model showed that the reduction in preferred length was mediated principally by a reduction in the summation area. Thus, the effects of ACh application on length

tuning were similar to the effects of voluntary attention in the majority of the cells in the current study.

The temporal profiles of the effect of ACh and the effect of attention were also similar. Response enhancement by attention and by ACh was found to be stronger in the late part of the response than in the early part. This made responses more tonic. I have argued that the temporal profile of the attentional effect is strongly influenced by the monkey's strategy; however, I do not argue that the monkey's strategy entirely controlled the temporal profile. In a recent study Ghose and Maunsell (2002) investigated how the temporal profile of attentional enhancement in area V4 was influenced by changing the hazard function of their experimental task. They report similar findings to my own, that the hazard function was reflected in the attentional effect. However, they also show that the hazard function did not fully predict the attentional profile; instead there were systematic differences. When behaviourally relevant events were most likely to occur at the end of the trial, they nevertheless found significant attentional enhancement of the response early on in the trial. By contrast when behaviourally relevant events were most likely to occur at the beginning of the trial and were unlikely at the end, they found that attentional enhancement lagged behind the hazard function by ~150msec. Moreover, under these conditions they nevertheless found a large degree of attention response enhancement at the end of the trial although behaviourally relevant events were unlikely. The authors interpret their findings as showing that the temporal profile of response enhancement by attention is to some extent fixed to be smaller at response onset than during later parts of the response, independent of task timing or strategy. My findings on the temporal profile of response enhancement by ACh could be the substrate of this fixed element in the temporal profile of response enhancement by attention, although this is a speculative proposal.

The similarities in the effects of ACh application and directing voluntary attention lend support to the hypothesis that ACh is involved in the neuronal processes that mediate attention. An important difference between ACh application and attention was that ACh caused suppression of the response in 37.9% of the cell population whilst attention suppressed the response of only 16.7% of the population (high contrast data). Although the possibility exists that the larger proportion of suppressed cells in the ACh experiments was due to an interaction with anaesthesia, it is almost certain that other mechanisms, such as feedback from higher areas,

mediate attentional effects in addition to ACh. Some of these other mechanisms may act to relieve suppression caused by ACh.

3.6 Conclusions

In this chapter I have demonstrated that directing voluntary visual attention towards the RF of a V1 neuron significantly alters the neurons length tuning. This result is compatible with a reduction in the efficacy of the neuron's nCRF in the attend-RF condition. Thus, attention caused the neuronal response to be more strongly driven by visual stimuli within the CRF and less strongly influenced by surrounding context (the nCRF). Such a reduction in contextual modulation is in line with my findings presented in Chapter 1, in which I demonstrated a reduction in contextual modulation in human orientation perception under conditions of full attention. It seems therefore that one function of attention is to dynamically control the flow of neuronal information, such that the efficacy of information arriving from the senses is boosted relative to information from within the cortex. This is, to my knowledge, the first study to provide a consistent demonstration of such an effect at the level of the primary visual cortex. In a previous study Ito et al. (1999) attempted to characterise the interaction of attention and context in V1, however they were unable to demonstrate consistent effects between their two monkeys. My findings concerning the importance of eccentricity put their results into a new light.

My findings on the effects of visual attention are in good agreement with my findings presented in Chapter 2, concerning the effects of external ACh application. I found that ACh application caused a reduction in the preferred length of V1 cells. This reduction was mediated by a reduction in summation area and an increase in summation gain. These effects match the effects of attention on length tuning in the $\sim 2^\circ$ eccentricity sample reported herein. Furthermore, I found that the temporal profile of the ACh effect on neuronal responses matched the temporal profile of attentional modulation. Attention is known to be associated with the natural release of ACh. The similarities between the effects of attention and the effects of ACh lend support to the hypothesis that ACh is a key pharmacological agent of the neuronal attentional network. In Chapter 4 the importance of cholinergic mechanisms on attentional processes is explored more rigorously, by testing the effect of external application of cholinergic agents on attentional modulation in primary visual cortex.

Chapter 4: The Cholinergic Contribution to Attentional Modulation in Alert Macaque Primary Visual Cortex

4.1 Abstract

States of attention are associated with increased neuronal responses and increased levels of cortical acetylcholine (ACh). To what extent attentional modulation can be attributed to cholinergic mechanisms is unknown, but in the preceding chapters I have demonstrated that both spatial attention and the external application of ACh cause a general increase in neuronal responses and a decrease in contextual modulation in primary visual cortex. The similarity between the effects of ACh and the effects of attention is suggestive that ACh may have a role in mediating attentional modulation. In this chapter I directly investigate the importance of cholinergic transmission on attentional modulation in V1, by assessing the effect of scopolamine application on the attentional modulation of neuronal responses.

Scopolamine was applied iontophoretically to the recorded cell via a newly-developed recording electrode/iontophoresis pipette, while the monkey was engaged in a task which required attention to be directed either towards or away from the location of the receptive field (RF) of the neuron under study. Stimuli were dark, medium-contrast bars which were of variable length and set to the cell's preferred orientation. Attention generally facilitated neuronal responses whilst scopolamine generally suppressed the response. Moreover, scopolamine reduced the effect of attention in many cells. This effect was significant across the population for short bar lengths (0.4°). The reduction in attentional modulation by cholinergic blockade demonstrates that cholinergic transmission is necessary for full attentional modulation to occur.

To perform these experiments, I needed to develop a recording electrode/iontophoresis pipette that was robust enough to pass through the intact dura yet fine enough to provide adequate recording and iontophoresis properties. During the development of these pipettes I tested the effect of ACh application on the contrast response functions of V1 cells and the effect of ACh application on attentional modulation.

4.2 Introduction

In previous chapters I have demonstrated that attention reduces contextual processing in vision, both at the level of perception (Chapter 1) and at the level of single neurons in primary visual cortex (Chapter 3). I have also demonstrated that contextual processing is reduced by external application of the neuromodulator acetylcholine (ACh, Chapter 2). The natural release of cortical ACh is strongly linked with states of arousal and attention (Blokland 1995; Everitt and Robbins 1997; Sarter and Bruno 1997), thus it seems plausible that the effect of attention on contextual processing is mediated at least in part by cholinergic mechanisms. However, the similarity between the effects of attention and the effects of ACh does not provide a conclusive demonstration of the role of cholinergic mechanisms in attentional function. To test this hypothesis it is necessary to manipulate cholinergic transmission in a behaving monkey, whilst also measuring the effect of attention on neuronal processing. If blocking local cholinergic transmission reduces or eliminates the effect of attention, it would be a clear demonstration that cholinergic transmission is necessary for the attentional modulation of neuronal responses. The goal of the work presented in this chapter is to test this proposal.

Cholinergic transmission was manipulated using iontophoretic application of cholinergic drugs (ACh and scopolamine) via a combined recording electrode and iontophoresis pipette. I used a similar approach in the marmoset experiments presented in Chapter 2; however in the anaesthetised preparation it is possible to open the dura to gain direct access to the cortex. In the behaving monkey it is undesirable to remove the dura, therefore I had to develop a recording electrode/iontophoresis pipette combination strong enough to pass through the intact dura yet fine enough to give adequate recording and iontophoresis properties.

In this chapter I describe the development of these methods, and present preliminary data from one monkey in which attentional modulation of neuronal responses was successfully recorded, under control conditions and under conditions where cholinergic transmission was manipulated by the application of either scopolamine or ACh. The first experiments I describe were performed during the development of the recording electrode/iontophoresis pipette combination. In these experiments I recorded the contrast tuning of V1 cells in an alert, passively fixating monkey under conditions of applied and not applied ACh. Since the data acquisition

in this paradigm was relatively straightforward (no attentional manipulation) I was able to concentrate on the development of the recording electrode/iontophoresis pipette combination. Moreover, I was already experienced in testing for the effects of ACh application on V1 neuronal responses (Chapter 2), therefore it was straightforward to test whether or not the drug application had worked. The effect of ACh on contrast tuning is in itself an interesting question, and I present findings from a small population of cells.

Once the method for iontophoretic drug application in the alert monkey had been established, I started experiments in which I measured the effect of attention on neuronal responses under control conditions and under conditions of ACh application. These experiments allowed me to test the hypothesis that the application of ACh in the absence of attention would mimic the effect of attention. In the final set of experiments discussed in this chapter I measured the effect of attention under control conditions and under conditions of scopolamine application. These experiments allowed me to test the hypothesis that attentional modulation would be blocked by the application of a cholinergic antagonist. This is a currently ongoing project, and I present the data acquired so far.

4.3 Methods

I recorded V1 neuronal activity from one macaque; this monkey was also used in the experiments described in Chapter 3. Details of the surgical preparation and training of the monkey (monkey B) are given in Chapter 3. All experiments were carried out in accordance with the European Communities Council Directive 1986 (86/609/EEC), the National Institutes of Health *Guidelines for the Care and Use of Animals for Experimental Procedures*, the Society for Neuroscience *Policies on the Use of Animals and Humans in Neuroscience Research*, and the UK Animals Scientific Procedures Act.

4.3.1 Electrode/pipette manufacture

The electrode/pipette combinations were made using tungsten wires (0.125mm diameter, Advent Research Materials), which were sharpened in etching solution (172.5g NaNO₂, 85g KOH, 375ml distilled water) and glued into one barrel of a 120mm three-barrel glass pipette (custom made, Hilgenberg-GmbH glass, Germany). I tried a number of different types of three-barrel pipette and found that the best type

was made from borosilicate glass and had the three barrels (capillaries) arranged in a row (Figure 4.1), where the flanking capillaries had a different outer and inner diameter than the central capillary (flanking capillaries: outer diameter (OD) 0.545 +/- 0.1mm, inner diameter (ID) 0.273 +/- 0.1mm; central capillary: OD 1.0 +/- 0.1mm, ID 0.6 +/- 0.1mm). The flanking capillaries, which were used for drug delivery, were each fitted with a filament (diameter 0.05mm) to ensure a fluid bridge across any bubbles of air which might occur in the drug solution held within the pipette. The central barrel was used for the tungsten electrode and was not fitted with a filament. The pipette, with the electrode inside, was pulled using a Narishige pipette puller (Narishige PE-21 puller). After pulling it was usually necessary to grind away excess glass from the tip (Thomas Recording electrode tip grinding machine). On the finished pipette the total tip diameter was ~20 μ m wide by ~5 μ m thick (Figure 4.2). This is comparable with typical tungsten in epoxy electrodes (e.g. Frederick Haer, FHC 2M Ω electrodes). The barrel openings were ~2-5 μ m in diameter. The distance between the pipette opening and the electrode tip was between 20 μ m and 5 μ m. The total width of the pipette increased with distance from the tip. At 500 μ m from the tip the width of the pipette was ~100 μ m.

Pipettes were partially filled with the appropriate drug either by capillary force or were back-filled with the aid of syringes, equipped with filter units (Millex $\text{\textcircled{R}}$ GV, 22 μ m pore diameter, Millipore Corporation), and fine flexible injection canulae (MicroFil 34 AWG, MF34G-5, World Precision Instruments, Ltd.). Currents were applied to the drug solution by inserting thin wires into the capillaries, whose ends were insulated to avoid contact between the capillaries and/or the recording electrode. These were connected to the iontophoresis unit (Neurophore- BH-2, Medical systems USA). Currents for drug application were typically 10 μ A to 30 μ A. Currents for drug retention was typically -10 μ A.

Illustration of electrode/pipette manufacture

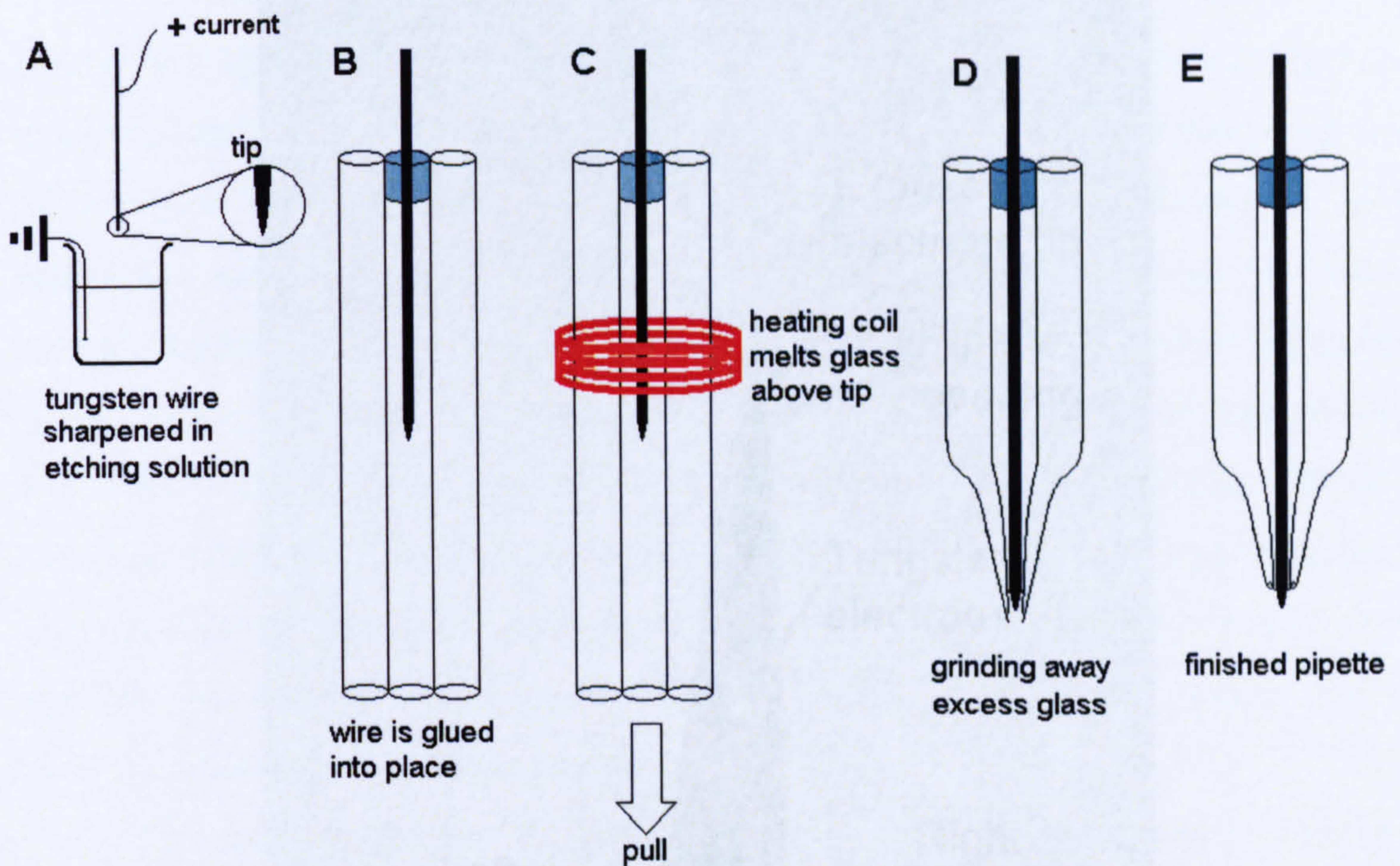


Figure 4.1 Illustration of electrode/pipette manufacture (not to scale). **A)** One end of a tungsten wire is sharpened by repeated dipping into etching solution (172.5g NaNO_2 , 85g KOH, 375ml distilled water) with a current applied (0.4 to 1.2 amps, 6 volts). **B)** The sharpened wire is glued into the central barrel of a three-barrel pipette. Enough wire is left exposed at the top to connect the pre-amplifier during recording. **C)** Once the glue is set the pipette is placed into the puller such that the heating element is 4-7mm above the tip of the electrode. As the pipette is pulled, melted glass coats the electrode tip. The lower half of the pipette breaks off at or just below the electrode tip. **D)** If the pipette breaks off below the electrode tip, excess glass is ground away. **E)** Barrel openings on the finished pipette are just behind the electrode tip.

Photograph of a typical electrode/pipette tip

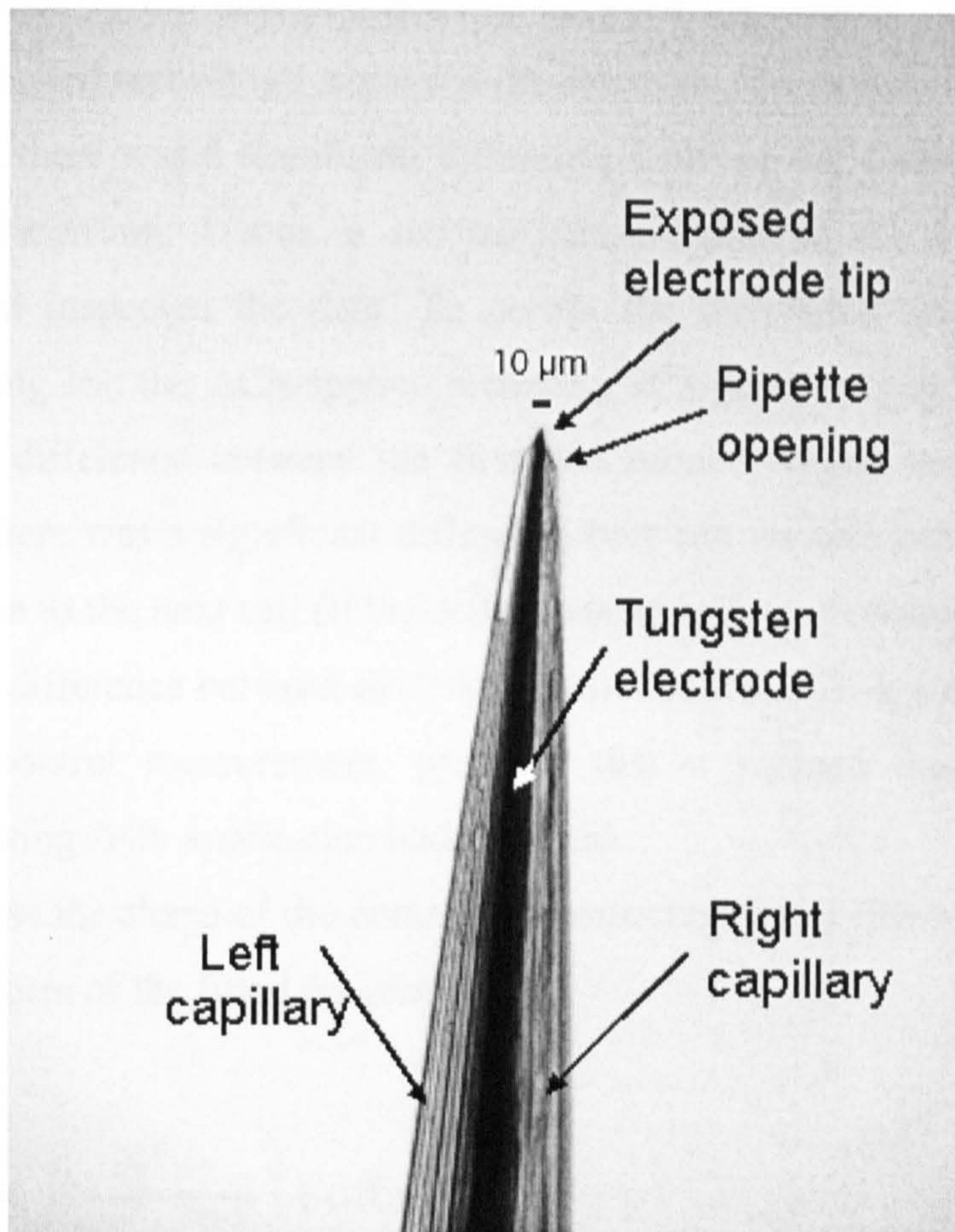


Figure 4.2 Photograph of the tip of a typical electrode/pipette. The central black region is the tungsten electrode coated in glass from the central glass barrel. On the left and right of the electrode are the two pipette barrels used for drug delivery. The openings of the pipette have been ground to produce a sharp profile at the tip. The electrode tip extends $<10\mu\text{m}$ beyond the end of the glass.

4.3.2 Contrast response measurement during passive viewing

Neuronal contrast response functions were mapped using eight bars (0.4° long, 0.1° wide) of varying contrast. The monkey's task was to fixate for 2000msec within a window of $\pm 0.5^\circ$ on a red dot (0.1°) presented in the centre of the screen. During each trial, four separate stimuli were presented at the location of the RF of the neuron under study. Stimuli were dark bars (0.1° wide, 0.4° long) set to the preferred orientation of the cell, with contrasts selected randomly from 8 possible contrasts (100%, 70.2%, 49.5%, 39.5%, 29.4%, 18.5%, 9% and 5.3%). Each stimulus was presented for 400msec, with a 400msec inter-stimulus interval. Each stimulus was presented 20 times during each full recording.

During each experiment I took a control recording (no ACh application) followed by a drug recording (ACh application) and then inspected the data. If there was no difference between the control recording and the ACh-applied recording, I

increased the drug application current and repeated the measurement. If there was still no difference in the neuronal activity between the control recording and the second ACh-applied recording I advanced the electrode to a new cell. If, as was more often the case, there was a significant difference between the control recording and ACh-applied recording, I took a second measurement in the absence of ACh application and inspected the data. To accept the difference between the initial control recording and the ACh-applied recording as a genuine drug effect I required no significant difference between the first and second control recordings (2-way ANOVA). If there was a significant difference between the two control recordings I either moved on to the next cell (if the difference between the control recordings was larger than the difference between the first control and the ACh-applied recording) or repeated the control measurement, provided that it seemed that only a partial recovery following ACh application had occurred.

To assess the shape of the contrast response function I fitted a Naka-Rushton function. The form of the fitted function was:

$$Y = \left(R_{\max} \times \frac{X^n}{C50^n + X^n} \right) + \text{offset} \quad (\text{Equation 4.1})$$

where 'Y' is the model's predicted response to a stimulus of contrast 'X'. 'Rmax' is the maximum response, 'C50' is the contrast which produces a response equal to 50% of the difference between 'Rmax' and the spontaneous activity 'offset'. The slope of the curve is given by the exponent 'n'. The four free parameters, 'Rmax', 'C50', 'offset' and 'n' were optimised by minimising the summed squared error between the model's predicted response 'Y' and the recorded response rate. To take the variance of the data into account I used a bootstrap method for fitting, as described in Chapter 2. I assessed the goodness of fit by calculating the percentage of variance accounted for, as described in Chapters 2 and 3.

4.3.3 The interaction of attention, drug application and stimulus length

The effect of attention on neuronal responses was assessed using the same method as described in Chapter 3. Briefly, test stimuli were dark bars of varying length. One bar was presented at the location of the RF of the neuron under study and a second identical bar was presented in the opposite hemifield. The contrast of the

bars was set to a value predicted to produce a response significantly below the response to a 100% contrast stimulus. The range of contrasts used in the ACh experiments was between 18% and 70%; for most cells the stimuli had 20% contrast. In the scopolamine experiments, 12 cells were recorded using stimuli of 20% contrast and 15 cells were recorded using stimuli of 18% contrast. Due to the already intensive recording protocol, I did not record contrast tuning functions for each cell. Instead I used a range of low to medium contrasts, which are generally below the saturation point of cells in primary visual cortex. In the ACh experiments and early scopolamine experiments I used six bar lengths (0.1°, 0.2°, 0.4°, 0.8°, 1.6° and 2.4°). In order to increase the number of trials recorded for each data point, in later scopolamine experiments I reduced the number of bar lengths to four (0.2°, 0.4°, 1.6° and 2.4°).

The monkey's task was to detect an increase in luminance at the centre of the bar presented at the cued location ('target brightening'), and to ignore changes that occurred at the un-cued location ('distracter brightening'). A brightening could occur at 500msec or 1500msec after the presentation of the test stimuli. The monkey reported the occurrence of a brightening in the cued location by releasing a touch bar. Attention was manipulated by cueing the monkey to respond to a brightening that occurred either at the location of the RF of the neuron under study (attend-RF condition) or in the opposite hemifield (attend-away condition).

For both the ACh and scopolamine experiments I recorded from cells in two recording locations in area V1. RF eccentricity was different at the two locations. In the ACh experiments I recorded from four cells where the RF eccentricity was ~2° and from five cells where the RF eccentricity was ~7°. In the scopolamine experiment I recorded from 14 cells where the RF eccentricity was ~2° and from 13 cells where the RF eccentricity was ~7°.

I recorded the effect of attention on neuronal responses in the presence and absence of applied ACh or applied scopolamine. In my early ACh recording I recorded 20 trials per bar length in both attention conditions (attend-RF and attend-away) in the absence of ACh, followed by 20 trials per bar length in both attention conditions during ACh application, followed by a final recording of 20 trials per bar length for both attention conditions in the absence of ACh. This regime had the disadvantage that often I was unable to complete the recovery measurement, either because the monkey stopped working or because the recorded activity changed due

to cell drift. A recovery measurement is vital, because without it it is impossible to distinguish drug effects from changes in activity due to cell drift. To reduce these problems I changed the regime such that I recorded eight trials per bar length under control and drug-applied conditions. Under this regime I was normally able to record several cycles of control measurements followed by drug-applied measurements. To be included for further analysis I required that there were at least two comparable recordings (i.e. either two control recordings or two drug-applied recordings) where the activity showed a trend for recovery following either a drug application recording (where two control recordings had been made) or a control recording (where two drug-applied recordings had been made).

In order to avoid frustrating the monkey I did not leave a time break between drug measurements and no-drug measurements (as I had done in the anaesthetised experiments presented in Chapter 2), instead I excluded from my data analysis the first two trials per bar length from each measurement. This ensured that only the full drug effect/full recovery occurred in the analysed data.

4.3.4 Data analysis

I tested for significant effects of attention and drug application using a 3-way ANOVA, where the factors were attended location, drug application and bar length. Only cells that showed either a significant effect of attention and drug application or a significant interaction between drug application and attention were included for further analysis. I have previously shown that the effects of attention and the effects of ACh application on firing rates are largest during the late part of the response (225-500msec, see Chapters 2 and 3); hence for individual cell analysis I only examined responses during this late period to test for the significance of effects.

I used receiver operating characteristic (ROC) analysis to assess the magnitude of attentional modulation in the presence and absence of drug application. I also used the ROC to assess the magnitude of the effect of drug application on neuronal responses in the attend-RF and attend-away conditions. Details of how ROC values are calculated are given in Chapter 3. To assess how the effects of drug application and attention changed over time, I performed this analysis separately over the early and late response periods (early period: 50-225msec post stimulus onset, late period: 225-500msec post stimulus onset) and over the full response period (50-500msec after stimulus onset).

4.4 Results

4.4.1 ACh application influences contrast response functions

I ran this experiment on 28 recording days. In this time I recorded from seven cells which showed a significant effect of ACh application on firing rate (2-way ANOVA) and a return to baseline following drug application. Of these cells, five showed response enhancement at all contrasts during ACh application, one cell (cell pen118, see Figure 4.3) showed response suppression at all contrasts and one (cell pen117) showed facilitation at high contrasts and suppression at low contrasts. Figure 4.3 shows the contrast response function of these seven cells in the presence and absence of applied ACh.

I quantified how ACh altered the shape of contrast response functions by fitting the data with a Naka-Rushton function (Equation 4.1). This function gave good fits to the data, accounting for >97% of the variance (median = 98.3%). The effect of ACh application on Naka-Rushton fitting parameters is shown in Figure 4.4. I used Fishers exact statistic (Fearon 2003) to assess the significance of differences in fitting parameters across the population. This method is appropriate for small sample sizes. Across the population ACh had no significant effect on any of the fitting parameters. It is likely that more data are needed for a trend to emerge.

The effect of ACh on contrast response functions

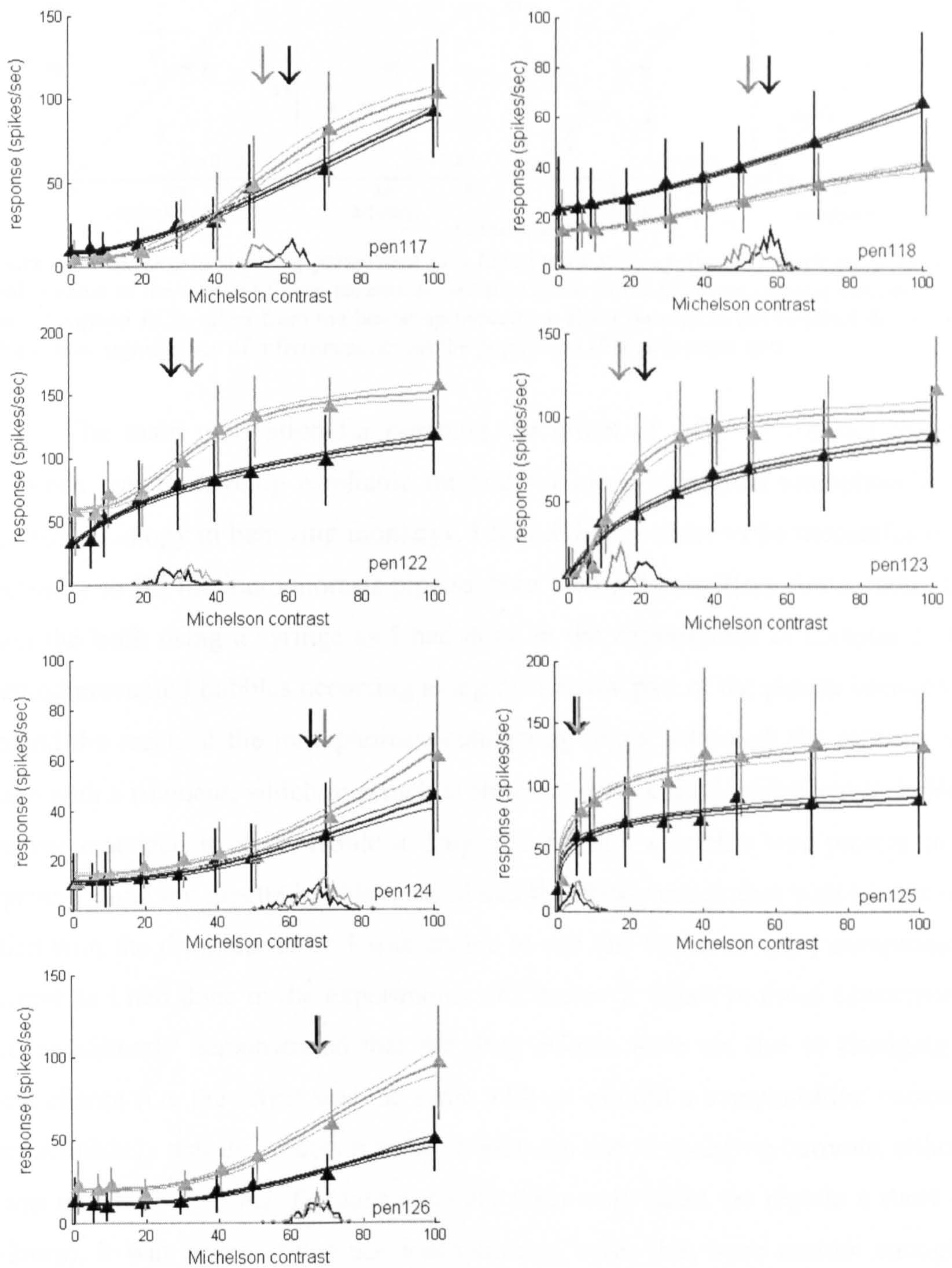


Figure 4.3 The contrast response function of seven cells where ACh application significantly altered firing rate. Triangles show mean response at each contrast, error bars show standard deviation. Bold line fitted to the data shows the median Naka-Rushton fit from the bootstrap procedure, flanking upper and lower narrow lines show the 75th and 25th percentile fits. Curves at the base of each plot show the distribution of the location of C50 taken from 100 iterations of the bootstrap procedure. The median C50 is marked with the downwards-pointing arrow. Black triangles, lines and arrows show data from the control (no drug application) condition; grey triangles, lines and arrows show data from the ACh-applied condition. Each cell is given a name after the number of the recording penetration. This name is shown at the base of each plot.

The effect of ACh on Naka-Rushton fitting parameters

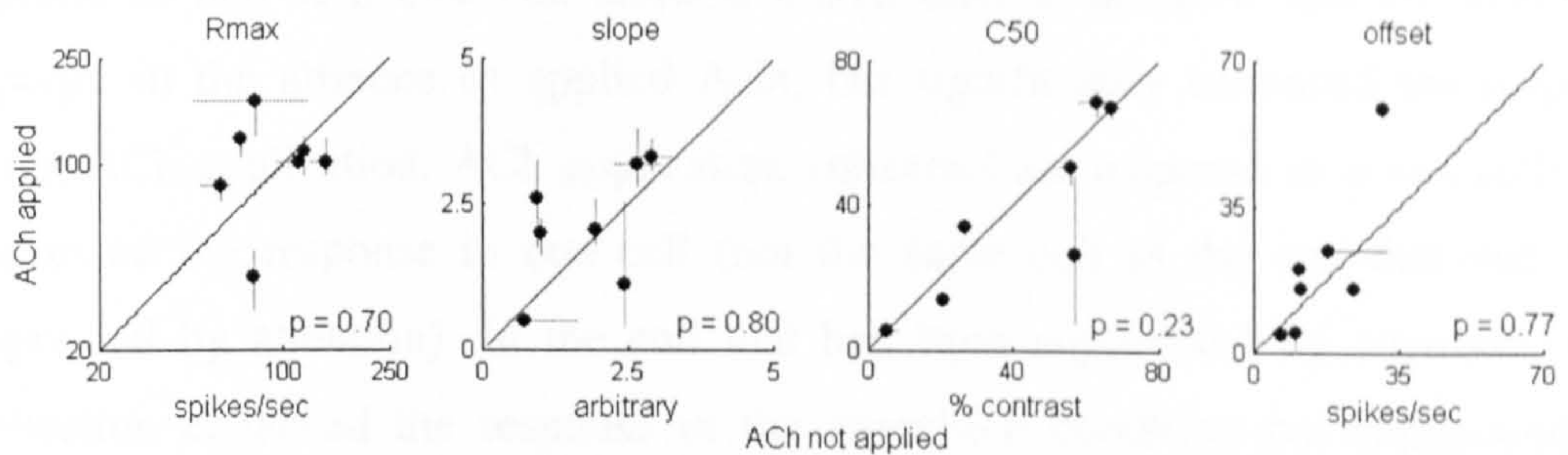


Figure 4.4 Naka-Rushton fitting parameters as a function of ACh application. Each point shows the median value of the relevant fitting parameter (see plot titles) in the presence (y-axis) and absence (x-axis) of applied ACh, taken from the bootstrap procedure. Error bars show the standard deviation. P-values show significance of differences across the population (Fisher's exact test).

The main motivation for pursuing the effect of ACh on contrast response functions was to develop a reliable method for using combined iontophoresis and electrophysiology in behaving monkeys. I found that in order to be successful it was necessary to fill the iontophoresis pipette from the tip by capillary force, rather than from the back using a syringe as I had done in the experiments of Chapter 2. This method prevented bubbles occurring along the narrow part of the pipette between the tip and the reach of the iontophoresis connecting wires. Although the pipettes were fitted with a filament, which in principal should ensure a fluid bridge across bubbles, I never managed to demonstrate a drug effect when a bubble was present in the pipette. Filling the pipette by this method had the disadvantage that both barrels were filled with the drug, therefore I was unable to use one barrel to apply compensation current as I had done in the experiments of Chapter 2. Since in those experiments I had consistently demonstrated that the drug effects were not due to changing the local charge (i.e. the effect was the same with or without a compensation current) it seems unlikely that the effects reported herein are due to changing currents, although I was unable to test this. Because capillary force only filled the pipette a short way (~2mm), it was necessary to use iontophoresis wires that were narrow enough to reach into the thin part of the pipette. These were fitted into the pipette under microscopic guidance.

4.4.2 ACh application reduces attentional modulation

I recorded from nine cells which showed a significant effect of attention and ACh application, or a significant interaction between ACh application and attention

(Table 4.1). Attention enhanced the response in seven cells and suppressed the response in one cell. One cell showed mixed effects; attention did not affect the response in the absence of applied ACh, but significantly enhanced the response during ACh application. ACh application enhanced the response in seven cells and suppressed the response in one cell (not the same cell as the one that had been suppressed by attention). In the cell that had been suppressed by attention, ACh application enhanced the response in the attend-RF condition but suppressed the response in the attend-away condition. Thus, across the population both attention and ACh application generally facilitated neuronal responses.

Factor	n cells where $p < 0.05$
Attention	8
Drug application	9
Bar length	7
Attention x drug	2
Attention x length	2
Drug x length	3
3-way interaction	0

Table 4.1 Numbers of cells in which a significant ($p < 0.05$) amount of variance is accounted for by each factor or by interactions between factors in a 3-way ANOVA.

The effects of attention and of ACh application are demonstrated in Figures 4.5 and 4.6. Figure 4.5 shows the response of one cell to one bar length (0.1°) in the attend-RF and attend-away conditions in the presence and absence of applied ACh. Both attention and ACh application enhanced the response. In the late part of the response, enhancement by ACh was larger in the attend-away conditions (compare data shown in blue with data in black) than in the attend-RF condition (compare data shown in red with data in green). The population histograms (Figure 4.6) indicate that this was typical of the population and also show that attentional modulation was reduced by the application of ACh, especially at short bar lengths.

Example of the effects of attention and of ACh application on neuronal response

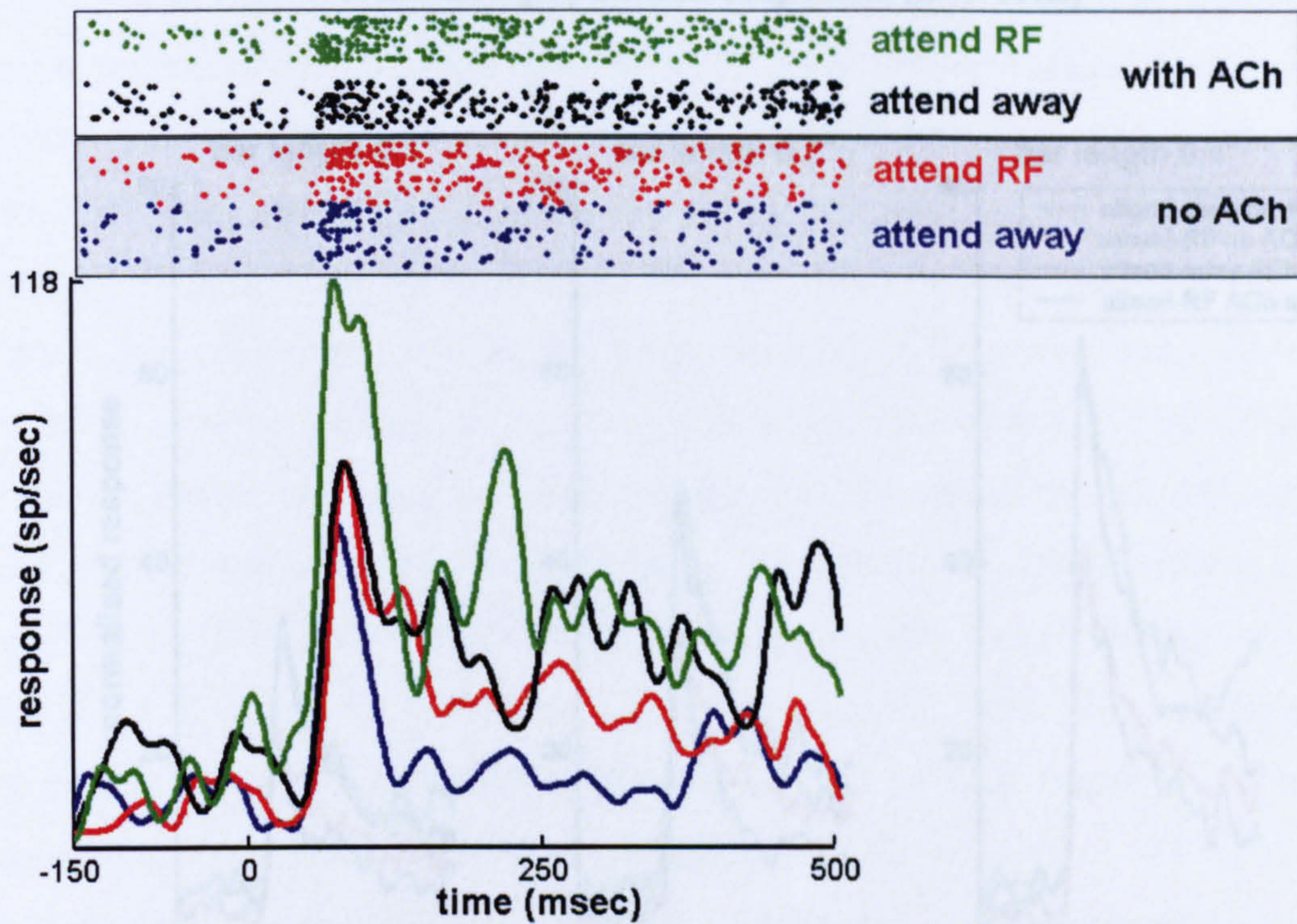


Figure 4.5 Response from one cell to one bar length (0.1°). Response is shown as raster plots and histograms. Data in green shows responses from the attend-RF condition with ACh applied and data in black shows responses in the attend-away condition with ACh applied; data in red shows responses from the attend-RF condition without ACh application and data in blue shows responses from the attend-away condition without ACh application. Time is shown relative to stimulus onset.

Normalised population responses (n=9 cells)

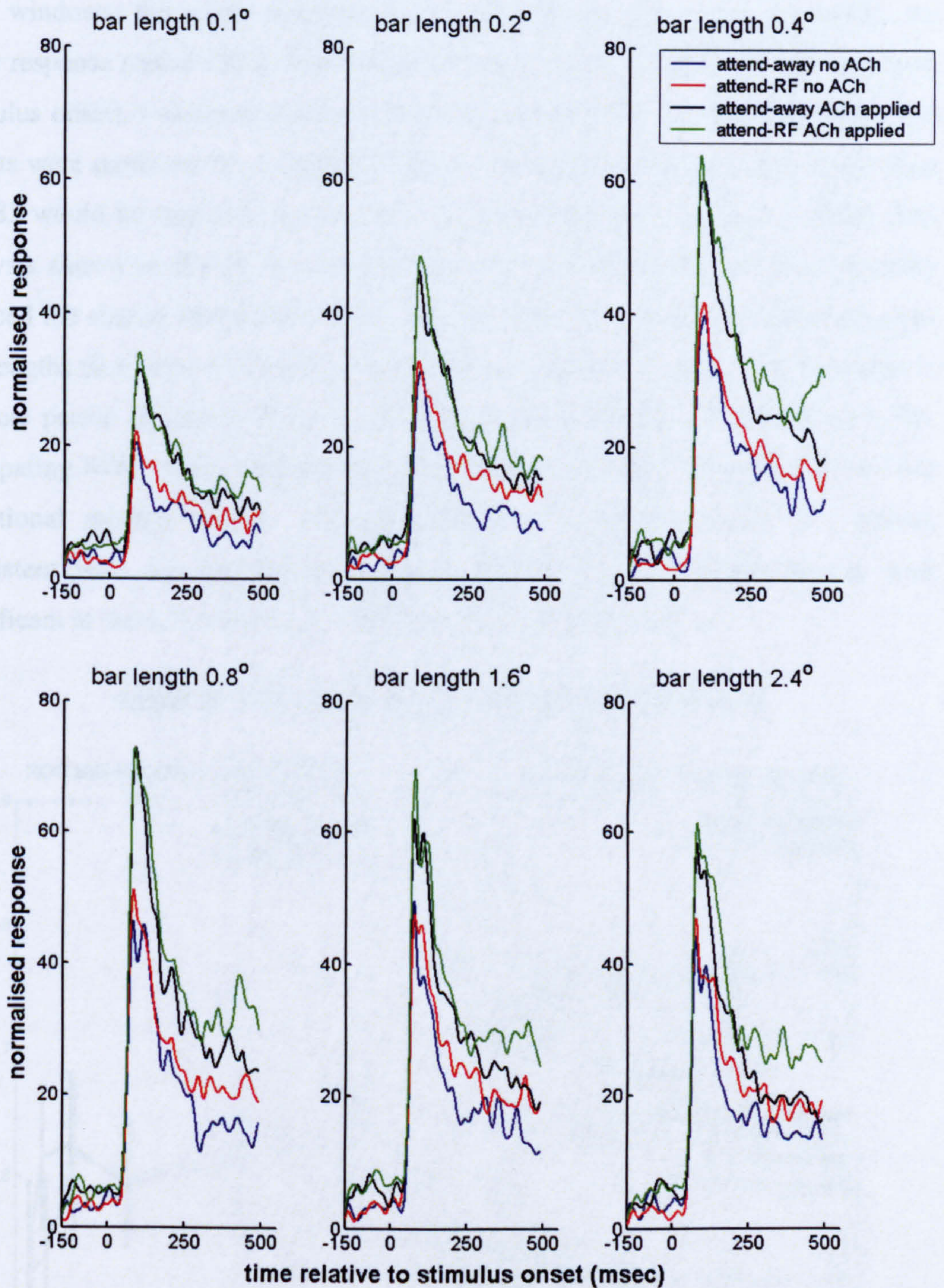


Figure 4.6 Normalised population responses (9 cells) to 6 bar lengths under conditions of attention towards and away from the RF of the cell under study, with and without ACh application (legend). Responses from each cell were normalised to the highest response for that cell before being added to the population, thus each cell contributes equally to the mean responses shown here.

To assess the significance of changes in attentional modulation with drug application, I calculated the size of attentional modulation as ROC values in the presence and absence of ACh application. This calculation was performed over three time windows: the whole response period (50-500msec post stimulus onset), the early response period (50-225msec) and the late response period (225-500msec post stimulus onset). I assessed significance using a paired t-test at each bar length. The results were corrected for multiple comparisons, meaning that a p-value of less than 0.0083 would be required to reject the null hypothesis for any one bar length. The analysis shown in Figure 4.7 demonstrates that the application of ACh generally reduced the size of attentional modulation. The effect was most prominent for short bar lengths (0.1° to 0.4°) but did not reach significance. The effect was strongest in the late period (Figure 4.7C) and was absent from the early period (Figure 4.7B). Comparing ROC values between the early and late periods (Figure 4.8) shows that attentional modulation was stronger (higher ROC values) in the late period, consistent with my findings presented in Chapter 3. This difference was only significant at the 0.2° bar length in the absence of ACh application.

Effect of ACh application on attentional modulation

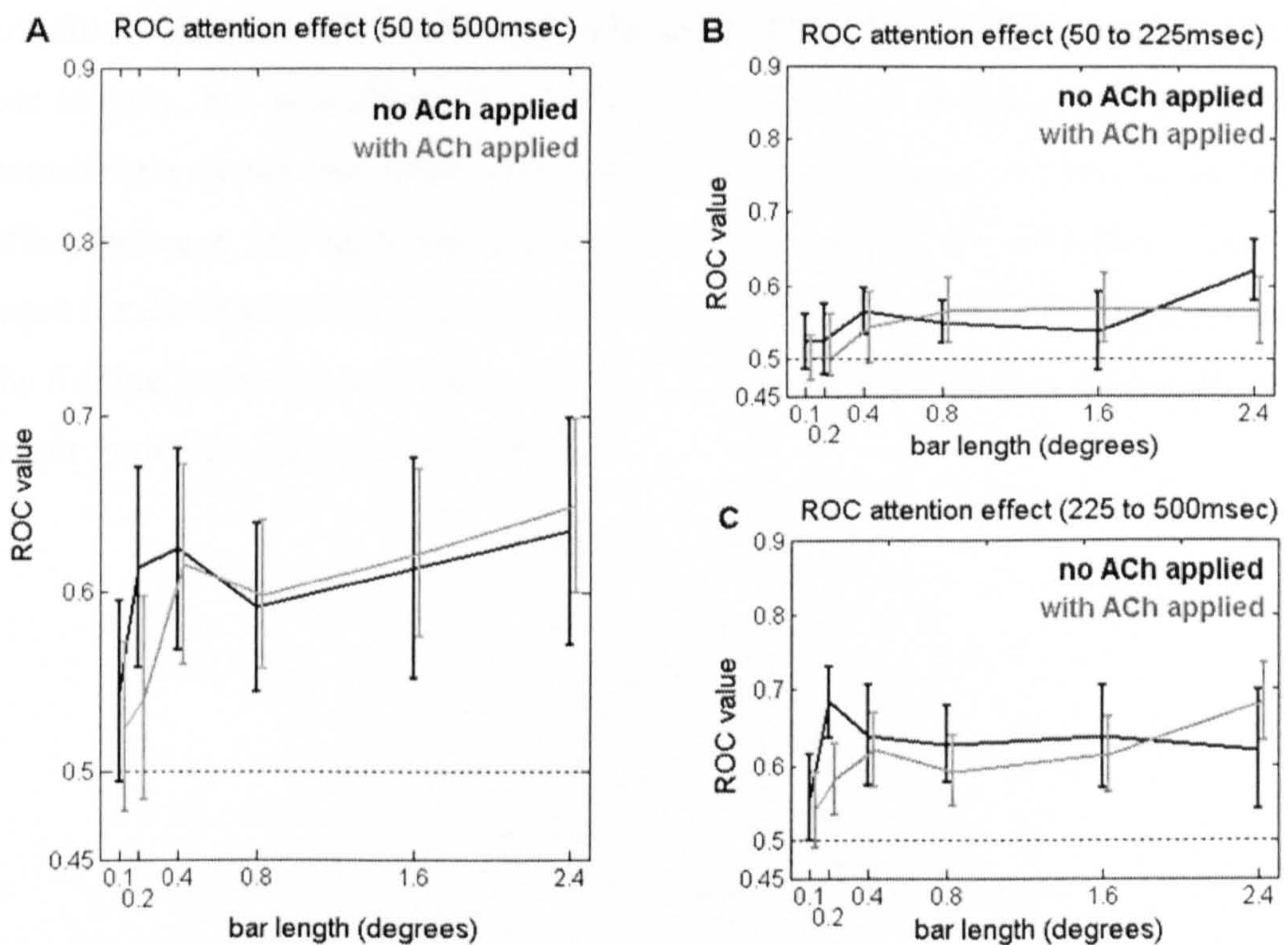


Figure 4.7 Attentional modulation expressed as ROC values as a function of bar length and drug application, during the entire response period (A) and separately for the early (B) and late periods (C) Error bars show standard error. Curves and error bars in black show data with no ACh applied, grey

curves and error bars show data with ACh applied. Differences were not significant ($p > 0.0083$, paired t-test).

Attentional modulation as a function of time and bar length

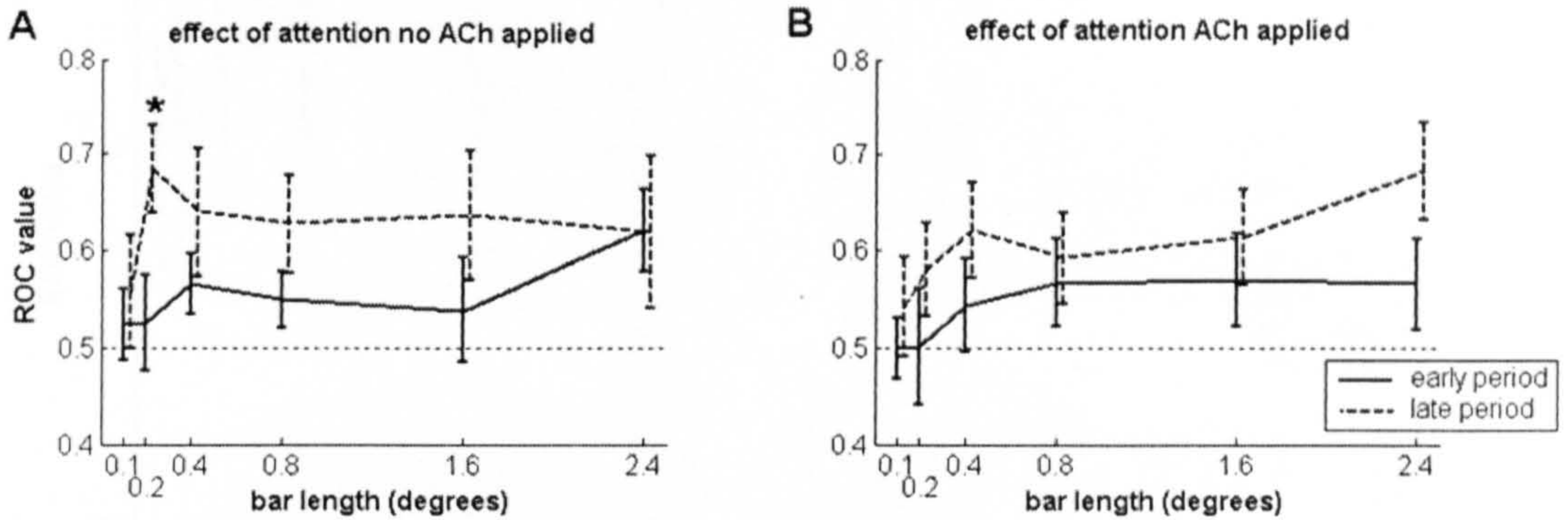


Figure 4.8 Attentional modulation in the early (solid lines) and late (dashed lines) periods expressed as mean ROC values **A**) without ACh applied and **B**) with ACh applied. Error bars show standard error. Asterisks mark significant difference between the time periods ($p < 0.0083$, paired t-test).

To further investigate the interaction between attention and ACh application, I assessed the effect of ACh application on neuronal responses separately in the attend-RF and attend-away conditions (Figure 4.9). Here I found that the effect of ACh application was smaller in the attend-RF condition than in the attend-away condition. This attention-mediated reduction in the effect of ACh was evident at most bar lengths, but was absent for the 0.8° bar length. Comparing the effect of ACh across time shows that there were no significant differences in the size of the ACh effect between the early and the late periods (Figure 4.10); however, there was a trend for the effect of ACh to be smaller in the late period. This finding is contrary to the finding presented in Chapter 2 where I found that the effect of ACh was generally larger in the late part of the response.

The effect of attention on response modulation by ACh

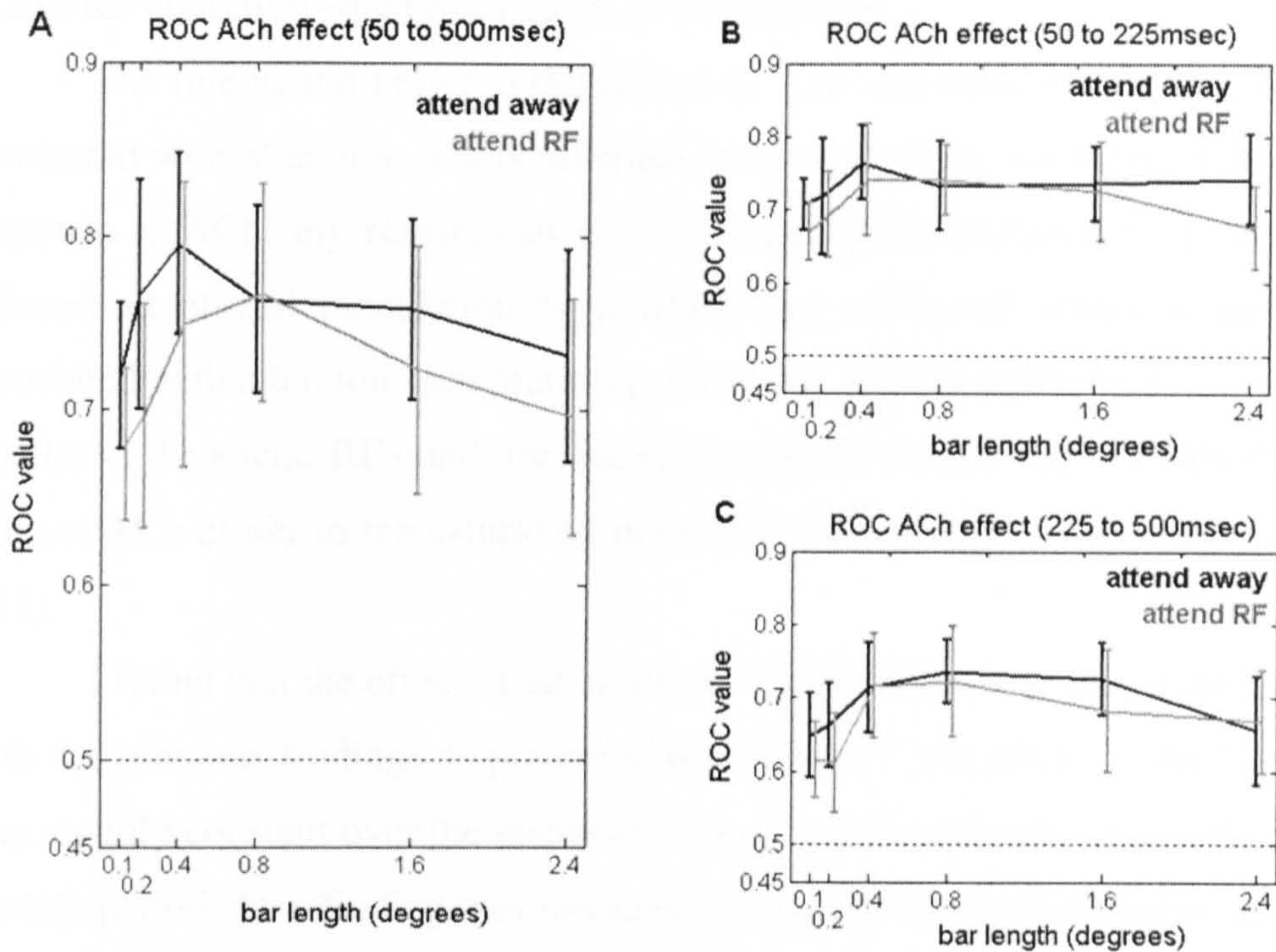


Figure 4.9 Effect of ACh application on neuronal responses expressed as ROC values as a function of bar length and attention condition, for the entire response period (**A**) and separately for the early (**B**) and late (**C**) periods. Error bars show standard error. Curves and error bars in black show data from the attend-away condition, in grey they show data from the attend-RF condition. Differences were not significant ($p > 0.0083$, paired t-test).

The effect of ACh application as a function of time and bar length

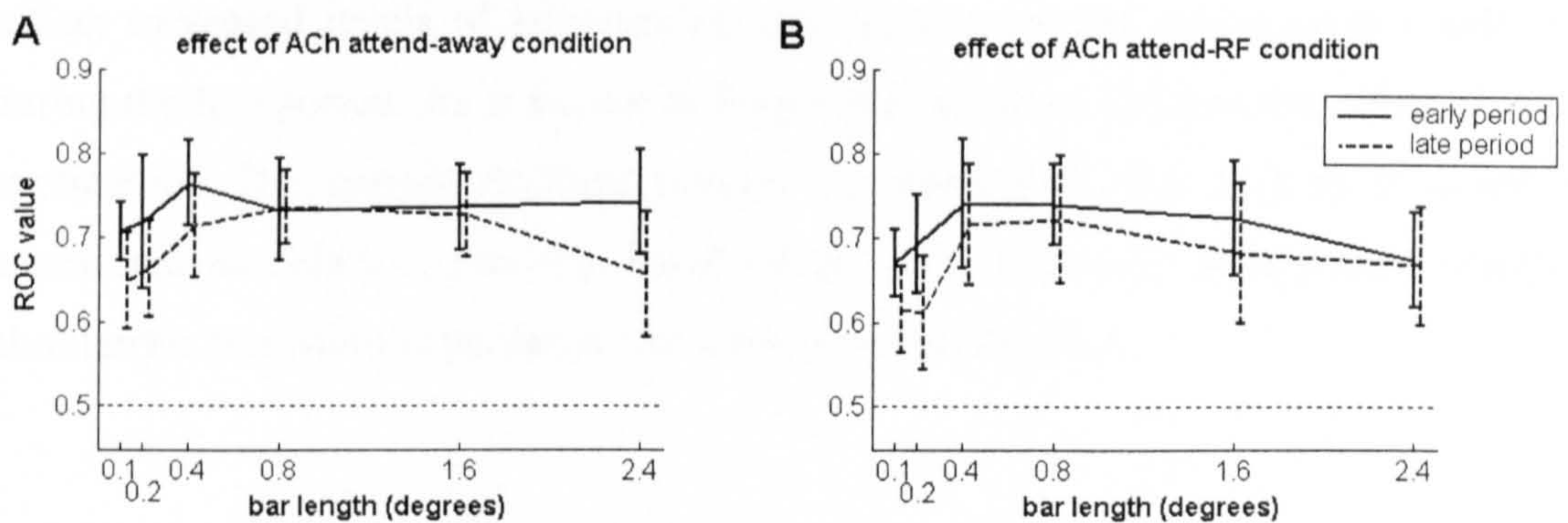


Figure 4.10 The effect of ACh application in the early (solid lines) and late (dashed lines) periods expressed as mean ROC values **A**) in the attend-away condition and **B**) in the attend-RF condition. Error bars show standard error. No differences between the periods were significant ($p > 0.0083$, paired t-test).

To summarise results from this experiment, I found that both attention and ACh application caused a general increase in neuronal responses. Moreover, I found that response enhancement by attention was reduced during ACh application, although this difference was not significant. The reduction in attentional modulation was due to a larger effect of ACh application in the attend-away condition. Thus,

responses in the attend-away condition were more similar to responses from the attend-RF condition when external ACh was applied.

The interaction between the effects of ACh and attention implies that ACh is associated with attention. If it is assumed that there can be saturation in the neuronal response to ACh, my results can be explained by the application of ACh causing reduced attentional modulation by masking any additional naturally-released ACh associated with attention. Alternatively, the effect of ACh application may have been smaller in the attend-RF condition because naturally released ACh raised the level of cortical ACh closer to the saturation point than in the attend-away condition (Figure 4.11).

I found that the effect of attention was larger during the late period, consistent with my previous findings as presented in Chapter 3. The effect of ACh application was roughly constant over the response period, with a tendency for smaller effects in the late period. This finding was inconsistent with my previous findings as presented in Chapter 2. In Chapter 3 I argued that the time course of the attentional modulation largely reflects the temporal profile of behaviourally relevant events (the hazard function), thus the difference in the time course between the effects of ACh application and the effects of attention does not necessarily point to different mechanisms. The somewhat weaker effect of ACh application in the late period may reflect increased levels of attention or arousal, even in the attend-away condition, during the late period. As is shown in Figure 4.9, attention reduces the effect of ACh application. The current findings support the hypothesis that ACh is involved in attentional modulation, however these results do not directly demonstrate whether cholinergic transmission is necessary for attentional modulation.

Possible explanation for the interaction between ACh application and attention

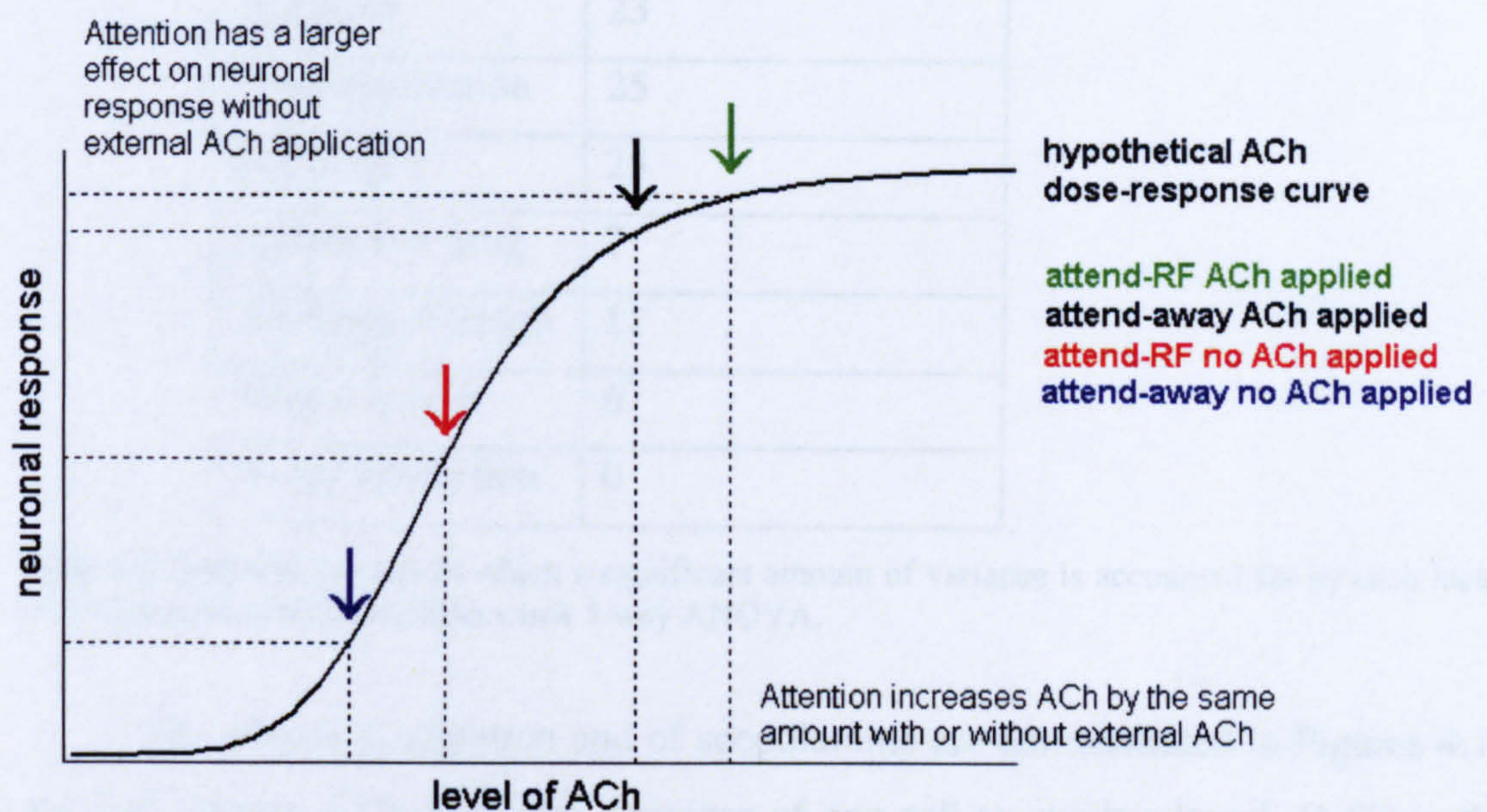


Figure 4.11 Model to explain the interaction between attention and ACh application. The solid black curve shows a hypothetical relationship between the level of cortical ACh and the neuronal response to a given stimulus. Downward-pointing arrows indicate the assumed level of ACh in each of the four experimental conditions (legend). Attention is assumed to increase neuronal responses by causing an increase of ACh. With no external ACh applied the level of ACh is in the steep part of the dose-response curve, thus a set increase in ACh with attention causes a large increase in the neuronal response. External ACh application puts the level of ACh into the shallow saturating part of the dose-response curve, therefore the same increase in ACh with attention causes only a small increase in the neuronal response.

4.4.3 Scopolamine application reduces attentional modulation

I recorded from 27 cells which showed either a significant effect of attention and scopolamine application or a significant interaction between attention and scopolamine application (Table 4.2). Nine of these cells were recorded with six bar lengths, 15 cells were recorded with four bar lengths (0.2° , 0.4° , 1.6° and 2.4°). Attention facilitated the response in 21 cells and suppressed the response in two cells. In two cells, attention facilitated the response in the absence of scopolamine but suppressed the response when scopolamine was applied, and in two other cells attention facilitated the response in the absence of scopolamine and had no significant effect on the response in the presence of scopolamine. Scopolamine suppressed the response of 25 cells and facilitated the response of two cells. The two cells facilitated by scopolamine were not the same two cells that were suppressed by attention. Thus across the population, attention generally enhanced the response, whilst scopolamine generally suppressed the response.

Factor	n cells where p<0.05
Attention	23
Drug application	25
Bar length	25
Attention x drug	7
Attention x length	11
Drug x length	6
3-way interaction	0

Table 4.2 Numbers of cells in which a significant amount of variance is accounted for by each factor or by interactions between factors in a 3-way ANOVA.

The effects of attention and of scopolamine are demonstrated in Figures 4.12 and 4.13. Figure 4.12 shows the response of one cell to one bar length (1.6°) in the attend-RF and attend-away conditions with and without scopolamine application. For this cell there was a large effect of attention in the absence of scopolamine. During scopolamine application, the effect of attention was eliminated. Data in the population histograms (Figure 4.13) suggest that attentional modulation was greatest at short bar lengths (0.1° to 0.8°). At these bar lengths scopolamine application caused the largest reduction in attentional modulation. At bar lengths of 1.6° and larger, there seemed to be no difference in attentional modulation during scopolamine application.

The effect of attention and scopolamine application on neuronal responses

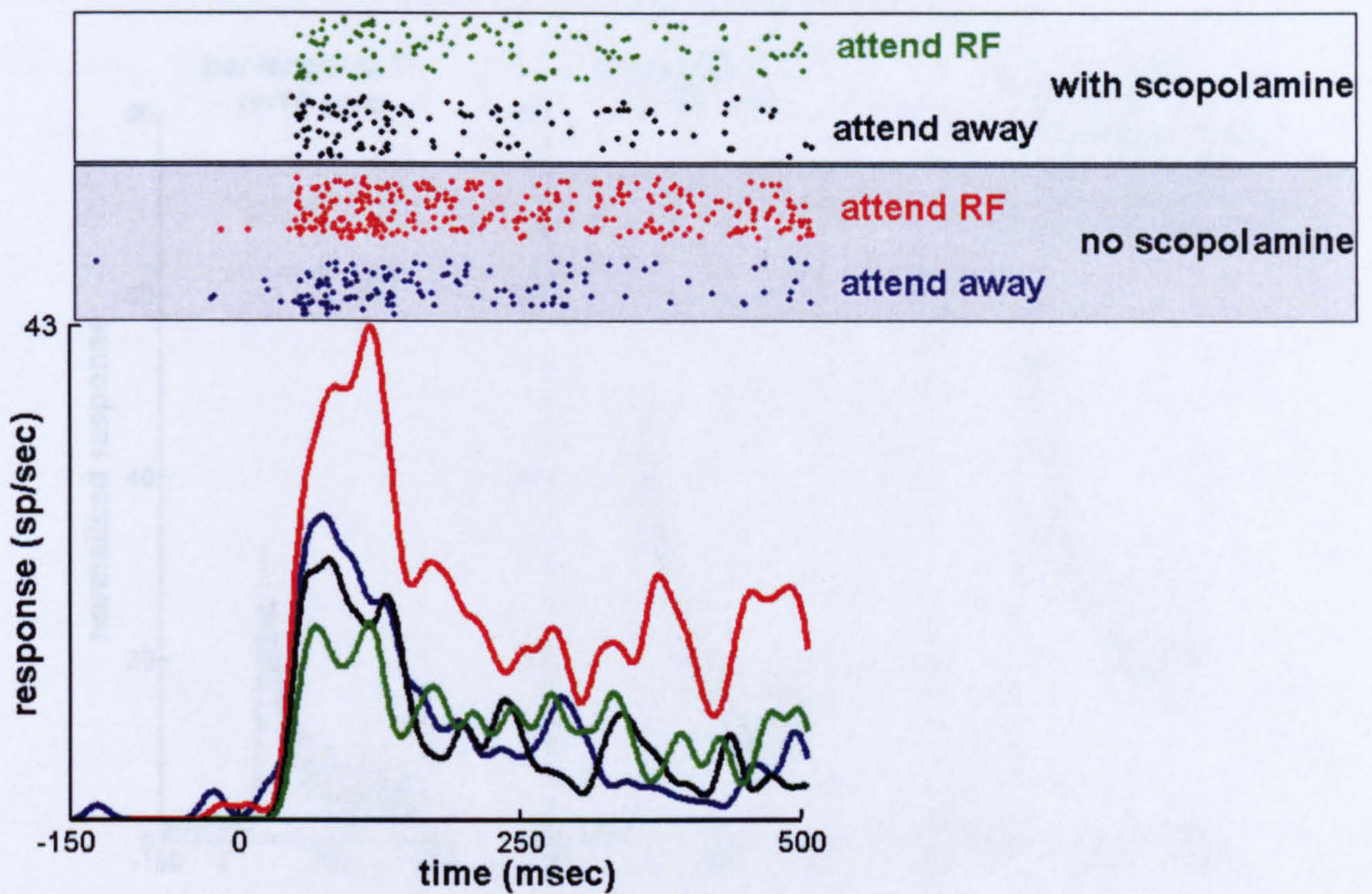


Figure 4.12 The response from one cell to one bar length (1.6°). Response is shown as raster plots and histograms. Data in green shows responses from the attend-RF condition with scopolamine applied and data in black shows responses in the attend-away condition with scopolamine applied; data in red shows responses from the attend RF condition without scopolamine and data in blue shows responses from the attend-away condition without scopolamine. Time is shown relative to stimulus onset.

Normalised population responses

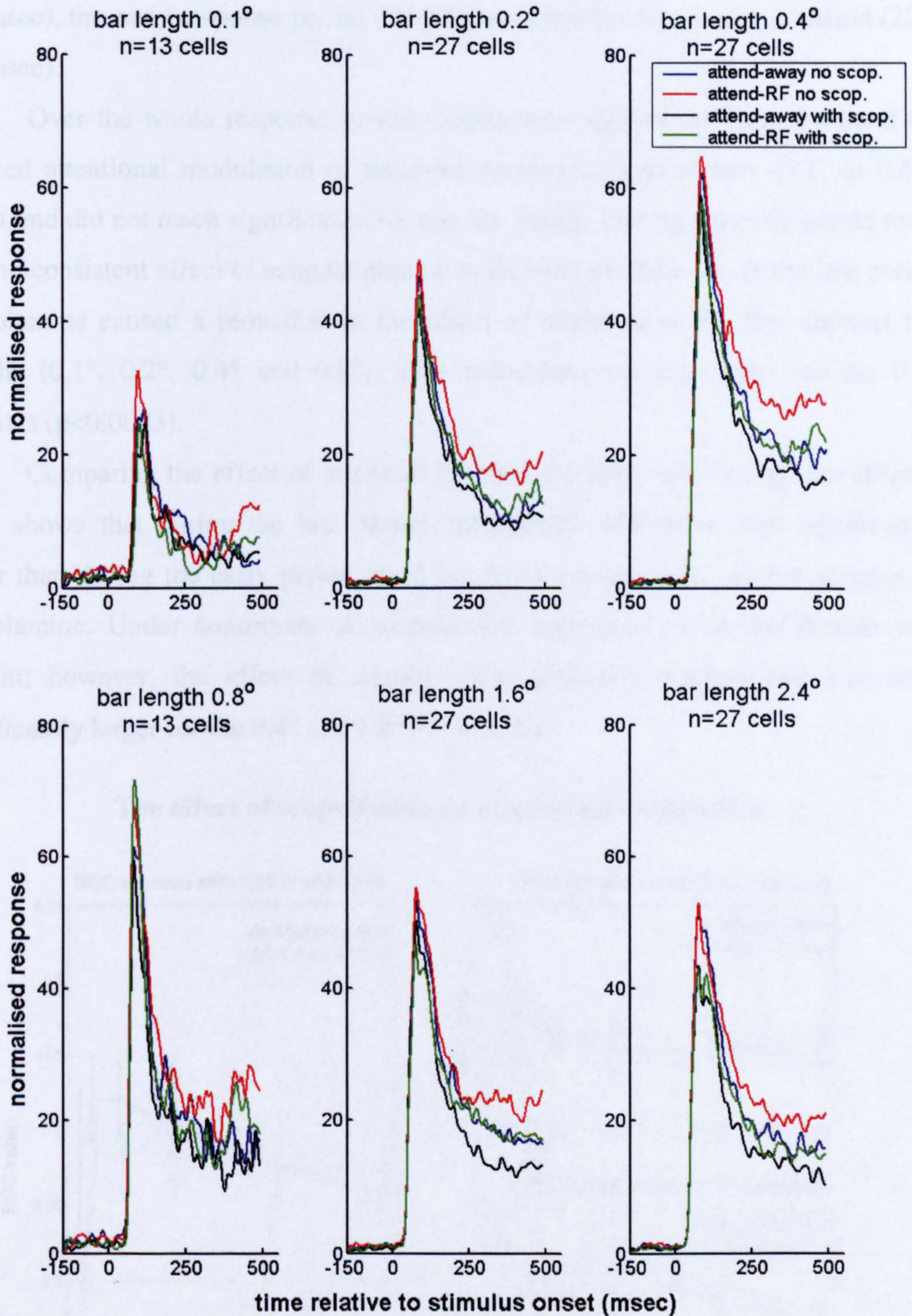


Figure 4.13 Normalised population responses to 6 bar lengths under attend-RF and attend-away conditions, with and without applied scopolamine (legend). 14 cells were recorded with only four bar lengths, 27 cells were recorded with 6 bar lengths. Responses from each cell were normalised to the highest response for that cell before being added to the population, thus each cell contributes equally to the mean responses shown here.

To test how scopolamine application influenced attentional modulation I calculated ROCs for the effect of attention separately for data recorded with and

without scopolamine application (Figure 4.14). To assess the temporal profile of the effects I calculated ROCs over three time windows: the whole response period (50-500msec), the early response period (50-225msec) and the late response period (225-500msec).

Over the whole response period scopolamine application caused a trend for reduced attentional modulation of neuronal responses to short bars (0.1° to 0.4°). This trend did not reach significance for any bar length. During the early period there was no consistent effect of scopolamine on attentional modulation. In the late period scopolamine caused a reduction in the effect of attention at the four shortest bar lengths (0.1° , 0.2° , 0.4° and 0.8°). This reduction was significant for the 0.2° stimulus ($p < 0.0083$).

Comparing the effect of attention between the early and late periods (Figure 4.15) shows that during the late period, attentional modulation was significantly larger than during the early period at all bar lengths except 0.1° , in the absence of scopolamine. Under conditions of scopolamine application a similar pattern was evident; however, the effect of attention was generally reduced and was only significantly larger for the 0.4° and 1.6° bar lengths.

The effect of scopolamine on attentional modulation

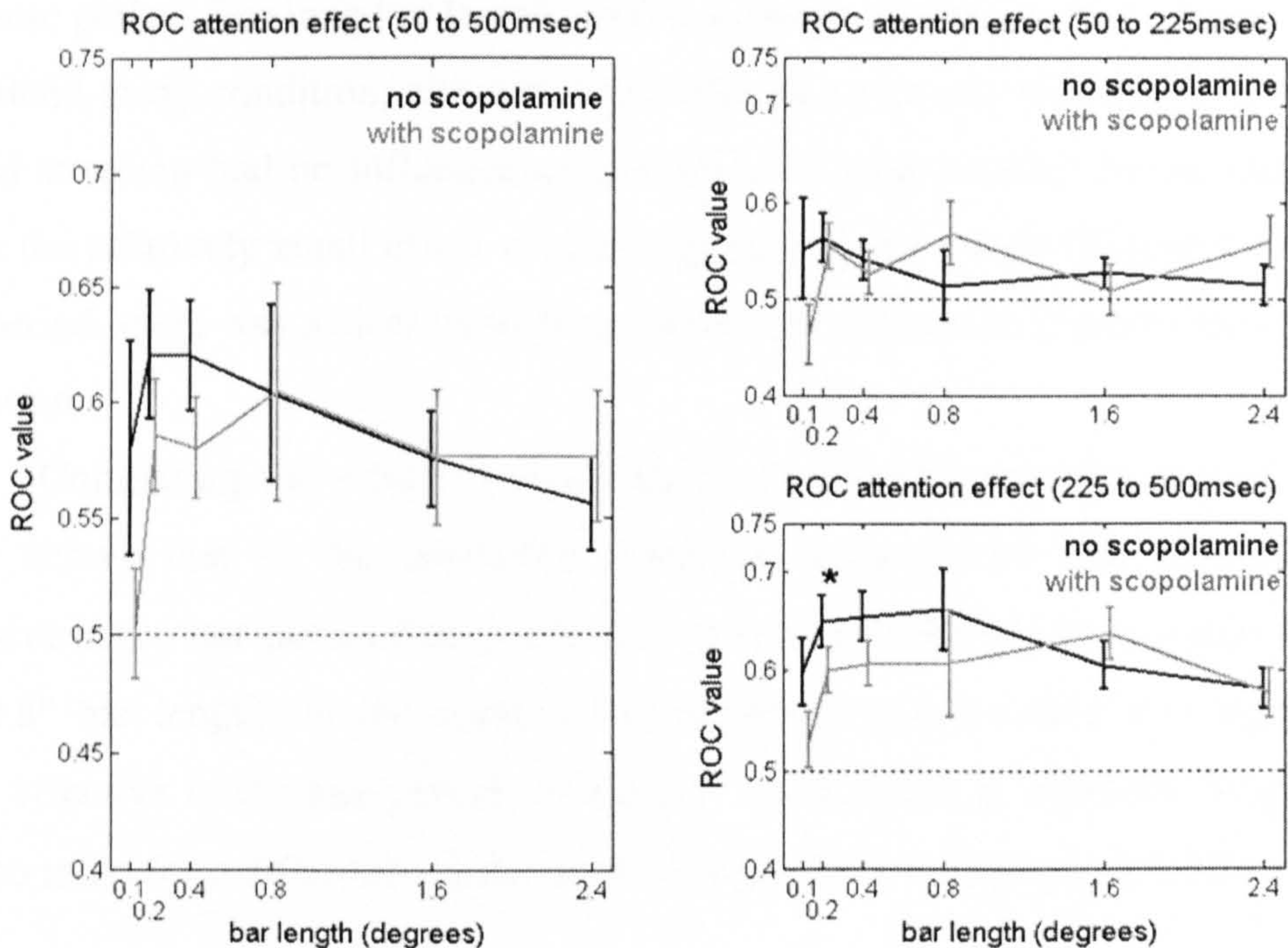


Figure 4.14 Attentional modulation expressed as ROC values as a function of bar length and drug application, for the whole response period (A) and separately for the early (B) and late (C) periods. Error bars show standard error. Curves and error bars in black show data with no scopolamine applied,

in grey they show data with scopolamine applied. Asterisks mark a significant effect of drug application ($p < 0.0083$, paired t-test).

Attentional modulation as a function of time and bar length

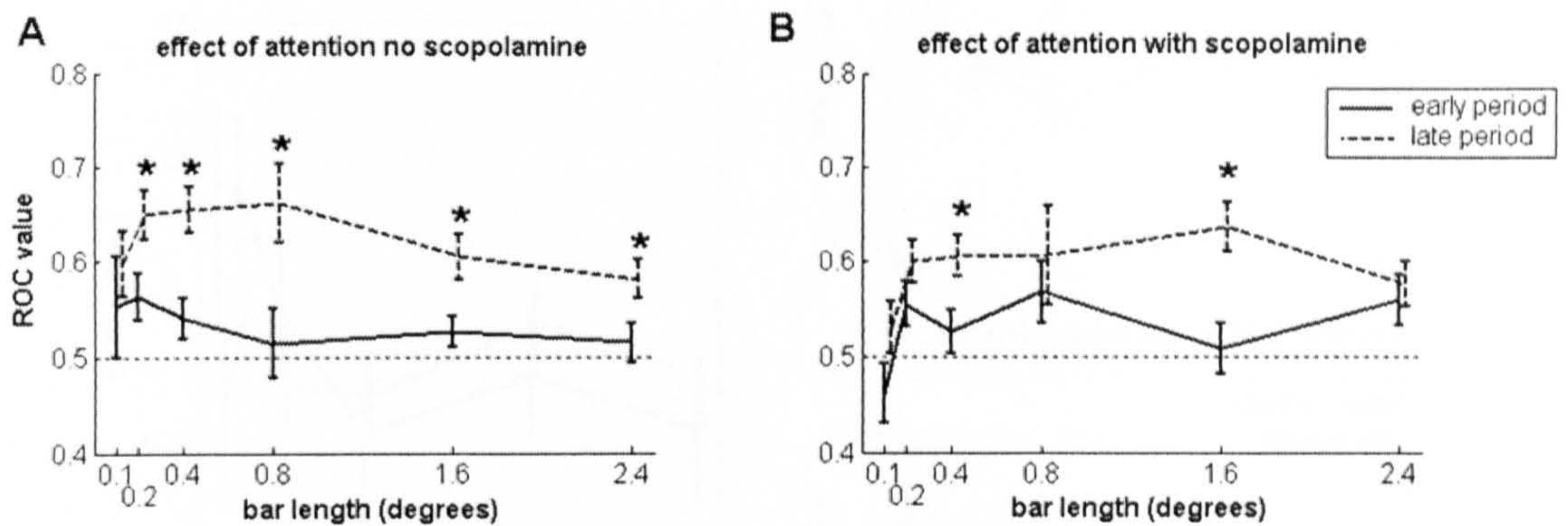


Figure 4.15 Attentional modulation in the early (solid lines) and late (dashed lines) periods expressed as mean ROC values **A**) without scopolamine applied and **B**) with scopolamine applied. Error bars show standard error. Asterisks mark significant differences between the time periods ($p < 0.0083$, paired t-test).

To further investigate the interaction of attentional modulation and scopolamine application, I compared the effect of scopolamine application in the attend-away and attend-RF conditions. For short bar lengths the effect of scopolamine was generally larger in the attend-RF condition (ROC values further below 0.5). This difference was significant for the 0.2° bar length in the whole response period. For long bar lengths in this period scopolamine had a larger effect in the attend-away condition, although this difference was not significant. In the early period attention had no influence on the effect of scopolamine; this is unsurprising given the relatively small effect of attention during this period (Figure 4.15). In the late period, there was a clear trend for a larger effect of scopolamine in the attend-RF condition.

Comparing the effect of scopolamine in the different time periods (Figure 4.17) shows that in the attend-RF condition scopolamine was generally more effective in the late period than in the early period; this difference was significant for the 0.8° bar length. In the attend-away condition, scopolamine was significantly more effective in the late period for the 1.6° bar lengths; at other bar lengths there was no trend for a difference in the effect of scopolamine application with time.

The effect of attention on response modulation by scopolamine

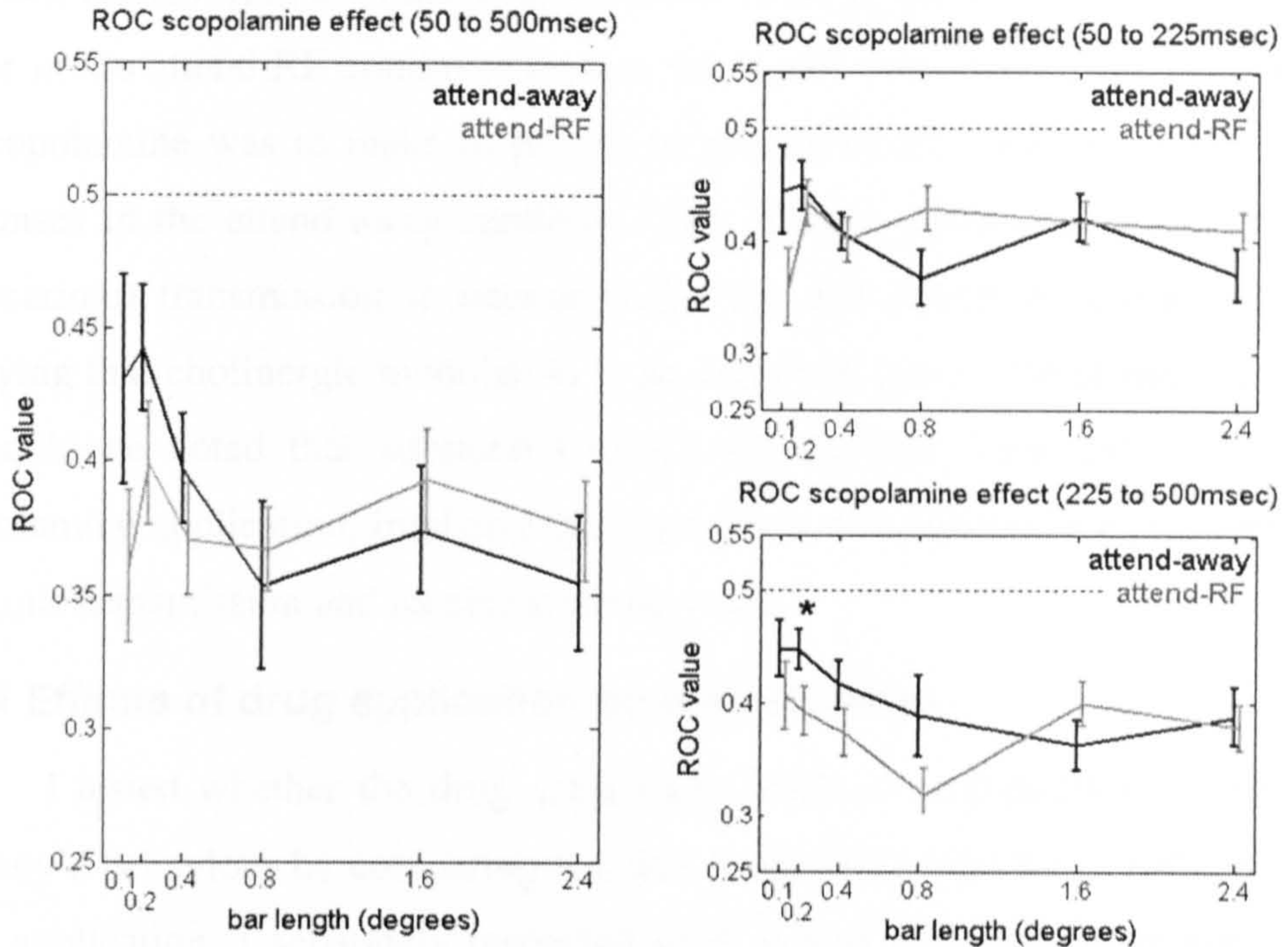


Figure 4.16 Effect of scopolamine application on neuronal responses expressed as ROC values as a function of bar length and attention condition, for the whole response period (A), and separately for the early (B) and late (C) periods. Error bars show standard error. Curves and error bars in black show data from the attend-away condition, in grey they show data from the attend-RF condition. Asterisks mark a significant effect of attention ($p < 0.0083$, paired t-test).

Effect of scopolamine application as a function of time and bar length

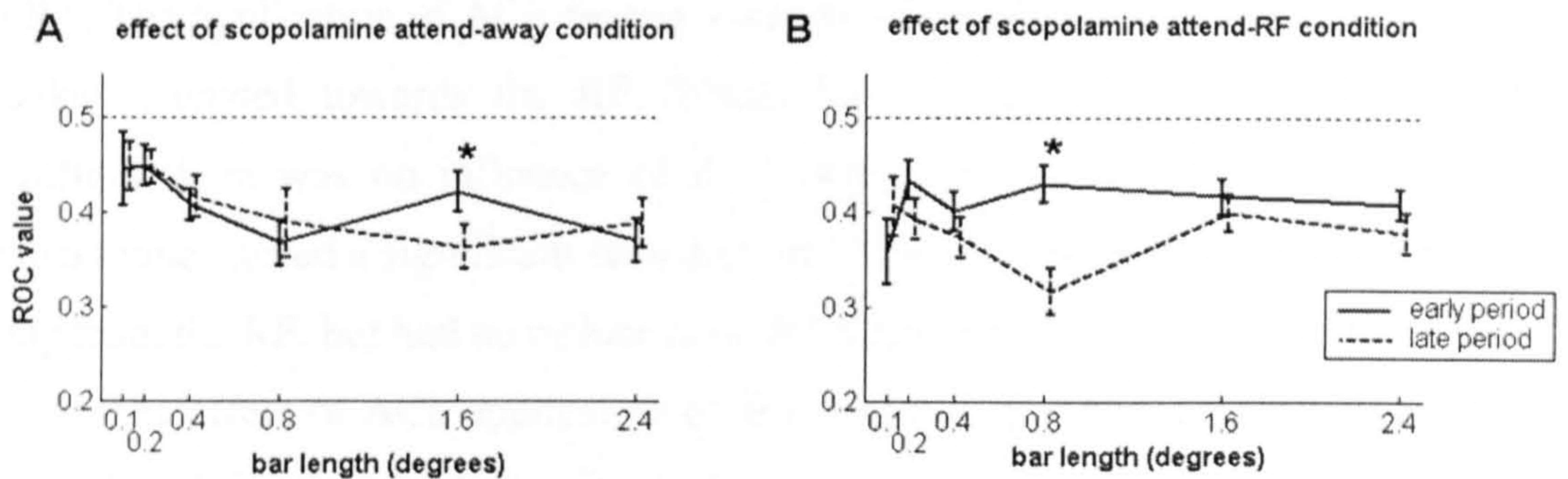


Figure 4.17 The effect of scopolamine application in the early (solid lines) and late (dashed lines) periods expressed as mean ROC values A) in the attend-away condition and B) in the attend RF condition. Error bars show standard error. Asterisks mark a significant effect of attention ($p < 0.0083$, paired t-test).

To summarise results from the scopolamine experiment: I found that attention generally facilitated neuronal responses whilst scopolamine generally suppressed the response. Moreover, I found that response enhancement by attention was reduced by scopolamine application. This result may seem surprising given the results from the ACh experiment showing that attentional modulation is also reduced by ACh

application (i.e. the effect of the antagonist appears the same as the effect of the agonist). However, in contrast with the effect of ACh, the effect of scopolamine was larger in the attend-RF condition than in the attend-away condition. Thus the effect of scopolamine was to make responses in the attend-RF condition more similar to responses in the attend-away condition. This finding demonstrates that cholinergic (muscarinic) transmission is necessary for the full effects of attention to occur, implying that cholinergic modulation is an important part of the attentional network. It should be noted that substantial effects of attention were still present during scopolamine application, implying the importance of additional mechanisms such as nicotinic transmission and feedback connections.

4.4.4 Effects of drug application on reaction time

I tested whether the drug application (ACh or scopolamine) influenced the monkey's behaviour by comparing reaction times (RT) from trials with and without drug application. I separately inspected trials where the monkey attended towards and away from the RF of the cell under study (and therefore the area of drug application). Due to the very small dose of the drug that was applied and due to the very local nature of the application, it seemed unlikely that the monkey's behaviour would be influenced. Nevertheless I did find that both drugs had significant effects on RT. The application of ACh caused a significant increase in RT in trials when the monkey attended towards the RF. When the monkey attended in the opposite hemifield there was no influence of drug application on RT. The application of scopolamine caused a significant reduction in RT in trials when the monkey attended away from the RF, but had no influence on RT when the monkey attended to the RF.

The effect of ACh application on RT suggests that ACh application in some way reduced the ability of the visual system to detect the target brightening. Since the drug application was very localised, there was no effect on RT when the target appeared in the opposite hemifield to the drug application (i.e. in the attend-away condition). The reduction in RT observed during scopolamine application is a surprising result since previous studies generally showed an increase in RT during scopolamine administration (Andrews et al. 1992; Blokland 1995). Importantly, I only found reductions in RT when the monkey attended in the opposite hemifield to the drug application. Since I found that scopolamine suppressed neuronal response,

the increase in RT may reflect the monkey being less distracted by stimuli in the RF location when attending to the opposite hemifield.

The effect of drug application on reaction time (RT)

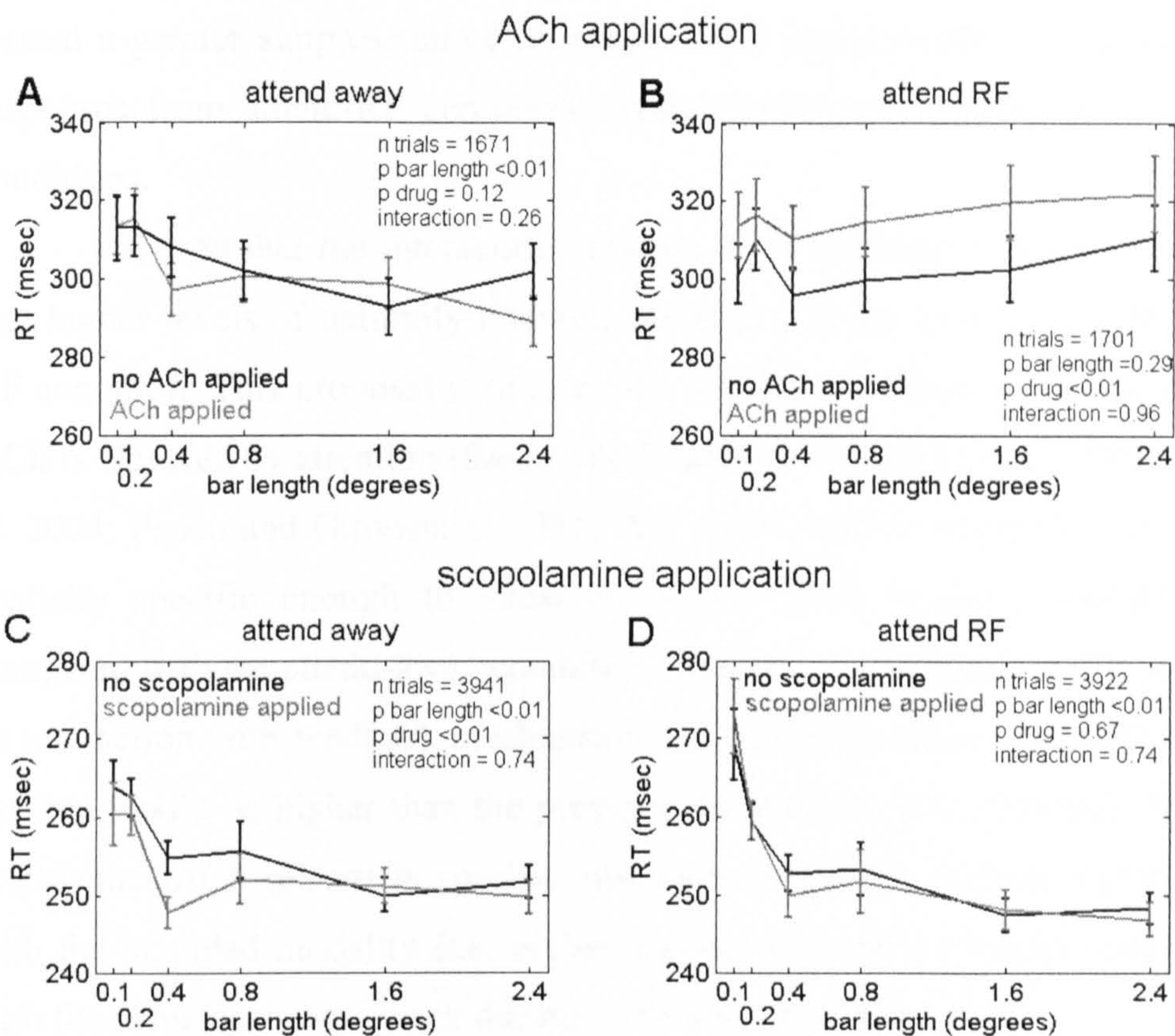


Figure 4.18 Reaction time as a function of bar length and drug application, separately for the attend-away and attend-RF conditions. In parts **A** and **B** grey lines show mean RTs during ACh application and black lines show RTs during control (no drug application) condition. Error bars show standard error. P-values are from a 2-way ANOVA. In parts **C** and **D** grey lines show RTs during scopolamine application and black lines show RTs during control conditions.

4.5 Discussion

In this chapter I investigated the effects of external administration of cholinergic drugs (ACh or scopolamine) on neuronal response and attentional modulation in primary visual cortex of one alert monkey. This is a currently ongoing project and the data presented here are preliminary. Further work will include testing a wider range of cholinergic antagonists, especially the nicotinic antagonist mecamylamine, and also recording in a second monkey.

My preliminary data show that both attention and external ACh application caused a general increase in neuronal responses, whilst scopolamine generally suppressed neuronal responses. Moreover, I show that the effect of attention is

reduced during the application of both cholinergic drugs. In the case of ACh application, this was achieved by a greater facilitation of responses from the attend-away condition than from the attend-RF responses, rendering responses in the attend-away condition more similar to responses in the attend-RF condition. Scopolamine caused a greater suppression of responses from the attend-RF condition, rendering responses from attend-RF conditions more similar to responses from attend-away conditions.

I argued that the interaction between ACh application and attention indicate that higher levels of naturally-released cortical ACh are associated with the attend-RF condition. This proposal is in line with a number of demonstrations that cortical ACh is elevated by attention (Sarter and Bruno 1997; Arnold et al. 2002; Fournier et al. 2004; Pepeu and Giovannini 2004). My results further imply that ACh release is spatially specific enough to allow for higher ACh in the attend-RF condition compared with the attend-away condition. This spatial specificity might arise through an interaction with feedback mechanisms from higher cortical areas. The specificity implied would be higher than the previous demonstration by Fournier, Semba et al. (2004) that ACh release is specific enough to target the cortical region associated with the attended modality (i.e. higher cortical ACh in the visual cortex compared with the somatosensory cortex during a visually demanding task).

The suppression of attentional modulation by scopolamine application is a clear demonstration that cholinergic (muscarinic) transmission is a necessary component of the network mediating attentional modulation.

4.5.1 Potential confounds

It may be argued that the application of ACh caused a saturation of the response in the attend-away condition, thus further enhancement of activity due to attention could not occur. Arguing against this possibility, I found reduced attentional modulation during ACh application, even at the 0.1° bar length (although this reduction was not significant), which typically gave lower responses than other bar lengths even during ACh application. Thus for this stimulus at least, saturation cannot account for my finding since the cell was demonstrably not saturated.

Due to the constraints of the pipette manufacturing process I was unable to apply a balance current during drug application. During my experiments as presented in Chapter 2 I repeatedly demonstrated that effects of ACh application were not due

to current effects. I have not investigated whether current effects could account or contribute to the effect of scopolamine application. In fact current effects are more likely to confound the effect of scopolamine (inhibitory) than of ACh (excitatory) since the increase in positively charged drug ions in the extra-cellular space would cause cells to become hyperpolarised, which would potentially have the effect of inhibiting neuronal activity. I am currently planning experiments to test for the possibility of current effects during scopolamine application.

4.5.2 Suppression by ACh in anaesthetised experiments

In Chapter 2 I presented data from experiments which investigated the effects of ACh application on the length tuning of V1 cells in anaesthetised primates. In those experiments I found that application of ACh caused a facilitation of responses in 62.1% of cells and a suppression of responses in 37.9% of cells compared to control conditions. This number is comparable to reports from earlier studies in anaesthetised animals (Sillito and Kemp 1983; Sato et al. 1987; Sillito and Murphy 1987; Metherate et al. 1988; Murphy and Sillito 1991). In Chapter 3 I suggested that the effects of attention were similar to the effects of ACh application; however, in contrast with the effect of ACh application I found that attention suppressed the response of only 16.7% of cells. I suggested that an interaction with anaesthesia may have contributed to the large proportion of suppressed cells in the anaesthetised experiments.

In this chapter I have presented data from 16 cells where the effect of ACh was investigated in the absence of anaesthesia (seven cells from the contrast tuning experiment and nine from the attention experiment). I found two cells (12.5%) in which ACh application caused a general suppression of the response and a further cell in which ACh suppressed the response in the attend-away condition but facilitated the response in the attend-RF condition. This proportion of cells suppressed by ACh is closer to the proportion of cells suppressed by attention than the proportion suppressed by ACh in the anaesthetised animal, thus the current findings suggest that an interaction with anaesthesia may have contributed to the results presented in Chapter 2. Obviously a larger population of cells where the effect of ACh is assessed in awake animals will be required before this assertion can be made with sufficient confidence. Such data are currently being obtained in Alexander Thiele's lab.

Grand summary, conclusions and outlook

In this thesis I have investigated how attention modulates contextual processing in vision. There are two components to this question. Firstly, what are the effects of attention on contextual processing. Secondly, what are the neurobiological mechanisms that mediate attentional processing. The hypothesis of the thesis was based on two previously-described findings: first, that attention is associated with increased levels of the neuromodulator acetylcholine (ACh) in the cortex; second, that ACh has been shown *in vitro* to selectively reduce the efficacy of intracortical synapses whilst leaving the efficacy of thalamocortical synapses unaffected or even enhanced. Thus ACh may alter the balance of the cortical network in favour of feed-forward inputs. In the visual system intracortical inputs are the major input of the non-classical receptive field (nCRF), which is the likely neural basis for contextual influences in perception. Based on these findings, my hypothesis was that attention would reduce contextual processing by the action of ACh.

In Chapters 1 and 3, I presented work to test the hypothesis that attention reduces contextual processing. In Chapter 1, it was shown that contextual influences in human orientation perception were reduced by full attention, compared with a reduced attention condition. Importantly, it was shown that attention reduced contextual influences independently of the nature of the influence (whether perceived orientation was attracted or repelled by the context). In Chapter 3, I presented work in which I tested the effect of attention on the strength of the nCRF of V1 cells, by measuring length tuning when the monkey attended either towards or away from the receptive field (RF) of the neuron under study. I found that attention altered length tuning, and that the nature of this influence depended on the eccentricity of the RF. At near-foveal eccentricities ($\sim 2^\circ$) attention reduced preferred length whilst in the periphery ($\sim 7^\circ$ eccentricity) attention increased the preferred length. This difference could be explained by differences in centre/surround interactions across eccentricities. Near the fovea there is a high degree of summation from the nCRF whilst in the periphery inhibitory interactions dominate the nCRF. Thus a reduction in the power of the nCRF will have different consequences at different eccentricities. Near the fovea summation from the nCRF will be reduced, resulting in reduced preferred length, whilst in the periphery inhibition from the nCRF will be reduced, resulting in increased preferred length. This is precisely the pattern found for the

effect of attention, and therefore the results are consistent with the hypothesis that attention causes a reduction in nCRF modulation. Taken together, results from Chapters 1 and 3 demonstrate that attention reduces contextual modulation at the level of perception and at the level of V1 processing, generally supporting my hypothesis.

The second part of my hypothesis was that the cholinergic system is involved in mediating the attentional modulation of neuronal responses and contextual processes. This part of the hypothesis was investigated in Chapters 2 and 4. In Chapter 2 it was shown that the application of ACh caused a reduction in the preferred length of cells in V1 of anaesthetised marmosets. This reduction in preferred length was mediated by a reduction in the size of the spatial summation area towards the size of the cell's classical RF. Thus the findings demonstrate that ACh application caused a reduction in nCRF modulation, mirroring the effect of attention shown in Chapters 1 and 3. In Chapter 4 I presented preliminary work in which I directly tested the contribution of cholinergic mechanisms to attentional processes. I measured attentional modulation of V1 responses in the presence and absence of a locally-applied cholinergic agonist (ACh) and antagonist (scopolamine). Attentional modulation was reduced by the application of both agents. ACh application caused greater facilitation of responses when attention was directed away from the RF of the cell under study, whilst scopolamine caused greater suppression of responses when attention was directed to the location of the RF of the cell under study. Thus ACh application somewhat mimicked the effect of attention whilst scopolamine blocked attentional modulation. These findings clearly demonstrate the importance of cholinergic transmission for attentional modulation of V1 responses. Taken together, my findings in Chapters 2 and 4 demonstrate that the effect of ACh is similar to the effect of attention, and moreover that cholinergic transmission is a necessary and permissive component for full attentional modulation of neuronal responses. My findings therefore fully support the hypothesis that effects of attention are to some extent dependent on cholinergic mechanisms.

In summary, this thesis set out to investigate how attention modulates contextual processing in vision. To answer this question I have presented experiments which investigated the effects of attention on contextual modulation, and experiments which investigated the neurobiological mechanisms mediating attentional modulation. I have shown that attention suppressed contextual influences

at the level of perception and at the level of the primary visual cortex. These effects were at least partly accounted for by cholinergic mechanisms.

Future work

Data presented in Chapter 4, although intriguing, are preliminary. Further data are currently being collected to test the effect of scopolamine on attentional modulation in a second monkey. Moreover, future work will also test the effect of the nicotinic antagonist mecamylamine or methyllycaconitine. Ultimately it will be desirable to test the effect on the same cell of either drug independently or both drugs combined, and so be able to test the relative contribution of muscarinic and nicotinic mechanisms in mediating attentional modulation. These experiments are to start in the near future.

In Chapter 1, I presented a biologically inspired model which could account for the observed shift in perceived target orientation either towards or away from the context bars, depending on the contrast of the target. The model suggested that the context bars facilitated the neuronal response to the target when it was presented at low contrast but suppressed the response when the target was presented at high contrast. To test this model, I have recently started to record the V1 cell responses of an alert macaque under stimulus conditions identical to those used in the psychophysical experiments, with the target bar centred over the RF of the cell under study. To date only a small sample of data have been collected and further work will be required before the model's predictions can be compared with neuronal data with any confidence. There are also a number of model parameters that could be tested using human psychophysics. The most obvious of these is the area over which contextual influences are effective. This could be assessed by testing how the number of context bars influenced the strength of the effect. It would also be interesting to assess how the speed of the apparent motion of the context bars influenced the size of the effect. This would provide information about the temporal profile of contextual integration.

References

- Abbott, L. F., Varela, J. A., Sen, K. and Nelson, S. B. (1997). "Synaptic depression and cortical gain control." Science **275**(5297): 220-4.
- Albright, T. D. and Stoner, G. R. (2002). "Contextual influences on visual processing." Annu Rev of Neurosci **25**: 339-379.
- Alitto, H. J. and Usrey, W. M. (2004). "Influence of contrast on orientation and temporal frequency tuning in ferret primary visual cortex." J Neurophysiol **91**(6): 2797-808.
- Alkire, M. T. and Haier, R. J. (2001). "Correlating in vivo anaesthetic effects with ex vivo receptor density data supports a gabaergic mechanism of action for propofol, but not for isoflurane." Brit J Anaesth **86**(5): 618-626.
- Andrews, J. S., Grutzner, M. and Stephens, D. N. (1992). "Effects of cholinergic and non-cholinergic drugs on visual discrimination and delayed visual discrimination performance in rats." Psychopharmacology (Berl) **106**(4): 523-30.
- Angelucci, A. and Bullier, J. (2003). "Reaching beyond the classical receptive field of V1 neurons: Horizontal or feedback axons?" J Physiol Paris **97**(2-3): 141-54.
- Angelucci, A., Levitt, J. B. and Lund, J. S. (2002a). "Anatomical origins of the classical receptive field and modulatory surround field of single neurons in macaque visual cortical area V1." Prog Brain Res **136**: 373-88.
- Angelucci, A., Levitt, J. B., Walton, E. J., Hupe, J. M., Bullier, J. and Lund, J. S. (2002b). "Circuits for local and global signal integration in primary visual cortex." J Neurosci **22**(19): 8633-46.
- Aoki, C. and Kabak, S. (1992). "Cholinergic terminals in the cat visual cortex: Ultrastructural basis for interaction with glutamate-immunoreactive neurons and other cells." Vis Neurosci **8**(3): 177-91.
- Arnold, H. M., Burk, J. A., Hodgson, E. M., Sarter, M. and Bruno, J. P. (2002). "Differential cortical acetylcholine release in rats performing a sustained attention task versus behavioral control tasks that do not explicitly tax attention." Neuroscience **114**(2): 451-60.
- Bair, W., Cavanaugh, J. R. and Movshon, J. A. (2003). "Time course and time-distance relationships for surround suppression in macaque V1 neurons." J Neurosci **23**(20): 7690-701.
- Barlow, H. B., Blakemore, C. and Pettigrew, J. D. (1967). "The neural mechanism of binocular depth discrimination." J Physiol **193**(2): 327-42.
- Blasdel, G. G. and Fitzpatrick, D. (1984). "Physiological organization of layer 4 in macaque striate cortex." J Neurosci **4**(3): 880-95.
- Blokland, A. (1995). "Acetylcholine: A neurotransmitter for learning and memory?" Brain Res Rev **21**(3): 285-300.
- Born, R. T. (2000). "Center-surround interactions in the middle temporal visual area of the owl monkey." J Neurophysiol **84**(5): 2658-2669.

- Bringuier, V., Chavane, F., Glaeser, L. and Fregnac, Y. (1999). "Horizontal propagation of visual activity in the synaptic integration field of area 17 neurons." Science 283(5402): 695-9.
- Britten, K. H., Newsome, W. T., Shadlen, M. N., Celebrini, S. and Movshon, J. A. (1996). "A relationship between behavioral choice and the visual responses of neurons in macaque mt." Vis Neurosci 13(1): 87-100.
- Carandini, M., Heeger, D. J. and Movshon, J. A. (1997). "Linearity and normalization in simple cells of the macaque primary visual cortex." J Neurosci 17(21): 8621-44.
- Carandini, M., Heeger, D. J. and Senn, W. (2002). "A synaptic explanation of suppression in visual cortex." J Neurosci 22(22): 10053-65.
- Carey, R. G. and Rieck, R. W. (1987). "Topographic projections to the visual cortex from the basal forebrain in the rat." Brain Res 424(2): 205-15.
- Carpenter, R. H. (2004). "Contrast, probability, and saccadic latency; evidence for independence of detection and decision." Curr Biol 14(17): 1576-80.
- Carrasco, M., Ling, S. and Read, S. (2004). "Attention alters appearance." Nat Neurosci 7(3): 308-13.
- Cavanaugh, J. R., Bair, W. and Movshon, J. A. (2002). "Nature and interaction of signals from the receptive field center and surround in macaque V1 neurons." J Neurophysiol 88(5): 2530-46.
- Cavanaugh, J. R., Bair, W. and Movshon, J. A. (2002). "Nature and interaction of signals from the receptive field center and surround in macaque V1 neurons." J Neurophysiol 88(5): 2530-46.
- Cavanaugh, J. R., Bair, W. and Movshon, J. A. (2002). "Selectivity and spatial distribution of signals from the receptive field surround in macaque V1 neurons." J Neurophysiol 88(5): 2547-56.
- Celebrini, S. and Newsome, W. T. (1994). "Neuronal and psychophysical sensitivity to motion signals in extrastriate area mst of the macaque monkey." J Neurosci 14(7): 4109-24.
- Chavane, F., Monier, C., Bringuier, V., Baudot, P., Borg-Graham, L., Lorenceau, J. and Fregnac, Y. (2000). "The visual cortical association field: A gestalt concept or a psychophysiological entity?" J Physiol Paris 94(5-6): 333-42.
- Chelazzi, L. (1995). "Neural mechanisms for stimulus selection in cortical areas of the macaque subserving object vision." Behav. Brain Res. 71: 125-134.
- Connor, C. E., Preddie, D. C., Gallant, J. L. and Van Essen, D. C. (1997). "Spatial attention effects in macaque area v4." J Neurosci 17(9): 3201-14.
- Cook, E. P. and Maunsell, J. H. R. (2002). "Attentional modulation of behavioral performance and neuronal responses in middle temporal and ventral intraparietal areas of macaque monkey." J Neurosci 22(5): 1994-2004.
- Corbetta, M., Miezin, F. M., Dobmeyer, S., Shulman, G. L. and Petersen, S. E. (1990). "Attentional modulation of neural processing of shape, color, and velocity in humans." Science 248(4962): 1556-1559.

- Crook, J. M., Engelmann, R. and Lowel, S. (2002). "Gaba-inactivation attenuates colinear facilitation in cat primary visual cortex." Exp Brain Res **143**(3): 295-302.
- Das, A. and Gilbert, C. D. (1999). "Topography of contextual modulations mediated by short-range interactions in primary visual cortex." Nature **399**(6737): 655-61.
- Dayan, P. and Yu, A. (2001). "Ach, uncertainty, and cortical inference." NIPS **13**(1).
- De Weerd, P., Gattass, R., Desimone, R. and Ungerleider, L. G. (1995). "Responses of cells in monkey visual-cortex during perceptual filling-in of an artificial scotoma." Nature **377**(6551): 731-734.
- DeAngelis, G. C., Freeman, R. D. and Ohzawa, I. (1994). "Length and width tuning of neurons in the cat's primary visual cortex." J Neurophysiol **71**(1): 347-74.
- Desimone, R. and Duncan, J. (1995). "Neural mechanisms of selective visual attention." Annu Rev Neurosci **18**: 193-222.
- Dick, M. and Hochstein, S. (1989). "Visual orientation estimation." Percept Psychophys **46**(3): 227-34.
- Disney, A. A. and Aoki, C. (2003). "Nicotinic, but not muscarinic, acetylcholine receptors are expressed by thalamic afferents and their terminals in layer 4c of macaque V1." Soc for Neurosci Abstract Viewer/Itinerary Planner Program No. 701.16.
- Douglas, R. J., Koch, C., Mahowald, M., Martin, K. A. C. and Suarez, H. H. (1995). "Recurrent excitation in neocortical circuits." Science **269**(5226): 981-985.
- Drachman, D. A. (1977). "Memory and cognitive function in man: Does the cholinergic system have a specific role?" Neurology **27**(8): 783-90.
- Dragoi, V. and Sur, M. (2000). "Dynamic properties of recurrent inhibition in primary visual cortex: Contrast and orientation dependence of contextual effects." J Neurophysiol **83**(2): 1019-1030.
- Driver, J. and Frackowiak, R. S. J. (2001). "Neurobiological measures of human selective attention." Neuropsychologia **39**(12): 1257-1262.
- Duncan, J. (1984). "Selective attention and the organization of visual information." J Exp Psycho-Gener **113**(4): 501-517.
- Dunnett, S. B., Everitt, B. J. and Robbins, T. W. (1991). "The basal forebrain-cortical cholinergic system: Interpreting the functional consequences of excitotoxic lesions." Trends Neurosci **14**(11): 494-501.
- Everitt, B. J. and Robbins, T. W. (1997). "Central cholinergic systems and cognition." Annu Rev Psychol **48**: 649-84.
- Eysel, U. T., Pape, H. C. and Van Schayck, R. (1986). "Excitatory and differential disinhibitory actions of acetylcholine in the lateral geniculate nucleus of the cat." J Physiol **370**: 233-54.
- Fearon, P. (2003). "Big problems with small samples." The Psychologist **16**(12): 632-635.
- Ferster, D., Chung, S. and Wheat, H. (1996). "Orientation selectivity of thalamic input to simple cells of cat visual cortex." Nature **380**(6571): 249-252.

- Fitzpatrick, D. (2000). "Seeing beyond the receptive field in primary visual cortex." Curr Opin Neurobiol 10(4): 438-43.
- Fjeld, I. T., Ruksenas, O. and Heggelund, P. (2002). "Brainstem modulation of visual response properties of single cells in the dorsal lateral geniculate nucleus of cat." J Physiol 543(Pt 2): 541-54.
- Fournier, G. N., Semba, K. and Rasmusson, D. D. (2004). "Modality- and region-specific acetylcholine release in the rat neocortex." Neuroscience 126(2): 257-62.
- Freeman, E., Driver, J., Sagi, D. and Zhaoping, L. (2003). "Top-down modulation of lateral interactions in early vision: Does attention affect integration of the whole or just perception of the parts?" Curr Biol 13(11): 985-9.
- Freeman, E., Sagi, D. and Driver, J. (2001). "Lateral interactions between targets and flankers in low-level vision depend on attention to the flankers." Nat Neurosci 4(10): 1032-6.
- Freeman, E., Sagi, D. and Driver, J. (2004). "Configuration-specific attentional modulation of flanker- -target lateral interactions." Perception 33(2): 181-94.
- Fries, P., Reynolds, J. H., Rorie, A. E. and Desimone, R. (2001). "Modulation of oscillatory neuronal synchronization by selective visual attention." Science 291(5508): 1560-3.
- Fuchs, A. F. and Robinson, D. A. (1966). "A method for measuring horizontal and vertical eye movement chronically in the monkey." J Appl Physiol 21(3): 1068-70.
- Gazzaley, A., Cooney, J. W., McEvoy, K., Knight, R. T. and D'Esposito, M. (2005). "Top-down enhancement and suppression of the magnitude and speed of neural activity." J Cogn Neurosci 17(3): 507-17.
- Georges, S., Series, P., Fregnac, Y. and Lorenceau, J. (2002). "Orientation dependent modulation of apparent speed: Psychophysical evidence." Vision Res 42(25): 2757-72.
- Ghose, G. M. and Maunsell, J. H. R. (2002). "Attentional modulation in visual cortex depends on task timing." Nature 419(6907): 616-620.
- Gil, Z., Connors, B. W. and Amitai, Y. (1997). "Differential regulation of neocortical synapses by neuromodulators and activity." Neuron 19(3): 679-686.
- Gil, Z., Connors, B. W. and Amitai, Y. (1999). "Efficacy of thalamocortical and intracortical synaptic connections: Quanta, innervation, and reliability." Neuron 23(2): 385-97.
- Gilbert, C., Ito, M., Kapadia, M. and Westheimer, G. (2000). "Interactions between attention, context and learning in primary visual cortex." Vision Res 40(10-12): 1217-26.
- Gilbert, C. D. and Wiesel, T. N. (1990). "The influence of contextual stimuli on the orientation selectivity of cells in primary visual cortex of the cat." Vision Res 30(11): 1689-701.
- Gioanni, Y., Rougeot, C., Clarke, P. B., Lepouse, C., Thierry, A. M. and Vidal, C. (1999). "Nicotinic receptors in the rat prefrontal cortex: Increase in glutamate

- release and facilitation of mediodorsal thalamo-cortical transmission." Eur J Neurosci 11(1): 18-30.
- Grinvald, A., Lieke, E. E., Frostig, R. D. and Hildesheim, R. (1994). "Cortical point-spread function and long-range lateral interactions revealed by real-time optical imaging of macaque monkey primary visual cortex." J Neurosci 14(5 Pt 1): 2545-68.
- Guo, K., Nevado, A., Robertson, R. G., Pulgarin, M., Thiele, A. and Young, M. P. (2004). "Effects on orientation perception of manipulating the spatio-temporal prior probability of stimuli." Vision Res 44(20): 2349-58.
- Habbicht, H. and Vater, M. (1996). "A microiontophoretic study of acetylcholine effects in the inferior colliculus of horseshoe bats: Implications for a modulatory role." Brain Res 724(2): 169-179.
- Hammett, S. T., Georgeson, M. A., Bedingham, S. and Barbieri-Hesse, G. S. (2003). "Motion sharpening and contrast: Gain control precedes compressive non-linearity?" Vision Res 43(10): 1187-99.
- Hasselmo, M. E. and Bower, J. M. (1992). "Cholinergic suppression specific to intrinsic not afferent fiber synapses in rat piriform (olfactory) cortex." J Neurophysiol 67(5): 1222-1229.
- Heeger, D. J. (1992). "Normalization of cell responses in cat striate cortex." Vis Neurosci 9(2): 181-97.
- Hsieh, C. Y., Cruikshank, S. J. and Metherate, R. (2000). "Differential modulation of auditory thalamocortical and intracortical synaptic transmission by cholinergic agonist." Brain Res 880(1-2): 51-64.
- Huang, L. and Dobkins, K. R. (2005). "Attentional effects on contrast discrimination in humans: Evidence for both contrast gain and response gain." Vision Res 45(9): 1201-12.
- Hupe, J. M., James, A. C., Girard, P. and Bullier, J. (2001). "Response modulations by static texture surround in area V1 of the macaque monkey do not depend on feedback connections from v2." J Neurophysiol 85(1): 146-163.
- Hupe, J. M., James, A. C., Payne, B. R., Lomber, S. G., Girard, P. and Bullier, J. (1998). "Cortical feedback improves discrimination between figure and background by V1, v2 and v3 neurons." Nature 394(6695): 784-787.
- Ito, M. and Gilbert, C. D. (1999). "Attention modulates contextual influences in the primary visual cortex of alert monkeys." Neuron 22(3): 593-604.
- Ito, M., Westheimer, G. and Gilbert, C. D. (1998). "Attention and perceptual learning modulate contextual influences on visual perception." Neuron 20(6): 1191-1197.
- Jancke, D., Chavane, F., Naaman, S. and Grinvald, A. (2004). "Imaging cortical correlates of illusion in early visual cortex." Nature 428(6981): 423-6.
- Jones, H. E., Wang, W. and Sillito, A. M. (2002). "Spatial organization and magnitude of orientation contrast interactions in primate V1." J Neurophysiol 88(5): 2796-808.

- Jones, J. P. and Palmer, L. A. (1987). "An evaluation of the two-dimensional gabor filter model of simple receptive fields in cat striate cortex." J Neurophysiol 58(6): 1233-58.
- Judge, S. J., Richmond, B. J. and Chu, F. C. (1980). "Implantation of magnetic search coils for measurement of eye position: An improved method." Vision Res 20(6): 535-8.
- Kapadia, M. K., Ito, M., Gilbert, C. D. and Westheimer, G. (1995). "Improvement in visual sensitivity by changes in local context: Parallel studies in human observers and in V1 of alert monkeys." Neuron 15(4): 843-56.
- Kapadia, M. K., Westheimer, G. and Gilbert, C. D. (1999). "Dynamics of spatial summation in primary visual cortex of alert monkeys." Proc Natl Acad Sci U S A 96(21): 12073-8.
- Kapadia, M. K., Westheimer, G. and Gilbert, C. D. (2000). "Spatial distribution of contextual interactions in primary visual cortex and in visual perception." J Neurophysiol 84(4): 2048-62.
- Kastner, S., De Weerd, P., Pinsk, M. A., Elizondo, M. I., Desimone, R. and Ungerleider, L. G. (2001). "Modulation of sensory suppression: Implications for receptive field sizes in the human visual cortex." J Neurophysiol 86(3): 1398-411.
- Kastner, S. and Pinsk, M. A. (2004). "Visual attention as a multilevel selection process." Cogn Affect Behav Neurosci 4(4): 483-500.
- Kersten, D., Mamassian, P. and Yuille, A. (2004). "Object perception as bayesian inference." Annu Rev Psychol 55: 271-304.
- Khoe, W., Freeman, E., Woldorff, M. G. and Mangun, G. R. (2004). "Electrophysiological correlates of lateral interactions in human visual cortex." Vision Res 44(14): 1659-73.
- Kimura, F. (2000). "Cholinergic modulation of cortical function: A hypothetical role in shifting the dynamics in cortical network." Neurosci Res 38(1): 19-26.
- Kimura, F. and Baughman, R. W. (1997). "Distinct muscarinic receptor subtypes suppress excitatory and inhibitory synaptic responses in cortical neurons." J Neurophysiol 77(2): 709-16.
- Kimura, F. and Baughman, R. W. (1997). "Distinct muscarinic receptor subtypes suppress excitatory and inhibitory synaptic responses in cortical neurons." J Neurophysiol 77(2): 709-16.
- Kimura, F., Fukuda, M. and Tsumoto, T. (1999). "Acetylcholine suppresses the spread of excitation in the visual cortex revealed by optical recording: Possible differential effect depending on the source of input." Eur J Neurosci 11(10): 3597-3609.
- Knierim, J. J. and van Essen, D. C. (1992). "Neuronal responses to static texture patterns in area V1 of the alert macaque monkey." J Neurophysiol 67(4): 961-80.
- Lamme, V. A. and Roelfsema, P. R. (2000). "The distinct modes of vision offered by feedforward and recurrent processing." Trends Neurosci 23(11): 571-9.

- Lamme, V. A. F., Zipser, K. and Spekreijse, H. (1998). "Figure-ground activity in primary visual cortex is suppressed by anesthesia." Proc Natl Acad Sci U S A **95**(6): 3263-3268.
- Lavine, N., Reuben, M. and Clarke, P. B. (1997). "A population of nicotinic receptors is associated with thalamocortical afferents in the adult rat: Laminar and areal analysis." J Comp Neurol **380**(2): 175-90.
- Levitt, J. B. and Lund, J. S. (1997). "Contrast dependence of contextual effects in primate visual cortex." Nature **387**(6628): 73-6.
- Li, W. and Gilbert, C. D. (2002). "Global contour saliency and local colinear interactions." J Neurophysiol **88**(5): 2846-56.
- Li, W., Piech, V. and Gilbert, C. D. (2004). "Perceptual learning and top-down influences in primary visual cortex." Nat Neurosci **7**(6): 651-7.
- Li, Z. (2003). "V1 mechanisms and some figure-ground and border effects." J Physiol Paris **97**(4-6): 503-15.
- Lucas-Meunier, E., Fossier, P., Baux, G. and Amar, M. (2003). "Cholinergic modulation of the cortical neuronal network." Pflugers Arch **446**(1): 17-29.
- Luck, S. J., Chelazzi, L., Hillyard, S. A. and Desimone, R. (1997). "Neural mechanisms of spatial selective attention in areas V1, v2, and v4 of macaque visual cortex." J Neurophysiol **77**(1): 24-42.
- Lund, J. S., Angelucci, A. and Bressloff, P. C. (2003). "Anatomical substrates for functional columns in macaque monkey primary visual cortex." Cereb Cortex **13**(1): 15-24.
- Maffei, L. and Fiorentini, A. (1976). "The unresponsive regions of visual cortical receptive fields." Vision Res **16**(10): 1131-9.
- Mamassian, P., Landy, M. S. and L.T., M. (2002). Bayesian modelling of visual perception. Probabilistic models of the brain: Perception and neural function. R. P. Rao, B. A. Olshausen and L. M.S. Cambridge MA, MIT Press: 13-36.
- Mareschal, I. and Shapley, R. M. (2004). "Effects of contrast and size on orientation discrimination." Vision Res **44**(1): 57-67.
- McAdams, C. J. and Maunsell, J. H. (1999). "Effects of attention on the reliability of individual neurons in monkey visual cortex." Neuron **23**(4): 765-73.
- McAdams, C. J. and Maunsell, J. H. R. (1999). "Effects of attention on orientation-tuning functions of single neurons in macaque cortical area v4." J Neurosci **19**(1): 431-441.
- McAdams, C. J. and Maunsell, J. H. R. (2000). "Attention to both space and feature modulates neuronal responses in macaque area v4." J Neurophysiol **83**(3): 1751-1755.
- McCormick, D. A. and Pape, H. C. (1988). "Acetylcholine inhibits identified interneurons in the cat lateral geniculate nucleus." Nature **334**(6179): 246-8.
- McCormick, D. A. and Prince, D. A. (1986). "Mechanisms of action of acetylcholine in the guinea-pig cerebral cortex in vitro." J Physiol **375**: 169-94.

- McCormick, D. A. and Prince, D. A. (1987). "Actions of acetylcholine in the guinea-pig and cat medial and lateral geniculate nuclei, in vitro." J Physiol **392**: 147-65.
- Metherate, R. and Hsieh, C. Y. (2004). "Synaptic mechanisms and cholinergic regulation in auditory cortex." Prog Brain Res **145**: 143-56.
- Metherate, R., Tremblay, N. and Dykes, R. W. (1988). "Transient and prolonged effects of acetylcholine on responsiveness of cat somatosensory cortical neurons." J Neurophysiol **59**(4): 1253-76.
- Mizobe, K., Polat, U., Pettet, M. W. and Kasamatsu, T. (2001). "Facilitation and suppression of single striate-cell activity by spatially discrete pattern stimuli presented beyond the receptive field." Vis Neurosci **18**(3): 377-91.
- Moran, J. and Desimone, R. (1985). "Selective attention gates visual processing in the extrastriate cortex." Science **229**(4715): 782-4.
- Mori, T., Zhao, X., Zuo, Y., Aistrup, G. L., Nishikawa, K., Marszalec, W., Yeh, J. Z. and Narahashi, T. (2001). "Modulation of neuronal nicotinic acetylcholine receptors by halothane in rat cortical neurons." Mol Pharmacol **59**(4): 732-43.
- Motter, B. C. (1993). "Focal attention produces spatially selective processing in visual cortical areas V1, v2, and v4 in the presence of competing stimuli." J Neurophysiol **70**(3): 909-919.
- Motter, B. C. (1994). "Neural correlates of feature selective memory and pop-out in extrastriate area v4." J Neurosci **14**(4): 2190-2199.
- Muir, J. L., Everitt, B. J. and Robbins, T. W. (1994). "Ampa-induced excitotoxic lesions of the basal forebrain: A significant role for the cortical cholinergic system in attentional function." J Neurosci **14**(4): 2313-26.
- Murphy, P. C. and Sillito, A. M. (1991). "Cholinergic enhancement of direction selectivity in the visual cortex of the cat." Neuroscience **40**(1): 13-20.
- Nagase, Y., Kaibara, M., Uezono, Y., Izumi, F., Sumikawa, K. and Taniyama, K. (1999). "Propofol inhibits muscarinic acetylcholine receptor-mediated signal transduction in xenopus oocytes expressing the rat m1 receptor." Jap J Pharmacol **79**(3): 319-325.
- O'Craven, K. M., Downing, P. E. and Kanwisher, N. (1999). "Fmri evidence for objects as the units of attentional selection." Nature **401**(6753): 584-587.
- O'craven, K. M., Rosen, B. R., Kwong, K. K., Treisman, A. and Savoy, R. L. (1997). "Voluntary attention modulates fmri activity in human mt-mst." Neuron **18**(4): 591-598.
- Oldford, E. and Castro-Alamancos, M. A. (2003). "Input-specific effects of acetylcholine on sensory and intracortical evoked responses in the "barrel cortex" in vivo." Neuroscience **117**(3): 769-78.
- Orban, G. A., Kato, H. and Bishop, P. O. (1979). "End-zone region in receptive fields of hypercomplex and other striate neurons in the cat." J Neurophysiol **42**(3): 818-32.
- Ozeki, H., Sadakane, O., Akasaki, T., Naito, T., Shimegi, S. and Sato, H. (2004). "Relationship between excitation and inhibition underlying size tuning and

- contextual response modulation in the cat primary visual cortex." J Neurosci 24(6): 1428-38.
- Pack, C. C., Hunter, J. N. and Born, R. T. (2005). "Contrast dependence of suppressive influences in cortical area mt of alert macaque." J Neurophysiol 93(3): 1809-15.
- Parkinson, D., Kratz, K. E. and Daw, N. W. (1988). "Evidence for a nicotinic component to the actions of acetylcholine in cat visual cortex." Exp Brain Res 73(3): 553-68.
- Pepeu, G. and Giovannini, M. G. (2004). "Changes in acetylcholine extracellular levels during cognitive processes." Learn Mem 11(1): 21-7.
- Perry, E., Walker, M., Grace, J. and Perry, R. (1999). "Acetylcholine in mind: A neurotransmitter correlate of consciousness?" Trends Neurosci 22(6): 273-80.
- Petrov, Y., Carandini, M. and McKee, S. P. (2004). "Surround suppression is strong in the periphery but absent in the fovea." Soc for Neurosci Abstract Program No. 713.5.
- Petrov, Y., Carandini, M. and McKee, S. P. (2005). "Two distinct mechanisms of suppression in human vision." J Neurosci 25(38): 8704-8707.
- Polat, U., Mizobe, K., Pettet, M. W., Kasamatsu, T. and Norcia, A. M. (1998). "Collinear stimuli regulate visual responses depending on cell's contrast threshold." Nature 391(6667): 580-4.
- Polat, U. and Norcia, A. M. (1996). "Neurophysiological evidence for contrast dependent long-range facilitation and suppression in the human visual cortex." Vision Res 36(14): 2099-109.
- Press, W. H., Teukolsky, S. A., Vetterling, W. T. and Flannery, B. P. (2002). Numerical recipes in C. Cambridge, Cambridge University Press.
- Price, J. and Stern, R. (1983). "Individual cells in the nucleus basalis-diagonal band complex have restricted axonal projections to the cerebral cortex in the rat." Brain res 269: 352-356.
- Prusky, G. T., Shaw, C. and Cynader, M. S. (1987). "Nicotine receptors are located on lateral geniculate nucleus terminals in cat visual cortex." Brain Res 412(1): 131-8.
- Quinn, P. C. (2004). "Visual perception of orientation is categorical near vertical and continuous near horizontal." Perception 33(8): 897-906.
- Reynolds, J. H., Chelazzi, L. and Desimone, R. (1999). "Competitive mechanisms subserve attention in macaque areas v2 and v4." J Neurosci 19(5): 1736-53.
- Reynolds, J. H. and Desimone, R. (1999). "The role of neural mechanisms of attention in solving the binding problem." Neuron 24: 19-29.
- Reynolds, J. H. and Desimone, R. (2003). "Interacting roles of attention and visual salience in v4." Neuron 37(5): 853-63.
- Reynolds, J. H., Pasternak, T. and Desimone, R. (2000). "Attention increases sensitivity of v4 neurons." Neuron 26(3): 703-14.

- Robbins, T. W., McAlonan, G., Muir, J. L. and Everitt, B. J. (1997). "Cognitive enhancers in theory and practice: Studies of the cholinergic hypothesis of cognitive deficits in alzheimer's disease." Behav Brain Res 83(1-2): 15-23.
- Roberts, M., Zinke, W., Guo, K., Robertson, R., McDonald, S. and Thiele, A. (2005). "Acetylcholine dynamically controls spatial integration in marmoset primary visual cortex." J Neurophysiol 93(4): 2062-72.
- Roberts, M. J. and Thiele, A. (2004). "Attention reduces spatial integration in primate primary visual cortex." Soc for Neurosci Abstract Viewer/Itinerary Planner Program No. 175.9.
- Roberts, M. J. and Thiele, A. (2005). "Interaction of context, contrast, and attention on orientation discrimination in human subjects." Soc for Neurosci Abstract Viewer/Itinerary Planner Program No. 286.7.
- Robinson, H. P. and Harsch, A. (2002). "Stages of spike time variability during neuronal responses to transient inputs." Phys Rev E Stat Nonlin Soft Matter Phys 66(6 Pt 1): 061902.
- Roelfsema, P. R., Lamme, V. A. and Spekreijse, H. (1998). "Object-based attention in the primary visual cortex of the macaque monkey." Nature 395(6700): 376-81.
- Roelfsema, P. R. and Spekreijse, H. (2001). "The representation of erroneously perceived stimuli in the primary visual cortex." Neuron 31(5): 853-63.
- Sahin, M., Bowen, W. D. and Donoghue, J. P. (1992). "Location of nicotinic and muscarinic cholinergic and mu-opiate receptors in rat cerebral neocortex: Evidence from thalamic and cortical lesions." Brain Res 579(1): 135-47.
- Sarter, M. and Bruno, J. P. (1997). "Cognitive functions of cortical acetylcholine: Toward a unifying hypothesis." Brain Res.Rev. 23: 28-46.
- Sarter, M. and Bruno, J. P. (1998). "Cortical acetylcholine, reality distortion, schizophrenia, and lewy body dementia: Too much or too little cortical acetylcholine?" Brain Cogn 38(3): 297-316.
- Sarter, M., Bruno, J. P. and Givens, B. (2003). "Attentional functions of cortical cholinergic inputs: What does it mean for learning and memory?" Neurobiol Learn Mem 80(3): 245-56.
- Sarter, M., Givens, B. and Bruno, J. P. (2001). "The cognitive neuroscience of sustained attention: Where top-down meets bottom-up." Brain Res Rev 35(2): 146-60.
- Sarter, M., Hasselmo, M. E., Bruno, J. P. and Givens, B. (2005). "Unraveling the attentional functions of cortical cholinergic inputs: Interactions between signal-driven and cognitive modulation of signal detection." Brain Res Rev 48(1): 98-111.
- Sarter, M. and Parikh, V. (2005). "Choline transporters, cholinergic transmission and cognition." Nat Rev Neurosci 6(1): 48-56.
- Sato, H., Hata, Y., Masui, H. and Tsumoto, T. (1987). "A functional role of cholinergic innervation to neurons in the cat visual cortex." J Neurophysiol 58(4): 765-80.

- Sceniak, M. P., Hawken, M. J. and Shapley, R. (2001). "Visual spatial characterization of macaque V1 neurons." J Neurophysiol 85(5): 1873-87.
- Sceniak, M. P., Hawken, M. J. and Shapley, R. (2002). "Contrast-dependent changes in spatial frequency tuning of macaque V1 neurons: Effects of a changing receptive field size." J Neurophysiol 88(3): 1363-73.
- Sceniak, M. P., Ringach, D. L., Hawken, M. J. and Shapley, R. (1999). "Contrast's effect on spatial summation by macaque V1 neurons." Nat Neurosci 2(8): 733-9.
- Scholte, H. S., Spekreijse, H. and Roelfsema, P. R. (2001). "The spatial profile of visual attention in mental curve tracing." Vision Res 41(20): 2569-80.
- Seidemann, E. and Newsome, W. T. (1999). "Effect of spatial attention on the responses of area mt neurons." J Neurophysiol 81(4): 1783-94.
- Seidemann, E., Poirson, A. B., Wandell, B. A. and Newsome, W. T. (1999). "Color signals in area mt of the macaque monkey." Neuron 24(4): 911-917.
- Series, P., Georges, S., Lorenceau, J. and Fregnac, Y. (2002). "Orientation dependent modulation of apparent speed: A model based on the dynamics of feed-forward and horizontal connectivity in V1 cortex." Vision Res 42(25): 2781-97.
- Series, P., Lorenceau, J. and Fregnac, Y. (2003). "The "silent" surround of V1 receptive fields: Theory and experiments." J Physiol Paris 97(4-6): 453-74.
- Shapley, R., Hawken, M. and Ringach, D. L. (2003). "Dynamics of orientation selectivity in the primary visual cortex and the importance of cortical inhibition." Neuron 38(5): 689-99.
- Sillito, A. M. (1977). "The spatial extent of excitatory and inhibitory zones in the receptive field of superficial layer hypercomplex cells." J Physiol 273(3): 791-803.
- Sillito, A. M. and Kemp, J. A. (1983). "Cholinergic modulation of the functional organization of the cat visual cortex." Brain Res 289(1-2): 143-55.
- Sillito, A. M., Kemp, J. A. and Berardi, N. (1983). "The cholinergic influence on the function of the cat dorsal lateral geniculate nucleus (dlgn)." Brain Res 280(2): 299-307.
- Sillito, A. M. and P.C.Murphy (1987). The cholinergic modulation of cortical function. Cerebral cortex. J. E. G. a. P. A., Plenum Press: 161-185.
- Sillito, A. M., Salt, T. E. and Kemp, J. A. (1985). "Modulatory and inhibitory processes in the visual cortex." Vision Res 25(3): 375-81.
- Skrandies, W. (1985). "Human contrast sensitivity: Regional retinal differences." Hum Neurobiol 4(2): 97-9.
- Spinks, R. L., Baker, S. N., Jackson, A., Khaw, P. T. and Lemon, R. N. (2003). "Problem of dural scarring in recording from awake, behaving monkeys: A solution using 5-fluorouracil." J Neurophysiol 90(2): 1324-32.
- Spitzer, H., Desimone, R. and Moran, J. (1988). "Increased attention enhances both behavioral and neuronal performance." Science 240(4850): 338-340.

- Stemmler, M., Usher, M. and Niebur, E. (1995). "Lateral interactions in primary visual cortex: A model bridging physiology and psychophysics." Science **269**(5232): 1877-80.
- Suzuki, T., Ueta, K., Sugimoto, M., Uchida, I. and Mashimo, T. (2003). "Nitrous oxide and xenon inhibit the human (alpha 7)5 nicotinic acetylcholine receptor expressed in xenopus oocyte." Anesth Analg **96**(2): 443-8, table of contents.
- Talgar, C. P. and Carrasco, M. (2002). "Vertical meridian asymmetry in spatial resolution: Visual and attentional factors." Psychon Bull Rev **9**(4): 714-22.
- Talgar, C. P., Pelli, D. and Carrasco, M. (2003). "Covert attention enhances letter identification without affecting channel tuning." J Vis **4**(1) 22-31.
- Tassonyi, E., Charpantier, E., Muller, D., Dumont, L. and Bertrand, D. (2002). "The role of nicotinic acetylcholine receptors in the mechanisms of anesthesia." Brain Res Bulletin **57**(2): 133-150.
- Theeuwes, J., Kramer, A. F. and Atchley, P. (2001). "Spatial attention in early vision." Acta Psychologica **108**(1): 1-20.
- Thiele, A. (2004). "Perceptual learning: Is V1 up to the task?" Curr Biol **14**: 671-673.
- Thiele, A., Distler, C., Korbmacher, H. and Hoffmann, K. P. (2004). "Contribution of inhibitory mechanisms to direction selectivity and response normalization in macaque middle temporal area." Proc Natl Acad Sci U S A **101**(26): 9810-5.
- Treue, S. (2001). "Neural correlates of attention in primate visual cortex." Trends Neurosci **24**(5): 295-300.
- Treue, S. (2004). "Perceptual enhancement of contrast by attention." Trends Cogn Sci **8**(10): 435-437.
- Treue, S. and Martinez-Trujillo, J. C. (1999). "Feature-based attention influences motion processing gain in macaque visual cortex." Nature **399**(6736): 575-579.
- Treue, S. and Maunsell, J. H. (1999). "Effects of attention on the processing of motion in macaque middle temporal and medial superior temporal visual cortical areas." J Neurosci **19**(17): 7591-602.
- Treue, S. and Trujillo, J. C. M. (1999). "Feature-based attention influences motion processing gain in macaque visual cortex." Nature **399**: 575-579.
- Van Essen, D. C., Anderson, C. H. and Felleman, D. J. (1992). "Information processing in the primate visual system: An integrated systems perspective." Science **255**: 419-423.
- Vidal, C. and Changeux, J. P. (1993). "Nicotinic and muscarinic modulations of excitatory synaptic transmission in the rat prefrontal cortex in vitro." Neuroscience **56**(1): 23-32.
- Vogels, R. (1990). "Population coding of stimulus orientation by striate cortical cells." Biol Cybern **64**(1): 25-31.
- Vogels, R. and Orban, G. A. (1990). "How well do response changes of striate neurons signal differences in orientation: A study in the discriminating monkey." J Neurosci **10**(11): 3543-58.

- Westheimer, G. (1990). "Simultaneous orientation contrast for lines in the human fovea." Vision Res 30(11): 1913-21.
- Westheimer, G. (2003). "The distribution of preferred orientations in the peripheral visual field." Vision Res 43(1): 53-7.
- Williams, A. L., Singh, K. D. and Smith, A. T. (2003). "Surround modulation measured with functional mri in the human visual cortex." J Neurophysiol 89(1): 525-33.
- Xing, J. and Heeger, D. J. (2000). "Center-surround interactions in foveal and peripheral vision." Vision Res 40(22): 3065-72.
- Yeshurun, Y. and Carrasco, M. (1998). "Attention improves or impairs visual performance by enhancing spatial resolution." Nature 396(6706): 72-5.
- Young, M. P. (2000). "The architecture of visual cortex and inferential processes in vision." Spat Vis 13(2-3): 137-46.
- Yu, A. J. and Dayan, P. (2002). "Acetylcholine in cortical inference." Neural Networks 15(4-6): 719-730.
- Yu, A. J. and Dayan, P. (2003). Expected and unexpected uncertainty: Ach & ne in the neocortex. Advances in neural information processing systems. Cambridge, MA, MIT Press. 15.
- Yu, C., Klein, S. A. and Levi, D. M. (2001). "Surround modulation of perceived contrast and the role of brightness induction." J Vis 1(1): 18-31.
- Yu, C., Klein, S. A. and Levi, D. M. (2003). "Cross- and iso- oriented surrounds modulate the contrast response function: The effect of surround contrast." J Vis 3(8): 527-40.
- Zenger, B., Braun, J. and Koch, C. (2000). "Attentional effects on contrast detection in the presence of surround masks." Vision Res 40(27): 3717-24.
- Zenger-Landolt, B. and Heeger, D. J. (2003). "Response suppression in V1 agrees with psychophysics of surround masking." J Neurosci 23(17): 6884-93.

Appendix

Chapter 2 appendix

Table 2.2 (page 241) Median, 25th and 75th percentile changes in peak length and DOG fitting parameters taken using SSE fitting, χ^2 fitting and bootstrap fitting. Data are shown for all cells, and separately for facilitated and inhibited cells. The table shows the raw differences in the parameter of interest and the percentage change. Significance was tested using a signed rank test.

Table 2.3 (page 242) Median, 25th and 75th percentile changes in peak length and ROG fitting parameters taken using SSE fitting, χ^2 fitting and bootstrap fitting. Data are shown for all cells, and separately for facilitated and inhibited cells. The table shows the raw differences in the parameter of interest and the percentage change. Significance was tested using a signed rank test.

Table 2.2		all cells			facilitated cells			inhibited cells						
		25th	50th	75th	signed rank test	25th	50th	75th	signed rank test	25th	50th	75th	signed rank test	
DOG model	peak (multiples of mRF diameter)	SSE fit	-0.77	-0.075	0.06		-0.6	0.07	0.083		-1.58	-0.08	0.04	
		X2 fit	-37.02%	-6.82%	7.20%	p=0.002	-36.70%	-7.39%	7.53%	p=0.064	-37.40%	-4.30%	4.30%	p=0.012
		bootstrap	-1.1	-0.11	0.06		-1.16	0.11	0.06		-1.19	-0.09	0.065	
summation area (multiples of mRF diameter)	SSE fit	-32.80%	-8.18%	7.14%	p=0.003	-38.80%	-8.77%	7.86%	p=0.013	-29.59%	-6.60%	10.31%	p=0.101	
	X2 fit	-0.82	-0.9	0.05		-0.43	-0.03	0.07		-2.02	-0.23	0.31		
	bootstrap	-31.8	-8.65	3.21	p=0.001	-27.70%	-2.59%	4.70%	p=0.054	-40.50%	-15.90%	3.45%	p=0.003	
summation gain (arbitrary)	SSE fit	-0.52	-1.169	0.131		-0.57	-0.14	0.14		-0.48	0.024	0.15		
	X2 fit	-25.80%	-6.92%	14.38%	p=0.041	-26.70%	-14.40%	15.32%	p=0.002	-23.46%	2.08%	15.80%	p=0.946	
	bootstrap	-0.56	-0.1	0.25		-0.9	0.23	0.12		-0.32	0.11	0.59		
inhibitory area (multiples of mRF diameter)	SSE fit	-29.65%	-6.13%	27.62%	p=0.099	-42.10%	-13.78%	16.80%	p=0.009	-18.08%	15.80%	37.96%	p=0.527	
	X2 fit	-0.48	-0.09	0.15		-0.54	-0.52	0.14		-0.44	-0.03	0.16		
	bootstrap	-23.71	-7.01	13.5	p=0.019	-27.64%	-10.26%	17.40%	p=0.026	-22.85%	-0.94%	13.05%	p=0.353	
inhibitory gain (arbitrary)	SSE fit	-4.85	5.29	31.46		-0.83	8.3	28.02		-7.59	0.24	50.5		
	X2 fit	-15.08%	27.93%	116.50%	p=0.039	-2.98%	30.15%	101.50%	p=0.041	-27.80%	0.57%	294.70%	p=0.51	
	bootstrap	-26.6	3.45	31.77		-70.59	3.79	24.2		-6.78	1.6	85.4		
inhibitory area (multiples of mRF diameter)	SSE fit	-42.68%	23.23%	134.40%	p=0.513	-48.30%	28.60%	106.20%	p=0.851	-31.90%	4.06%	608.70%	p=0.326	
	X2 fit	-4	7.84	40.5		-0.81	10.43	45.06		-4.6	1.25	30.11		
	bootstrap	-11.10%	34.70%	117.90%	p=0.022	-1.98%	54.70%	98.90%	p=0.033	-20.50%	2.30%	320.70%	p=0.412	
inhibitory gain (arbitrary)	SSE fit	-0.66	-0.001	1.38		-0.65	0.15	3.38		-0.71	-0.05	0.41		
	X2 fit	-25.81%	-51.00%	38.01%	p=0.404	-26.80%	8.60%	74.90%	p=0.084	-24.60%	-1.92%	14.30%	p=0.353	
	bootstrap	-0.75	-0.07	1.89		-0.68	0.13	3.4		-1.02	-0.33	0.68		
inhibitory area (multiples of mRF diameter)	SSE fit	-26.43%	-2.76%	74.90%	p=0.458	-24.10%	13.10%	97.80%	p=0.093	-30.70%	-13.00%	32.60%	p=0.382	
	X2 fit	-0.58	-0.08	-0.8		-0.6	0.009	1.5		-0.45	-0.19	0.37		
	bootstrap	-23.98%	-2.70%	27.90%	p=0.77	-25.80%	0.12%	51.80%	p=226	-20.20%	-6.62%	15.53%	p=0.353	
inhibitory gain (arbitrary)	SSE fit	-8.6	6.94	42.42		-11.16	6.9	44.29		-5.76	7.33	55.2		
	X2 fit	-47.80%	62.76%	237.10%	p=0.075	-58.29%	54.90%	169.40%	p=0.241	-32.20%	91.50%	186.30%	p=0.166	
	bootstrap	-21.48	3.79	38.85		-82.13	2	30.1		-1.3	8.29	85.18		
inhibitory area (multiples of mRF diameter)	SSE fit	-52.40%	76.30%	115.30%	p=0.033	-79.20%	36.30%	492.70%	p=0.79	-2.10%	10.90%	227.10%	p=0.058	
	X2 fit	-3.56	8.89	38.07		-4.8	10.39	41.3		-0.97	8.84	26.5		
	bootstrap	-28.15%	69.10%	229.40%	p=0.022	-42.90%	68.40%	185.70%	p=0.088	13.90%	69.70%	160.80%	p=0.104	

Table 2.3		all cells			facilitated cells			inhibited cells					
ROG model		25	median	75	signed rank test	25	median	75	signed rank test	25	median	75	signed rank test
peak (multiples of mRF diameter)	SSE fit	-1.65	-0.18	0.03		-1.23	-0.09	0.03		-2.88	-0.46	0.015	
		-50.00%	-15.20%	3.13%	p<0.001	-49.50%	-5.38%	3.90%	p=0.005	-57.70%	-28.05%	2.06%	p=0.001
	X2 fit	-2.28	-0.315	0.01		-1.35	-0.22	0.015		-3.06	-0.42	0.01	
		-57.60%	-21.86%	1.36%	p<0.001	-53.18%	-17.14%	2.85%	p=0.001	-60.90%	-27.00%	1.48%	p=0.007
	bootstrap	-1.45	-0.17	0.05		-1.29	0.11	0.06		-2.63	-0.2	0.013	
		-49.22%	-10.67%	5.71%	p<0.001	-44.80%	-9.57%	6.22%	p=0.011	-52.20%	-18.77%	1.45%	p=0.002
summation area (multiples of mRF diameter)	SSE fit	-7.3	-0.18	0.04		-3.54	-0.76	0.1		-13.7	-2.03	0.03	
		-69.35%	-28.83%	3.31%	p<0.001	-63.10%	-29.67%	7.06%	p=0.001	-78.20%	-18.50%	1.50%	p=0.001
	X2 fit	-6.55	-0.75	0.1		-6.05	-1	0.09		-16.17	-0.71	0.16	
		-78.50%	-31.52%	9.04%	p<0.001	-77.50%	-34.70%	5.23%	p=0.002	82.35%	-20.39%	27.40%	p=0.035
	bootstrap	-7.17	-0.8	0.04		-3.54	-0.61	0.11		-13.34	-2.41	-0.07	
		-67.94%	-25.00%	5.52%	p<0.001	-64.10%	-25.47%	9.22%	p<0.001	-76.13%	-24.50%	-4.43%	p<0.001
summation gain (arbitrary)	SSE fit	-920.1	-10.61	10.35		-354	-2.64	25.6		-1405.5	-16.9	2.4	
		-87.80%	-19.30%	24.84%	p=0.013	-78.80%	-4.05%	99.30%	p=0.354	-94.50%	-43.20%	2.50%	p=0.005
	X2 fit	-530	-14.5	7.41		-556	-3.6	15.2		-480.15	-15.12	2.8	
		-96.90%	-30.80%	42.90%	p=0.01	-94.48%	-9.70%	115.90%	p=0.069	-98.70%	-60.40%	8.20%	p=0.058
	bootstrap	-318.95	-3.5	8.09		-216.8	0	17.5		-577.4	-7.19	0.27	
		-79.67%	-5.95%	34.93%	p=0.018	-70.30%	0.00%	103.80%	p=0.35	-94.70%	-23.00%	0.63%	p=0.005
inhibitory area (multiples of mRF diameter)	SSE fit	-4.13	0	2.55		-1.8	0.29	9.75		-13.08	-0.76	0.35	
		-46.06%	0.00%	46.67%	p=0.663	21.90%	1.00%	134.70%	p=0.204	-68.60%	-19.30%	4.35%	p=0.014
	X2 fit	-8.79	-0.04	4.5		-6.14	1.04	7.66		-17.2	-0.08	1.92	
		-73.11%	-0.88%	83.70%	p=0.608	-51.26%	1.15%	121.50%	p=0.83	-79.06%	-1.76%	37.80%	p=0.33
	bootstrap	-4.22	0	2.12		-1.9	0	3.8		-11.3	-0.15	0.7	
		-39.96%	0.00%	37.07%	p=0.508	-31.90%	0.00%	99.70%	p=0.536	-67.02%	-2.20%	-4.94%	p=0.05
inhibitory gain (arbitrary)	SSE fit	-38.1	-2.06	2.27		-25.38	-2.7	2.45		-52.06	-1.84	1.13	
		-89.45%	-42.04%	130.80%	p=0.35	-84.27%	-35.80%	172.30%	p=0.16	-91.70%	-48.20%	91.90%	p=0.093
	X2 fit	-61.3	-2.08	1.53		-52.5	-4.05	1.18		-83.6	-2.01	3.8	
		-98.00%	-49.50%	99.10%	p=0.016	-98.70%	-39.50%	79.70%	p=0.029	-97.40%	-55.40%	153.90%	p=0.313
	bootstrap	-38.5	-2.7	1.14		-29.7	-3.87	1.26		-53.15	-1.73	-1.2	
		-89.75%	-36.10%	76.79%	p=0.016	-78.05%	-39.14%	76.89%	p=0.088	-92.80%	-33.05%	88.70%	p=0.094

Chapter 3 appendix

Communication with M Ito regarding RF eccentricity

Message from Mark Roberts, 03 August 2005

Dear Dr. Ito,

I have a quick question regarding your 1999 neuron paper 'attention modulates contextual influences in primary visual cortex of alert monkeys'. You report that receptive field eccentricity was ranged from 1.9 deg to 5.3 deg, I was wondering whether the RF eccentricity in one monkey was different from the other or whether you recorded RFs across the same range in both monkeys.

Many thanks

Mark Roberts

Message from Minami Ito, 04 August 2005

Dear Dr. Roberts

The range of eccentricity was different between two monkeys. The range (mean+SEM) was 1.85-3.22 degree (2.56+0.04, n=84) for one monkey, and 3.68-5.25 degree (3.68+0.1, n=50) for another. Number of units was slightly larger than those reported in the paper due to some additional experiments. I hope this information may help you.

Best regards,

Minami Ito

Message from Mark Roberts, 05 August 2005

Dear Dr. Ito

Thank you that is really helpful, can you remember which monkey was which?

Many thanks

Mark

Message from Minami Ito, 05 August 2005

Dear Dr. Roberts

First monkey was indicated as SA (with the range of 1.85-3.22 degree) and second as UM in our paper.

Best regards,

Table 3.1		all cells						Monkey B			Monkey D		
parameter	contrast	25th	50th	75th	signed rank test	25th	50th	75th	signed rank test	25th	50th	75th	signed rank test
peak (degrees)	high	-0.11	-0.03	0.01	n=96	-0.08	-0.02	0.01	n=80	-0.18	-0.05	0.00	n=16
		-29.48%	-7.22%	2.07%	p<0.001	-25.04%	-6.08%	2.07%	p<0.001	-32.68%	-13.96%	-0.21%	p=0.09
	mid	-0.13	-0.07	-0.01	n=53	-0.12	-0.07	0.00	n=19	-0.15	-0.08	-0.02	n=34
	low	-28.94%	-12.93%	-0.31%	p<0.001	-35.52%	-16.67%	0.00%	p<0.05	-28.41%	-12.91%	-4.13%	p=0.005
		-0.31	-0.01	0.26	n=15	-0.31	-0.01	0.26	n=15	-0.31	-0.01	0.26	n=15
		-24.40%	-2.27%	59.84%	p=0.89	-24.40%	-2.27%	59.84%	p=0.89	-24.40%	-2.27%	59.84%	p=0.90
summation area (degrees)	high	-0.09	-0.03	0.03	p<0.001	-0.09	-0.03	0.02	p<0.001	-0.09	-0.01	0.05	p=0.44
		-28.45%	-11.48%	9.37%	p<0.001	-27.78%	-11.86%	8.07%	p<0.001	-38.54%	-6.75%	26.47%	p=0.44
	mid	-0.26	-0.11	-0.03	p<0.001	-0.23	-0.10	-0.01	p<0.005	-0.29	-0.12	-0.03	p<0.001
	low	-40.84%	-24.75%	9.73%	p<0.001	-43.74%	-24.66%	-2.01%	p<0.005	-39.42%	-25.87%	-12.66%	p<0.001
		-0.06	0.03	0.20	p=0.52	-0.06	0.03	0.20	p=0.52	-0.06	0.03	0.20	p=0.52
		12.29%	5.59%	46.72%	p=0.52	12.29%	5.59%	46.72%	p=0.52	-12.29%	5.59%	46.72%	p=0.52
summation gain (arbitrary)	high	-2.55	8.07	27.14	p<0.001	-2.55	7.00	25.03	p<0.001	-11.35	11.06	60.97	p=0.26
		-3.66%	14.40%	39.08%	p<0.001	-3.66%	14.43%	38.25%	p<0.001	-2.18%	13.59%	53.72%	p=0.26
	mid	-71.06	-7.06	23.23	p=0.16	-36.32	-0.03	11.51	p=0.52	-84.13	-12.10	27.77	p=0.29
	low	-49.76%	-8.14%	24.74%	p=0.16	-46.36%	-1.03%	27.92%	p=0.52	-48.97%	-16.41%	22.67%	p=0.29
		-147.18	-39.91	5.06	p=0.12	-147.18	-39.91	5.06	p=0.12	-147.18	-39.91	5.06	p=0.12
		-57.65%	-41.29%	25.82%	p=0.12	-57.65%	-41.29%	25.82%	p=0.12	-57.65%	-41.29%	25.82%	p=0.12
inhibitory area (degrees)	high	-0.25	0.05	0.67	p=0.17	-0.24	0.02	0.59	p=0.22	-0.58	0.15	1.82	p=0.53
		-23.09%	3.92%	45.88%	p=0.17	-23.07%	1.57%	42.81%	p=0.22	-43.02%	13.99%	326.60%	p=0.53
	mid	-1.13	-0.06	1.14	p=0.82	-1.04	-0.03	0.63	p=0.57	-1.21	-0.10	1.40	p=0.90
	low	-57.62%	-10.65%	72.21%	p=0.82	-51.29%	-7.39%	35.01%	p=0.57	-59.57%	-14.92%	76.15%	p=0.90
		-0.31	0.10	0.61	p=0.64	-0.31	0.10	0.61	p=0.64	-0.31	0.10	0.61	p=0.64
		-24.72%	27.33%	61.93%	p=0.64	-24.72%	27.33%	61.93%	p=0.64	-24.72%	27.33%	61.93%	p=0.64
inhibitory gain (arbitrary)	high	-8.16	1.94	26.12	p=0.10	-4.03	1.94	23.03	p=0.08	-30.54	4.82	98.86	p=0.72
		-18.31%	6.68%	69.32%	p=0.10	-11.73%	6.68%	59.92%	p=0.08	-46.30%	27.70%	137.02%	p=0.72
	mid	-179.84	-6.04	35.36	p=0.21	-165.78	-16.87	5.85	p=0.13	-181.04	0.02	91.61	p=0.66
	low	-68.70%	-6.23%	32.10%	p=0.21	-67.92%	-11.77%	18.51%	p=0.13	-70.02%	-0.74%	161.62%	p=0.66
		-152.80	-27.43	91.11	p=0.60	-152.80	-27.43	91.11	p=0.60	-152.80	-27.43	91.11	p=0.60
		-64.01%	-23.92%	55.05%	p=0.60	-64.01%	-23.92%	55.05%	p=0.60	-64.01%	-23.92%	55.05%	p=0.60

Table 3.1 Median, 25th and 75th percentile change in peak length and fitting parameters between the attend-away and attend-towards conditions in high, medium (mid) and low contrast data. The table shows both the raw difference in the parameter of interest and the percentage change (from attend-away to attend-towards condition). Negative values indicate that the parameter of interest was reduced in attend-towards condition. Significance was tested by a signed rank test. Data is shown for all cells combined and separately for each monkey.

Effect of attention on length tuning in cells recorded from monkey B when data are cut at 200msec post stimulus onset

Table 3.2		Monkey B first 200ms			
parameter	contrast	25th percentile	50th percentile	75th percentile	signed rank test
peak (degrees)	high	-0.08 -18.97%	-0.01 -3.18%	0.05 20.03%	n=80 p=0.28
	mid	-0.10 -23.39%	-0.03 -6.98%	0.01 1.88%	n=19 p=0.01
summation Area (degrees)	high	-0.08 -19.13%	-0.02 -8.48%	0.03 14.99%	p=0.01
	mid	-0.25 -32.14%	-0.06 -7.31%	0.00 -0.26%	p=0.01
summation Gain (arbitrary)	high	-10.29 -11.87%	3.35 4.13%	21.20 19.62%	p=0.21
	mid	-179.67 -53.81%	3.18 2.78%	10.38 23.18%	p=0.18
Inhibitory Area (degrees)	high	-0.47 -33.41%	-0.02 -2.64%	0.82 47.17%	p=0.81
	mid	-0.87 -46.08%	-0.05 -7.74%	0.09 10.01%	p=0.21
Inhibitory Gain (arbitrary)	high	-25.31 -29.49%	-0.98 0.02%	19.09 50.10%	p=0.69
	mid	-235.45 -64.82%	-12.50 -4.54%	6.75 21.44%	p=0.08

Table 3.2 25th, 50th and 75th percentile change in peak length and fitting parameters between the attend-away and attend-towards conditions in high and medium (mid) contrast data. The table shows both the raw difference in the parameter of interest and the percentage change (from attend-away to attend-towards condition). Negative values indicate that the parameter of interest was reduced in attend-towards condition. Significance was tested by a signed rank test. This table includes only data from monkey B when mean neuronal responses were calculated from 30msec to 200msec after stimulus onset.

Effect of attention on length tuning in cells with RF eccentricity recorded at ~7°

Table 3.3		~7° eccentricity sample			
Parameter	contrast	25th percentile	50th percentile	75th percentile	signed rank test
peak (degrees)	mid	0.00 0.00%	0.07 20.00%	0.75 64.95%	n=22 p<0.05
	low	-0.23 -26.53%	0.02 3.92%	0.09 43.18%	n=13 p>0.99
Summation Area (degrees)	mid	-0.03 -5.31%	0.04 19.19%	0.16 62.38%	p<0.05
	low	-0.05 -12.82%	0.05 4.66%	0.12 38.83%	p=0.38
Summation Gain (arbitrary)	mid	-2.26 -7.76%	3.17 9.17%	24.09 45.61%	p=0.14
	low	-8.59 -28.23%	0.01 0.01%	30.52 101.10%	p=0.79
Inhibitory Area (degrees)	mid	-0.35 -21.78%	0.27 21.85%	1.90 95.29%	p=0.17
	low	-0.26 -17.57%	0.54 39.10%	1.32 79.25%	p=0.34
Inhibitory Gain (arbitrary)	mid	-2.46 -18.29%	5.35 15.49%	49.15 166.90%	p=0.16
	low	-19.24 -39.17%	-4.76 -6.90%	31.72 127.65%	p=0.89

Table 3.3 25th, 50th and 75th percentile change in peak length and fitting parameters between the attend-away and attend-towards conditions in medium (mid) and low contrast data. The table shows both the raw difference in the parameter of interest and the percentage change (from attend-away to attend-towards condition). Negative values indicate that the parameter of interest was reduced in attend-towards condition. Significance was tested by a signed rank test. This table includes only data from the ~7° sample from monkey B.

Comparison of DOG fitting parameters between cells with RFs at $\sim 2^\circ$ and $\sim 7^\circ$ eccentricity

parameter	Data sample	25th percentile	50th percentile	75th percentile	2 sample t-test
Peak (degrees)	~2 deg attend RF	0.20	0.34	0.41	
	~7 deg attend RF	0.24	0.46	1.31	p=0.12
	~2 deg attend away	0.28	0.40	0.58	
	~7 deg attend away	0.24	0.35	0.59	p=0.78
Summation Area (degrees)	~2 deg attend RF	0.17	0.34	0.57	
	~7 deg attend RF	0.20	0.43	0.66	p=0.30
	~2 deg attend away	0.24	0.40	0.75	
	~7 deg attend away	0.22	0.29	0.59	p=0.18
Summation Gain (arbitrary)	~2 deg attend RF	27.47	59.88	115.28	
	~7 deg attend RF	16.32	56.80	107.57	p=0.58
	~2 deg attend away	26.34	45.54	170.81	
	~7 deg attend away	17.03	43.57	68.31	p=0.11
Summation Strength (arbitrary)	~2 deg attend RF	6.56	14.10	60.68	
	~7 deg attend RF	6.49	28.14	60.25	p=0.81
	~2 deg attend away	7.71	17.31	125.41	
	~7 deg attend away	4.90	12.84	25.85	p=0.088
Inhibitory Area (degrees)	~2 deg attend RF	0.57	0.85	2.69	
	~7 deg attend RF	0.92	1.54	4.81	p=0.84
	~2 deg attend away	0.82	1.36	2.08	
	~7 deg attend away	1.15	1.57	3.09	p=0.28
Inhibitory Gain (arbitrary)	~2 deg attend RF	26.19	45.56	106.69	
	~7 deg attend RF	16.59	61.27	96.59	p=0.32
	~2 deg attend away	18.51	96.12	214.27	
	~7 deg attend away	13.44	33.15	78.03	p=0.20
Inhibitory Strength (arbitrary)	~7 deg attend RF	18.48	72.03	112.66	
	~2 deg attend away	20.40	56.71	233.23	p=0.32
	~7 deg attend away	24.10	73.37	258.60	
	~2 deg attend RF	15.50	65.59	111.73	p=0.25

Table 3.4 Comparison of peak length, fitting parameters, total facilitation and total inhibition between the $\sim 2^\circ$ and $\sim 7^\circ$ eccentricity samples in monkey B (medium contrast). Values show median, 25th and 75th percentiles of the parameter of interest (row headings). Significance of differences between the two samples was tested by a two sample t-test, p values are shown in the final column.

Table 3.6		all cells				Monkey B				Monkey D			
parameter	contrast	25th	50th	75th	signed rank test	25th	50th	75th	signed rank test	25th	50th	75th	signed rank test
peak (degrees)	hi/mid out	0.05	0.20	0.33	n=28 p<0.001	0.02	0.10	0.23	n=17	0.23	0.26	0.54	n=11
	hi/mid att	15.61%	63.61%	111.90%		7.50%	43.90%	99.29%	p<0.001	30.77%	92.86%	184.97%	p<0.005
	mid/lo out	0.06	0.10	0.24	n=128 p<0.001	0.00	0.07	0.10	n=17	0.12	0.22	0.72	n=11
	mid/lo in	13.36%	34.67%	94.08%		0.00%	21.21%	46.85%	p=0.09	35.83%	67.86%	185.07%	p<0.001
summation area (degrees)	hi/mid out	-0.19	-0.05	0.09	n=15 p=0.45	-0.01	0.19	0.42		-0.19	-0.05	0.09	n=15
	hi/mid att	-51.12%	-23.08%	31.40%		-6.74%	51.59%	157.49%	p<0.05	-51.12%	-23.08%	31.40%	p=0.45
	mid/lo out	-0.22	0.03	0.48	n=15 p=0.60	-0.01	0.11	0.28		-0.22	0.03	0.48	n=15
	mid/lo in	-46.67%	14.29%	170.05%		-2.60%	44.85%	104.99%	p<0.05	-46.67%	14.29%	170.05%	p=0.60
summation gain (arbitrary)	hi/mid out	0.02	0.35	0.48	p<0.001	-0.01	0.19	0.42		0.34	0.45	0.62	
	hi/mid att	4.10%	102.80%	193.72%		-6.74%	51.59%	157.49%	p<0.05	81.38%	166.45%	249.97%	p<0.01
	mid/lo out	0.00	0.20	0.30	p<0.01	-0.01	0.11	0.28		0.17	0.21	0.30	
	mid/lo in	0.54%	66.62%	115.42%		-2.60%	44.85%	104.99%	p<0.05	29.23%	86.45%	142.03%	p<0.05
inhibitory area (degrees)	hi/mid out	-0.20	-0.04	0.26	p=0.64	-0.20	-0.04	0.26		-0.20	-0.04	0.26	
	hi/mid att	-45.40%	-13.05%	108.72%		-45.40%	-13.05%	108.72%		-45.40%	-13.05%	108.72%	
	mid/lo out	-0.21	0.06	0.30	p=0.42	-0.21	0.06	0.30		-0.21	0.06	0.30	
	mid/lo in	-52.10%	20.89%	106.28%		-52.10%	20.89%	106.28%		-52.10%	20.89%	106.28%	
inhibitory gain (arbitrary)	hi/mid out	-23.95	-6.54	113.04	p=0.73	-20.96	-11.44	98.49		-107.45	-0.12	177.36	
	hi/mid att	-43.18%	-20.63%	160.83%		-46.46%	-27.77%	202.81%	p=0.69	-22.93%	-0.17%	130.75%	p=0.97
	mid/lo out	-85.88	-16.13	51.82	p=0.25	-38.96	-9.48	21.86		-153.63	-56.92	103.16	
	mid/lo in	-48.49%	-30.56%	83.91%		-40.09%	-30.93%	36.27%	p=0.33	-55.64%	-30.20%	237.53%	p=0.58
inhibitory area (degrees)	hi/mid out	-53.38	2.49	62.81	p=0.76	-53.38	2.49	62.81		-53.38	2.49	62.81	
	hi/mid att	-59.82%	6.64%	83.11%		-59.82%	6.64%	83.11%		-59.82%	6.64%	83.11%	
	mid/lo out	-84.87	-1.22	55.92	p=0.93	-84.87	-1.22	55.92		-84.87	-1.22	55.92	
	mid/lo in	-64.83%	-4.25%	102.77%		-64.83%	-4.25%	102.77%		-64.83%	-4.25%	102.77%	
inhibitory gain (arbitrary)	hi/mid out	-0.51	-0.17	0.66	p=0.97	-0.40	-0.17	0.84		-3.04	-0.23	0.62	
	hi/mid att	-37.80%	-15.70%	67.26%		-37.77%	-14.31%	62.90%	p=0.98	-54.56%	-24.32%	77.63%	p=0.46
	mid/lo out	-0.61	-0.12	0.63	p=0.78	-0.51	-0.08	0.47		-1.40	-0.30	1.75	
	mid/lo in	-48.30%	-19.61%	48.30%		-39.29%	-16.39%	31.84%	p=0.69	-66.53%	-22.82%	505.95%	p=0.90
inhibitory area (degrees)	hi/mid out	-0.59	0.58	1.49	p=0.33	-0.59	0.58	1.49		-0.59	0.58	1.49	
	hi/mid att	-42.49%	47.36%	289.55%		-42.49%	47.36%	289.55%		-42.49%	47.36%	289.55%	
	mid/lo out	-1.06	-0.53	0.72	p=0.52	-1.06	-0.53	0.72		-1.06	-0.53	0.72	
	mid/lo in	-63.78%	-32.51%	71.53%		-63.78%	-32.51%	71.53%		-63.78%	-32.51%	71.53%	
inhibitory gain (arbitrary)	hi/mid out	-31.67	33.35	221.75	p=0.15	-12.41	70.44	238.40		-226.40	-15.94	224.96	
	hi/mid att	-43.75%	58.89%	544.84%		-41.37%	119.38%	582.46%	p=0.06	-62.65%	-1.60%	442.72%	p=0.97
	mid/lo out	-42.64	-3.88	122.72	p=0.57	-24.36	-4.02	48.72		-132.68	88.05	425.01	
	mid/lo in	-41.71%	-10.70%	301.36%		-36.66%	-13.15%	118.50%	p=0.87	-56.78%	30.48%	1138.49%	p=0.52
inhibitory gain (arbitrary)	hi/mid out	-9.66	50.42	92.04	p=0.07	-9.66	50.42	92.04		-9.66	50.42	92.04	
	hi/mid att	-13.02%	182.46%	794.68%		-13.02%	182.46%	794.68%		-13.02%	182.46%	794.68%	
	mid/lo out	-21.96	14.23	51.74	p=0.45	-21.96	14.23	51.74		-21.96	14.23	51.74	
	mid/lo in	-49.77%	51.96%	132.92%		-49.77%	51.96%	132.92%		-49.77%	51.96%	132.92%	

Table 3.6. 25th, 50th and 75th percentile change in peak length and fitting parameters between contrasts in the attend-towards and attend-away conditions. The table shows both the raw difference in the parameter of interest and the percentage change (from lower contrast to the upper contrast). Negative values indicate that the parameter of interest was reduced by increased contrast. Significance was tested by a signed rank test. Data is shown for all cells combined and separately for each monkey.

Effect of contrast on length tuning for cells with RF eccentricity $\sim 7^\circ$

Table 3.7		Monkey B $\sim 7^\circ$ sample			
parameter	contrast	25th percentile	50th percentile	75th percentile	signed rank test
peak (degrees)	mid/lo out	-0.08 -21.27%	0.12 40.00%	0.25 123.76%	n=13 p=0.22
	mid/lo in	-0.12 -33.50%	0.08 27.59%	0.15 77.90%	n=13 p=0.68
summation area (degrees)	mid/lo out	-0.01 -3.42%	0.22 66.40%	0.47 159.53%	p<0.05
	mid/lo in	0.02 7.09%	0.12 64.98%	0.24 117.25%	p=0.09
summation gain (arbitrary)	mid/lo out	-26.14 -64.95%	0.65 1.56%	73.98 110.34%	p=0.74
	mid/lo in	-69.59 -68.79%	-5.71 -49.08%	12.23 37.38%	p=0.38
inhibitory area (degrees)	mid/lo out	-1.04 -46.92%	-0.38 -21.90%	0.20 35.27%	p=0.34
	mid/lo in	-1.34 -63.20%	-0.25 -24.95%	0.75 78.81%	p=0.64
inhibitory gain (arbitrary)	mid/lo out	-6.11 -39.25%	9.77 31.37%	203.65 599.75%	p=0.17
	mid/lo in	-29.82 -63.38%	0.29 1.05%	14.77 48.20%	p=0.74

Table 3.7 25th, 50th and 75th percentile change in peak length and fitting parameters between contrasts in the attend-towards and attend-away conditions for cells recorded with RFs at $\sim 7^\circ$ eccentricity. The table shows both the raw difference in the parameter of interest and the percentage change (from lower contrast to the upper contrast). Negative values indicate that the parameter of interest was reduced by increased contrast. Significance was tested by a signed rank test. Data is only included from the $\sim 7^\circ$ sample in monkey B.